Assessment of Stormwater Metals on Receiving Water Sediment Recontamination

by

Ilektra Drygiannaki, B.Sc., M.Sc.

A Dissertation

In

Civil Engineering

Submitted to the Graduate Faculty
of Texas Tech University in
Partial Fulfillment of
the Requirements for
the Degree of

DOCTOR OF PHILOSOPHY

Approved

Dr. Danny D. Reible
Chair of the Committee

Dr. Andrew W. Jackson

Dr. Weile Yan

Dr. John A. Dawson

Mark Sheridan
Dean of the Graduate School

August 2020

In loving memory of my uncle, Georgios Petrakakis

ACKNOWLEDGMENTS

I would like to express my deepest appreciation to my supervisor Dr. Danny Reible for his relentless support and guidance throughout my entire academic and career path. I will be always grateful to you because you gave true meaning to the word “mentor” for me. Your ingenious vision and charismatic personality will be memorable to me. Thank you very much for providing me the means to conduct my research in a well-equipped laboratory and an excellent facility.

I would like to thank very much my Ph.D. committee members, Dr. John A. Dawson, Dr. Andrew W. Jackson, and Dr. Weile Yan for being always available to provide guidance and useful comments for my research since the beginning of my academic path.

I would also like to thank very much Dr. Jeong-Hee Kim for agreeing to be present as the Dean’s representative in my dissertation defense and for being a supportive friend.

I would like to gratefully acknowledge the financial support provided by the Strategic Environmental Research and Development Program (SERDP) that made my studies possible.

Special thanks to Dr. Balaji Rao for being an exceptional colleague, providing valuable advices and great support throughout my entire Ph.D. path, which I will never forget.

I would like to thank very much Dr. Marienne Colvin, Mr. Gunther Rosen, Mr. Nicholas Hayman, and Dr. Bart Chadwick from the Naval Information Warfare Center Pacific (NIWC) for their contribution to the SERDP project and for performing the bioassays and passive sampling exposures. Many thanks to Michelle Bejar for performing the chemical analysis of these exposures at Texas Tech University.

I would like to thank very much Dr. Robert Pitt for his advices and help regarding the WinSLAMM modeling, as well as Mrs. Megan Otto. Mr. Brandon Steets, and Dr. Jared Ervin from Geosyntec Consultants Inc. for their contribution to the SERDP project and stormwater sampling in San Diego Bay.

I would like to acknowledge my colleagues in "Reible Research Group" for sharing valuable academic knowledge. I would also like to express my appreciation to Mr. Brad Thornhill for being always willing to provide valuable instrumental advices and for taking good care of the laboratory safety. Thanks to Dr. Magdalena Rakowska for her help in the SERDP project and also in the lab safety and instruments.

I would like to wholeheartedly thank my dear friends at Texas Tech University and in Lubbock, Texas; each of you made my Ph.D. life happier, and I could not be more grateful to you for creating a healthy and respectful life environment in Lubbock. Thank you for being there for me in the good and the difficult times. I will always remember our shared moments, our funny times during the happy hours, our parties, the trips together, and our sharing laughs, stories, and life experiences. You made Lubbock a great place to live and I will keep our memories in my heart forever. I also wish to thank a lot my dear friends from Greece for their valuable advices and understanding although so many miles apart.

I would like to extend my deepest gratitude to my mother, Anastasia, for showing me the importance of education and for teaching me through her way of life that kindness is a virtue. I would like to thank my father, Eleftherios, for his support and understanding in every situation I was going through during my entire Ph.D. life. Finally, special thanks to my brother, Myronas, for giving me great comfort with his positive attitude and love always.

TABLE OF CONTENTS

ABSTRACT

Contaminated sediments serve as the sink and source of contaminants, and pose one of the most difficult and cost-effective remediation challenges. Continued metal inputs from stormwater discharges may result in significant discharges into receiving waters and remediating sediments; presenting a challenge from both regulatory and assessment perspective. Metals, like cadmium (Cd), copper (Cu), mercury (Hg), lead (Pb), zinc (Zn), nickel (Ni), and the metalloid arsenic (As), are non-degradable and toxic, posing biological risks by accumulation on living organisms entering the food chain. Stormwater sources are difficult to understand due to the poor characterization of the irregular, event-driven inputs, and the difficulty of managing these diffuse sources of large volumes. Effective means of evaluating the significance of stormwater inputs is particularly important when examining the long-term effectiveness of sediment remedial efforts. This dissertation presents improved approaches for assessing the impact of metals in stormwater on receiving sediments at Paleta Creek in San Diego Naval Base, USA. First aim of the study presents the stormwater assessment and characterization and the exploration of useful indicators for associating metal discharges to sediment recontamination. Second goal presents the evaluation of seasonal storm effects to biologically available metals and biota accumulation in sediments as well as to bulk sediment chemistry. Intensive stormwater and receiving waters sampling was coupled with sediment trap and seasonal sediment core collections, *ex situ* bioassays, and porewater passive sampling via DGTs during the wet and dry seasons.

The first part identified that the most successful indicators of stormwater impacts on sediment recontamination were the size segregated stormwater discharges both in water

and on suspended solids, total (>0.45 μm), sand (>63 μm), coarse silt (20-63 μm), fine silt (5-20 μm), clay (0.45-5 μm), as well as the dissovled phase (<0.45 μm) combined with sediment traps in the receiving waters. The stormwater concentrations, characterized by particle size distribution, provided the potential of the discharged mass and resulting deposition on sediments. The sediment traps provided an indication of the short-term sediment deposition and recontamination resulting from the storm events. The comparison of these various indicators allowed the estimation of the proportion of sediment recontamination likely due to stormwater and the proportion that might be caused by other sources, including resuspension of sediment in the receiving waters. Among the metals studies, Cd was clearly associated with large (>63 μm) particles and was found to settle quickly into locations immediately downstream. Cu, however, was associated with a range of particle sizes and was found in all sediment traps, even those located with some distance from the stormwater discharge. Other constituents, like Pb, Zn, Ni, Hg, and As, showed behavior intermediate to these two extremes suggesting both stormwater and other sources were likely important for these metals.

In the second part, the synthesis of multiple lines of evidence successfully evaluated the biota accumulation due to contamination of sediments by stormwater heavy metals. The metal uptake in *Macoma nasuta* in bioaccumulation assays using sediments collected after the storm seasons were reduced with statistical certainty relative to pre-storm season samples for all measured metals, Cd, Hg, Cu, Pb, Zn, Ni, and the metalloid As; suggesting deposition of stormwater contaminants in low bioavailable forms. Similar reductions were observed after the storms in porewater of sediments measured by DGTs for all measured metals. Interestingly, sediment recontamination as indicated by stormwater loads and bulk

chemistry of the receiving sediments did not indicate biological impacts as indicated by bioaccumulation. Moreover, the bulk sediment chemistry did not correlate with bioaccumulation with the exception of Pb. Analysis of the metal biota accumulation and DGT measured porewater concentrations showed statistically significant positive correlations ($p<0.05$, $\alpha=0.05$) for most metals; suggesting that porewater concentrations can successfully indicate metal availability.

In conclusion, sediment recontamination should be assessed by the combination of size-segregated stormwater discharges and settling traps to identify short term deposition resulting from those storms. Any observed sediment recontamination should also be subjected to bioassays or other bioavailability assessments because bulk sediment recontamination may not lead to negative impacts on benthic organisms.

LIST OF TABLES

LIST OF FIGURES

CHAPTER 1

INTRODUCTION

1.1. Background

Contaminated sediments pose one of the most difficult and cost-effective remediation challenges (Rosengard *et al.*, 2010; USEPA, 1998). Contaminated sediment mega-sites are among the most cost-effective sites in the USA. As an example, 13 of these mega-sites are estimated to cost about $3 billion and these sites cover only a subset of contaminated-sediment sites (NRC, 2007). Much of the current sediment contamination has resulted from historic activities that have now ceased or been improved. However, many of the activities that caused the historic contamination can continue in some form, indicating the need for monitoring of such sources. Sediment sites under remediation can become contaminated by continued inputs from off-site sources, including permitted discharges, transport from upstream areas, or from stormwater discharges. Current urban and industrial discharges are regulated to prevent the release of significant quantities of the contaminants that have caused site contamination. Stormwater sources are particularly difficult to understand and manage because of the generally poor characterization of the irregular, event-driven inputs from such sources and the difficulty of managing diffuse sources of large volumes of runoff (Pitt *et al.*, 1995). Stormwater must be identified and controlled, however, the tools available to quantify these sources and their characteristics are limited, as is the ability to relate those sources to resulting chemical and biological impacts in sediments. These methodologies can also be integrated with models to identify impacts on remedies and, specifically, to identify the resilience of proposed and/or implemented remedies. The

assessment of sediment recontamination and biological impacts due to stormwater along with the integration of multiple lines of evidence in the sediment complex systems using statistcal certainty are crucial to all activities related to monitoring, management, and remediation of sediments (Burton *et al.*, 2002; Reible, 2014).

1.2. Objective

The scope of the study is to develop, test, and assess the effectiveness of approaches in characterizing stormwater discharges and their impact on sediment recontamination on remediating site and living organisms living on these sediments. A comprehensive set of laboratory, field, modeling, and statistical approaches is conducted which is focused on the development and application of techniques to assess the magnitude and characteristics of stormwater and the effects on sediments and the benthos. The method development, testing, and data acquisition are conducted at Paleta Creek, an urban watershed partially that encompasses Naval Base San Diego and drains to San Diego Bay.

The research study includes sampling under dry and wet weather seasonal conditions, stormwater assessment by direct sampling under selected storm events, and receiving water sediment assessment to link stormwater loads to sediment recontamination. Moreover, modeling of the stormwater discharges from the watershed and receiving water hydrodynamic conditions is applied to extrapolate the measurements to annual discharges and to simulate the depositional rate of the contaminants in receiving waters. Bulk sediment contamination is integrated with site-specific bioavailability and bioaccumulation and statistical analysis to identify the biological impacts due to storm-related deposited contaminants. This provides a foundation for a decision-making framework to identify

stormwater sources and their consequences, to design effective source controls, and to propose realistic and cost-effective remedial plans.

The study is conducted in eight coupled and integrated phases:

- Seasonal sediment sampling to characterize dry and wet weather conditions as well as spatial sampling to identify near-shore discharged impacts
- Stormwater loading assessment by direct sampling in various locations at mixed-use urban/industrial watershed
- Receiving waters assessment for associating stormwater loads to sediment recontamination
- Stormwater modeling to extrapolate stormwater metal discharges over a longer period
- Hydrodynamic currents simulations in San Diego Bay to predict the depositional rates of storm-discharged particle-bound contaminants in receiving waters
- *Ex situ* and *in situ* bioassays along with passive sampling techniques for biota accumulation and porewater assessment
- Statistical analysis of seasonal and spatial measurements to identify significant changes related to biological impacts in sediments due to stormwater
- Prediction of the best indicator for biota accumulation when assessing biological impacts in sediments

1.3. Content of the dissertation

In Chapter 2, the literature review provides the research gap statement, the scientific background of the key issues of the dissertation, and the tools that were used to assess the stormwater impacts on remediating sediments. The gaps in the literature are initially stated, continuing with an introduction to contaminated sediment and metal contamination in the environment. The role of stormwater in sediment contamination and the importance of particle size distribution characterization are further explored. The literature for assessing the biological effects in sediments due to stormwater is presented, including the approaches to identify the biota accumulation as well as the biological availability evaluation measuring the labile contaminants from sediments to biota. Finally, the importance of statistics for strengthening the multidisciplinary conclusions is reviewed.

In Chapter 3, the comprehensive methodology to evaluate the stormwater impacts on sediment recontamination and biological effects in sediments is presented. The methods involve field approaches, sampling efforts of stormwater and sediments, laboratory/analytical methods, particle size distribution characterization, and water and sediment metal extraction, and chemical analysis. In addition, the extrapolation of measured monitored discharges into annual storm discharges using WinSLAMM modeling, and the modeling of the depositional rates in receiving waters using CH3D are introduced. *In situ* and *ex situ* bioaccumulation exposure methods are presented as well as tissue extraction and chemical analysis for assessing the biota responses on sediments. Inorganic passive sampling using DGTs and chemical metal extraction and analysis of the DGTs are also evaluated to identify the labile metals of concern in sediment porewater.

Finally, the statistical methods using software R for identifying the statistical certainty of the conclusions from multiple lines of evidence are presented.

In Chapter 4, the stormwater metal impacts on bulk sediment recontamination are assessed. Size-segregated stormwater contaminant loads with simultaneous receiving water and sediment measurements are used to identify dominant sources and contaminants with respect to their impact on sediment recontamination. Stormwater in time series is sampled to evaluate the impacts on receiving waters over time. Stormwater characterization in different particle sizes for key storm discharges is critical to understand the settling potential of particle-bound contaminants on the sediment bed. Settling traps identify the depositional rate of the metal contaminants in receiving waters during the monitored storm events. Size-segregated stormwater contaminant mass and concentrations along with simultaneous deposition in sediment traps could distinguish recontamination by stormwater from other sources. Two-way ANOVA and correlations are applied in stormwater concentrations from different stormwater outlets to investigate the sources of contamination in the critical storm outlet that directly discharges on the sediment bed. Finally, seasonal and spatial evaluations of the surficial sediment core alterations due to stormwater are made using Fisher's exact test and Gamma regression. This chapter is identical to the paper published on the 27th of May 2020 to the journal *Science of the Total Environment*.

In Chapter 5, the approaches to assess biota accumulation from sediments contaminated by stormwaters are presented. Intensive stormwater sampling, before and after the winter wet season, is coupled with surficial sediment sampling, sediment collection via deposition

traps, porewater measurements using diffusion gradient in thin film devices, and metal accumulation in the marine clam, *Macoma nasuta*, using *ex situ* bioassays. Statistical analyses are applied to identify the biological alterations of tissue and porewater concentrations in sediments as well as the surficial seasonal changes in sediment chemistry. Finally, statistical correlations identify the best predictor of bioaccumulation in marine clams, *Macoma Nasuta,* comparing bulk sediment and porewater. This chapter is identical to a paper submitted on the 27th of June 2020 to the journal *Environmental Toxicology and Chemistry*. Another part of this study (presented in Appendix D) has already been published on the 11th October 2019 to the journal *Environmental Toxicology and Chemistry*, suggesting pyrethroids pesticides due to stormwater discharge as the sources for seasonal toxicity observed with Amphipods (*Eohaustorius estuarius*) at Paleta Creek (Hayman *et al.*, 2020).

Finally, *in Chapter 6,* the conclusions of the study are summarized and recommendations are made for future research activities.

1.4. References

Burton, G. A., Jr., Batley, G. E., Chapman, P. M., Forbes, V. E., Smith, E. P., Reynoldson, T., Schlekat, C. E., Besten, P. J., Bailer, A. J., & Green, A. S. (2002). A weight-of-evidence framework for assessing sediment (or other) contamination: Improving certainty in the decision-making process. *Human and ecological risk assessment, 8*(7), 1675-1696.

Hayman, N. T., Rosen, G., Colvin, M. A., Chadwick, B. D., Rao, B., Athanasiou, D., Rakowska, M., Drygiannaki, I., Burton, G. A., Jr., & Reible, D. D. (2020). Seasonal Toxicity Observed with Amphipods (Eohaustorius estuarius) at Paleta Creek, San Diego Bay, USA. *Environmental toxicology and chemistry, 39*(1), 229-239.

NRC. (2007). *Sediment Dredging at Superfund Megasites: Assessing the Effectiveness*. Washington, DC: The National Academies Press.

Pitt, R., Field, R., Lalor, M., & Brown, M. (1995). Urban stormwater toxic pollutants: assessment, sources, and treatability. *Water Environment Research, 67*(3), 260-275.

Reible, D. D. (2014). *Processes, assessment and remediation of contaminated sediments*: Springer.

Rosengard, J., Wallace, J., Otten, M., MacDonald, A., & Lafrenz, R. (2010). A Parametric Model For Estimating Costs For Remediating Contaminated Sediment Sites Using A Dredging Method-A Budgetary & Planning Tool For Decision-Makers. *International Journal of Soil, Sediment and Water, 3*(2), 9.

USEPA. (1998). Assessment and Remediastion of Contaminated Sediments (ARCS) Program: Guidance for in-situ subaqueous capping of contaminated sediments.

CHAPTER 2

LITERATURE REVIEW

2.1 Research gap statement

Contaminated sediment sites occur from legacy contamination of past discharge practices and accumulation of toxic contaminants. Stormwater is considered a major source of nonpoint contamination to surface waters (USEPA, 1993, 1998b) and therefore to receiving sediments through particle deposition as the transport process. In the United States, stormwater was classified as a source of contamination that needs to be subjected to controls in 1987, when the Clean Water Act was modified to include stormwater in the National Pollution Discharge Elimination System (NRC, 2009). Stormwater is generally characterized by contaminant loads (Lee & Bang, 2000). However, several runoff studies have implied the importance of the distribution of contaminants by particle size or settling characteristics, when designing parameters for best management practices (BMPs) of stormwater targeting particle removal efficiency (Hilliges *et al.*, 2017; Li *et al.*, 2005; River & Richardson, 2018; Selbig *et al.*, 2016; Windt *et al.*, 2017).

Recent efforts have been made to associate stormwater with sediments, such as the evaluation of stormwater BMPs performance on suspended sediment based on total and suspended solids and metals concentrations obtained by BMPs databases (Fassman, 2012). Moreover, the relationship between metals in road-deposited sediment particles versus wash off particles have been examined using artificial rainfall and different particle size characterization of metals (Zhao & Li, 2013). Research has also been conducted to measure the metal concentrations and toxicity in sedimentation tanks and stormwater ponds

(Karlsson *et al.*, 2010), as well as the chemical speciation of metals from source to deposition in stormwater pond sediments (Camponelli *et al.*, 2010). However, none of these studies have evaluated the transport of particle-associated stormwater contaminants with simultaneous monitoring of the depositional rates in receiving waters as well as surficial biological impacts in receiving sediments.

Over the last years, the emphasis of sediment risk assessment is often on ecological risk and particularly on benthic community impacts when evaluating the sediment quality (Reible, 2014). Contaminated sediments can serve as sink and source of many hazardous constituents and present an ecological threat to anthropogenic and aquatic organisms that reside in or on the sediments. Previous studies have highlighted the importance of stormwater impacts when evaluating sediment quality and benthic community impacts in sediments (Hatch & Burton, 1999; House *et al.*, 1993; Schiff & Bay, 2003). When assessing biological effects in sediments, a comprehensive assessment of key approaches, and not only a simple assessment of sediment toxicity using laboratory tests, on field-collected sediments is especially important. The examination of only one or two methods can be misleading and resulting in conclusions with high uncertainty (Reible, 2014). The complexity of stressor pathways to exposure and of contaminant fate and multiple factors that affect bioavailability make the assessment of biological effects in sediments particularly challenging (Reible, 2014). Numerous studies have indicated that integrating multiple methods, such as biota community assessments along with physicochemical sediment characterizations, laboratory testing, and in-situ approaches, is the way to go for

quality and risk associated assessment of sediments (Adams *et al.*, 2005; Burton, 1991; Burton *et al.*, 2005; Greenberg *et al.*, 2002).

Sediment quality assessment guidelines suggest physicochemical characterizations of sediments or one-time collections of sediment samples (Wenning, 2005). However, for regulatory and decision-making purposes the complex, dynamic and non-static environment of sediments requires comprehensive monitoring and sufficient sampling efforts (Greenberg *et al.*, 2000). Moreover, sampling and analysis of chemical and biological measurements should be performed simultaneously recognizing the spatial and seasonal heterogeneity and the instability in biological exposures (Reible, 2014).

Contaminated sediment systems contain a pool of contaminants with varying chemical behavior, forms, and transport properties relative to seasonal and spatial changes. Thus, when assessing a sediment system is important to evaluate integrated pieces of information and to strengthen the certainty of the measurements and conclusions (Burton *et al.*, 2002b). There is an increasing interest in approaches, often described as "weight of evidence" assessments, WoE, to promote and associate different lines of experimental pieces of evidence using statistical designs (Benedetti *et al.*, 2012; Burton *et al.*, 2002a; Burton *et al.*, 2002b). Statistical analysis of the generated measurements can provide strong "WoE" conclusions when assessing sediment contamination (Burton *et al.*, 2002a; Burton *et al.*, 2002b; Reible, 2014). However, there is not available guidance on how to compare data and integrate different types of information to support decision making for sediment management (Bates *et al.*, 2018). The importance of approaches that predict and assess the

biological alterations on sediment systems has been previously addressed in the literature (Reible, 2014; Wenning R. J., 2005).

2.2 Contaminated sediments

During the decades of the 1960s and 1970s, the increase of environmental consciousness in the USA resulted in the "Superfund" legislation of 1980, which aimed regulatory actions focusing on soil and groundwater contamination in the decades that followed. Water and wastewater treatment technology improvements in the 70s showed that despite the decreasing contamination of the surface waters, many of these contaminants were persistent in the sediment environment (Reible, 2014). This fact signified the importance of the legacy contamination in the sediments that served as the ultimate sink and source for solid-associated persistent contaminants (Durán *et al.*, 2012; Reible, 2014; Superville *et al.*, 2014). At the beginning of this century contaminated sediment sites, which pose some of the most difficult site remediation issues, began to receive remedial attention (Reible, 2014; USEPA, 1998a). The high cost of contaminated sediments' cleanup emphasizes the importance of source control and mitigation of contamination loadings into aquatic ponds. Contaminated sediments may occupy tens of miles of a river and millions of cubic yards of sediment and contain large amounts of waters, that add complexity to the management and the impacts of the sediment contamination (Reible, 2014). Several efforts have been made to regulate and manage decisions as to how to deal with these complex polluted sediment systems (Bianchini *et al.*, 2019; Mulligan *et al.*, 2001) and to assess sediment quality on these sites (Power & Chapman, 2018).

An ecological related risk is often posed by sediments to benthic microorganisms (Brusven & Prather, 2019; Ryu *et al.*, 2011) with a connection to human health risks through the food chain. The extent of the risk posed by sediment contaminants is a function of both the contaminants and the processes that control their behavior and transport. Significant negative impacts occur when the contaminants are sufficiently mobile to transfer into the biologically active zone, or if the sediment processes can expose buried contaminants (Droppo *et al.*, 2016; Lau & Chu, 1999; Reible, 2014; Zoumis *et al.*, 2001).

The assessment and remediation of contaminated sediments can be challenging compared to contaminated soil since sediments exist in dynamic aquatic environments that promote contaminant transport. The processes that typically influence the contaminant transport in the sediment aquatic environment are the sorption characteristics of fine sediments, the non-erosive nature of sediments, diffusion, advection, dispersion, dynamic processes such as hyporheic exchange, and bioturbation as shown in Figure 2.1 (Reible, 2014).

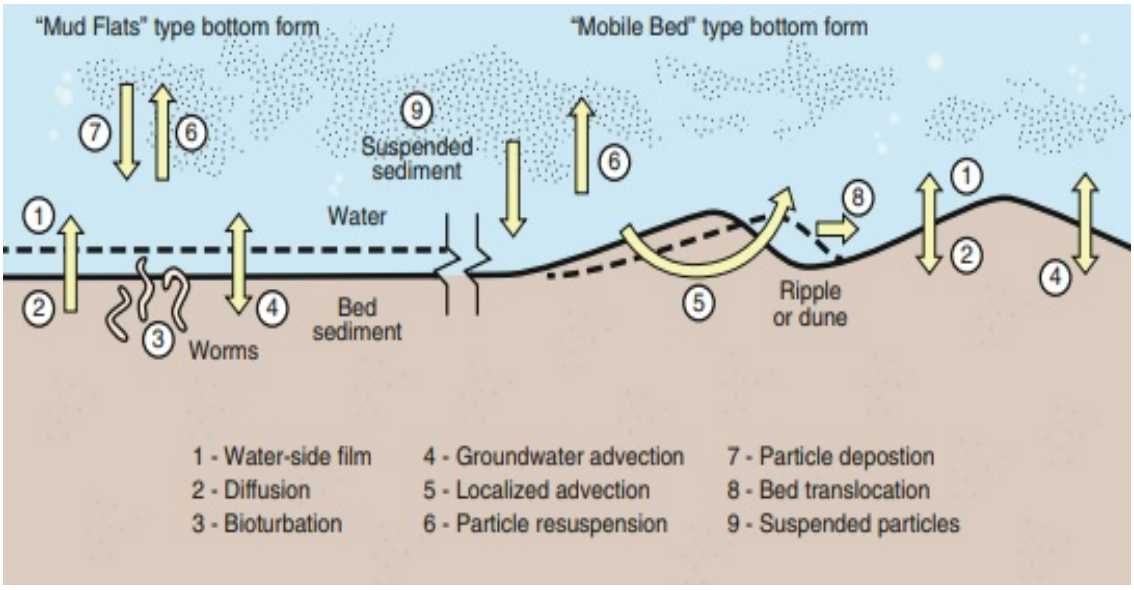

Figure 2.1: Processes that influence the fate and transport of contaminants on sediments (Reible, 2014).

These mechanisms are unique for sediment systems and present an assessment challenge due to their complexity, site-specificity, and spatial variability within a site. The groundwater upwelling and hyporheic exchange as well as bioturbation, which is the normal mixing and transport activities of benthic organisms that live at the sediment-water interface, may lead to a significant flux of sediment contaminants into the overlying waters or porewater (Reible *et al.*, 1996; Sawyer *et al.*, 2009). In particular, bioturbation is an important transport mechanism for strongly solid-associated contaminants in surficial sediments (Garcia, 2008).

Particle deposition and turbulent flow conditions associated with storms or seasonal floodings periodically remobilize surficial sediments and expose anoxic sediment to oxic conditions changing the sediment chemistry. Unavailable forms of metals may sometimes be transformed by exposure to oxic overlying waters to more available and mobile forms of the metals (Warner *et al.*, 2003). Particle-associated contaminant transport in surface waters and receiving sediments is particularly important when evaluating the particle sediment deposition (Burt & Parker, 1984; Christensen, 1965). Settling characteristics of the suspended solids due to different diameter size, such as sand (>60μm), silt (2–60 μm) and clays (<2μm), define the contamination/deposition of these particles on sediments due to their depositional rates in the aquatic environment (Reible, 2014). Fine-grained material remain suspended and settle with lower settling speed compared to sand solids (Cheng, 1997). The settling velocity for individual sediment particles, w (m/s), is described by the equation given by Cheng N. S., 1997:

$$\frac{w*d}{v} = \left(\sqrt{25 + 1.2 * d_*^2} - 5\right)^{1.5} \quad (2.1)$$

Where d is the diameter of particle (m), v the kinematic viscosity of the fluid (m^2/s), d^* dimensionless particle parameter given by the equation:

$$d_* = \left(\frac{\Delta g}{\nu^2}\right)^{1/3} * d \tag{2.2}$$

Where Δ the difference of the density of the fluid to the density of the sediment particle (kg/m^3) and g the gravitational acceleration (m/s^2).

The time that is required for particles with different particle sizes to settle 10m in receiving waters is presented in Figure 2.2. Particles with a diameter greater than 63 μm would require about 30 minutes to settle 10 m (Figure 2.2), and far-field effects (20 to 63 μm size particles) would require about 5 hours to settle 10 m, according to equation 2.1. The smallest fractions (<20 μm particles) would require more than 100 hours to settle this length (Figure 2.2), and therefore finer sized solids might represent a minimum risk to local sediment recontamination.

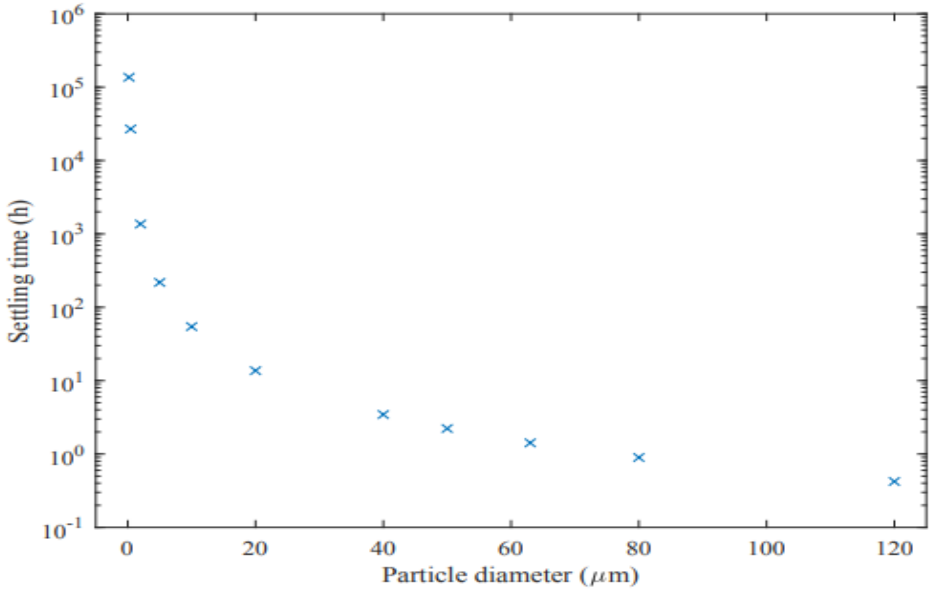

Figure 2.2: Calculated time of flocculated particles in receiving waters to settle 10m in receiving waters using equation 2.1.

The strong association of toxic contaminants to sediment deposited solids suggests the importance of assessment and monitoring of sediment deposition processes, which can be further evaluated by sediment practitioners for proposing effective remedial approaches. Finally, anthropogenic activities such as dredging and disposal of historically contaminated estuarine sediments may also result in major sediment disturbances (Eggleton & Thomas, 2004). Resuspension events caused by natural (erosion into a contaminated layer) or human-driven (propeller wash) activities can dramatically change the sediment redox environment, influencing redox-sensitive contaminants, or lead to direct release of contaminants due to partitioning into the water column (Hong *et al.*, 2011; Reible, 2014).

2.3 Heavy metal contamination

Heavy metals, like lead (Pb), arsenic (As), zinc (Zn), cadmium (Cd), copper (Cu), mercury (Hg), and nickel (Ni) are non-degradable and toxic; they can pose risks and hazards to humans and the ecosystem (Bi *et al.*, 2017). Heavy metals are naturally occurring elements found throughout the earth's crust and considered as trace elements because of their presence in trace concentrations (ppb range to less than 10 ppm) in various environmental matrices (Kabata-Pendias & Pendias, 2001). Most environmental metal pollution and human exposure are coming from anthropogenic activities, such as mining operations, industrial production, traffic activities, and domestic and agricultural use of metals and metal-containing compounds (Goyer & Clarkson, 1996; He *et al.*, 2005; Herawati *et al.*, 2000; Tchounwou *et al.*, 2012). Environmental contamination can also occur through metal corrosion, atmospheric deposition, soil erosion of metal ions and leaching, sediment

resuspension, as well as metal evaporation from water resources to soil and groundwater (Kabata-Pendias & Pendias, 2001).

2.3.1 Heavy metals in sediment

Sediment contamination is associated with legacy metal and metalloid contaminants that are released to the streams and lakes or onto soil that wash into surface waters and settle on the sediment bottom (Reible, 2014). The mobilization of surface metals through urban storm events may result in significant discharges into downstream areas (Lee *et al.*, 2002; Soller *et al.*, 2005). Previous studies have identified that sediments in urban water basins can accumulate metal contamination from traffic, such as exhaust, oil spills, tires and vehicles, and from residential activities, such as building paint, renovation, and demolition (Andersson *et al.*, 2004; Jartun *et al.*, 2003; Ottesen & Langedal, 2001).

Trace metals and metalloids have several bounding routes in sediments depending on the various physicochemical phases of sediment. This selective partitioning of particulate metals into sediment has been used in sediment extraction techniques (Tessier *et al.*, 1979). The metals can be bound in carbonates, sulphides, iron and/or manganese oxyhydroxides (e.g., cement between particles, coatings on particles) and in organic matter in either living or detrital form. Moreover, metals can be adsorbed at particle surfaces (e.g., clays, humic acids, metal oxyhydroxides), or can be matrix-bound (e.g., bound in lattice positions in aluminosilicates, in resistant oxides or sulphides) (Tessier & Campbell, 1987).

2.3.2 Heavy metals in water environment

In marine and freshwater environment, metal partitioning and distribution of metals in the suspended particulate matter are mostly influenced by physicochemical interactions between the dissolved and particulate components. These interactions are driven by sorption kinetics (Hering & Morel, 1990; Jannasch *et al.*, 1988), adsorption-desorption phenomenon (Di Toro & Horzempa, 1982; O'Connor & Connolly, 1980), surface chemistry variations (Hamilton-Taylor *et al.*, 1993), particle-particle interactions (Di Toro *et al.*, 1986), and the role of partitioning with colloids in the filtrate fraction (Benoit *et al.*, 1994; Benoit & Rozan, 1999; Morel, 1987). Finally, metals can be also present in solutions as free ions and inorganic complexes.

Water-quality parameters (e.g. pH, water hardness) may affect metal speciation and partitioning in the water environment. For example, water hardness ions may reduce zinc uptake through chemical mechanisms (e.g. inhibition of metal absorption) or biological mechanisms (reduction in membrane permeability) (Barron & Albeke, 2000). Moreover, the presence of chlorides in the water environment can cause the desorption of metals from particulate surfaces into the dissolved phase, where chloride complexes are formed and the metals become more bioavailable to aquatic organisms (Begeal, 2008).

2.4 Stormwater and particle size fractionation characterization

Stormwater occurs in an inconsistent pattern over a diffuse area and originates from watersheds whose characteristics and pollutant loadings vary through time and space (Burton & Pitt, 2001). Continued inputs from off-site sources, including permitted discharges, transport from upstream areas, or from stormwater metal discharges can result

in a significant deposition to near zone sediments that can slow or reverse sediment recovery and limit the effectiveness of remediating sediments. As stormwater management regulations in the United States and Europe mature, questions are raised concerning the evaluation of how metal releases from stormwater can be related to the recontamination of the sediment bed (Reible, 2014). Heavy metals in roadway runoff can affect receiving waters by increasing toxicity in the water column and sediments by bioaccumulation in living organisms entering the food chain (Greenstein *et al.*, 2004; Marsalek *et al.*, 1999).

Previous studies have identified the importance of size fractionation and measurement of all the forms, particulate and dissolved fractions, of heavy metals in runoff and discharge for better understanding of the fate, effects and treatability of stormwater (Burton & Pitt, 2001; Maniquiz-Redillas & Kim, 2014; Morquecho & Pitt, 2005; Pitt *et al.*, 1995). Best management practices for stormwater management are designed to treat only the particulate fractions (Maniquiz-Redillas & Kim, 2014; Minton, 2011). In order to improve the designing of stormwater treatment technologies, it is important to understand the metal associations with different sized particles. Knowing the distribution of pollutants associated with different sized storm particles allows accurate determinations of their sources, transport, and removal control. The particle size distribution can then be incorporated in receiving water models to calculate the fate and effect of the discharged contaminants (Pitt *et al.*, 1995; Pitt & Voorhees, 1995).

The contaminant concentrations associated with the suspended solids in different particle sizes, also known as particulate strength, can be used successfully for source identification of the associated contaminants based on their similar values to particulates found within

the watershed ("fingerprinting") (Pitt *et al.*, 2005). Particulate strengths are determined by calculating the pollutant concentration associated with the solids in stormwater (mg/kg) using the following equation:

$$\frac{(total\ water\ conc. - <0.45\mu m\ filtered\ conc.)}{solids\ conc.} = \frac{\mu g/L}{mg/L} \quad (2.3)$$

Equation 2.3 describes the concentration associated with solids in the runoff. These values are very useful when identifying erosion and other sources of the particulate-bound pollutants in the runoff, in contrast to the water concentrations (µg/L) that are affected by site hydrology and subsequent dilution (Burton & Pitt, 2001).

The evaluation of the metals' association to filterable (<0.45 µm) and non-filterable (particulate, >0.45 µm) fractions is of high importance when defining the optimum stormwater treatment technologies. Contaminants found in particulate forms (suspended solids) are controlled by stormwater practices like sedimentation and filtration processes. However, the constituents that are mostly associated with filterable fractions can potentially affect the groundwater and are difficult to mitigate. The particle association of storm-discharged contaminants has been examined several times in the literature. A large fraction of metal load in runoff from the roadway found to be associated with suspended solids (Florea & Büsselberg, 2006; Hatje *et al.*, 2003; Pitt *et al.*, 1995). Several researchers identified that metals, like Pb, Zn, Cu, and Cd, in runoff and catch basins partitioned mostly with solids (Glenn *et al.*, 2001; Karlsson & Viklander, 2008; Maestre, 2005). A previous study, that analyzed metal contaminants from 550 stormwater samples, indicated that most of Cu and Pb were associated with particles, while most of Zn was in the operationally

dissolved fraction (<0.45μm), as presented in Table 2.1 (Pitt *et al.*, 1998). Other study associated the stormwater metal concentrations with particle sizes less than 10μm diameter (Andral *et al.*, 1999).

Table 2.1: Average particulate metal fractions from 550 nationwide samples (Pitt et al., 1998).

Constituents	Total concentration	Filtered concentration (< 0.45 μm)	Filtered fraction (<0.45 μm)	Particulate, non-filtered (>0.45 μm)
Turbidity (NTU)	13	1.2	8%	91%
Copper (μg/L)	29	9.5	33%	67%
Lead (μg/L)	14	3	21%	79%
Zinc (μg/L)	230	160	70%	30%

2.5 Biota accumulation and metal availability in sediments

2.5.1 Assessing bioaccumulation in sediments

Bioaccumulation of metals and metalloids can be a representative indicator of chemical exposures of the biota in contaminated ecosystems (Borgmann, 2000; Goretti *et al.*, 2016; Phillips & Rainbow, 1994; Simpson & Batley, 2007). Bioaccumulation, which is the net accumulation of contaminants from the sediment into the tissues of the organisms, is included in sediment quality evaluations because it provides a direct measurement of the sediment-dwelling organisms' exposure (ASTM, 2006; Reible, 2014). Diagnostics of presence or absence of exposure and tissue concentrations of a given metal can be helpful for an organism's exposure evaluation (McCarty *et al.*, 2011).

Bioaccumulation of sediment-associated metals can be complex due to multiple influencing factors, such as multiple routes of exposure and geochemical effects on metal bioavailability (Luoma & Rainbow, 2005). Unlike organic contaminants, there is no dominant factor that governs the bioaccumulation of metals (McCarty *et al.*, 2011).

Bioaccumulation is depending on the exposed species because of the diversity of feeding ecology and living habits of benthic communities (Gewurtz *et al.*, 2000; Lake *et al.*, 1990; Watling, 1991). Exposure pathways from sediment-associated contaminants to biota include a) exposure to sediment pore water (interstitial water), b) ingestion of sediment particles and dissolved organic matter, c) direct contact of sediment with body surfaces, and d) exposure to the boundary layer of overlying water to sediment (Knezovich *et al.*, 1987). Particularly, the particle ingestion via filtration of the water column or direct consumption may be a significant path of exposure and preferable to many organisms (Landrum & Faust, 1991). When assessing metal bioaccumulation is recommended to take into consideration all the possible exposure routes, overlying water, porewater, and sediment (Boese *et al.*, 1990; Luoma *et al.*, 1992; Simpson & Batley, 2007; Winsor *et al.*, 1990).

Factors that influence contaminant bioaccumulation can be the ventilation of porewater by burrowing organisms (e.g., amphipods), or the tube and burrow formation that can affect the spatial distribution of contaminants (Lee, 1991) Also, the heterogeneous nature of sediment with spatial variability in the composition can ultimately influence the contaminant bioaccumulation in benthic organisms (Watling, 1991). Other factors influencing metal accumulation on sediments can be metal speciation, transformation (e.g., methylation to form hydrophobic alkyl metals), interactions of different metals, sediment chemistry (salinity, redox, pH), and binding to dissolved organic matter (DOM) (Farrington, 1991; Lee, 1991).

Sediment bioassays are useful approaches to assess bioaccumulation and exposure of marine organisms within sediment quality programs (ASTM, 2006; Chapman, 1986; Giesy *et al.*, 1988; Vethaak *et al.*, 2017). Field related influences on exposures have been recently evaluated using *ex situ* and *in situ* bioassays (Janssen *et al.*, 2011; Martins *et al.*, 2015). Bioaccumulation tests performed in the laboratory, *ex situ*, generate comparable results to the exposure tests on the field site, *in situ*, if the exposed organisms are similar to the biota inhabiting the field sediments. The species of *Macoma nasuta* are recommended and have been used in bioaccumulation exposure testing of marine and estuarine sediments (Kirtay *et al.*, 2018; Werner *et al.*, 2004). *Macoma nasuta* belongs to bivalve species that can be deposited-feed and/or suspended-feed and not only are associated with metal particles through ingestion but also through porewater, burrow, and overlying water (Hylleberg & Gallucci, 1975; Winsor *et al.*, 1990).

2.5.2 Assessing bioavailability using freely available porewater concentrations

Aquatic sediments are created from particle deposition and colloids and can act both as sink and source of contaminants. Long-term input deposition leads to sediment concentrations that exceed the water concentrations by several orders of magnitude because of the partitioning of chemicals onto sediment-binding sites. Physical and chemical interactions between contaminants and sediments can determine the bioavailable contaminants in aquatic sediments (Barron, 2003). Bioavailability of sediment-associated contaminants can be quantified by estimations of the freely dissolved concentrations in sediment porewater (Ghosh *et al.*, 2014; Lampert *et al.*, 2015; Reible, 2014) and can reflect the true exposure of organisms in sediments (Lydy *et al.*, 2014).

For the assessment of contaminated sediment effects to ecosystem, total bulk sediment concentration can present an initial screening; however, they are not enough because the bioavailable fraction is related to sulfides concentrations, iron oxides and organic contents that are not reflected in the sediment bulk concentrations (Chapman *et al.*, 1999; Di Toro *et al.*, 1990). The calculation of the fraction of the total metal concentration that is biologically available presents a challenge since metal bioavailability rapidly changes with speciation and complexation (Burton, 2010; Hamelink *et al.*, 1994; Maruya *et al.*, 2012). Previous research has shown that particular metal-binding phases, such as acid-volatile sulfide (AVS), particulate organic carbon, iron, and manganese oxyhydroxides are driving factors to metal speciation in sediments, e.g. Cu^{2+} binds with sulfide and organic matter, and Cd^{2+} partitions with Fe/Mn oxides, organic matter, and exchangeable cations/carbonates. In oxic sediments, Fe and Mn oxides/hydroxides along with organic matter are important binding sites for metals, while in anoxic sediments the formation of metal sulfides present major control (Eggleton & Thomas, 2004).

Other factors that affect metal bioavailability can be physical factors, such as temperature, adsorption, and sequestration (Hamelink *et al.*, 1994), as well as biological factors, such as species characteristics, trophic interactions, and physiological adaptation (Verkleji, 1993). Geochemical properties of colloids and the chemical properties of metals are critical in affecting the bioavailability of colloid-bound metals to marine bivalves. A greater emphasis is also beginning to appear on the role of colloids in the fate and effects of metals. Mechanisms of colloidal-bound metals associated with the truly dissolved phase need a further examination of how they affect metal bioavailability (Pan & Wang, 2002).

Labile metal concentrations represent the chemically available forms of metals in porewater media that can potentially interact with organisms in aquatic sediments. Diffusive gradient in thin-film devices (DGTs) can successfully determine metals in sediment porewater (Harper *et al.*, 1999; Wu *et al.*, 2011; Xu *et al.*, 2017; Zhang *et al.*, 1995) as well as remobilization fluxes of metals in sediments (Harper *et al.*, 1998). The DGT consists of a filter membrane that is exposed to the environment for filtering the porewater concentrations, a diffusive hydrogel where dissolved metals diffuse, and finally a resin gel where the metals are accumulated. Assuming steady-state diffusion, the device provides the porewater concentration, C_{pw}, based the followed equation:

$$C_{pw} = \frac{m_{resin} * \Delta z_{gel}}{D_{gel} * \Delta t} \quad (2.4)$$

Where Δz_{gel} is the hydrogel layer thickness, D_{gel} the diffusivity, m_{resin} the mass accumulated in the resin, and Δt the exposure time (Zhang *et al.*, 1995). DGTs is a robust passive sampling technique, that has been widely used to a variety of sediment and soils, for measuring successfully porewater concentrations by applying different types of resins and diffusive layers depending on the targeted contaminants (Clarisse & Hintelmann, 2006; Ernstberger *et al.*, 2005; Li *et al.*, 2009; Nowack *et al.*, 2004; Zhang & Davison, 1995).

2.6 Improving certainty using statistics

Sediments represent complex ecosystems with a variety of factors affecting their contamination (Reible, 2014); therefore it is difficult to distinguish which factors contribute to the recontamination and biological effects in sediments majorly and to what extent. Particularly in field studies, there is a high need of developing conclusions from

multiple lines of evidence, such as before/after treatment, spatial-location impacts, multi-component measurements and datasets. "Weight of evidence" (WoE) investigations that provide definitive conclusions strengthen the observed relationships/outcomes, quantify or reduce uncertainty, and even select what information are necessary for arriving at definitive conclusions (Burton *et al.*, 2002b; Chapman, 2007; Linkov *et al.*, 2009). WoE assessment presents a method of comparison of the examined lines of evidence, such as sediment chemistry, bioavailability assessment, bioassays (McPherson *et al.*, 2008; Piva *et al.*, 2011), that promotes the best judgment and improves the reporting in sediment quality assessments (Batley *et al.*, 2002; Burton *et al.*, 2002b).

There is no standardized approach on how to conduct the WoE assessment (Reible, 2014) and WoE approaches vary broadly from qualitative to quantitative. However, there have been studies that propose quantification approaches of the WoE assessment for establishing sediment quality (Burton *et al.*, 2002a; Chapman *et al.*, 1997; Chapman & McDonald, 2005). These approaches include statistical analysis such as regression methods, paired reference tests e.g. before/after control impact, ANOVA methods, multiple reference tests e.g. ANOVA and multivariate methods, and combination use of them e.g. regression, ANOVA and multivariate methods (Burton *et al.*, 2002a). WoE assessment can be most effective when incorporated into the initial design stage of field efforts as well as into the final data interpretation/analysis stage to promote on-going reassessment and help decision-making processes (Burton *et al.*, 2002a). WoE provides a promising tool to support and evaluate complex processes included in environmental contamination assessments.

2.7 Site description

The studied location is a mixed-used watershed (including urban, highways, and industrial areas) that encompasses 8,094,000m^2 in the Pueblo San Diego hydrologic unit. It also includes portions of the cities of San Diego and National City and a small portion of the tidelands immediately adjacent to San Diego Bay under the jurisdiction of the U.S. Navy. The majority of the tributary area is categorized as single-family detached residential (42%), followed next by upstream, military uses (20%) downstream of associated with the U.S. Navy Base, and the roads (11%). More than 96% of the watershed is developed (i.e., not characterized as recreation or open space parks). Paleta Creek itself is a channelized urban/industrial creek with the highest flow rates associated with flashy winter storm events and low and highly variable dry weather flows for the rest of the year. Extended periods with no flows usually occur during the dry season and particularly during drought conditions (Reible *et al.*, 2018). The mouth of the Paleta Creek site is located on the eastern shoreline in the central portion of San Diego Bay and flows directly through Naval Base San Diego, CA (32°40'27.9192"N, 117°6'55.998"W) (Figure 2.3).

The State Water Board characterized the Paleta Creek as a high priority candidate toxic hot spot due to amphipod sediment toxicity findings and the presence of multiple degraded benthic communities in the Consolidated Toxic Hotspots Cleanup Plan (SWRCB, 1999). Toxicity and chemistry of wet weather runoff have been routinely measured in outfalls and receiving water in NBSD for compliance with National Pollutant Discharge Elimination System (NPDES) stormwater discharge permits (Reible *et al.*, 2018). Pollutants include bacteria, pesticides, heavy metals and organic contaminants. The areas of concern involve

marinas, shipyards, and outlet discharges of creeks. Recent studies have indicated pyrethroids pesticides to attribute to the seasonal toxicity of sediments in Southern California (Hayman *et al.*, 2020; Lao *et al.*, 2012).

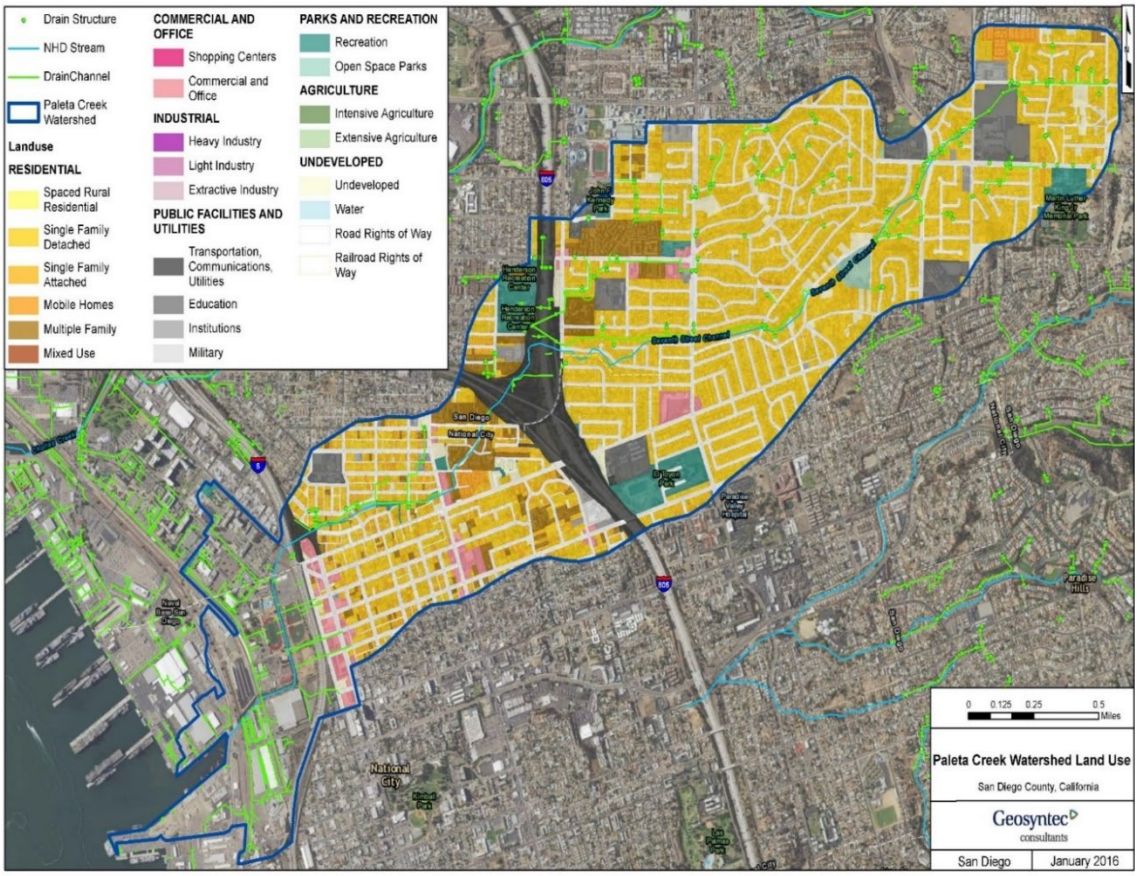

Figure 2.3: Studied watershed at Paleta Creek in San Diego, CA (Reible et al., 2018).

2.8 References

Adams, W. J., Green, A. S., Ahlf, W., Brown, S. S., Burton, G. A., Jr., Chadwick, B., Crane, M., Gouget, R., Ho, K. T., & Hogstand, C. (2005). Using sediment assessment tools and a weight of evidence approach. *Use of Sediment Quality Guidelines and Related Tools for the Assessment of Contaminated Sediments. Society of Environmental Toxicology and Chemistry, Pensacola, FL, USA*, 163-225.

Andersson, M., Ottesen, R. T., & Volden, T. (2004). Building materials as a source of PCB pollution in Bergen, Norway. *Science of the total environment, 325*(1-3), 139-144.

Andral, M. C., Roger, S., Montrejaud-Vignoles, M., & Herremans, L. (1999). Particle size distribution and hydrodynamic characteristics of solid matter carried by runoff from motorways. *Water Environment Research, 71*(4), 398-407.

ASTM. (2006). *Standard Guide for Determination of the Bioaccumulation of Sediment-Associated Contaminants by Benthic Invertebrates.*

Barron, M. G. (2003). Bioaccumulation and bioconcentration in aquatic organisms. *Handbook of Ecotoxicology. Lewis Publishers, Boca Raton, Florida*, 877-892.

Barron, M. G., & Albeke, S. (2000). Calcium control of zinc uptake in rainbow trout. *Aquatic Toxicology, 50*(3), 257-264.

Bates, M. E., Massey, O. C., & Wood, M. D. (2018). *Weight-of-evidence concepts: introduction and application to sediment management*. Retrieved from

Batley, G. E., Burton, G. A., Jr., Chapman, P. M., & Forbes, V. E. (2002). Uncertainties in Sediment Quality Weight-of-Evidence (WOE) Assessments. *Human and Ecological Risk Assessment: An International Journal, 8*(7), 1517-1547. doi:10.1080/20028091057466

Begeal, C. (2008). The Effect of Chloride Ion on Heavy Metal Partitioning and Transport in an Urban Watershed: Patroon Creek, Albany, NY.

Benedetti, M., Ciaprini, F., Piva, F., Onorati, F., Fattorini, D., Notti, A., Ausili, A., & Regoli, F. (2012). A multidisciplinary weight of evidence approach for classifying polluted sediments: Integrating sediment chemistry, bioavailability, biomarkers responses and bioassays. *Environment international, 38*(1), 17-28. doi:https://doi.org/10.1016/j.envint.2011.08.003

Benoit, G., Oktay-Marshall, S. D., Cantu Ii, A., Hood, E. M., Coleman, C. H., Corapcioglu, M. O., & Santschi, P. H. (1994). Partitioning of Cu, Pb, Ag, Zn, Fe, Al, and Mn between filter-retained particles, colloids, and solution in six Texas estuaries. *Marine Chemistry, 45*(4), 307-336.

Benoit, G., & Rozan, T. F. (1999). The influence of size distribution on the particle concentration effect and trace metal partitioning in rivers. *Geochimica et Cosmochimica Acta, 63*(1), 113-127. doi:https://doi.org/10.1016/S0016-7037(98)00276-2

Bi, S., Yang, Y., Xu, C., Zhang, Y., Zhang, X., & Zhang, X. (2017). Distribution of heavy metals and environmental assessment of surface sediment of typical estuaries in eastern China. *Marine pollution bulletin, 121*(1-2), 357-366.

Bianchini, A., Cento, F., Guzzini, A., Pellegrini, M., & Saccani, C. (2019). Sediment management in coastal infrastructures: Techno-economic and environmental impact assessment of alternative technologies to dredging. *Journal of environmental management, 248*, 109332.

Boese, B. L., Lee, I. H., Specht, D. T., Randall, R. C., & Winsor, M. H. (1990). Comparison of aqueous and solid-phase uptake for hexachlorobenzene in the tellinid clam Macoma nasuta (conrad): A mass balance approach. *Environmental Toxicology and Chemistry: An International Journal, 9*(2), 221-231.

Borgmann, U. (2000). Methods for assessing the toxicological significance of metals in aquatic ecosystems: bio-accumulation-toxicity relationships, water concentrations and sediment spiking approaches. *Aquatic Ecosystem Health & Management, 3*(3), 277-289.

Brusven, M. A., & Prather, K. V. (2019). Influence of stream sediments on distribution of macrobenthos. *Journal of the Entomological Society of British Columbia, 71*, 25-32.

Burt, T. N., & Parker, W. R. (1984). *Settlement and density in beds of natural mud during successive sedimentation*: Hydraulics Research Limited.

Burton, G. A., Jr. (1991). Assessing the toxicity of freshwater sediments. *Environmental Toxicology and Chemistry: An International Journal, 10*(12), 1585-1627.

Burton, G. A., Jr. (2010). Metal bioavailability and toxicity in sediments. *Critical Reviews in Environmental Science and Technology, 40*(9-10), 852-907.

Burton, G. A., Jr., Batley, G. E., Chapman, P. M., Forbes, V. E., Smith, E. P., Reynoldson, T., Schlekat, C. E., Besten, P. J., Bailer, A. J., & Green, A. S. (2002a). A weight-of-evidence framework for assessing sediment (or other) contamination: Improving certainty in the decision-making process. *Human and ecological risk assessment, 8*(7), 1675-1696.

Burton, G. A., Jr., Chapman, P., & Smith, E. (2002b). Weight-of-evidence approaches for assessing ecosystem impairment. *Human and ecological risk assessment, 8*(7), 1657-1673.

Burton, G. A., Jr., Nguyen, L. T. H., Janssen, C., Baudo, R., McWilliam, R., Bossuyt, B., Beltrami, M., & Green, A. (2005). Field validation of sediment zinc toxicity. *Environmental Toxicology and Chemistry: An International Journal, 24*(3), 541-553.

Burton, G. A., Jr., & Pitt, R. (2001). *Stormwater effects handbook: A toolbox for watershed managers, scientists, and engineers*: CRC Press.

Camponelli, K. M., Lev, S. M., Snodgrass, J. W., Landa, E. R., & Casey, R. E. (2010). Chemical fractionation of Cu and Zn in stormwater, roadway dust and stormwater pond sediments. *Environmental pollution, 158*(6), 2143-2149. doi:https://doi.org/10.1016/j.envpol.2010.02.024

Chapman, P. M. (1986). Sediment quality criteria from the sediment quality triad: an example. *Environmental Toxicology and Chemistry: An International Journal, 5*(11), 957-964.

Chapman, P. M. (2007). Determining when contamination is pollution — Weight of evidence determinations for sediments and effluents. *Environment international, 33*(4), 492-501. doi:https://doi.org/10.1016/j.envint.2006.09.001

Chapman, P. M., Anderson, B., Carr, S., Engle, V., Green, R., Hameedi, J., Harmon, M., Haverland, P., Hyland, J., Ingersoll, C., Long, E., Rodgers, J., Salazar, M., Sibley, P. K., Smith, P. J., Swartz, R. C., Thompson, B., & Windom, H. (1997). General guidelines for using the sediment quality triad. *Marine pollution bulletin, 34*(6), 368-372. doi:https://doi.org/10.1016/S0025-326X(96)00138-5

Chapman, P. M., & McDonald, B. G. (2005). Using the Sediment Quality Triad (Sqt) in ecological risk assessment. In C. Blaise & J.-F. Férard (Eds.), *Small-scale Freshwater Toxicity Investigations: Hazard Assessment Schemes* (pp. 305-329). Dordrecht: Springer Netherlands.

Chapman, P. M., Wang, F., Adams, W. J., & Green, A. (1999). Appropriate applications of sediment quality values for metals and metalloids. In: ACS Publications.

Cheng, N. S. (1997). Simplified settling velocity formula for sediment particle. *Journal of hydraulic engineering, 123*(2), 149-152.

Christensen, B. A. (1965). Discussion of 'Erosion and Deposition of Cohesive Soils'. *J. Hydraul. Div. Am. Soc. Civ. Eng, 9*(5), 301-308.

Clarisse, O., & Hintelmann, H. (2006). Measurements of dissolved methylmercury in natural waters using diffusive gradients in thin film (DGT). *Journal of Environmental Monitoring, 8*(12), 1242-1247.

Di Toro, D., Mahony J., Hansen D., Scott K., Hicks M., Mayr S., & Redmond M. (1990). Toxicity of cadmium in sediments: the role of acid volatile sulfide. *Environmental Toxicology and Chemistry: An International Journal, 9*(12), 1487-1502.

Di Toro, D. M., & Horzempa, L. M. (1982). Reversible and resistant components of PCB adsorption-desorption: Isotherms. *Environmental Science & Technology, 16*(9), 594-602.

Di Toro, D. M., Mahony, J. D., Kirchgraber, P. R., O'Byrne, A. L., Pasquale, L. R., & Piccirilli, D. C. (1986). Effects of nonreversibility, particle concentration, and ionic strength on heavy-metal sorption. *Environmental Science & Technology, 20*(1), 55-61.

Droppo, I. G., Krishnappan, B. G., & Lawrence, J. R. (2016). Microbial interactions with naturally occurring hydrophobic sediments: influence on sediment and associated contaminant mobility. *Water research, 92*, 121-130.

Durán, I., Sánchez-Marín, P., & Beiras, R. (2012). Dependence of Cu, Pb and Zn remobilization on physicochemical properties of marine sediments. *Marine environmental research, 77*, 43-49.

Eggleton, J., & Thomas, K. (2004). A review of factors affecting the release and bioavailability of contaminants during sediment disturbance events. *Environment international, 30*(7), 973-980.

Ernstberger, H., Zhang, H., Tye, A., Young, S., & Davison, W. (2005). Desorption kinetics of Cd, Zn, and Ni measured in soils by DGT. *Environmental Science & Technology, 39*(6), 1591-1597.

Farrington, J. W. (1991). Biogeochemical processes governing exposure and uptake of organic pollutant compounds in aquatic organisms. *Environmental health perspectives, 90*, 75-84.

Fassman, E. (2012). Stormwater BMP treatment performance variability for sediment and heavy metals. *Separation and Purification Technology, 84*, 95-103. doi:https://doi.org/10.1016/j.seppur.2011.06.033

Florea, A.-M., & Büsselberg, D. (2006). Occurrence, use and potential toxic effects of metals and metal compounds. *Biometals, 19*(4), 419-427.

Garcia, M. (2008). *Sedimentation engineering: processes, measurements, modeling, and practice*.

Gewurtz, S. B., Lazar, R., & Douglas Haffner, G. (2000). Comparison of polycyclic aromatic hydrocarbon and polychlorinated biphenyl dynamics in benthic invertebrates of Lake Erie, USA. *Environmental Toxicology and Chemistry: An International Journal, 19*(12), 2943-2950.

Ghosh, U., Kane Driscoll, S., Burgess, R. M., Jonker, M. T. O., Reible, D. D., Gobas, F., Choi, Y., Apitz, S. E., Maruya, K. A., & Gala, W. R. (2014). Passive sampling methods for contaminated sediments: practical guidance for selection, calibration, and implementation. *Integrated environmental assessment and management, 10*(2), 210-223.

Giesy, J. P., Graney, R. L., Newsted, J. L., Rosiuand, C. J., Benda, A., Kreis Jr, R. G., & Horvath, F. J. (1988). Comparison of three sediment bioassay methods using Detroit River sediments. *Environmental Toxicology and Chemistry: An International Journal, 7*(6), 483-498.

Glenn, D. W., Tribouillard, T., & Sansalone, J. J. (2001). Temporal Deposition of Anthropogenic Pollutants in Urban Snow as Generated by Traffic. WEFTEC 2001 Conf. *Proc. CD-ROM*.

Goretti, E., Pallottini, M., Ricciarini, M., Selvaggi, R., & Cappelletti, D. (2016). Heavy metals bioaccumulation in selected tissues of red swamp crayfish: an easy tool for monitoring environmental contamination levels. *Science of the total environment, 559*, 339-346.

Goyer, R. A., & Clarkson, T. W. (1996). Toxic effects of metals. *Casarett and Doull's toxicology: the basic science of poisons, 5*, 696-698.

Greenberg, M. S., Burton, G. A., Jr., & Duncan, P. B. (2000). Considering groundwater-surface water interactions in sediment toxicity assessment. *SETAC Globe, 1*(2), 42-44.

Greenberg, M. S., Burton, G. A., Jr., & Rowland, C. D. (2002). Optimizing interpretation of in situ effects of riverine pollutants: Impact of upwelling and downwelling. *Environmental Toxicology and Chemistry: An International Journal, 21*(2), 289-297.

Greenstein, D., Tiefenthaler, L., & Bay, S. (2004). Toxicity of parking lot runoff after application of simulated rainfall. *Archives of Environmental Contamination and Toxicology, 47*(2), 199-206.

Hamelink, J., Landrum, P. F., Bergman, H., & Benson, W. H. (1994). *Bioavailability: physical, chemical, and biological interactions*: CRC press.

Hamilton-Taylor, J., Kelly, M., Titley, J. G., & Turner, D. R. (1993). Particle-solution behaviour of plutonium in an estuarine environment, Esk Estuary, UK. *Geochimica et Cosmochimica Acta, 57*(14), 3367-3381.

Harper, M. P., Davison, W., & Tych, W. (1999). Estimation of Pore Water Concentrations from DGT Profiles: A Modelling Approach. *Aquatic Geochemistry, 5*(4), 337-355. doi:10.1023/A:1009620412373

Harper, M. P., Davison, W., Zhang, H., & Tych, W. (1998). Kinetics of metal exchange between solids and solutions in sediments and soils interpreted from DGT measured fluxes. *Geochimica et Cosmochimica Acta, 62*(16), 2757-2770. doi:https://doi.org/10.1016/S0016-7037(98)00186-0

Hatch, A. C., & Burton, G. A., Jr. (1999). Sediment toxicity and stormwater runoff in a contaminated receiving system: consideration of different bioassays in the laboratory and field. *Chemosphere, 39*(6), 1001-1017.

Hatje, V., Apte, S. C., Hales, L. T., & Birch, G. F. (2003). Dissolved trace metal distributions in port jackson estuary (sydney harbour), Australia. *Marine pollution bulletin, 46*(6), 719-730.

Hayman, N. T., Rosen, G., Colvin, M. A., Chadwick, B. D., Rao, B., Athanasiou, D., Rakowska, M., Drygiannaki, I., Burton, G. A., Jr., & Reible, D. D. (2020). Seasonal Toxicity Observed with Amphipods (Eohaustorius estuarius) at Paleta Creek, San Diego Bay, USA. *Environmental toxicology and chemistry, 39*(1), 229-239.

He, Z. L., Yang, X. E., & Stoffella, P. J. (2005). Trace elements in agroecosystems and impacts on the environment. *Journal of Trace elements in Medicine and Biology, 19*(2-3), 125-140.

Herawati, N., Suzuki, S., Hayashi, K., Rivai, I. F., & Koyama, H. (2000). Cadmium, copper, and zinc levels in rice and soil of Japan, Indonesia, and China by soil type. *Bulletin of environmental contamination and toxicology, 64*(1), 33-39.

Hering, J. G., & Morel, F. M. M. (1990). Kinetics of trace metal complexation: ligand-exchange reactions. *Environmental Science & Technology, 24*(2), 242-252.

Hilliges, R., Endres, M., Tiffert, A., Brenner, E., & Marks, T. (2017). Characterization of road runoff with regard to seasonal variations, particle size distribution and the correlation of fine particles and pollutants. *Water Science and Technology, 75*(5), 1169-1176.

Hong, Y. S., Kinney, K. A., & Reible, D. D. (2011). Acid volatile sulfides oxidation and metals (Mn, Zn) release upon sediment resuspension: Laboratory experiment and model development. *Environmental toxicology and chemistry, 30*(3), 564-575.

House, M., Ellis, J., Herricks, E., Hvitved-Jacobsen, T., Seager, J., Lijklema, L., Aalderink, H., & Clifforde, I. (1993). Urban drainage–impacts on receiving water quality. *Water Science and Technology, 27*(12), 117-158.

Hylleberg, J., & Gallucci, V. (1975). Selectivity in feeding by the deposit-feeding bivalve Macoma nasuta. *Marine Biology, 32*(2), 167-178.

Jannasch, H. W., Honeyman, B. D., & Balistrieri, L. S. (1988). Kinetics of trace element uptake by marine particles. *Geochimica et Cosmochimica Acta, 52*(2), 567-577.

Janssen, E. M. L., Oen, A. M. P., Luoma, S. N., & Luthy, R. G. (2011). Assessment of field-related influences on polychlorinated biphenyl exposures and sorbent amendment using polychaete bioassays and passive sampler measurements. *Environmental toxicology and chemistry, 30*(1), 173-180.

Jartun, M., Ottesen, R. T., & Steinnes, E. (2003). *Urban soil pollution and the playfields of small children.* Paper presented at the Journal de Physique IV (Proceedings).

Kabata-Pendias, A., & Pendias, H. (2001). Trace elements in soils and plants, 3rd edn CRC Press. *Boca Raton, FL, USA*.

Karlsson, K., & Viklander, M. (2008). Trace metal composition in water and sediment from catch basins. *Journal of Environmental Engineering, 134*(10), 870-878.

Karlsson, K., Viklander, M., Scholes, L., & Revitt, M. (2010). Heavy metal concentrations and toxicity in water and sediment from stormwater ponds and sedimentation tanks. *Journal of Hazardous Materials, 178*(1), 612-618. doi:https://doi.org/10.1016/j.jhazmat.2010.01.129

Kirtay, V., Conder, J., Rosen, G., Magar, V., Grover, M., Arblaster, J., Fetters, K., & Chadwick, B. (2018). Performance of an in situ activated carbon treatment to reduce PCB availability in an active harbor. *Environmental toxicology and chemistry, 37*(6), 1767-1777.

Knezovich, J. P., Harrison, F. L., & Wilhelm, R. G. (1987). The bioavailability of sediment-sorbed organic chemicals: a review. *Water, Air, and Soil Pollution, 32*(1-2), 233-245.

Lake, J. L., Rubinstein, N. I., Lee, H., Lake, C. A., Heltshe, J., & Pavignano, S. (1990). Equilibrium partitioning and bioaccumulation of sediment-associated contaminants by infaunal organisms. *Environmental Toxicology and Chemistry: An International Journal, 9*(8), 1095-1106.

Lampert, D. J., Thomas, C., & Reible, D. D. (2015). Internal and external transport significance for predicting contaminant uptake rates in passive samplers. *Chemosphere, 119*, 910-916.

Landrum, P. F., & Faust, W. (1991). Effect of variation in sediment composition on the uptake rate coefficient for selected PCB and PAH congeners by the amphipod, Diporeia sp. In *Aquatic Toxicology and Risk Assessment: Fourteenth Volume*: ASTM International.

Lao, W., Tiefenthaler, L., Greenstein, D. J., Maruya, K. A., Bay, S. M., Ritter, K., & Schiff, K. (2012). Pyrethroids in southern California coastal sediments. *Environmental toxicology and chemistry, 31*(7), 1649-1656.

Lau, S. S. S., & Chu, L. M. (1999). Contaminant release from sediments in a coastal wetland. *Water research, 33*(4), 909-918.

Lee, H. (1991). A clam's eye view of the bioavailability of sedimentassociated pollutants. *Organic substances and sediments in water, 3*, 73-93.

Lee, J. H., & Bang, K. W. (2000). Characterization of urban stormwater runoff. *Water research, 34*(6), 1773-1780. doi:https://doi.org/10.1016/S0043-1354(99)00325-5

Lee, J. H., Bang, K. W., Ketchum, L. H., Choe, J. S., & Yu, M. J. (2002). First flush analysis of urban storm runoff. *Science of the total environment, 293*(1-3), 163-175.

Li, W., Wang, F., Zhang, W., & Evans, D. (2009). Measurement of stable and radioactive cesium in natural waters by the diffusive gradients in thin films technique with new selective binding phases. *Analytical chemistry, 81*(14), 5889-5895.

Li, Y., Lau, S.-L., Kayhanian, M., & Stenstrom Michael, K. (2005). Particle Size Distribution in Highway Runoff. *Journal of Environmental Engineering, 131*(9), 1267-1276. doi:10.1061/(ASCE)0733-9372(2005)131:9(1267)

Linkov, I., Loney, D., Cormier, S., Satterstrom, F. K., & Bridges, T. S. (2009). Weight-of-evidence evaluation in environmental assessment: review of qualitative and quantitative approaches. *Science of the total environment, 407*(19), 5199-5205.

Luoma, S. N., Johns, C., Fisher, N. S., Steinberg, N. A., Oremland, R. S., & Reinfelder, J. R. (1992). Determination of selenium bioavailability to a benthic bivalve from particulate and solute pathways. *Environ. Sci. Technol., 26*, 485.

Luoma, S. N., & Rainbow, P. S. (2005). Why is metal bioaccumulation so variable? Biodynamics as a unifying concept. *Environmental Science & Technology, 39*(7), 1921-1931.

Lydy, M. J., Landrum, P. F., Oen, A. M. P., Allinson, M., Smedes, F., Harwood, A. D., Li, H., Maruya, K. A., & Liu, J. (2014). Passive sampling methods for contaminated sediments: State of the science for organic contaminants. *Integrated environmental assessment and management, 10*(2), 167-178.

Maestre, M. A. A. (2005). Stormwater characteristics as described in the National Stormwater Quality Database.

Maniquiz-Redillas, M., & Kim, L.-H. (2014). Fractionation of heavy metals in runoff and discharge of a stormwater management system and its implications for treatment. *Journal of Environmental Sciences, 26*(6), 1214-1222.

Marsalek, J., Rochfort, Q., Brownlee, B., Mayer, T., & Servos, M. (1999). An exploratory study of urban runoff toxicity. *Water Science and Technology, 39*(12), 33-39.

Martins, C., de Matos, A. P. A., Costa, M. H., & Costa, P. M. (2015). Alterations in juvenile flatfish gill epithelia induced by sediment-bound toxicants: A comparative in situ and ex situ study. *Marine environmental research, 112*, 122-130.

Maruya, K. A., Landrum, P. F., Burgess, R. M., & Shine, J. P. (2012). Incorporating contaminant bioavailability into sediment quality assessment frameworks. *Integrated environmental assessment and management, 8*(4), 659-673.

McCarty, L. S., Landrum, P. F., Luoma, S., Meador, J., Merten, A., Shephard, B., & Van Wezel, A. (2011). Advancing environmental toxicology through chemical dosimetry: external exposures versus tissue residues. *Integrated environmental assessment and management, 7*(1), 7-27.

McPherson, C., Chapman, P. M., deBruyn, A. M. H., & Cooper, L. (2008). The importance of benthos in weight of evidence sediment assessments — A case study. *Science of the total environment, 394*(2), 252-264. doi:https://doi.org/10.1016/j.scitotenv.2008.01.027

Minton, G. R. (2011). *Stormwater treatment: biological, chemical & engineering principles*: Sheridan Books.

Morel, F. M. M. (1987). The role of colloids in the partitioning of solutes in natural waters. *Aquatic surface chemistry*, 405-422.

Morquecho, R., & Pitt, R. (2005). Pollutant associations with particulates in stormwater. *Proceedings of the Water Environment Federation, 2005*(11), 4973-4999.

Mulligan, C. N., Yong, R. N., & Gibbs, B. F. (2001). An evaluation of technologies for the heavy metal remediation of dredged sediments. *Journal of Hazardous Materials, 85*(1-2), 145-163.

Nowack, B., Koehler, S., & Schulin, R. (2004). Use of diffusive gradients in thin films (DGT) in undisturbed field soils. *Environmental Science & Technology, 38*(4), 1133-1138.

NRC. (2009). *Urban stormwater management in the United States*: National Academies Press.

O'Connor, D. J., & Connolly, J. P. (1980). The effect of concentration of adsorbing solids on the partition coefficient. *Water research, 14*(10), 1517-1523. doi:https://doi.org/10.1016/0043-1354(80)90018-4

Ottesen, R. T., & Langedal, M. (2001). Urban geochemistry in Trondheim, Norway. *Norges Geologiske Undersokelse, 438*, 63-69.

Pan, J.-F., & Wang, W.-X. (2002). Comparison of the bioavailability of Cr and Fe bound with natural colloids of different origins and sizes to two marine bivalves. *Marine Biology, 141*(5), 915-924.

Phillips, D. J. H., & Rainbow, P. S. (1994). Biomonitoring of trace aquatic contaminants. *Environmental Management Series, Chapman & Hall, London*.

Pitt, R., Bannerman, R., Clark, S., & Williamson, D. (2005). Sources of pollutants in urban areas (Part 1)-Older Monitoring Projects. *Journal of Water Management Modeling*.

Pitt, R., Clark, S., Lantrip, J., & Day, J. (1998). Telecommunication manhole water and sediment study. *Special report SR-3841, 2*.

Pitt, R., Field, R., Lalor, M., & Brown, M. (1995). Urban stormwater toxic pollutants: assessment, sources, and treatability. *Water Environment Research, 67*(3), 260-275.

Pitt, R., & Voorhees, J. (1995). *Source loading and management model (SLAMM).* Paper presented at the Seminar Publication: National Conference on Urban Runoff Management: Enhancing Urban Watershed Management at the Local, County, and State Levels.

Piva, F., Ciaprini, F., Onorati, F., Benedetti, M., Fattorini, D., Ausili, A., & Regoli, F. (2011). Assessing sediment hazard through a weight of evidence approach with bioindicator organisms: A practical model to elaborate data from sediment chemistry, bioavailability, biomarkers and ecotoxicological bioassays. *Chemosphere, 83*(4), 475-485. doi:https://doi.org/10.1016/j.chemosphere.2010.12.064

Power, E. A., & Chapman, P. M. (2018). Assessing sediment quality. In *Sediment toxicity assessment* (pp. 1-18): CRC Press.

Reible, D. D. (2014). *Processes, assessment and remediation of contaminated sediments*: Springer.

Reible, D. D., Popov, V., Valsaraj, K. T., Thibodeaux, L. J., Lin, F., Dikshit, M., Todaro, M. A., & Fleeger, J. W. (1996). Contaminant fluxes from sediment due to tubificid oligochaete bioturbation. *Water research, 30*(3), 704-714.

Reible, D. D., Rao, B., Rakowska, M., Athanasiou, D., Drygiannaki, I., Bejar, M., Chadwick, B., Colvin, M., Rosen, G., Burton, G. A., Jr., Stecker, E., Steets, B., Otto, M., & Pitt, R. (2018). Assessment and Management of Stormwater Impacts on Sediment Recontamination. ER-2428, Final Report. *Strategic Environmental Research and Development Program, Alexandria, VA, USA*.

River, M., & Richardson, C. J. (2018). Particle size distribution predicts particulate phosphorus removal. *Ambio, 47*(1), 124-133. doi:10.1007/s13280-017-0981-z

Ryu, J., Khim, J., Kang, S., Kang, D., Lee, C., & Koh, C. (2011). The impact of heavy metal pollution gradients in sediments on benthic macrofauna at population and community levels. *Environmental pollution, 159*(10), 2622-2629.

Sawyer, A. H., Cardenas, B. M., Bomar, A., & Mackey, M. (2009). Impact of dam operations on hyporheic exchange in the riparian zone of a regulated river. *Hydrological Processes: An International Journal, 23*(15), 2129-2137.

Schiff, K., & Bay, S. (2003). Impacts of stormwater discharges on the nearshore benthic environment of Santa Monica Bay. *Marine environmental research, 56*(1-2), 225-243.

Selbig, W. R., Fienen, M. N., Horwatich, J. A., & Bannerman, R. T. (2016). The effect of particle size distribution on the design of urban stormwater control measures. *Water, 8*(1), 17.

Simpson, S., & Batley, G. (2007). Predicting metal toxicity in sediments: a critique of current approaches. *Integrated Environmental Assessment and Management: An International Journal, 3*(1), 18-31.

Soller, J., Stephenson, J., Olivieri, K., Downing, J., & Olivieri, A. W. (2005). Evaluation of seasonal scale first flush pollutant loading and implications for urban runoff management. *Journal of environmental management, 76*(4), 309-318.

Superville, P.-J., Prygiel, E., Magnier, A., Lesven, L., Gao, Y., Baeyens, W., Ouddane, B., Dumoulin, D., & Billon, G. (2014). Daily variations of Zn and Pb concentrations in the Deûle River in relation to the resuspension of heavily polluted sediments. *Science of the total environment, 470*, 600-607.

SWRCB. (1999). Consolidated Toxic Hot Spots Cleanup plan List and Findings Volume I: Policy, Toxic Hot Spots List and Findings. In (Vol. I).

Tchounwou, P. B., Yedjou, C. G., Patlolla, A. K., & Sutton, D. J. (2012). Heavy metal toxicity and the environment. In *Molecular, clinical and environmental toxicology* (pp. 133-164): Springer.

Tessier, A., Campbell, P. G., & Bisson, M. (1979). Sequential extraction procedure for the speciation of particulate trace metals. *Analytical chemistry, 51*(7), 844-851.

Tessier, A., & Campbell, P. G. C. (1987). Partitioning of trace metals in sediments: relationships with bioavailability. In *Ecological Effects of In Situ Sediment Contaminants* (pp. 43-52): Springer.

USEPA. (1993). Natural Wetlands and Urban Stormwater: Potential Impacts and Management. *O. a. WWD Office of Wetlands, ed. Washington, DC*.

USEPA. (1998a). Assessment and Remediastion of Contaminated Sediments (ARCS) Program: Guidance for in-situ subaqueous capping of contaminated sediments.

USEPA. (1998b). *National Water Quality Inventory: 1996 report to Congress*: US Environmental Protection Agency, Office of Water.

Verkleji, J. (1993). The effects of heavy metals stress on higher plants and their use as biomonitors. *Plant as bioindicators: indicators of heavy metals in the terrestrial environment. VCH, New York*, 415-424.

Vethaak, A. D., Hamers, T., Martínez-Gómez, C., Kamstra, J., de Weert, J., Leonards, P., & Smedes, F. (2017). Toxicity profiling of marine surface sediments: a case study using rapid screening bioassays of exhaustive total extracts, elutriates and passive sampler extracts. *Marine environmental research, 124*, 81-91.

Warner, K. A., Roden, E. E., & Bonzongo, J.-C. (2003). Microbial mercury transformation in anoxic freshwater sediments under iron-reducing and other electron-accepting conditions. *Environmental Science & Technology, 37*(10), 2159-2165.

Watling, L. (1991). The sedimentary milieu and its consequences for resident organisms. *American Zoologist, 31*(6), 789-796.

Wenning R. J. (2005). *Use of sediment quality guidelines and related tools for the assessment of contaminated sediments*: SETAC.

Wenning, R. J. (2005). *Use of sediment quality guidelines and related tools for the assessment of contaminated sediments*: SETAC.

Werner, I., Teh, S. J., Datta, S., Lu, X., & Young, T. M. (2004). Biomarker responses in Macoma nasuta (Bivalvia) exposed to sediments from northern San Francisco Bay. *Marine environmental research, 58*(2-5), 299-304.

Windt, C., Ebrahimian, A., & Traver, R. (2017). *Flow Characterization of Stormwater Runoff in Philadelphia.* Paper presented at the World Environmental and Water Resources Congress 2017.

Winsor, M. H., Boese, B. L., Lee Ii, H., Randall, R. C., & Specht, D. T. (1990). Determination of the ventilation rates of interstitial and overlying water by the clam Macoma nasuta. *Environmental Toxicology and Chemistry: An International Journal, 9*(2), 209-213.

Wu, Z., He, M., & Lin, C. (2011). In situ measurements of concentrations of Cd, Co, Fe and Mn in estuarine porewater using DGT. *Environmental pollution, 159*(5), 1123-1128. doi:https://doi.org/10.1016/j.envpol.2011.02.015

Xu, J., Zhang, J., Huo, S., Xi, B., He, Z., & Xu, Y. (2017). High-resolution profiles of trace metals assessed by DGT techniques in lake sediment porewaters. *Environmental Earth Sciences, 76*(8), 319. doi:10.1007/s12665-017-6642-5

Zhang, H., & Davison, W. (1995). Performance characteristics of diffusion gradients in thin films for the in situ measurement of trace metals in aqueous solution. *Analytical chemistry, 67*(19), 3391-3400.

Zhang, H., Davison, W., Miller, S., & Tych, W. (1995). In situ high resolution measurements of fluxes of Ni, Cu, Fe, and Mn and concentrations of Zn and Cd in porewaters by DGT. *Geochimica et Cosmochimica Acta, 59*(20), 4181-4192.

Zhao, H., & Li, X. (2013). Understanding the relationship between heavy metals in road-deposited sediments and washoff particles in urban stormwater using simulated rainfall. *Journal of Hazardous Materials, 246-247*, 267-276. doi:https://doi.org/10.1016/j.jhazmat.2012.12.035

Zoumis, T., Schmidt, A., Grigorova, L., & Calmano, W. (2001). Contaminants in sediments: remobilisation and demobilisation. *Science of the total environment, 266*(1-3), 195-202.

CHAPTER 3

METHODS TO ASSESS STORMWATER IMPACTS ON SEDIMENTS

A comprehensive set of laboratory, field, modeling, and statistical approaches was conducted at Paleta Creek, CA to characterize and assess the chemical and biological effects of stormwater metals to the contamination of sediments and remediated sites. This chapter provides a detailed description of the field monitoring, analytical, modeling, and statistical methods used in the study.

At the beginning of the chapter, *section 3.1*, describes the sampling stormwater collections that occurred at the NBSD in San Diego, CA in order to capture freshwater discharges. Then, the novel method of particle size distribution provides the characterization of the discharged solids and contaminants in the sizes of the filtered fraction (<0.45μm), clay (0.45-5 μm**),** fine silts (5-20 μm), coarse silts (20-63 μm) and sands (>63 μm). Analytical methods that involve metal extractions and chemical analysis using ICP-MS and Merx-T autosampler are also discussed for obtaining the stormwater concentrations of Cd, Cu, Zn, Ni, Pb, As, and THg. WinSLAMM modeling, calibrated in wide ranges of rain conditions at Paleta Creek, is also presented that was used to extrapolate the measured water concentrations and to provide the annual watershed discharges at Paleta Creek in different particle sizes.

Section 3.2 of the chapter presents the sediment sampling using sediment traps and seasonal surficial sediment cores as well as the analytical methods used for the metal extraction and chemical analysis of the collected sediment samples. In addition, the method of particle size characterization of sediment samples is described, which was useful to better understand the solid depositional rates during the trap deployment at the sediment bed.

Finally, the estuary model CH3D is presented which simulated based on modeled hydrodynamic currents and conditions in San Diego bay the depositional rates of the suspended solids in receiving waters at Paleta Creek during the monitored storm events.

Section 3.3 continues with additional analytical methods that were simultaneously applied to the sediment collections in order to assess the biological stormwater effects in sediments. The methods involved tissue bioaccumulation assessment using *in situ* and *ex situ* bioassays as well as sediment porewater assessment using DGTs as inorganic passive samplers.

Finally, *section 3.4* presents the statistical approaches that served as "weight of evidence assessment" of the multidisciplinary analytical measurements of the study. The statistical tools are presented that were used to identify contributing source locations for metals in stormwater, to assess the seasonal and spatial alterations on sediment and biological effects in sediments due to stormwater, as well as to evaluate the best predictor of biota accumulation in sediments. The statistical methods include two-way ANOVA, Fisher's exact test, Gamma regression, and Spearman's rank correlations using the software R.

3.1 Stormwater

3.1.1 Sampling collection

Intensive stormwater sampling occurred at six different locations and an ambient grab sampling in time series within the Paleta Creek Watershed during the 2015/2016 wet season. Six monitoring locations were selected within the lower Paleta Creek watershed representing NBSD land uses, the upper urbanized watershed, and a downstream creek

location affected by mixed flows from both NBSD and the upper watershed area. The sample locations described below are shown in Figure 3.1:

- Creek location upstream (C2W; Paleta Creek at Main Street): This location reflects the Creek upstream that is tidally influenced and is upstream of NBSD outfall discharges.
- Creek location downstream (C1W; Paleta Creek at Cummings Road): This location is within the tidal portion of the Creek and is representative of the entire watershed.
- Ambient grab sampling in time series close to the location C1W (A(1-3)W; represented by the red mark in Figure 3.1): This sampling reflects the discharged deposition overtime during the monitored storm events.
- Storm drain outfall 1 (O1W; NBSD outfall): This outfall discharge is representative of stormwater runoff from industrial areas on the west side of NBSD.
- Storm drain outfall 2 (O2W; NBSD outfall): This outfall discharge is representative of stormwater runoff from industrial areas on the east side of NBSD.
- Storm drain outfall 3 (O3W; NBSD outfall north of railroad crossing): This outfall discharge is representative of a large, central, mixed-used portion of the NBSD facility that includes residential areas, parking, and an auto-shop.

- Storm drain outfall 4 (O4W; NBSD outfall at Paunack and Division Streets): This outfall discharge represents a large, central, mixed-use portion of the NBSD facility that includes apartment buildings, activity fields, and parking lots.

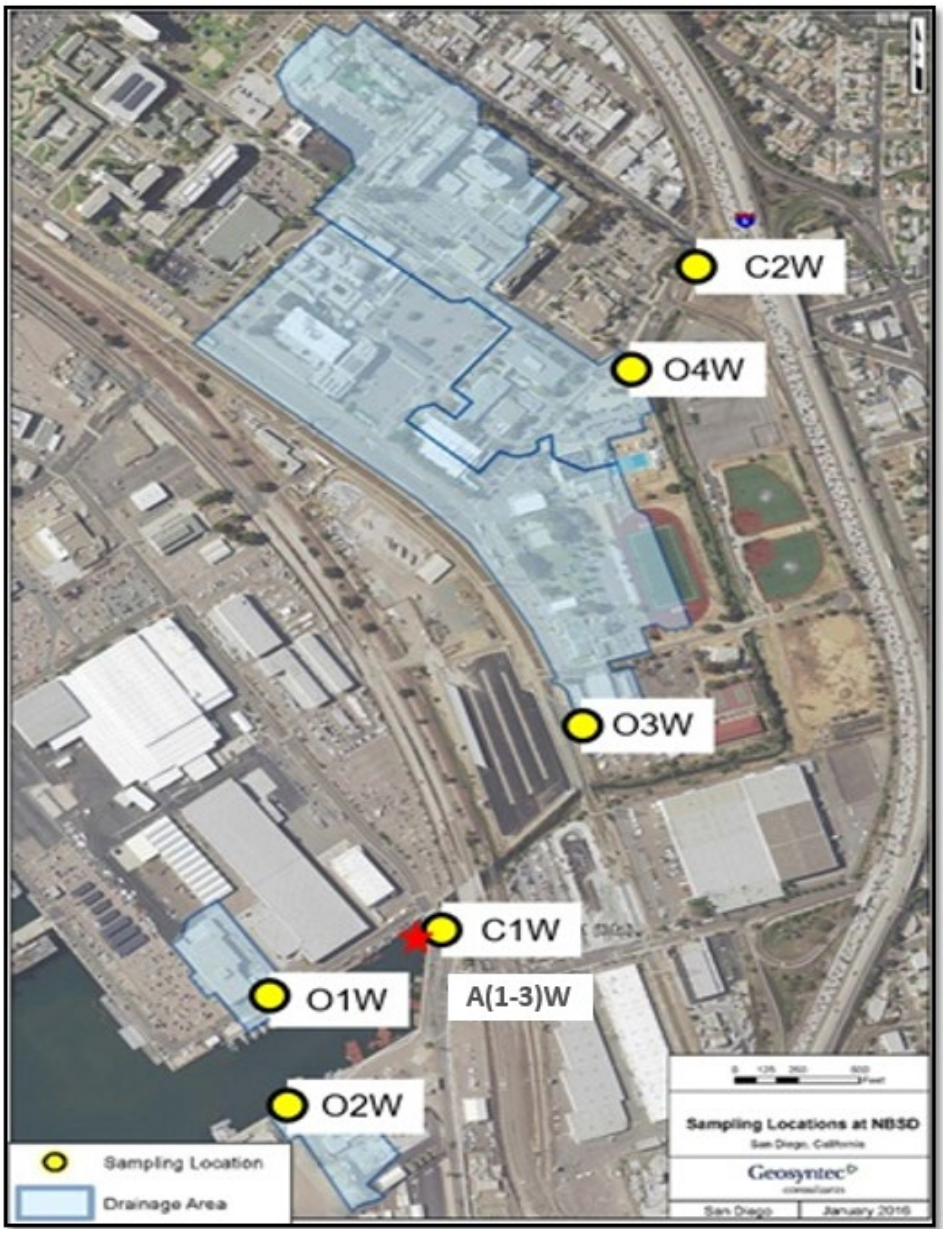

Figure 3.1: Paleta Creek watershed stormwater sampling locations. The red star indicates time-series sampling location A(1-3)W (Reible et al., 2018).

Automated time-integrated samples were collected by Geosyntec personnel using American Sigma 900 and ISCO 6712 auto-samplers installed at each monitoring location

at Paleta Creek. ISCO AQ702 multi-parameter meters were also deployed at tidally influenced monitoring locations (C1W, O1W, O2W, and O3W) to measure salinity and target the collection of freshwater samples. ISCO 750 area-velocity (AV) meters were deployed at flow or depth-triggered monitoring locations (C2W, O1W, O2W, O3W, and O4W). Figure 3.2 shows the installations of automatic water samplers at manhole and surface locations. Intensive stormwater sampling was conducted during two storm events in January 2016. ISCO 6712 automatic water samplers were deployed at all monitoring locations at Paleta Creek for the collection of time-spaced composite samples. The first event was on January 5th to 7th in 2016 and had 2.82 inches of precipitation over 26 hours of sampling and 4.65 inches over the entire event. The second event was from January 31th to February 1st, 2016, and had 0.20 inches of precipitation over 7.25 hours. These two rainfalls represented both small and large rains in the sampling watershed. Approximately 75% of the storms during 2015-2017 were similar in duration and intensity of the two selected events, and 90% of the total precipitation occurred while sediment traps were deployed in the receiving waters (Drygiannaki *et al.*, 2020). Supplementary ambient grab samples, A(1-3)W, were also collected near C1W, as shown in Figure 3.1, in time series including the beginning of the first storm event on 1/5/2016 at 13:27h (A1W), after 6h at 19:47h (A2W), and after 14h on 1/6/2016 at 03:33h (A3W), as shown in Figure 3.1. For the second storm event, A1W sample was collected on 1/31/2016 at 09:00h and A2W sample was collected after 6h on 1/31/2016 at 15:00h.

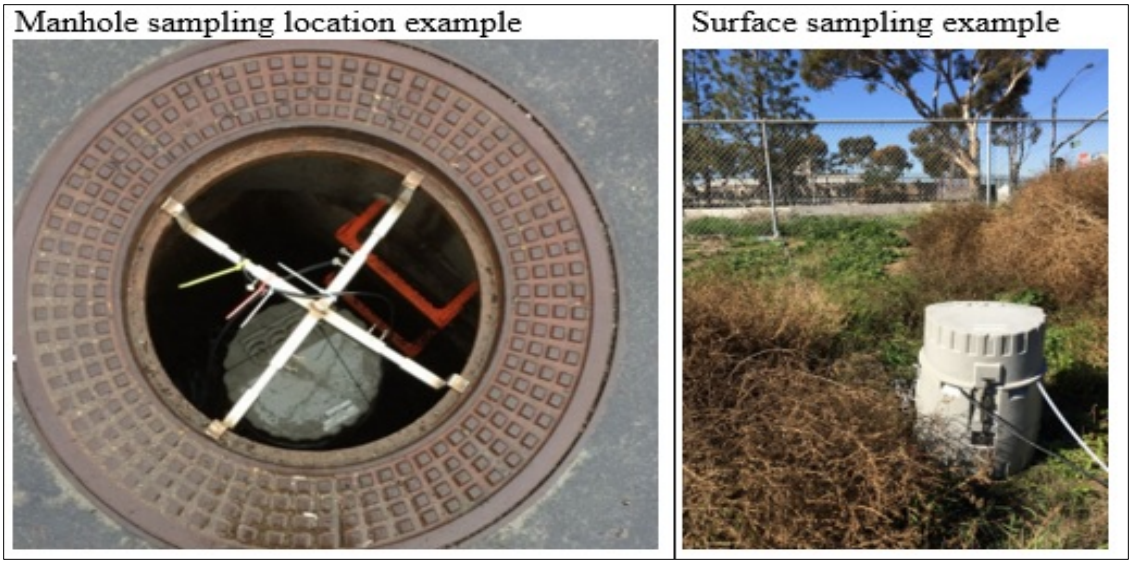

Figure 3.2: Automatic water sampler installations (Reible et al., 2018).

3.1.2 Particle size fractionation in water samples

Samples were collected in 10L pre-cleaned glass jars. Once the samples were collected, the bottles were wrapped carefully and transported by Geosyntec personnel to the SSC Bioassay Laboratory. Ambient samples, A(1-3)W, were collected by SSC Pac personnel. The stormwater samples from each event were split using a Teflon™ Dekaport splitter. The Dekaport Sample Splitter (Figure 3.3) is a pour-through device machined from a solid fluoropolymer used for splitting water samples in a wide range of particle sizes and water volumes. The bottles that were used to contain the stormwater samples after splitting for trace metal analysis were from high-density polyethylene (HDPE).

The HDPE bottles that have been selected to contain the water samples were trace metal clean cylinder bottles of 1L from VWR, quality-assured for trace metal analysis. Before each of the stormwater sampling, the bottles were precleaned at TTU, using a cleanup protocol based on modification from EPA specification and guidance for contaminant-free

sample containers (USEPA, 1992b). The cleanup procedure involved rinsing with ultra-pure water (purity ≤18MΩ.cm) and filling the bottles with 10% v/v HCl overnight. After removing the acidified water, the bottles were dried before shipping to Paleta Creek. This procedure helped to distinguish actual site concentrations as opposed to bottle contamination.

Figure 3.3: Dekaport splitter setup from TTU.

Briefly, two analytical blank samples were collected by pouring distilled deionized (DDI) water through the sampler into HDPE and amber glass bottles. Next, 7 Amber glass and 3 HDPE bottles were placed under the Dekaport splitter and 10L of the mixed stormwater sample was poured into the Dekaport for each sampling location. The samples contained in the amber glass bottles subjected to organic contaminant analysis. However, this study focused only on metal contaminants. Samples were poured into the splitter through a 0.5mm sieve to remove debris at a rate that would allow constant pressure and thus

consistent flow through all the tubings of the Dekaport splitter. After the first splitting, all 7 Amber glass bottles and one HDPE bottle (served as contingency sample) with the equal volumes were capped and stored in the cold room (4ºC). The remaining 2 HDPE bottles (approximately 2L of the sample) were then passed through the Dekaport splitter for the second splitting into 5 HDPE bottles of equal volume, approximately 400mL each. For the stormwater collection of the 2nd event, when 20L were collected per location, the splitting process duplicated for the additional 10L of sample volume that was collected. The Dekaport splitter was thoroughly rinsed with DDI water between samples. All bottles were immediately shipped on ice to Texas Tech University (TTU) for further processing and analytical chemical measurements as shown in Figure 3.4.

For each stormwater location, one out of the five HDPE bottles was kept aside for bulk chemical analysis. The remaining four HDPE bottles were used for fractionation with sieving and vacuum filtration systems. One HDPE bottle was proceeded for sieving with a sieve of 63μm opening size, and another HDPE bottle with a sieve of 20μm opening size. One HDPE bottle was used for vacuum filtration using 0.45μm hydrophilic polytetrafluoroethylene (PFTE) filters and another one using 5μm PFTE filters. PFTE filters are compatible with all solvents, acids, and alkaline solutions. The particles on the filters that are greater than 0.45 and 5μm and the retained solids greater than 63 and 20μm, were collected, dried at 45ºC for obtaining the solid concentration per fraction, and stored in the 4ºC cold room for chemical characterization. Also, samples of ultra-pure water poured into three extra HDPE of 1L containers in the NIWC Pacific lab, processed through the Dekaport splitter, and shipped along with the rest of the samples to TTU laboratory. One of these HDPE bottles was used as a bulk trip blank and was extracted without size

fractionation. The other two were used as sieved and filtered trip blanks and were passed through the sieve and vacuum filtration system, respectively. The trip blanks, bulk, sieved and filtered water samples were preserved with 0.5%v/v HCl to reach pH<2, before the storage in the 4°C cold room. The acid preservative is designed to keep the metallic content of the water sample in solution and in some cases will actually leach metals from the small particles present in the water sample.

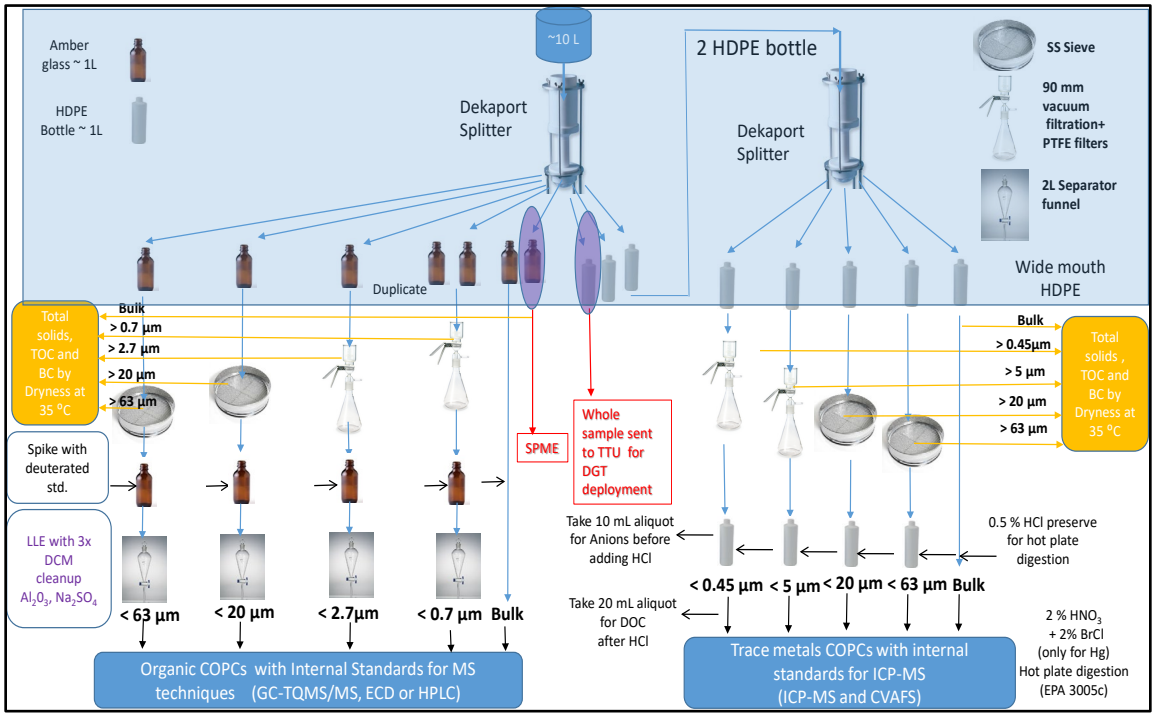

Figure 3.4: Composite sample splitting schematic for stormwater samples collected Jan-2016 (Reible et al., 2018).

3.1.3 Trace metal digestion for bulk and fractionated water samples

The bulk, fractionated, and field blank water samples/bottles were digested using the modified EPA method 3005A (USEPA, 1992a). Triplicates of 35mL per water sample/bottle were used for bulk and fractionated water digestion. The procedure was performed using aqua-regia digestion, solution of concentrated nitric acid (HNO_3) and

hydrochloric acid (HCl) with a molar ratio of about 1:3. After the digestion, 15mL of each digested sample were stored in the 4ºC cold room for trace metal analysis using ICP-MS (USEPA, 1994), and the remaining 20mL were preserved with 2% v/v BrCl and stored, separately, in the cold room for total mercury analysis using MERX-T (USEPA, 2002). Each digestion set was accompanied by triplicates of digestion blanks, which were vials with 35mL ultra-pure water, to control there is no cross-contamination during the digestion process. Spiked blank water samples were digested and analyzed for obtaining the method recoveries for each of the metals of interest.

3.1.4 Inductively coupled plasma mass spectrometry (ICP-MS) for trace metal analysis (other than THg)

The trace metal analysis was obtained using the modified EPA method 200.8, Revision 5.4 for Inductively coupled plasma mass spectrometry (ICP-MS), using the Perkin-Elmer SCIEX ELAN DRC II (USEPA, 1994). The trace metals, Cu, Ni, Zn, Cd, Pb, and the metalloid As were analyzed for the bulk and fractionated water samples as well as the bulk sediment samples. Before the analysis, all the samples that contained particles were centrifuged to remove any residual particles that would interfere with the analytical instrument. Furthermore, selected samples were analyzed to decide the dilution of the to-be-analyzed samples. Each run of the instrument was consisted initially of the calibration range, with at least five calibration points. After the calibration run, every 10 samples were in the sequence were followed by an instrument blank, which was a sample of 2%v/v HNO_3, and a quality control (QC) sample, which was the same sample that was used for one of the calibration points of the instrument. The acceptable QC recoveries for the measured metals are within the range of 80-120%. Additionally, the internal standards

(Scandium, Terbium, and Indium) were added to each of the samples, before the analysis. The internal standards were compounds that could not interfere with the sample components and were added to control the loss of the analyte during the sample preparation or sample inlet. The acceptable recoveries of the internal standards were within the range of 60-125%. The set of samples that did not meet the recovery criteria of the internal standards and QCs was re-analyzed.

3.1.5 THg analysis using the MERX-T Autosampler

Total Mercury was analyzed following the EPA method 1631E: Mercury in Water by Oxidation, Purge, and Trap, and Cold Vapor Atomic Fluorescence Spectrometry using the MERX total Hg system of Brooks Rand™ (USEPA, 2002). Before the analysis, selected samples were analyzed to decide the dilution of the to-be-analyzed samples. Each run of the instrument was consisted initially of the calibration range, with at least five calibration points. After the calibration run, every 10 samples were in the sequence were followed by a reagent blank and a quality control (QC) sample. The acceptable QC recoveries for the measured metals are within the range of 77-123%. The set of samples that were not meet the recovery criteria of the QCs or the equipment blank criteria was re-analyzed.

Table 3.1: List of metals that were analyzed using ICP-MS and MERX-T.

Metals	Lower calibration point (ppb)	Higher calibration point (ppb)
Cd	0.2	50
Pb	0.5	50
Cu	1	500
Ni	1	500
Zn	1	500
As	1	100
	Lower calibration point (pg)	Higher calibration point (pg)
THg	25	2,500

3.1.6 Evaluation of extraction recoveries for trace metals in water matrices

Spiked blank water samples were digested and analyzed for obtaining the method recoveries for each of the metals of interest. The blank spiked water samples, that were prepared with ultra-pure water and stock metal solution, were digested with the digestion procedure for water samples from EPA 300.5 (USEPA, 1992a), and finally analyzed using ICP-MS. Table 3.2 presents the blank spiked recoveries for particular metals as they were measured at TTU.

Table 3.2: Blank spiked water sample recoveries for trace metal digestion of water samples.

Metal	Expected value (μg/L)	Measured value (μg/L)	% Recovery
Copper (Cu)	10	10.1	101
Cadmium (Cd)	1	1	100
Nickel (Ni)	10	9.4	94
Zinc (Zn)	10	10.5	105
Arsenic (As)	2	2.2	112

3.1.7 Stormwater solid and metal loading calculations

The equations that are described below, were used to obtain the sold, and the metal water and particulate concentrations in different size ranges and their standard deviations (Stdev):

Solids*:*

Solids for normalizing the metal aqueous measurements:

$$TFS_{0.45-5\mu m} = TFS_{>0.45um} - TFS_{>5\mu m} \quad (3.1)$$

$$TFS_{5-20\mu m} = TFS_{>5um} - TFS_{>20\mu m} \quad (3.2)$$

$$TFS_{20-63\mu m} = TFS_{>20um} - TFS_{>63\mu m} \quad (3.3)$$

Example of calculating the solid concentration (mg/L), TFS, in the coarse silt interval (20-63μm) in location C1W of event 1:

TFS in the fraction >20μm was 171.8mg/L and TFS in the fraction >63μm was 63.5mg/L. The TFS in the (20-63μm) interval was:

$$TFS_{20-63\mu m} = 171.8\frac{mg}{L} - 63.5\frac{mg}{L} = 108.3\frac{mg}{L} \quad (3.4)$$

In the cases that the TFS calculation gave negative value, the solid concentration was reported as 0.0.

For Metals:

Equations involved in the calculation of aqueous concentrations of metals, C(μg/L), in the corresponding size intervals:

For the C(>0.45μm):

$$C_{>0.45\mu m} = C_{Bulk} - C_{<0.45\mu m}\left(\frac{\mu g}{L}\right) \quad (3.5)$$

$$Stdev_{(>0.45)\mu m} = \sqrt{(Stdev_{Bulk})^2 + (Stdev_{<0.45\mu m})^2} \quad (3.6)$$

For the C(0.45-5μm):

$$C_{0.45-5\mu m} = C_{<5um} - C_{<0.45\mu m}(\frac{\mu g}{L}) \quad (3.7)$$

$$Stdev_{(0.45-5)\mu m} = \sqrt{(Stdev_{<5\mu m})^2 + (Stdev_{<0.45\mu m})^2} \quad (3.8)$$

For the C(5-20μm):

$$C_{5-20\mu m} = C_{<20um} - C_{<5\mu m}(\frac{\mu g}{L}) \quad (3.9)$$

$$Stdev_{(5-20)\mu m} = \sqrt{(Stdev_{<20\mu m})^2 + (Stdev_{<5\mu m})^2} \quad (3.10)$$

For the C(20-63μm):

$$C_{20-63\mu m} = C_{<63um} - C_{<20\mu m}(\frac{\mu g}{L}) \quad (3.11)$$

$$Stdev_{(20-63)\mu m} = \sqrt{(Stdev_{<63\mu m})^2 + (Stdev_{<20\mu m})^2} \quad (3.12)$$

For the C(>63μm):

$$C_{>63\mu m} = C_{Bulk} - C_{<63\mu m}(\frac{\mu g}{L}) \quad (3.13)$$

$$Stdev_{(>63)\mu m} = \sqrt{(Stdev_{Bulk})^2 + (Stdev_{<63\mu m})^2} \quad (3.14)$$

Example of calculating the Cu aqueous concentration (μg/L), C, in the coarse silt interval (20-63μm) in location C1W of event 1:

C in the fraction <63μm is 15.05±0.2 μg/L and C in the fraction <20μm is 9.88±0.3 μg/L.

The C in the interval (20-63μm) for Cu is:

$$C_{20-63\mu m} = 15.05\,\frac{\mu g}{L} - 9.88\,\frac{\mu g}{L} = 5.17\,\frac{\mu g}{L} \quad (3.15)$$

And the standard deviation is:

$$Stdev_{(20-63)\mu m} = \sqrt{(0.2)^2 + (0.3)^2} = 0.4 \quad (3.16)$$

In the cases that the C calculation gave negative value, the metal aqueous concentration was reported as 0.0 with standard deviation "NA" and the flag "M<0".

Equations involved in the calculation of metal concentrations on solids, C (mg/kg), in the corresponding size intervals:

For the C(>0.45μm):

$$C_{>0.45\mu m} = \frac{C_{Bulk} - C_{<0.45\mu m}\,(\frac{\mu g}{L})}{TFS_{>0.45um}(\frac{mg}{L})} * 1000\,\frac{mg}{g} = \frac{\mu g}{g} = \frac{mg}{kg} \tag{3.17}$$

$$Stdev_{(>0.45)\mu m} = \frac{\sqrt{(Stdev_{\mathrm{Bulk}})^2 + (Stdev_{<0.45\mu m})^2}}{TFS_{>0.45\mu m}} \tag{3.18}$$

For the C(0.45-5μm):

$$C_{0.45-5\mu m} = \frac{C_{<5\mu m} - C_{<0.45\mu m}\,(\frac{\mu g}{L})}{TFS_{>0.45um} - TFS_{>5\mu m}(\frac{mg}{L})} * 1000\,\frac{mg}{g} = \frac{\mu g}{g} = \frac{mg}{kg} \tag{3.19}$$

$$Stdev_{(0.45-5)\mu m} = \frac{\sqrt{(Stdev_{<5\mu\mathrm{m}})^2 + (Stdev_{<0.45\mu m})^2}}{TFS_{>0.45\mu m} - TFS_{>5\mu\mathrm{m}}} \tag{3.20}$$

For the C(5-20μm):

$$C_{5-20\mu m} = \frac{C_{<20\mu m} - C_{<5\mu m}\,(\frac{\mu g}{L})}{TFS_{>5um} - TFS_{>20\mu m}(\frac{mg}{L})} * 1000\,\frac{mg}{g} = \frac{\mu g}{g} = \frac{mg}{kg} \tag{3.21}$$

$$Stdev_{(5-20)\mu m} = \frac{\sqrt{(Stdev_{<20\mu\mathrm{m}})^2 + (Stdev_{<5\mu m})^2}}{TFS_{>5\mu m} - TFS_{>20\mu\mathrm{m}}} \tag{3.22}$$

For the C(20-63μm):

$$C_{20-63\mu m} = \frac{C_{<63\mu m} - C_{<20\mu m}\,(\frac{\mu g}{L})}{TFS_{>20um} - TFS_{>63\mu m}(\frac{mg}{L})} * 1000\,\frac{mg}{g} = \frac{\mu g}{g} = \frac{mg}{kg} \tag{3.23}$$

$$Stdev_{(20-63)\mu m} = \frac{\sqrt{(Stdev_{<63\mu\mathrm{m}})^2 + (Stdev_{<20\mu m})^2}}{TFS_{>20\mu m} - TFS_{>63\mu\mathrm{m}}} \tag{3.24}$$

For the C(>63μm):

$$C_{>63\mu m} = \frac{C_{Bulk} - C_{<63\mu m}\,(\frac{\mu g}{L})}{TFS_{>63um}(\frac{mg}{L})} * 1000\,\frac{mg}{g} = \frac{\mu g}{g} = \frac{mg}{kg} \tag{3.25}$$

$$Stdev_{(>63)\mu m} = \frac{\sqrt{(Stdev_{\text{Bulk}})^2 + (Stdev_{<63\mu m})^2}}{TFS_{>63\mu\text{m}}} \tag{3.26}$$

Example of calculating the Cu concentration on the solids (mg/kg), C, in the coarse silt interval (20-63µm) in location C1W of event 1:

$$C_{20-63\mu m} = \frac{15.05\frac{\mu g}{L} - 9.88\frac{\mu g}{L}}{171.8\frac{mg}{L} - 63.5\frac{mg}{L}} * 1000\,\frac{mg}{g} = 47.8\ \frac{mg}{kg} \tag{3.27}$$

And the standard deviation is:

$$Stdev_{(20-63)\mu m} = \frac{\sqrt{(0.2)^2 + (0.3)^2}}{108.3} = 0.004 \tag{3.28}$$

In the cases that the numerator was negative, the metal concentration on solids was reported as 0.0 with Stdev "NA" and the flag "M<0". In the cases that the denominator was negative, the metal concentration on solids was reported as the metal aqueous concentration with the standard deviation of the metal aqueous concentration and the flag "µg/L". Moreover, for the samples with high salinity that the salt precipitated in the pores of the filters presented interference >20%, the flag "S" (salinity) was used for identification. Finally, the flag "LS" (low solids) was used in the stormwater samples that presented less than 10mg/L solid concentration.

3.1.8 Prediction of long term storm discharges using WinSLAMM modeling

The Paleta Creek stormwater measured data were used along with the WinSLAMM stormwater quality model that was previously calibrated for the Paleta Creek area during previous NBSD projects (Reible *et al.*, 2018). WinSLAMM was developed to evaluate stormwater runoff volumes and pollutant loadings in developed areas during a wide range

of rain conditions, not just very large storms that are the focus of conventional drainage design models. WinSLAMM can use any length of rainfall record as determined by the user, from single rainfall events to several decades of rains (Pitt & Voorhees, 1995).

The stormwater modeling enabled calculations of stormwater discharge characteristics as determined by specific drainage areas at Paleta Creek watershed; allowing the extrapolation of individual monitored storm events to annual discharges. The generated data in annual unit area discharges with units g/ha/yr were also distributed in different particle size ranges (<20μm), (20-63μm), (>63μm), as well as in total watershed contributions, as shown in Appendix A in Table A1. The annual metal discharges obtained by WinSLAMM were particularly useful to calculate the modeled discharged metals during the trap deployment period and used for comparison with the extrapolated total metal mass deposition in the total trap deployment vicinity at the sediment bed of Paleta Creek.

3.2 Sediment

3.2.1 Sediment sampling of seasonal surficial cores and trap material

Sediment core collections occurred throughout the dry and wet weather seasons 2015/2016 and 2016/2017. The sampling months of July, October 2015 and September 2016 represented the "dry weather" or pre storm season, while the February 2016 and March 2017 represented the "wet weather" or post storm season (Figure 3.5). Intact sediment cores were hand-collected by SCUBA divers or using a Van Veen grab sampler. Divers descended and pushed a core liner into the sediment approximately 5 inches and then carefully capped the cores, or multiple core samples were collected with the Van Veen grab from each station to obtain enough material to collect intact cores. The sediment sampling locations included the P01, far from the Paleta Creek discharge, P08, P11, and P17,

progressively closer to the Paleta Creek discharge (Figure 3.6). P08 is located in the outer creek area, while P11 and P17 are located in the inner creek area.

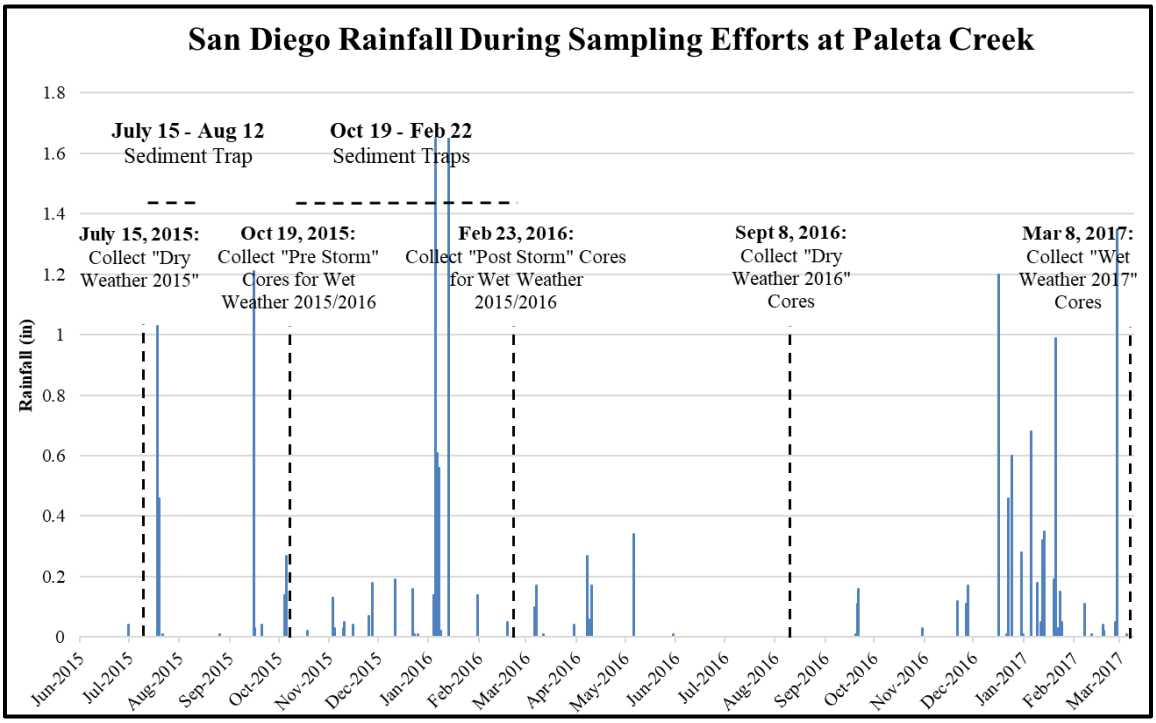

Figure 3.5: Sampling efforts at Paleta Creek (Reible et al., 2018).

Figure 3.6: Sediment sampling locations at Paleta Creek.

Sediment trap deployment at Paleta Creek was crucial for capturing the suspended particles from stormwater discharge. The settling traps were the incorporation of three cylindrical traps with dimensions 81.3cm x 15.2cm and were deployed at each of the monitoring stations, P01, P08, P11, and P17 from 19th of October 2015 through 23rd of February 2016, during the monitored storm events 1 and 2.

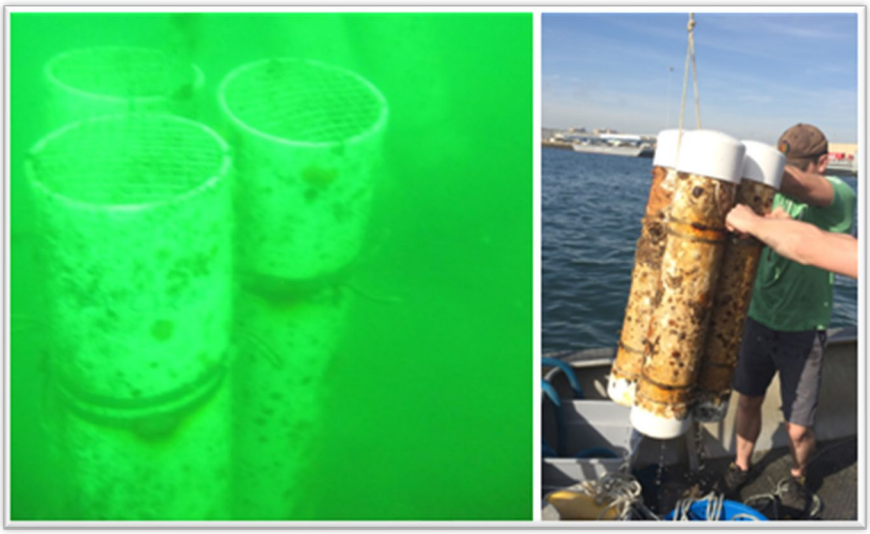

Figure 3.7: Cylindrical sediment trap deployment at Paleta Creek (Reible et al., 2018).

Each of the sediment traps was prefilled with hypersaline brine and topped off with ambient seawater. Traps were capped and lowered into the water to divers who secured the traps to pre-deployed posts on the sediment surface. Once dive activities were completed, divers carefully removed caps from each sediment trap. Sediment traps were capped when any diving related activities occurred on station to avoid potential deposition from those efforts. At the termination of the sediment trap deployment period, divers placed caps back on the traps and recovered and transferred to the surface crew with the assistance of a boat-mounted davit. The traps were transported back to the NIWC Pacific laboratory and

allowed to settle. Once the sediment trap material sufficiently settled, the overlying water was removed, and the remaining material was subjected to chemical analysis but also was used as part of bioassays treatments. All three traps at a given location were combined prior to analysis and were to TTU for further processing.

3.2.2 Particle size fractionation in sediments using the pipette method

Triplicates of the sediment trap material in each of the four locations were used for particle size fractionation. An aliquot-replicate of well-homogenized wet sediment (~20g) was dried. 1% w/v of sodium hexametaphosphate dispersant was added to the sample in a 1,000mL glass cylinder bottle and was filled up to 400mL with ultra-pure water. After sonication and mixing overnight, the mixed sample of 400mL was sieved through a stainless-steel sieving system with 63μm opening size. The retained sand (>63μm) was collected from the sieve and stored at 4ºC cold room for further physiochemical characterization. The filtrate sample was transferred into the 1,000mL glass cylinder bottle and filled up to 800mL with ultra-pure water. After mixing the sample overnight, the pipette method was applied, and the fractions: clay (< 2μm), fine silt (2-20μm), and coarse silt (20-63μm) were obtained using the Stoke's equation. The TTU process is evolved from the modification of the method described by (Haywick, 2004).

3.2.3 Trace metal (other than THg) digestion for sediment samples

The bulk sediment samples were digested using the modified EPA method 3050B (USEPA, 1996). Triplicates of ~1g dry sediment per location/bottle were used for trace metal extraction. The sediment digestion was performed using nitric acid, HNO_3, and hydrogen peroxide, H_2O_2. After the digestion, ~33mL of the sample was stored in the 4ºC cold room for metal analysis using ICP-MS. Each digestion set was accompanied with triplicates of

digestion blanks, which were initially empty trace metal clean vials. The standard reference material 1944 was also digested along with the sediment samples, and the recoveries for the preferred metals were in the range of 87-103%. The metals were analyzed using ICP-MS following the same QAQCs as described in the section 3.1.3.2.

3.2.4 Total mercury (THg) digestion for sediment samples

The bulk sediment samples were digested using an adaptation of the "EPA-821-R-01-013" (USEPA, 2013). Triplicates of ~1g of dry sediment per location were used for THg digestion. The sediment digestion was performed with aqua-regia digestion, using a solution of concentrated hydrochloric acid, HCl, and nitric acid, HNO_3. The acid digested mixture was further oxidized with concentrated solution 0.2N of bromine monochloride, BrCl, and then diluted to 40 ± 0.5 mL with ultra-pure water. After the digestion, 40mL of the final digested sample was stored in the 4^{o}C cold room for THg analysis using MERX-T Autosampler (USEPA, 2002). Each digestion set was accompanied with triplicates of digestion blanks, which were initially empty trace metal clean vials. The standard reference material 2702, with low levels of THg similarly to the expected concentrations, was also digested following the THg digestion procedure, and the acceptable recovery was within the range of 80-120%. THg was analyzed using Merx-T following the same QAQCs as described in the section 3.1.3.3.

3.2.5 Evaluation of extraction recoveries of sediment matrices

Regarding THg digestion method performance in sediment matrices, the standard reference material 2702 with low-level THg, was also digested following the THg digestion procedure. Table 3.3 presents the SRM 2702 recoveries for total mercury as they were measured in TTU.

Table 3.3: SRM 2702 recoveries for THg sediment digestion performance.

ID	Expected THg value (mg/kg)	Measured THg value (mg/kg)	Recovery%	Average Recovery%	STDEV
SRM 2702_1	0.4474	0.398	88.9	91.2	1.9
SRM 2702_2	0.4474	0.415	92.7		
SRM 2702_3	0.4474	0.411	91.9		

The metal digestion performance for sediment matrices was evaluated using the National Institute of Standards and Technology (NIST) sediment standard reference material "1944". Table 3.4 presents the SRM 1944 recoveries for particular metals as they were measured in TTU.

Table 3.4: SRM 1944 recoveries for metal sediment digestion performance.

Metal	Expected value (mg/kg)	Measured value (mg/kg)	% Recovery
Copper (Cu)	380	371	97.6
Cadmium (Cd)	8.8	8.7	98.5
Lead (Pb)	330	290	87.9
Nickel (Ni)	76.1	66.4	87.3
Zinc (Zn)	656	645	98.3
Arsenic (As)	18.9	19.5	103

3.2.6 Depositional rate modeling in receiving waters

The model 3-dimensional CH3D (Curvilinear Hydrodynamics in 3-Dimensions) was applied by (Wang *et al.*, 1998) to study the transport patterns of the storm-discharged particles in San Diego Bay. CH3D simulates hydrodynamic currents in 3D (x,y,z spatial plus time) and the fate and transport of contaminants in harbors under the forcing of tides, wind, and freshwater inflows. The same model has been used for a number of studies focusing on fate and transport, including sewage spills near the entrance of the bay and the south bay, copper discharge from the convention center dewatering facility, and migration of contaminated sediments resuspended by propeller wash (Wang *et al.*, 2000) and copper

concentrations in the bay (Wang *et al.*, 2006). The existing CH3D-San Diego Bay model domain covers an area of approximately 110 km^2 and uses a total of approximately 6214 grid elements, with an average resolution of approximately 100 meters (Wang *et al.*, 1998).

The field measurements of flowrate and solid concentrations of the particle sizes, clay, silt, and sand, from the storm discharge C1W, that were conducted during the two monitoring storm events in 2016, were used to calculate the field sediment loads on receiving waters using the CH3D based the following equation:

$$S_i = FC_i\left(\frac{30.48^3}{10^6}\right) \tag{3.29}$$

Where S_i represents the sediment load (g/s) for the different particle sizes i=1-clay,2-silt,3=sand, F is the creek flow rate (f^3/s) and C_i is the solid concentrations (mg/L) for the different particle sizes, i. The number in parenthesis is the conversion constant. The field data were used for comparison with the simulated modeled results.

The model simulations were conducted for event 1 (5^{th} Jan 2016) and event 2 (31^{th} Jan 2016). For each event, model simulations were run for 15 days. Model output of net sediment deposition mass (g/cm^2) for clay silt and sand particles were stored. Simulated sediment deposition rates (g/cm^2/day) in receiving water were calculated by dividing the net simulated sediment deposition mass by the total length of the time window of the loads for each event. The selection of the time window is representative of the field data sampling. The simulated deposition rates (g/cm^2/d), obtained from the CH3D, were used for comparison to the field calculated rates. The results of the model, as shown in Appendix A, include simulated and field depositional rates for both events, which were particularly useful to identify that stormwater discharges from Paleta Creek were expected to settle

with the highest rate in P17 location; while with the lowest rate in P01 (P17>P11>P08>P01) as shown in Figure A1, Appendix A.

3.3 *In situ* and *ex situ* bioassays

3.3.1 *In situ* bioaccumulation monitoring

Sediment Ecosystem Assessment Rings (SEA Rings) were used for the *in situ* bioaccumulation to obtain the tissue metal concentrations. For the metal contaminants, SEA Rings Version 3.0 (Figure 3.8) were deployed only during the wet weather season.

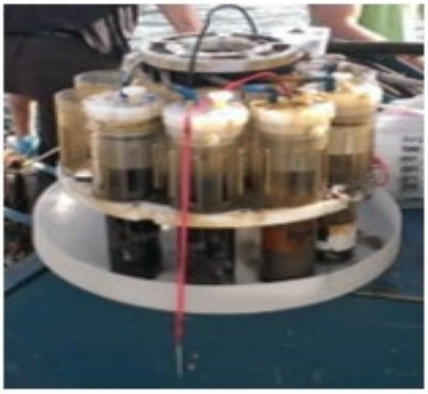

Figure 3.8: Version 3.0 SEA Rings that were deployed at Paleta Creek for in situ bioaccumulation studies (Reible et al., 2018).

The wet weather deployments utilized Version 3.0 SEA Rings which consisted of ten exposure chambers with integrated multifunctional caps. Caps include both water intake and outlet ports, and an organism delivery port. For each station, 8 of the 10 potential replicates on a given SEA Ring were initiated with 5 clams each. Four of the eight replicates were equipped with an 80µm pre-filter and the remaining four replicates were equipped with a 500µm pre-filter. Additionally, an open cage with 15 clams was deployed adjacent to the SEA Ring. The purpose of the filters or lack of filter was to potentially isolate depositing particle fraction contributions to the certain exposure chambers. SEA

Rings were deployed for a wet weather characterization of the bioavailability of contaminants associated with the sediments at Paleta Creek. Organisms were either purchased from commercial vendors or field-collected and acclimated to site conditions prior to deployment. For the Wet Weather evaluation beginning in January 2016, SEA Rings were deployed at all four receiving water locations, P17, P11, P08, and P01 for 28-d. Each SEA Ring consisted of ten exposure chambers with organisms for bioaccumulation analysis. The clam used for the *in situ* evaluations was the bivalve *Macoma nasuta* (bent-nosed clam) (Figure 3.9). On the day of deployment, five clams were directly loaded into exposure chambers with coarse stainless-steel mesh fastened to the bottom (to aid in the recovery of organisms). Stainless steel mesh was also fastened to the top of each exposure chamber to allow for passive settling of particulate matter and to allow for the flushing of ambient water conditions. SEA Rings were held in 17-gallon plastic. Following the 14- or 28-d exposure, SEA Rings were recovered by divers. Following an initial visual assessment of each SEA Ring, the device was gently lifted out of the sediment and brought to the surface. Once at the surface, the stainless-steel mesh was removed, and the clams were recovered by hand and enumerated for survival. Organisms were depurated overnight in clean seawater and prepared for chemical analysis. The Wet Weather *in situ* exposures at all four receiving locations P17, P11, P08, and P01 that occurred in January 2016 were compared with the *ex situ* tissue concentrations of the same period exposures from the same locations. Figure A2 and Table A2 in Appendix A indicate that the *ex situ* tissue concentrations were lower than the *in situ* tissue with statistical significance, $p<0.05$ $\alpha=0.05$, for all the examined metals, except Pb.

Figure 3.9: Macoma nasuta (bent-nosed clam) used for in situ bioaccumulation studies (Reible et al., 2018).

The clams were purged in clean seawater overnight after the recovery, and the soft-body portion saved for tissue analysis. Wet tissue weights were assessed on a per replicate basis, then typically composited on a per station basis, and tissues were frozen and shipped on blue ice to TTU chemistry laboratory, where digestion, extraction, and analysis were conducted.

3.3.2 *Ex situ* bioaccumulation monitoring

Ex situ exposures were conducted at the SSC Pacific Bioassay Laboratory using the bent-nosed marine clam *Macoma nasuta* (Figure 3.10). The sediment intact cores were placed into 1L glass mason jars with 750mL of overlying uncontaminated 0.45µm filtered natural seawater (FSW) collected near the mouth of San Diego. In addition to the sediment core samples collected from Paleta Creek at NBSD, sediment trap material collected over the course of the wet season was placed as an additive treatment on the top of the pre storm cores, named as "pre+". No significant differences were noted between "pre+" and "post" storm tissue measurements and these treatments were also simply treated as "post" storm season treatments for the *ex situ* tissue data interpretation. The amount of trap material

added on the top of the intact cores was proportional to the volume of sediment trap material recovered from each station.

Overlying water in all exposures was continuously aerated with filtered laboratory air delivered through Pasteur pipettes at a rate of approximately 100 bubbles per minute. A 24-h equilibration period with the overlying water was allowed prior to the introduction of test organisms or passive sample devices (Day 0). For all sediment samples, 1-inch small adult clams were exposed to sediments for a 28-d bioaccumulation assay. The *ex situ* bioassays were conducted with 3 replicates using intact sediment of approximately 100g dry weight. Organisms were introduced randomly to test chambers on test "Day 0" with sufficient organisms reserved for characterization of initial metal bioaccumulation. Renewals of the overlying water, filtered (0.45 μm) natural seawater collected from San Diego Bay, were made three times per week over the course of the 28-d exposure. Upon termination of the exposure period (Day 28), surviving organisms were recovered by sieving sediment using a 500 μm sieve, enumerated, and then transferred to clean freshwater overnight to purge digested sediment. On Day 29, the soft body portions from the clams were dissected from each replicate, rinsed with milli-q deionized water, weighed and frozen in sample collection jars until shipment to the analytical laboratory at TTU for metal digestion, extraction, and analysis using test protocols for sediment bioaccumulation exposures (ASTM, 2000; USEPA, 1991). Trace metals (except Hg) in tissue were extracted using HNO_3. Hg was extracted from tissue using HNO_3 and sulfuric acid (H_2SO_4). BrCl was also added to the digested Hg to prevent the reabsorption of Hg to carbon particles if present. The procedure is based on the EPA method 1631B (USEPA, 1999).

3.4 Inorganic passive sampling using Diffusive Gradients in Thin films

Diffusive Gradients in Thin films (DGTs) were acquired from DGT Research, Lancashire, UK (Figure 3.10) for measuring the cationic metals, including Cd, Cu, Ni, Pb, and Zn. The DGTs consisted of a plastic molded base (2.5 cm diameter) and a plastic top with a 3.14 cm^2 diameter window, which allows the exposure to a layered setup of a polyethersulphone filter-membrane, 0.78mm cross-linked polyacrylamide (APA) diffusive gel and 0.4 mm Chelex binding resin gel. When deployed either in solution or into sediments, metal ions diffuse through the filter membrane and diffusive gel and bind to the resin gel which continues to accumulate ions over the course of a deployment. In sediment applications, DGT measures the mean flux of labile metals at the interface between the device and the sediment, or the labile porewater concentrations. DGTs were stored in sealed, plastic bags at 0-4°C prior to deployment. Each bag contained a few drops of 0.01M $NaNO_3$ solution and was maintained moist throughout storage periods. The DGTs were pressed gently into the surface of the sediments to ensure full contact between the sediment and the exposure window/membrane of the DGT.

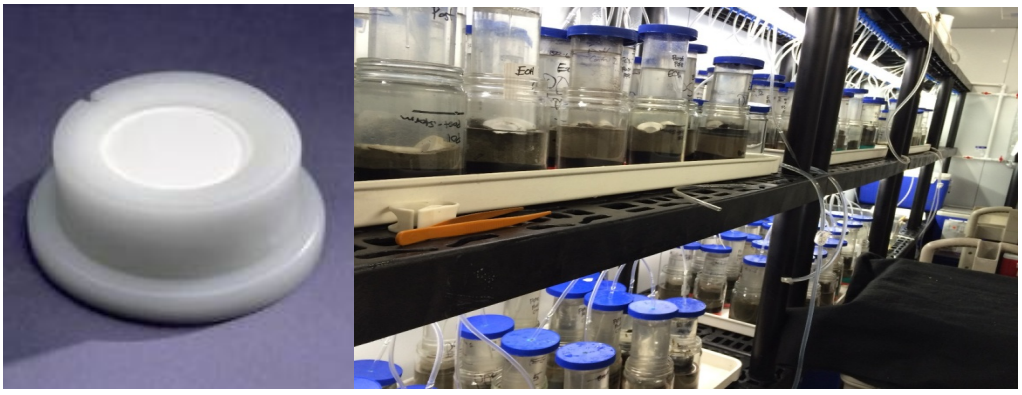

Figure 3.10: Diffusive Gradients in Thin-film (DGT) device and ex situ DGT exposures on the sediment cores (Reible et al., 2018).

DGTs for measuring Hg were fabricated by TTU using an agarose based resin-gel layer based on an adaptation of the method described by (Amirbahman *et al.*, 2013). The DGTs under-went pre-treatment prior to use by purging in a 10mM solution of $NaNO_3$ with polyacrylamide resin strips. The solution, strips, and DGTs were placed in a N_2 glove box and were bubbled with N_2 overnight. On exposure Day 0, Hg DGTs were removed from the N_2 box and immediately deployed into the exposure chambers in the same manner as the trace metals. DGTs were exposed for 2 or 3-d and deployment and recovery times were recorded to the minute. Upon termination of exposure periods, DGTs were rinsed immediately with distilled-deionized water to remove sediment. DGTs were placed in a labeled and clean plastic bag with minimal airspace and stored at 0-4°C until shipment to TTU laboratory for chemical extraction and analysis.

Briefly, once the trace metal and Hg DGTs were received at TTU, they were disassembled and the Chelex resin gels removed and placed in clean micro-centrifuge tubes. All laboratory manipulation and analysis were done in <0.2μm high-efficiency particulate air (HEPA) filtered working stations using acid-cleaned material. The resin gel was exposed to 1000 μL quartz-still grade nitric acid (Q-HNO_3) for 24 hours before analysis in order to dissolve the metals back in solution; allowing the resin gel to stay as a solid membrane instead of partially dissolving in solution. The digestion method of Hg from the DGT resin involved the treatment of cold (room temperature) HCl followed by BrCl oxidation (USEPA, 2002). Other trace metals were extracted from DGT's resins using the same method to tissue metal extraction as mentioned above. Metals were quantified in the acidic solution using ICP-MS. The acidic solution was diluted in metal-free water (18 MΩ/cm

H_2O), acidified to pH 2 with Q-HNO_3, and analyzed following the USEPA method 200.8, Revision 5.4 (USEPA, 1994).

The mass of the metal accumulated in the resin gel layer (M) was calculated using:

$$M = \frac{C_e * (V_{HNO3} + V_{gel})}{fe} \quad (3.30)$$

where Ce is the concentration of metals in the 1M HNO_3 elution solution (in µg/l), V_{HNO3} is the the volume of HNO_3 added to the resin gel, Vgel is the volume of the resin gel, typically 0.15 mL, and fe is the elution factor for each metal, typically 0.8.

The concentration of metal measured by DGT (C_{DGT}) was calculated using:

$$C_{DGT} = \frac{M * \Delta g}{D * t * A} \quad (3.31)$$

where Δg is the thickness of the diffusive gel (0.8 mm) plus the thickness of the filter membrane (typically, 0.14 mm), D is the diffusion coefficient of each metal in the gel, t is deployment time and A is the exposure area (A=3.14 cm^2).

3.5 Statistical analysis

Statistical approaches were used to strengthen the conclusions of the study and improve the certainty among different measurements. Firstly, two-way ANOVA was applied in the fractionated stormwater discharges for source identification of the associated contaminants based on their similar values to particulates found within the watershed. For biological effects in sediment assessment, statistical analysis were applied to evaluate the seasonal and spatial alterations of the bulk sediment metal concentrations, the DGT porewater, and the bioassay tissue concentrations among the sampling locations, P01, P08, P11 and P17 and between the sampling seasons 2015/2016 and 2016-2017. The statistical effects were evaluated using a “two-step model” that included Fisher’s exact test and a generalized

linear model using gamma regression. Finally, Spearman's correlation applied to the dataset for both seasons of pre and post measurements to identify the correlations among sediment, porewater, and tissue, and to evaluate the best predictor of biota accumulation. All statistical analyses were performed using the software R. The R coding that was used for each statistical test can be found in Appendix A.

3.5.1 Two-way ANOVA

Two-way ANOVA method is a hypothesis-based test that was used to examine the effect of two factors on a dependent variable (Swearer *et al.*, 2003). The two examined factors were, the location, C1W, C2W, O3W, and O4W, and the particle size, (>63 μm), (20-63 μm), (5-20 μm), and (0.45-5 μm), on the variable water metal concentrations (mg/kg). All analyses were done on log-transformed data in order to meet the normality and homogeneity of variance assumptions of ANOVA and the assumptions of multivariate normality and homoscedasticity. The method detection limits per metal (mg/kg) were placed instead of zero concentrations. Two-way ANOVA was used to identify the statistically significant differences ($p<0.05$, $\alpha=0.05$) of the metal concentrations (mg/kg) among the C1W discharges, that were directly deposited on the receiving sediments at Paleta Creek, the discharges from the industrial outlets O3W and O4W, and the highway/residential influenced creek location C2W.

3.5.2 "Two-step model" using Fisher's exact test and gamma regression

Statistical tools were used to identify whether or not the differences that were seen between the tissue, porewater and sediment measurements among different sampling locations P17, P11, P08, and P01 and different seasons, pre-storm, and post-storm were statistically significant with a confidence level of $\alpha=0.05$. The interaction effect of period and location

was also examined and represents whether, or not, the effect of the period depends on the location and likewise the effect of location depends on the period. The excessive 0 values in the dataset for some metal concentrations created a boundary condition that caused the analysis to occur in two steps. The first step included Fisher's exact test (Agresti, 2003) in order to identify whether or not the probability of the concentrations to be 0 is driven/associated by location or by period. The second step included a generalized linear model using gamma regression (similar hypothesis testing as the two-way ANOVA) that was applied only to the non-0, positive values of the dataset to examine the main effects of the period, the location, and their interaction effect. In the cases that the dataset consisted only of non-0 positive values then only the gamma regression was applied to the dataset.

3.5.3 Spearman's rank correlations

Spearman's rank correlation, which is the non-parametric version of the Pearson correlation, was applied to measure the strength of the association between the metal accumulation of biota on sediments and the metal bioavailability measured by DGTs porewater, but also between the metal bioaccumulation and the bulk sediment concentrations. Spearman's rank correlations were chosen due to the sparse nature of the study's dataset since Spearman's method is less sensitive to outliers (Hauke & Kossowski, 2011) and can also capture non-linear relationships. P-values were used to determine whether or not the statistical significance of the results can be repeated. However, the p-values are generally influenced by the effect size, the sample size, and the spread of the data. Therefore, p-values should not be the ultimate reference for whether or not the study is statistically significant. Confidence intervals (CI) were also determined in the study,

along with the p-values, to evaluate the magnitude of the size of the effect and the precision of the statistical estimation (Dahiru, 2008; Palesch, 2014).

3.6 References

Agresti, A. (2003). *Categorical data analysis* (Vol. 482): John Wiley & Sons.

Amirbahman, A., Massey, D. I., Lotufo, G., Steenhaut, N., Brown, L. E., Biedenbach, J. M., & Magar, V. S. (2013). Assessment of mercury bioavailability to benthic macroinvertebrates using diffusive gradients in thin films (DGT). *Environmental Science: Processes & Impacts, 15*(11), 2104-2114.

ASTM. (2000). Standard Guide for Determination of the Bioaccumulation of Sediment-Associated Contaminants by Benthic Invertebrates. In.

Dahiru, T. (2008). P-value, a true test of statistical significance? A cautionary note. *Annals of Ibadan postgraduate medicine, 6*(1), 21-26.

Drygiannaki, I., Rao, B., Dawson, J. A., Rakowska, M., Reible, D. D., Hayman, N. T., Rosen, G. H., Colvin, M. A., Chadwick, D. B., Pitt, R., Otto, M., Steets, B., & Ervin, J. (2020). Assessing sediment recontamination from metals in stormwater. *Science of the total environment*, 139726. doi:https://doi.org/10.1016/j.scitotenv.2020.139726

Hauke, J., & Kossowski, T. (2011). Comparison of values of Pearson's and Spearman's correlation coefficients on the same sets of data. *Quaestiones geographicae, 30*(2), 87-93.

Haywick, D. W. (2004). Pipette and sieve grain size analysis: Procedure Guides. In.

Palesch, Y. (2014). Some common misperceptions about P values. *Stroke, 45*(12), e244-e246.

Pitt, R., & Voorhees, J. (1995). *Source loading and management model (SLAMM).* Paper presented at the Seminar Publication: National Conference on Urban Runoff Management: Enhancing Urban Watershed Management at the Local, County, and State Levels.

Reible, D. D., Rao, B., Rakowska, M., Athanasiou, D., Drygiannaki, I., Bejar, M., Chadwick, B., Colvin, M., Rosen, G., Burton, G. A., Jr., Stecker, E., Steets, B., Otto, M., & Pitt, R. (2018). Assessment and Management of Stormwater Impacts on Sediment Recontamination. ER-2428, Final Report. *Strategic Environmental Research and Development Program, Alexandria, VA, USA*.

Swearer, S. E., Forrester, G. E., Steele, M. A., Brooks, A. J., & Lea, D. W. (2003). Spatio-temporal and interspecific variation in otolith trace-elemental fingerprints

in a temperate estuarine fish assemblage. *Estuarine, coastal and shelf science, 56*(5), 1111-1123. doi:https://doi.org/10.1016/S0272-7714(02)00317-7

USEPA. (1991). Evaluation of Dredged Material Proposed for Ocean Disposal_Testing Manual_ EPA 503/8-91/001.

USEPA. (1992a). *ACID DIGESTION OF WATERS FOR TOTAL RECOVERABLE OR DISSOLVED METALS FOR ANALYSIS BY FLAA OR ICP SPECTROSCOPY*.

USEPA. (1992b). *Specifications and Guidance for Contaminant-free Sample Containers*: U.S. Environmental Protection Agency, Office of Emergency and Remedial Response, Office of Solid Waste and Emergency Response.

USEPA. (1994). DETERMINATION OF TRACE ELEMENTS IN WATERS AND WASTES BY INDUCTIVELY COUPLED PLASMA - MASS SPECTROMETRY.

USEPA. (1996). *EPA Method 3050B: Acid Digestion of Sediments, Sludges, and Soils*.

USEPA. (1999). Method 1631, Revision B: Mercury in Water by Oxidation, Purge and Trap, and Cold Vapor Atomic Fluorescence Spectrometry Retrieved from https://nepis.epa.gov/Exe/ZyPDF.cgi/40001EQ2.PDF?Dockey=40001EQ2.PDF

USEPA. (2002). *Method 1631, Revision E:Mercury in Water by Oxidation, Purge and Trap, and Cold Vapor Atomic Fluorescence Spectrometry*

USEPA. (2013). *Appendix to Method 1631 : total mercury in tissue, sludge, sediment, and soil by acid digestion and BrCl oxidation*. [Anchorage]: [Susitna-Watana Hydroelectric Project].

Wang, P. F., Chadwick, D. B., Johnson, C., & Grovhoug, J. (2006). *Modeling Copper and Biocide Concentrations from Hull Paint Leachate in San Diego Bay*. Retrieved from

Wang, P. F., Cheng, R. T., Richter, K., Gross, E., Sutton, D., & Gartney, J. W. (1998). MODELING TIDAL HYDRODYNAMICS OF SAN DIEGO BAY, CALIFORNIA. *JAWRA Journal of the American Water Resources Association, 34*(5), 1123-1140.

Wang, P. F., Sutton, D., Richte, K., & Chadwick, B. (2000). *Modeling Migration of Sediment and Sorbed Contaminants Resuspended by Ship Docking in San Diego Bay.* Paper presented at the Proceedings of the 4th International Conference on Hydroscience & Engineering.

CHAPTER 4

ASSESSING SEDIMENT RECONTAMINATION FROM METALS IN STORMWATER[1]

[1]**Published as:** I. Drygiannaki, B. Rao, J. A. Dawson, M. Rakowska, D. D. Reible, N. T. Hayman, G. Rosen, M. A. Colvin, B. D. Chadwick, R. Pitt, M. Otto, B. Steets, J. Ervin, "Assessing Sediment Recontamination from Metals in Stormwater", *Science of the Total Environment*, *Vol 737*, 2020.

4.1 Abstract

Recontamination of sediments by stormwater is a major concern when evaluating the potential effectiveness of sediment remediation. Stormwater and sediment sampling were conducted in a mixed-use watershed at Paleta Creek in San Diego, CA to evaluate methods for assessing sediment recontamination by metals. Size-segregated stormwater contaminant loads with simultaneous receiving water and sediment measurements were used to identify dominant sources and contaminants with respect to their impact on sediment recontamination. Most of the stormwater contaminant loads of Cd, Cu, Pb, and Zn were associated with residential and highway sources from the upstream portions of the watershed and As, Ni and Hg were more significantly influenced by the downstream area of the watershed. Cd was strongly associated with large particles (>63 μm) and observed to settle in near shore areas with some attenuation due to mixing and dilution. Cu, in contrast, was associated more with the filtered fraction (<0.45 μm) and clay fraction (0.45-5 μm), resulting in less near shore sediment recontamination. Depositing sediment and other metals, particularly Cu and Hg, exhibited greater accumulation in settling traps than could be attributed to stormwater loads indicating the importance of other sources or resuspension of bay sediments on surficial sediment concentrations. Pb, Zn, Ni, and As showed influences of both stormwater and other sources. The study showed that measurement of size-segregated stormwater contaminant mass and concentrations

combined with simultaneous measurements of deposition in sediment traps could differentiate between recontamination by stormwater and that of other sources.

4.2 Introduction

Sediments may act as a sink or source of various contaminants and play a significant role in their storage and transport (Burton *et al.*, 2006; Durán *et al.*, 2012; Superville *et al.*, 2014). Sediments serve as a reservoir for metal and metalloid contaminants such as cadmium (Cd), copper (Cu), mercury (Hg), lead (Pb), arsenic (As), zinc (Zn) and nickel (Ni) that have been linked to ecological and chronic human health risks (Arambourou *et al.*, 2020; Bi *et al.*, 2017; Reible, 2014; Tchounwou *et al.*, 2012). Stormwater is considered a major source of nonpoint contamination to surface waters, and the mobilization of contaminants through stormwater discharges may result in significant deposition to near zone sediments that can slow or reverse sediment recovery and limit the effectiveness of remediating sediments (Burton & Pitt, 2001; Camponelli *et al.*, 2010; Reible, 2014; Reible *et al.*, 2018; Zhao & Li, 2013). The high cost of remediating contaminated sediments makes understanding continuing sources of potential recontamination, such as stormwater, especially important.

Stormwater discharges occur in an inconsistent pattern (e.g. varying discharge volume and duration) over a diffuse area. It is often difficult to adequately characterize their contributions to sediments, since the characteristics of the watersheds and pollutant loadings vary through time and space (Burton & Pitt, 2001; Pitt *et al.*, 1995). The approaches to quantify stormwater sources and their characteristics are limited, as is the ability to relate those sources to resulting sediment recontamination following remediation and biological impacts on sediments (Reible, 2014). Metal contaminants in runoff can

occur as ionic and colloidal species as well as adsorbed or precipitated on particulates of various sizes and settling rates. The distribution of metal contaminants in particulates of different settling rates is particularly important to the resulting spatial distribution of sediment recontamination (Loch, 2001; Reible *et al.*, 2018; Zhu *et al.*, 2020).

Stormwater is generally characterized by contaminant load (Lee & Bang, 2000), but usually not distribution of contaminants by particle size or settling characteristics. Some work has examined relationships between metals in wash off particles versus road-deposited sediment particles using artificial rainfall and different particle size characterization (Zhao & Li, 2013). Research has also been conducted to measure the metal concentrations and toxicity in sedimentation tanks and stormwater ponds (Karlsson *et al.*, 2010). However, none of these studies evaluated the transport of particle-associated stormwater contaminants with simultaneous monitoring of the depositional rates in receiving waters and sediments. Transport of contaminants in large catchments can be difficult to link to stormwater discharges due to the complexity of the system (Cho & Lee, 2017; Peng *et al.*, 2016). Previous observations of stormwater discharges have primarily been monitored in relatively small catchments, 4-34 ha (Fai & Yusop, 2017). Substantially contaminated sediments can be flushed from the system during the initial stage of storms, and this “first flush phenomena” has been demonstrated numerous times (Schiff *et al.*, 2016; Soller *et al.*, 2005; Zuraini *et al.*, 2018). Moreover, in arid climates with extended dry periods, pollutants may build-up on impervious surfaces and wash-off into nearby water bodies once the wet season begins (Al Mamoon & Rahman, 2017; Tu & Smith, 2018). Southern California exhibits this type of behavior with over 84% of the annual average rainfall of approximately 10 inches occurring during the winter months from

November to March (based upon the years 1982-2012), while there is often no precipitation during the summer months of July, August, and September. The period with no precipitation can last six months or longer (Baguskas *et al.*, 2016; Vasey *et al.*, 2012).

The objective of this study is to improve the understanding of the contribution of stormwater discharges to sediment recontamination and identify useful tools to characterize that impact. The focus was on a watershed in San Diego that had both residential, commercial and highway sources of stormwater runoff as well as industrial stormwater runoff associated with Navy Base San Diego (NBSD). Particle size distribution of stormwater discharges was used as an indicator of the particle settling rates. Seasonal sampling of surficial sediments was coupled with sediment traps during the storm season. Sediment traps have been successfully used in previous studies providing an assessment of particle-associated contaminants contributing to sediment recontamination (Chadwick *et al.*, 2017). The study was conducted in three phases including sampling of sediment (surficial sediment) before and after the storm season, sampling of depositing sediments (settling traps) during the storm season, and stormwater assessment by direct sampling under selected storm events. The study is part of a larger effort to characterize the sediment recontamination and biological effects of stormwater contaminants at Paleta Creek in San Diego Bay, CA (Reible *et al.*, 2018). Previous work had focused on identifying the causes of stormwater toxicity in this creek (Hayman *et al.*, 2020). The current work is focused on assessing the characteristics of stormwater from the various source areas and evaluating approaches to assess the resulting sediment recontamination that can be useful not only in Paleta Creek but also in other areas that are facing sediment recontamination issues related to stormwater discharges.

4.3 Materials and methods

4.3.1 Sediment sampling of seasonal surficial cores and trap material

Multiple intact cores were hand-collected with SCUBA divers or using a Van Veen grab sampler in the receiving water locations P17, P11, P08 and P01 (Fig. 4.1). The sediment material that was used for chemical analysis was approximately the top 5cm (~100g) of a collected core. Triplicates of the homogenized surficial sediment from each intact sediment core were analyzed to obtain the bulk sediment concentrations. Station P17 is located close to the Paleta Creek discharge, C1W, and the other locations are located progressively further from the creek mouth to P01, was taken to represent background conditions in San Diego Harbor. The sediment cores were sampled in 2015, 2016 and 2017, as shown in Fig. 4.2 and Table 4.1.

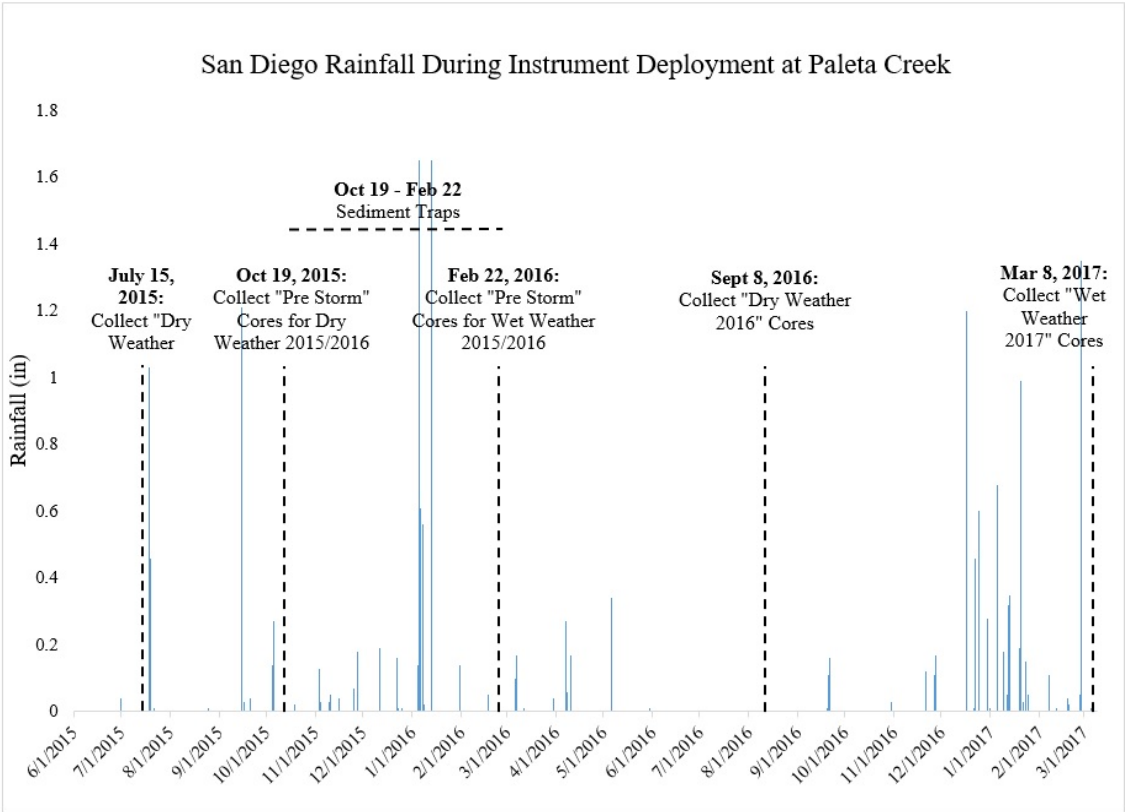

Figure 4.1: Sediment sampling efforts at Paleta Creek.

Three PVC cylindrical sediment traps with dimensions 81.3cm x 15.2cm were deployed in each of the sediment sampling stations P17, P11, P08 and P01 (captured masses~500-1,300g) on 19th of October 2015 and retrieved on 23rd of February 2016 and thus represent the composite sediment deposition through the entire wet season (Fig. 4.2 and Table 4.1). Each of the sediment traps was prefilled with hypersaline brine and topped off with ambient seawater. The traps were capped and lowered into the water with divers who secured the traps to pre-deployed posts on the sediment surface. Once dive activities were completed, divers removed caps from each sediment trap. Sediment traps were capped when diving related activities occurred on station to avoid potential deposition from those efforts. At the termination of the sediment trap deployment period, divers placed caps back on the traps and recovered and transferred to the surface crew with the assistance of a boat-mounted davit. The traps were transported back to the Space and Naval Warfare Systems Center Pacific (SSC Pac) laboratory and allowed to settle. Once the trap material sufficiently settled, the overlying water was removed, and the remaining material was subjected to chemical analysis. All three traps at a given location were combined prior to analysis. The sediment metal concentrations (mg/kg) in the settling traps were multiplied with the total collected mass of each trap and divided by the surface area of the cylindrical trap and by the time of deployment to provide the deposition flux of the metals in each sediment trap location.

4.3.2 Site description

The study area was Paleta Creek in San Diego, CA which drains a mixed-use urban watershed above the naval base and discharges into San Diego Bay at NBSD (32°40'27.9192"N, 117°6'55.998"W) (Fig. 4.1). San Diego Bay is relatively long and

narrow, 25km length and 1-3km wide, and tides and currents within the bay can move sediment around and in and out of the bay as can storm events and propeller wash from ships (Wang *et al.*, 2000). The Paleta Creek watershed is approximately 8.1 square kilometers and consists of residential (42%), and commercial (27%) land uses as well as roads (20%) upstream and industrial/military uses (11%) associated with NBSD downstream (Reible *et al.*, 2018). The State Water Resources Control Board characterizes Paleta Creek as a high priority toxic hot spot due to amphipod sediment toxicity findings in the Consolidated Toxic Hotspots Cleanup Plan (SWRCB, 1999). Stormwater from the watershed discharges primarily during seasonal rains in the winter months November until March; while the summer months are considered dry.

4.3.3 Stormwater sampling

Intensive stormwater sampling occurred during the 2015/2016 rain season using ISCO 6712 automatic water samplers to capture time-integrated water samples of stormwater at the locations shown in Fig. 4.1. The samplers at all locations were programmed for time-spaced composite sampling and adjusted to reflect the predicted storm intensity and duration, as forecasted by the National Weather Service (NWS). Salinity and area-velocity meters were used to trigger the start of sampling to ensure collection of stormwater rather than tidal return flows.

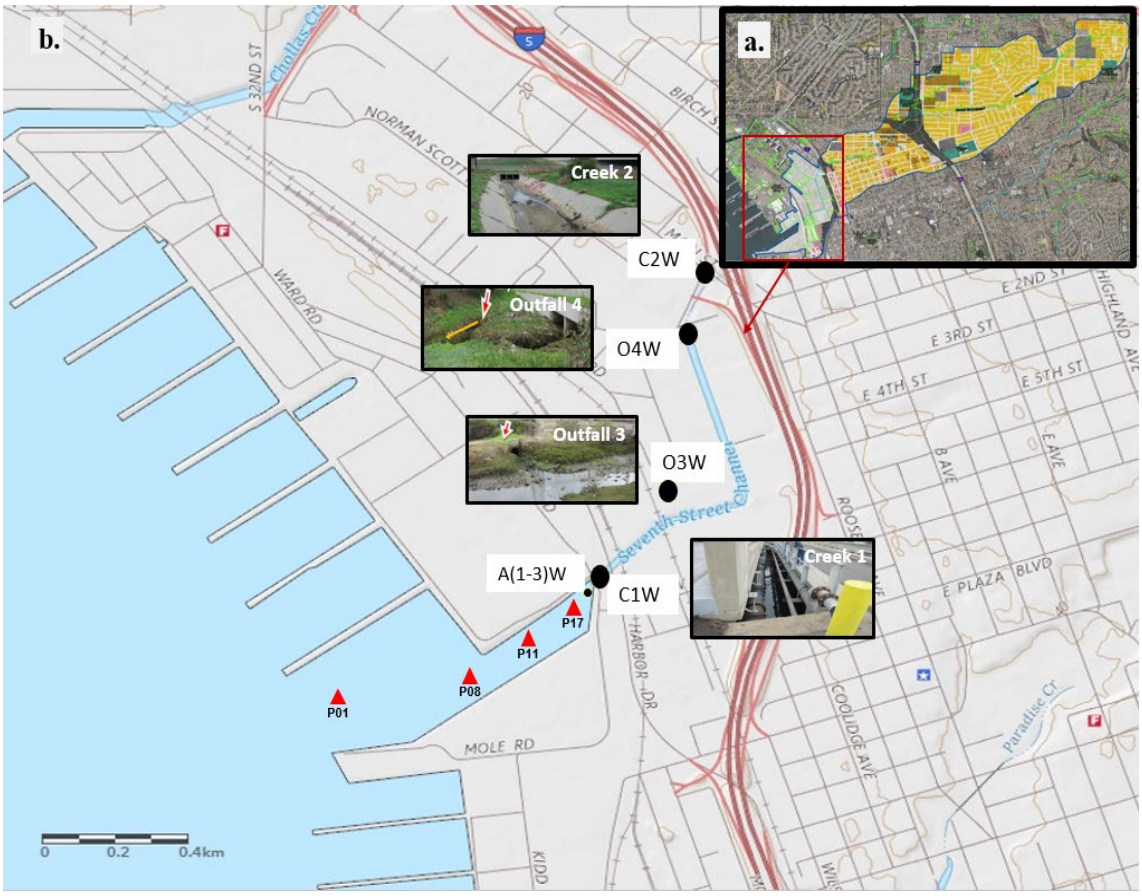

Figure 4.2: Map of the Paleta Creek site (California, USA) with (a) the map of the Paleta Creek watershed, and (b) the locations of the stormwater samples collection (in yellow) and the sediment samples collection (in red) in the lower watershed mouth area.

The captured events that will be discussed in this study were collected from 5th-7th of January 2016 (event 1 of 2.82 inches of precipitation over 26 hours of sampling and 4.65 inches over the entire event) and 30th January-1st February 2016 (event 2 of 0.20 inches of precipitation over 7.25 hours). The stormwater sampling efforts are presented in Table 4.1. Together these two storms represented 90% of the total precipitation in San Diego during the period of trap deployment in the receiving waters during the 2015-2016 wet season (Fig. S1, supplementary information). The storm intensity and duration of these two storms were also similar to at least 75% of the storms that occurred during the 2015-2017 study period (Fig. S2, supplementary information). Typically, approximately half of the total

seasonal precipitation comes from a small number of events with greater than 1inch total precipitation (represented by event 1), while the bulk of the remaining precipitation falls in more numerous events with 0.1-0.2 inches total precipitation (represented by event 2). The discharge sampling location from Paleta Creek, C1W into San Diego Bay is of primary interest here although integrated samples were also collected at other outfalls, O3W and O4W, contributing stormwater to the creek and receiving waters (Fig. 4.1 and Table 4.1). Automated time-integrated samples were also collected at location C2W, which is upstream of the Naval Base (Fig. 4.1 and Table 4.1) and reflects discharges from the upper urbanized reaches of the watershed. Supplementary ambient grab samples, A(1-3)W, were also collected in the receiving waters near C1W in a time series.

Table 4.1: Stormwater sampling locations and events.

Location	Event 1	Event 2	Year	Description
C2W	5th-7th Jan	30th Jan-1st Feb	2016	Upstream creek, close to highway
O4W	5th-7th Jan	30th Jan-1st Feb	2016	Outfalls, close to industrial use areas
O3W	5th-7th Jan	30th Jan-1st Feb	2016	
C1W	5th-7th Jan	30th Jan-1st Feb	2016	Downstream creek, primary discharge in San Diego Bay
A1W	5th of Jan at 13:27h	31st Jan at 09:00h	2016	Ambient sampling in time series, close to the primary discharge C1W
A2W	5th of Jan at 19:47h	31st Jan at 15:00h	2016	
A3W	6th of Jan at 03:33h	NA[a]	2016	

[a]not applicable (NA) due to no sampling in the 2nd event.

Sediment sampling locations and seasons.

Type of sediment	Location	Date
Surficial cores	P17, P11, P08, P01	July 15, 2015
		Oct 19, 2015
		Sep 8, 2016
		Feb 22, 2016
		Mar 8, 2017
Sediment traps	P17, P11, P08, P01	Oct 19th, 2015 -Feb 22nd, 2016

4.3.4 Stormwater particle size distribution characterization

Particle size fractionation of the stormwater samples was conducted to identify the settling characteristics of the particles in stormwater after discharge into receiving waters. The

water samples were fractionated using stainless steel sieves of 63 and 20μm opening size and polytetrafluoroethylene (*PTFE*) membrane filters of 5 and 0.45μm pore size to obtain the contaminant and solid loads associated with various size fractions. The solids that were accumulated on the sieves were transferred into a 0.45μm pore size PFTE membrane filter for solid mass measurements. The total solids in sand (>63 μm), coarse silt (20-63 μm), fine silt (5-20μm) and clay (0.45-5 μm) fractions were measured by the differences in the solids collected on filters in adjacent size ranges. The bulk, sieved and filtered water samples were preserved simultaneously with 0.5%v/v hydrochloric acid (HCl) to reach pH<2 and were stored at 4^{o}C.

4.3.5 Metal extraction and chemical analysis of stormwater samples

Triplicate sets of the water filtrates were subjected to metal extraction using nitric acid (HNO_3) and HCl digestion (USEPA, 1992). Triplicate aliquots of the digested samples were analyzed using ICP-MS (EPA Method 200.8) to obtain the total recoverable concentrations per fraction and the final filtered concentrations for the metals Cd, Cu, Ni, Zn, As, and Pb. A separate set of aliquots was preserved with 2% bromine monochloride (BrCl) for Hg analysis, using the MERX-T automated system (EPA 1631) from Brooks Rand (USEPA, 2002).

The contaminant concentration in the filtered fraction (<0.45 μm) was measured directly in the filtrate, while the contaminant concentrations in the various size fractions were measured by the differences in concentration between filtrates, i.e. sand (bulk analyses minus <63μm fraction), coarse silt (<63 minus <20 μm), fine silt (<20μm minus <5 μm), clay (<5μm minus <0.45 μm) (Gee & Or, 2002; Reible, 2014). The schematic representation of the stormwater particle size characterization and analysis of metal

contaminants is presented in Fig. S3 of supplementary information. Details of the particle size fractionation method for stormwater samples are described by (Reible *et al.*, 2018).

The metal constituents in stormwater discharges were characterized by a *stormwater metal concentration* either in the bulk stormwater or associated with a particular filtered particle size range (e.g. μg/L), or as a *stormwater metal solid concentration* which is contaminant concentration normalized by the mass of solids in the stormwater volume, i.e. stormwater metal concentration divided by the suspended solids concentration (e.g. mg/kg). These quantities can also be defined on the basis of the total stormwater or in a particular particle size interval.

4.3.6 Metal extraction and chemical analysis of sediment samples

Triplicates of 1g dry weight sediment samples from each settling traps and sediment cores were digested using HNO_3 and hydrogen peroxide, H_2O_2, and the extracted metal concentrations of Cd, Cu, Ni, Zn, Pb, and As were analyzed by the inductively coupled plasma mass spectrometry, ICP-MS, using the Perkin-Elmer SCIEX ELAN DRC II (USEPA, 1996), EPA Method 200.8. For total mercury extraction from the sediment a modified EPA Method 1631 (USEPA, 2013) was applied. Triplicates of 1g dry weight sediment per sample were treated with HNO_3 and HCl for 24h at room temperature and the acid digested mixture was further oxidized with BrCl to prevent reabsorption of mercury to carbon particles, if present in the sample. The extracted Hg concentrations were analyzed by EPA Method 1631 using the Brooks Rand MERX-T automated system.

4.3.7 Particle size fractionation in sediments

To characterize the settling particles on the sediment bed, particle size fractionation was applied to the sediment trap material. The total deposition was measured, and triplicates of

the cylindrical trap material were analyzed from each of the four sampling sites. For each sediment trap, an aliquot of well homogenized sediment or solids was dried. Dispersant of 1% w/v of sodium hexametaphosphate, $(NaPO_3)_6$, was added to the sample in a1L glass cylinder bottle and was filled up with ultra-pure water. After sonication and mixing overnight, the mixed sample was sieved through a stainless-steel sieving system with 63μm opening size to obtain the sand-sized particles (>63μm). After that, the pipette method was applied and the fractions of clay (<2μm), fine silt (2-20μm) and coarse silt (20-63μm) were obtained using Stoke's equation. The process was adapted from the method described by (Haywick, 2004) and provided the mass of the different particle size fractions per trap. The mass per fraction divided by the surface area of each trap and by the time of deployment provided the deposition flux of flocculated sediment in each sediment trap location.

4.4 Results and Discussion

4.4.1 Stormwater concentration

The stormwater metal concentrations (e.g. in μg/L), metal concentrations on the solids in stormwater (e.g. in mg/kg) as well as the total suspended solids concentration (e.g. mg/L) are presented in Tables S1-S4 of supplementary information for the main Paleta Creek C1W discharge, the upstream C2W location, the sampled outfalls O3W and O4W, and the time series A(1-3)W in the receiving water adjacent to the stormwater discharge. Fig. 4.3 summarizes the solids (by particle size) that were discharged from Paleta Creek to San Diego Bay, C1W, as measured in the time-integrated samples collected over the entire period of events 1 and 2. Less than 10% of the total solids, by mass, were associated with the finest clay size particles (0.45-5μm) in either event (Fig.4.3). Sand-sized particles constituted 26% of the total particulates in stormwater that were discharged from Paleta

Creek in C1W during the high precipitation event, but only 7% during the low precipitation event (Fig. 4.3). This occurred even though 60% of the total stormwater solids at the C2W location, which includes stormwater from the upstream highway, residential and commercial areas, was associated with the coarse sand-sized particles during the low precipitation storm event (Table S2 of supplementary information). The low proportion of the coarse particles at the C1W discharge compared to the upstream C2W was apparently due to deposition and accumulation of these particles in the downstream portions of the stormwater conveyance system.

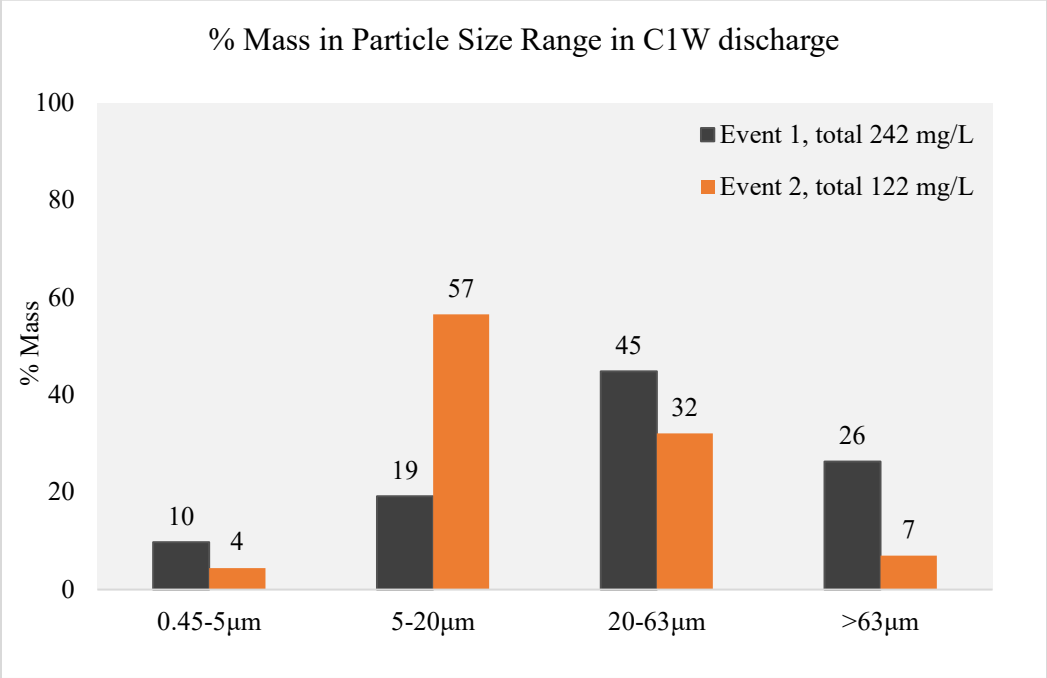

Figure 4.1: Percentage of mass of solids by particle size distribution in location C1W for events 1 and 2 (the total (>0.45 µm) concentrations for the key events are also shown).

The association of Cd with rapidly settling sand-sized particles in the first event is illustrated in Fig. 4.4 and would be expected to lead to rapid settling in receiving waters. Approximately 50% of the Cu discharged from C1W, however, was associated with particles smaller than 63µm with a substantial fraction (22%) passing a 0.45µm filter and

operationally defined as filtered (<0.45µm) during the first event (Fig. 4.4). The Cu association with fine fractions in both events could potentially lead to sediment bed contamination in locations further away from the Paleta Creek discharge or in water column impacts not reflected in sediment deposition.

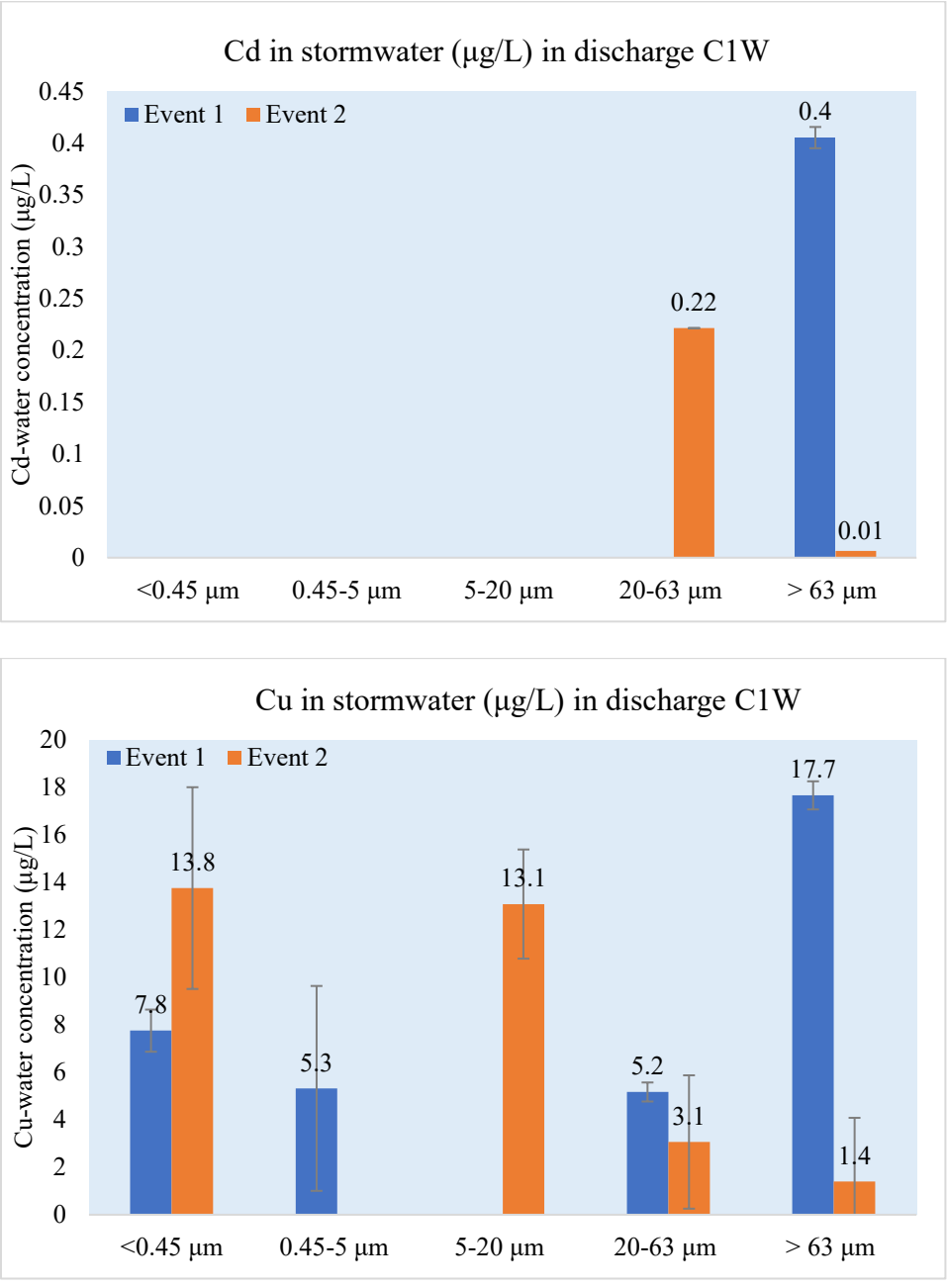

Figure 4.2: Cd and Cu stormwater concentration (µg/L) by particle size in C1W.

The rest of the measured metals showed behavior intermediate between that of Cd and Cu. In time-integrated sampling at C1W during event 1, approximately 60% of Hg, 70% of Zn and 90% of As were associated with fast-settling >63μm solids, that could lead to near shore deposition (Table S3, supplementary information). In C1W during the 2nd lower rainfall event, Hg and Zn were mostly associated with finer and dissolved fractions that could travel further before settling onto the sediment bed (Table S4, supplementary information). Most of the Pb at C1W in the 1st event was associated with sand-sized particles (>63μm), while during the second event was associated to a greater extent with the fine silts. During both events, the bulk of the Ni was associated with the non-particulate fraction (defined as passing the 0.45μm filter) (Tables S3 and S4, supplementary information) that would be expected to pose minimal sediment recontamination risk, if there is no aggregation and growth of colloidal particles.

Despite the significant difference in magnitude of the precipitation events, the contaminant concentrations were similar (less than a factor of two difference) at the C1W discharge and the *stormwater metal concentrations* (in mass per volume stormwater) during the low precipitation event were 56-93% of that during the high precipitation event. Cd exhibited the largest difference (56%), due to its association almost entirely with sand-sized particles (Tables S1-S4, supplementary information), which, as noted above, apparently deposited within the watershed. The *stormwater metal solids concentrations*, that is the average metal concentration on the suspended solids, were also similar between the events with the lower precipitation event showing 11-37% higher stormwater solids concentrations than during the high precipitation event. The similarity of the metal concentrations in both stormwater and on solid concentrations is useful in extrapolating results to other events.

The suspended solids normalized stormwater metal concentrations, i.e. the stormwater metal solid concentrations were also compared between the upstream C2W location and the downstream C1W location to evaluate the importance of the highway and residential sources from the upper watershed, C2W, and industrial sources from NBSD, O3W, O4W, to the creek stormwater discharge at C1W. As an overall indication of similarity, the stormwater metal solid concentrations of specific metals in individual particulate size fractions (N=7 metals x 4 size fractions x 2 events= 56) showed that C2W and C1W were well correlated (r^2 =0.82 and cosine θ similarity of 0.91). However, the other outfalls O3W and O4W were essentially uncorrelated with the C1W (r^2~0 and cosine θ similarity of 0.09) and effectively introduced significant volume into the stormwater flow but with minimal contamination.

This was further investigated by using two-way ANOVA and R to identify the statistically significant differences in metal concentrations among the outfalls C1W, C2W, O3W, and O4W. A log transformation was used to handle non-Normality, and the method detection limit was used in place of zero concentrations (Table S5, supplementary information). Table 4.2 shows that no significant differences were observed between C1W and C2W for any of the metals ($p>0.05$); however, significant and marginally statistically significant differences were observed between the discharge C1W and the NBSD outfalls O3W and O4W. This suggests again that the upstream residential, commercial and highway sources are dominant in the C1W discharge. Highway sources have been found to contribute Pb and Zn from exhaust particulates (Ellis *et al.*, 1987) as well as from tire wear (Davis *et al.*, 2001) and Cd from roadway sources such as brake components (McKenzie *et al.*, 2009). Only Ni and As and to a lesser extent Hg appear to be influenced significantly by the two

NBSD outfalls and the upstream sources from C2W since there are similar p values between all three locations and the discharge C1W.

Table 4.2: Significance of metal concentration differences between various outfalls. $p<0.05$ suggests significant differences among the metals concentrations between the primary stormwater discharge, C1W and the outfalls , O3W and O4W that directly discharge downstream of the primary discharge, as well as between the C1W and the C2W a measurement point upstream of the primary discharge). The significance levels were obtained from two-way ANOVA.

	Cd	Pb	Cu	Ni	Hg	Zn	As
C1W vs C2W	0.19	0.97	0.60	0.22	0.65	0.84	0.48
C1W vs O3W	NA[a]	0.002	0.03	0.18	0.09	0.006	0.18
C1W vs O4W	NA[a]	0.001	0.10	0.31	0.41	0.02	0.51

[a]not applicable (NA) due to no measurable values in O3W and O4W.

4.4.2 Receiving Water Impacts

A time series of samples were collected in the receiving waters near the primary discharge location C1W (Fig. 4.1 and Table 4.1). For the high precipitation event 1, the discharged solids (mg/L) were more concentrated in the initial flush A1W sample and decreased about 80% by the end of the event sample, A3W (Fig. 4.5). Similar trends were observed in the lower precipitation second event. Fine and coarse silt solids (5-20 and 20-63 μm) were dominant in the first flush with coarse solids decreasing over the course of the precipitation events (Tables S2, supplementary information). Particles with a diameter greater than 63 μm would require only a few minutes to settle in 3 m of water while 20 to 63 μm size particles in 3m would require more than an hour and <20 μm particles would require more than a day (Cheng, 1997). Water and particulate metal concentrations, like Cd and Cu, also showed the “first-flush phenomena”, as presented in Tables S1 and S2 of supplementary information.

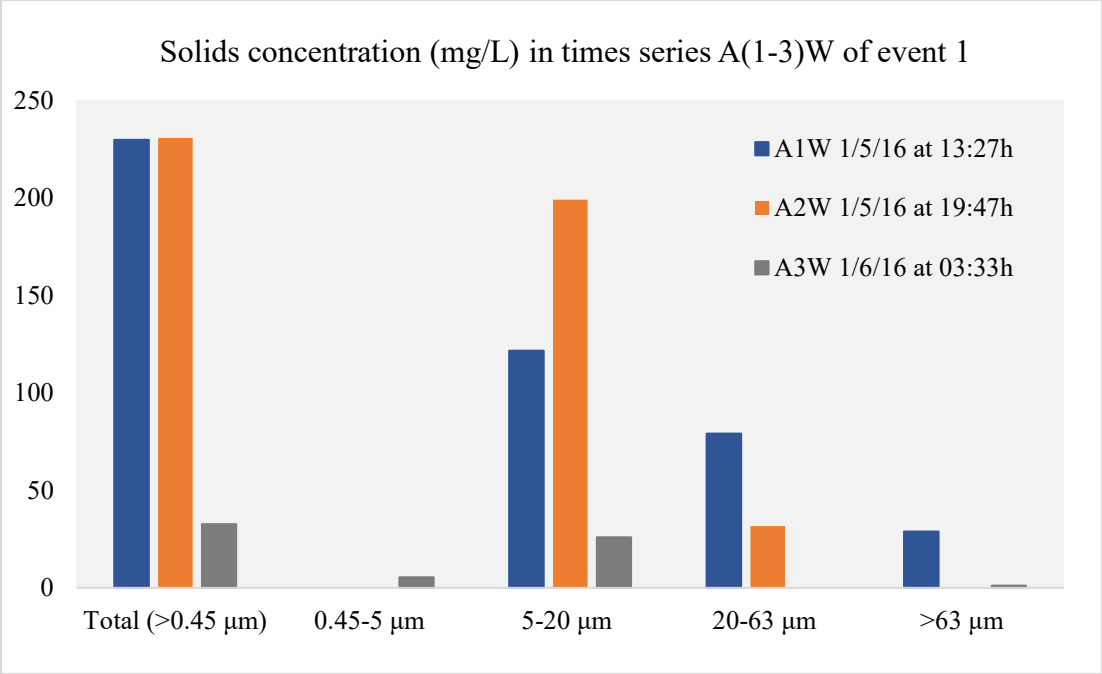

Figure 4.3: Solid concentrations in time series of samples, A(1-3)W, during the high precipitation event.

4.4.3 Sediment Recontamination

Metal recontamination of sediments due to Paleta Creek stormwater discharges was evaluated by surficial sediments collected pre and post storm seasons at the four receiving water sampling locations (P17, P11, P08, P01) (Fig. 4.1) in both 2015-2016 and 2016-2017 and with sediment traps placed at the same locations during the 2015-2016 wet season (Fig. 4.2 and Table 4.1). Pre-storm sediment cores were collected in July 2015, October 2015 and September 2016 to represent the dry season, while post-storm cores were collected in February 2016 and March 2017 near the end of the wet season (Fig. 4.2 and Table 4.1).

Statistical analysis of the surficial sediment concentrations was used to identify whether there were significant changes in sediment concentrations as a result of the wet season stormwater discharges. The effect of stormwater on the surficial sediment cores was evaluated by examining the statistically significant differences using gamma regression in

R (confidence level of α=0.05) of the sediment metal concentrations, location-wise, among the stations P17, P11, P08, and P01, and period-wise, between pre and post-storm season, during the sampling years 2015/2016 and 2016/2017 (Table S6). As noted in Table S6, sediment concentrations collected near the stormwater discharge were higher ($p<0.05$) for Cd, Cu, Ni and As but were only higher during post-storm season sampling for Ni. Significant interaction (of period and location) were noted for Cd, Hg, Pb, Zn and As making it impossible to identify the significance of either period or location. The results were also complicated by high variability at location P11 which contributed to the interaction effects and limited conclusions relative to both period and location.

Cd concentrations were significantly higher near stormwater discharge locations P11 and P17 locations compared to the more distant P08 and P01 locations (Fig. 4.6). As noted above, Cd in the stormwater discharge was primarily associated with sand-size particles, consistent with the apparent deposition in the near shore area. In contrast, Cu was widely distributed in surficial cores among the locations P17, P11, and P08 (Fig. S4, supplementary information) and were not easily connected to the stormwater discharges. This was also true of most other metals. As discussed below, it was generally not possible to identify statistically significant changes in sediment concentrations by location or between pre and post season likely due to the fact that sediment samples also reflected historical contamination. Recent deposition was much more clearly observed in settling traps as discussed below.

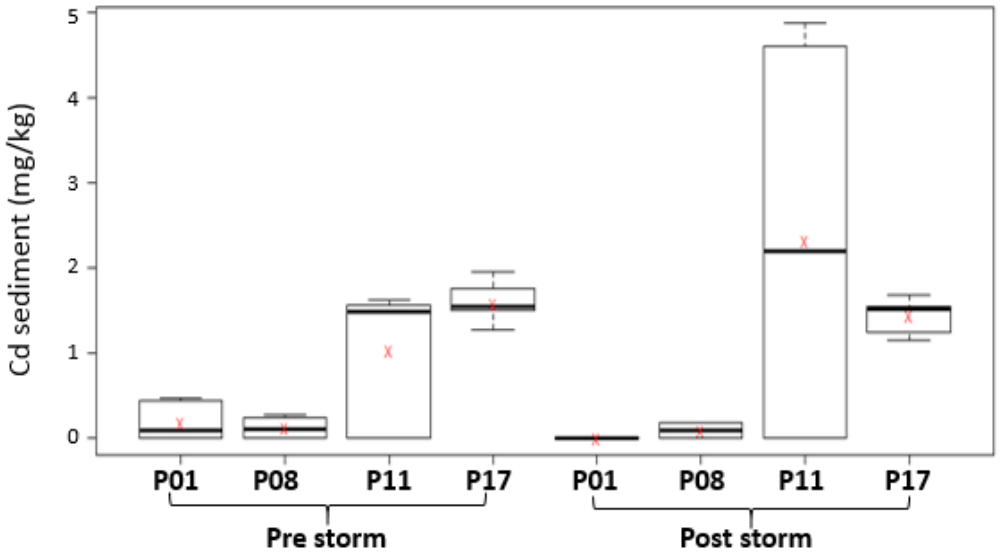

Figure 4.4: Boxplot of Cd sediment core concentrations (mg/kg) in the P17, P11, P08, and P01 for the "pre" and "post" seasons from 2015 until 2017. The red mark indicates the mean value of each dataset.

Sediment traps that directly measure depositing sediment were used to better link sediment recontamination to stormwater discharges. Sediment traps were deployed from October 19th, 2015 until February 22th, 2016 to monitor the particle deposition through the entire storm season of 2015-2016. Fig. 4.7 summarizes the deposition flux in different particle sizes for the traps at the sediment monitoring locations P17, P11, P08, and P01 using the sediment mass deposition divided by the surface area of each trap, 182.4 cm^2, and deployment time of 127 d. Substantial mass flux, 18.6 $mgcm^{-2}d^{-1}$, was observed for the solids in P17 trap close to the discharge C1W, which was about 50% greater than the fluxes measured at sites P11 and P08. Figure 4.7 shows that sand-sized particles settled relatively quickly with the greatest deposition at the near discharge location P17 and that finer particles were more important further from the discharge point.

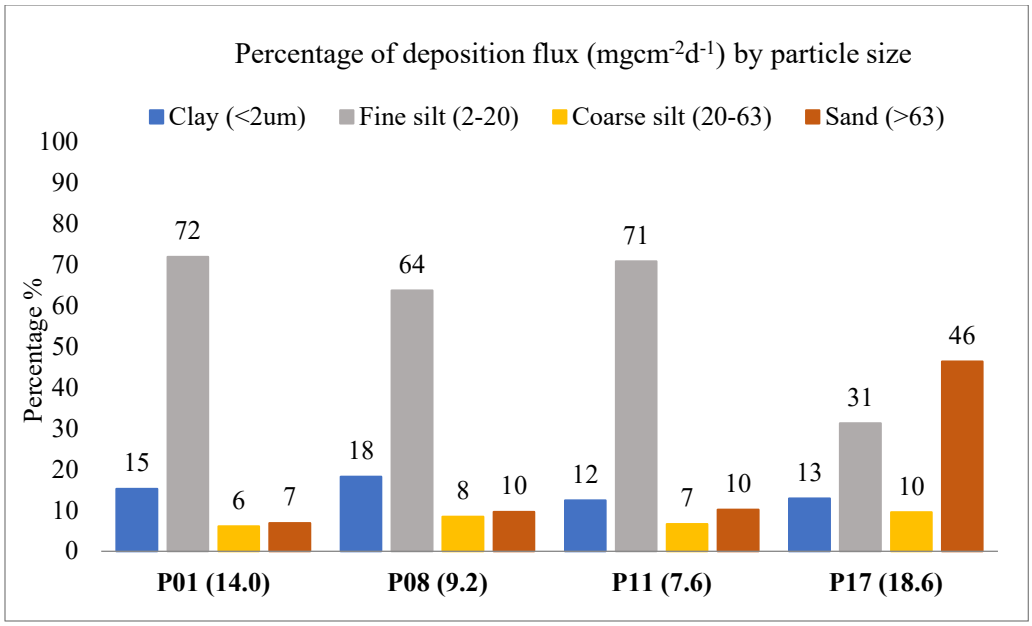

Figure 4.5: Percentage of deposition flux ($mgcm^{-2}d^{-1}$) by particle size of flocculated sediment from Paleta Creek. The total deposition flux for each site P01, P08, P11, and P17 presented in parentheses ().

Fig. 4.8 illustrates the solid-associated Cd and Cu deposition flux in the settling traps at the various locations. The Cd flux was the highest in the near-discharge P17 trap, consistent with the association with large particles in the stormwater discharge. The Cd flux in P11 and P08 was smaller by a factor of 5 and 7, respectively, compared to P17. The trap furthest away from the storm discharge, P01, had essentially zero Cd flux (Fig. 4.8, top figure). In contrast to Cd, the Cu deposition flux increased in the sites furthest away from the storm discharge, P08 and P01 (Fig. 4.8, bottom figure).

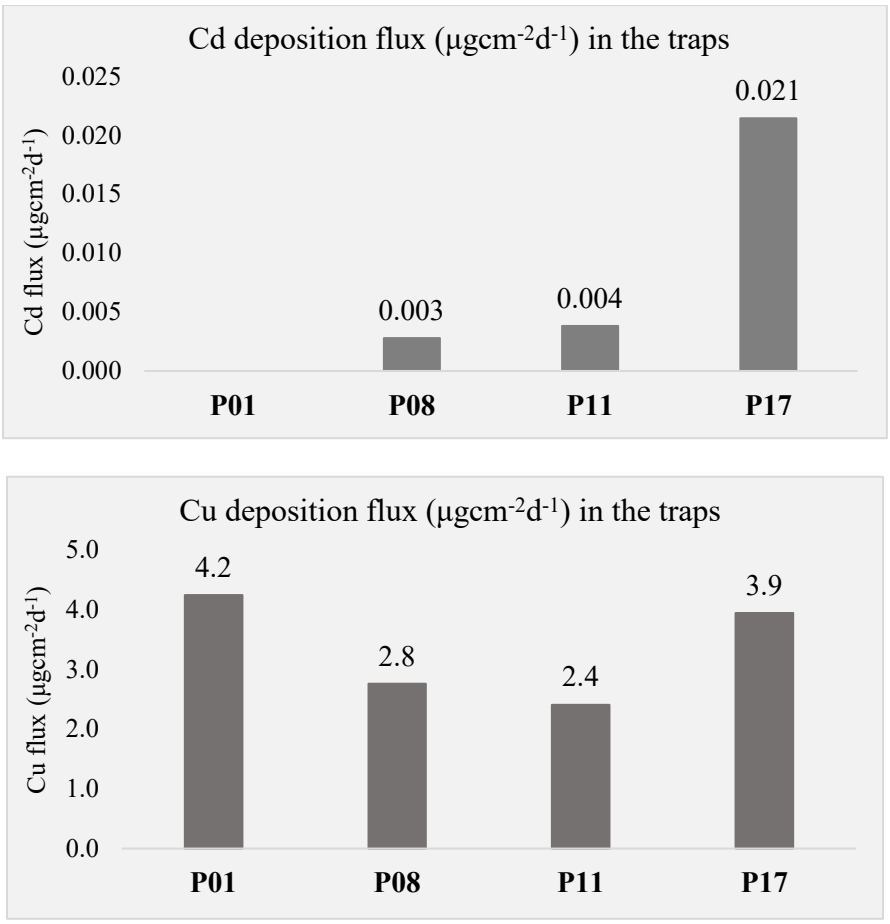

Figure 4.6: Cd and Cu deposition flux (µgcm^{-2}d^{-1}) in the traps during the 2015-2016 season.

As noted above, only stormwater discharges of particles >63 µm are expected to be able to settle in the P17 trap. Cd, which is largely associated with these coarse particles was largely observed to settle at this location and there is little Cd observed away from the stormwater discharge point. Cd can be used as an "indicator" of the settling of these large particles from the stormwater discharges. If a metal shows substantially greater amounts of contamination in the P17 trap than expected from their association with large particles in the stormwater discharge, it would be expected that other sources or resuspension and settling from the portions of the bay well away from the Paleta Creek discharge may be responsible for the observed sediment contamination. The ratio of the metal contaminant

mass collected in the P17 trap relative to the coarse particle discharge in the Paleta Creek stormwater was used to identify the expected metal deposition in the P17 sediment trap.

$$\frac{M_d^{P17} W_i}{V_w C_{C1W}^{>63\mu m}} = \frac{[kg][mg_i / kg]}{[L][\mu g_i / L]}\left[10^9\ \mu g / kg\right] = \frac{mg_i}{kg_i} \quad (4.1)$$

Here, M_d^{P17} is the deposited solid mass at P17 trap (kg) and W_i is the metal sediment concentration in the P17 trap (mg/kg) which should be the dominant trap recipient of these coarse particles. $C_{C1W}^{>63\mu m}$is the metal concentration in the largest particles in the C1W stormwater discharge (µg/L) and V_W is the total C1W outflow (L) during the high precipitation event 1 (~10^8L).

For Cd, this calculated ratio was 37.3 mg Cd deposited at P17 per kg of Cd in > 63 µm particles discharged at the mouth of Paleta Creek, C1W. The ratios for total particles and the other metals are shown in Table 4.3. For total sediment, the ratio is 207 mg of total particles were deposited per kg of >63 µm particles in the stormwater effluent during the high precipitation event 1. The larger ratio of total particles compared to sand-sized particles as well as the higher ratios of all metals except As (Table 4.3) suggest that additional sediment is being deposited in sediment traps from sources other than stormwater from Paleta Creek including potentially sediment resuspension from the bay (Frémion *et al.*, 2016; Reible, 2014; You & Chen, 2019).

Table 4.3: Ratio (mg/kg) of deposited total mass of contaminants/particles in near shore P17 sediment trap (mg) to the discharged sand-associated contaminants/particles of event 1 (kg).

	Particles	Cd	Pb	Cu	Ni	Hg	Zn	As
P17 mass collected (mg)	1,300,000	1.5	163	274	29.9	0.4	727	9.5
$C1W_{(>63\mu m)}$ mass discharge (kg)	6,260	0.04	1.2	1.7	0.49	0.0027	10.4	3.5
Ratio (P17/Discharge) (mg/kg)	207	37.3	136	158	61.0	165	70.1	2.7

As a further indication of the significance of other sources, Cu and Hg in the most distant sediment trap, P01, were more concentrated on the solids than the suspended solids in the stormwater discharged from Paleta Creek during either storm event (Tables S1, S2, S3, S4 and S7, supplementary information). This suggests that Cu and Hg collecting in the sediment trap at P01 were likely from sources other than the Paleta Creek stormwater discharge. Resuspension or return tidal flow in San Diego Bay of more concentrated bay sediment and/or discharges from other more concentrated sources were likely leading to the higher sediment concentrations in P01 and also the apparent increases in sediment deposition of metals such as Cu and Hg relative to discharge in the stormwater.

In an effort to estimate annual stormwater discharges, a WinSLAMM model (Pitt, 2014) was calibrated to the measured stormwater discharges and used to estimate contaminant loads during all storm events during the 2015-2016 sediment trap deployment period (Reible *et al.*, 2018). WinSLAMM was developed to evaluate stormwater runoff volumes and pollutant loadings in developed areas during a wide range of rain conditions, not just very large storms that are the focus of conventional drainage design models. WinSLAMM

can use any length of rainfall record as determined by the user, from single rainfall events to several decades of rains (Pitt & Voorhees, 1995).

The stormwater discharges obtained from WinSLAMM modeling were also compared to contaminant mass deposited in the areas around each of the sediment traps close to the Paleta Creek discharge, P17, P08, and P11. The measured deposition at these locations were assumed applicable to the center of a rectangular area around each settling trap location with dimensions equal to the half of the distance to the boundaries of the channel. This is equivalent to assuming that the deposition was a maximum at the settling locations but decreased linearly to the boundary around these deposition measurement locations. This suggests an effective settling area around P17 of 0.4 hectares, P11, 0.5 hectares and P08, 0.6 hectares as shown in Table 4.4. The comparison of the discharges to the deposition showed that essentially 100% of the Cd was deposited within the studied area, as expected from the association of Cd with large particles noted earlier. However, the deposition of other metals appeared to be significantly more than what can be accounted for from the Paleta Creek discharge at C1W (Table 4.4). This is further evidence that there is more sediment settling in this area and leading to recontamination than is apparently being discharged from Paleta Creek.

Table 4.4: Percentage of WinSLAMM estimated total mass release (kg) during trap deployment period to the total mass deposited in the settling traps (kg) at Paleta Creek, CA locations P17, P11 and P08.

	Particles	Cd	Pb	Cu	Ni	Hg	Zn	As
WinSLAMM mass discharge (kg)	37,000	0.15	4.2	10.1	1.85	0.040	49	2.48
P17 mass deposited (0.4)[a]	92,000	0.10	11.6	19.5	2.12	0.032	52	0.67
P11 mass deposited (0.5)[a]	52,000	0.03	5.5	16.6	1.52	0.030	24	0.66
P08 mass deposited (0.6)[a]	68,000	0.02	5.8	20.3	1.91	0.042	27	0.84
Total mass deposited (kg)	212,000	0.15	22.9	56.4	5.55	0.104	103	2.17
Percentage (Discharge/Total)	18%	100%	18%	18%	33%	39%	48%	114%

[a] estimated area of each trap in hectares.

4.5 Conclusions

The primary goal of this study was to explore approaches to characterize stormwater contamination by metals and their association with sediment recontamination using the Paleta Creek watershed as a case study. To identify sediment recontamination from stormwater discharges, the most useful tools were stormwater monitoring of concentrations by particle size combined with sediment settling traps. Measurement of total contaminant loads (that are, not size segregated) would not be as useful in estimating the effects on sediment recontamination since it would provide no information on settling characteristics. Sediment trap information was also necessary to confirm sediment recontamination by stormwater and to indicate where sediment deposition could not be associated solely with stormwater sources. Bulk sediment concentrations, even of surficial sediment, were complicated by historical sources and sediment redistribution that made it difficult to link to stormwater discharges. Moreover, sampling at both the primary discharge of the watershed as well as upstream locations allowed inferences to be made as to the primary

sources of metals and the dynamics of different size particle transport in the stormwater conveyance system.

The results suggested that the association of Cd with large particles in stormwater, likely generated from upstream highway sources, led to readily detectable sediment recontamination near the creek discharge. The broader distribution of Cu with particle size led to more distant sediment recontamination and the evaluation of the concentration of depositing particles as well as the total mass of depositing particles suggested that sources other than the stormwater discharge from Paleta Creek were likely contributing to the sediment recontamination in the receiving waters.

Although stormwater characterization combined with receiving water sediment settling traps can identify sediment recontamination, additional information is needed to evaluate the implications of that recontamination such as effects on benthic or aquatic organisms. The relatively large particles associated with Cd, for example, may limit biological exposure and effects, and separate studies of these effects are ongoing.

4.6 References

Al Mamoon, A., & Rahman, A. (2017). Rainfall in Qatar: Is it changing? *Natural Hazards, 85*(1), 453-470.

Arambourou, H., Llorente, L., Moreno-Ocio, I., Herrero, Ó., Barata, C., Fuertes, I., Delorme, N., Méndez-Fernández, L., & Planelló, R. (2020). Exposure to heavy metal-contaminated sediments disrupts gene expression, lipid profile, and life history traits in the midge Chironomus riparius. *Water research, 168*, 115165.

Baguskas, S. A., Still, C. J., Fischer, D. T., D'Antonio, C. M., & King, J. Y. (2016). Coastal fog during summer drought improves the water status of sapling trees more than adult trees in a California pine forest. *Oecologia, 181*(1), 137-148.

Bi, S., Yang, Y., Xu, C., Zhang, Y., Zhang, X., & Zhang, X. (2017). Distribution of heavy metals and environmental assessment of surface sediment of typical estuaries in eastern China. *Marine pollution bulletin, 121*(1-2), 357-366.

Burton, E. D., Phillips, I. R., & Hawker, D. W. (2006). Factors controlling the geochemical partitioning of trace metals in estuarine sediments. *Soil and Sediment Contamination: An International Journal, 15*(3), 253-276.

Burton, G. A., Jr., & Pitt, R. (2001). *Stormwater effects handbook: A toolbox for watershed managers, scientists, and engineers*: CRC Press.

Camponelli, K. M., Lev, S. M., Snodgrass, J. W., Landa, E. R., & Casey, R. E. (2010). Chemical fractionation of Cu and Zn in stormwater, roadway dust and stormwater pond sediments. *Environmental pollution, 158*(6), 2143-2149. doi:https://doi.org/10.1016/j.envpol.2010.02.024

Chadwick, B., Colvin, M., Davidson, B., Rosen, G., & Burton, G. A., Jr. (2017). *Remedy and Recontamination Assessment Array*.

Cheng, N. S. (1997). Simplified settling velocity formula for sediment particle. *Journal of hydraulic engineering, 123*(2), 149-152.

Cho, J. H., & Lee, J. H. (2017). Stormwater runoff characteristics and effective management of nonpoint source pollutants from a highland agricultural region in the Lake Soyang watershed. *Water, 9*(10), 784.

Davis, A. P., Shokouhian, M., & Ni, S. (2001). Loading estimates of lead, copper, cadmium, and zinc in urban runoff from specific sources. *Chemosphere, 44*(5), 997-1009.

Durán, I., Sánchez-Marín, P., & Beiras, R. (2012). Dependence of Cu, Pb and Zn remobilization on physicochemical properties of marine sediments. *Marine environmental research, 77*, 43-49.

Ellis, J. B., Revitt, D. J., Harrop, D. O., & Beckwith, P. R. (1987). The contribution of highway surfaces to urban stormwater sediments and metal loadings. *Science of the total environment, 59*, 339-349. doi:https://doi.org/10.1016/0048-9697(87)90457-8

Fai, C. M., & Yusop, Z. (2017). Determination of stormwater first flush treatment strategies at tropical urban catchments. *Desalin. Water Treat, 79*, 196-203.

Frémion, F., Courtin-Nomade, A., Bordas, F., Lenain, J.-F., Jugé, P., Kestens, T., & Mourier, B. (2016). Impact of sediments resuspension on metal solubilization and water quality during recurrent reservoir sluicing management. *Science of the total environment, 562*, 201-215. doi:https://doi.org/10.1016/j.scitotenv.2016.03.178

Gee, G. W., & Or, D. (2002). 2.4 Particle-size analysis. *Methods of soil analysis. Part, 4*(598), 255-293.

Hayman, N. T., Rosen, G., Colvin, M. A., Chadwick, B. D., Rao, B., Athanasiou, D., Rakowska, M., Drygiannaki, I., Burton, G. A., Jr., & Reible, D. D. (2020). Seasonal Toxicity Observed with Amphipods (Eohaustorius estuarius) at Paleta Creek, San Diego Bay, USA. *Environmental toxicology and chemistry, 39*(1), 229-239.

Haywick, D. W. (2004). Pipette and sieve grain size analysis: Procedure Guides. In.

Karlsson, K., Viklander, M., Scholes, L., & Revitt, M. (2010). Heavy metal concentrations and toxicity in water and sediment from stormwater ponds and sedimentation tanks. *Journal of Hazardous Materials, 178*(1), 612-618. doi:https://doi.org/10.1016/j.jhazmat.2010.01.129

Lee, J. H., & Bang, K. W. (2000). Characterization of urban stormwater runoff. *Water research, 34*(6), 1773-1780. doi:https://doi.org/10.1016/S0043-1354(99)00325-5

Loch, R. J. (2001). Settling velocity – a new approach to assessing soil and sediment properties. *Computers and Electronics in Agriculture, 31*(3), 305-316. doi:https://doi.org/10.1016/S0168-1699(00)00189-7

McKenzie, E., Money, J., Green, P., & Young, T. (2009). Metals associated with stormwater-relevant brake and tire samples. *Science of the total environment, 407*(22), 5855-5860.

Peng, H.-Q., Liu, Y., Wang, H.-W., Gao, X.-L., & Ma, L.-M. (2016). Event mean concentration and first flush effect from different drainage systems and functional areas during storms. *Environmental Science and Pollution Research, 23*(6), 5390-5398. doi:10.1007/s11356-015-5657-2

Pitt, R. (2014). *The Use of WinSLAMM at Naval Bases to Predict Stormwater Pollutant Sources and to Identify Treatment Options*. Retrieved from http://unix.eng.ua.edu/~rpitt/Publications/8_Stormwater_Management_and_Modeling/WinSLAMM_modeling_examples/Site_Descriptions_Calibration_and_Sources_Feb_17_2014.pdf

Pitt, R., Field, R., Lalor, M., & Brown, M. (1995). Urban stormwater toxic pollutants: assessment, sources, and treatability. *Water Environment Research, 67*(3), 260-275.

Pitt, R., & Voorhees, J. (1995). *Source loading and management model (SLAMM).* Paper presented at the Seminar Publication: National Conference on Urban Runoff Management: Enhancing Urban Watershed Management at the Local, County, and State Levels.

Reible, D. D. (2014). *Processes, assessment and remediation of contaminated sediments*: Springer.

Reible, D. D., Rao, B., Rakowska, M., Athanasiou, D., Drygiannaki, I., Bejar, M., Chadwick, B., Colvin, M., Rosen, G., Burton, G. A., Jr., Stecker, E., Steets, B., Otto, M., & Pitt, R. (2018). Assessment and Management of Stormwater Impacts on Sediment Recontamination. ER-2428, Final Report. *Strategic Environmental Research and Development Program, Alexandria, VA, USA*.

Schiff, K. C., Tiefenthaler, L. L., Bay, S. M., & Greenstein, D. J. (2016). Effects of rainfall intensity and duration on the first flush from parking lots. *Water, 8*(8), 320.

Soller, J., ,, Stephenson, J., Olivieri, K., Downing, J., & Olivieri, A. W. (2005). Evaluation of seasonal scale first flush pollutant loading and implications for urban runoff management. *Journal of environmental management, 76*(4), 309-318.

Superville, P.-J., Prygiel, E., Magnier, A., Lesven, L., Gao, Y., Baeyens, W., Ouddane, B., Dumoulin, D., & Billon, G. (2014). Daily variations of Zn and Pb concentrations in the Deûle River in relation to the resuspension of heavily polluted sediments. *Science of the total environment, 470*, 600-607.

SWRCB. (1999). Consolidated Toxic Hot Spots Cleanup plan List and Findings Volume I: Policy, Toxic Hot Spots List and Findings. In (Vol. I).

Tchounwou, P. B., Yedjou, C. G., Patlolla, A. K., & Sutton, D. J. (2012). Heavy metal toxicity and the environment. In *Molecular, clinical and environmental toxicology* (pp. 133-164): Springer.

Tu, M.-C., & Smith, P. (2018). Modeling pollutant buildup and washoff parameters for SWMM based on land use in a semiarid urban watershed. *Water, Air, & Soil Pollution, 229*(4), 121.

USEPA. (1992). *ACID DIGESTION OF WATERS FOR TOTAL RECOVERABLE OR DISSOLVED METALS FOR ANALYSIS BY FLAA OR ICP SPECTROSCOPY*.

USEPA. (1996). *EPA Method 3050B: Acid Digestion of Sediments, Sludges, and Soils*.

USEPA. (2002). *Method 1631, Revision E:Mercury in Water by Oxidation, Purge and Trap, and Cold Vapor Atomic Fluorescence Spectrometry*

USEPA. (2013). *Appendix to Method 1631 : total mercury in tissue, sludge, sediment, and soil by acid digestion and BrCl oxidation*. [Anchorage]: [Susitna-Watana Hydroelectric Project].

Vasey, M. C., Loik, M. E., & Parker, V. T. (2012). Influence of summer marine fog and low cloud stratus on water relations of evergreen woody shrubs (Arctostaphylos: Ericaceae) in the chaparral of central California. *Oecologia, 170*(2), 325-337. doi:10.1007/s00442-012-2321-0

Wang, P. F., Sutton, D., Richte, K., & Chadwick, B. (2000). *Modeling Migration of Sediment and Sorbed Contaminants Resuspended by Ship Docking in San Diego Bay.* Paper presented at the Proceedings of the 4th International Conference on Hydroscience & Engineering.

You, Z.-J., & Chen, C. (2019). Coastal dynamics and sediment resuspension in Laizhou bay. In *Sediment Dynamics of Chinese Muddy Coasts and Estuaries* (pp. 123-142): Elsevier.

Zhao, H., & Li, X. (2013). Understanding the relationship between heavy metals in road-deposited sediments and washoff particles in urban stormwater using simulated rainfall. *Journal of Hazardous Materials, 246-247*, 267-276. doi:https://doi.org/10.1016/j.jhazmat.2012.12.035

Zhu, X., Chatain, V., Gautier, M., Blanc-Biscarat, D., Delolme, C., Dumont, N., Aubin, J.-B., & Kouyi, G. L. (2020). Combination of Lagrangian Discrete Phase Model and sediment physico-chemical characteristics for the prediction of the distribution of trace metal contamination in a stormwater detention basin. *Science of the total environment, 698*, 134263.

Zuraini, N. A., Alias, N., Yusof, Z. M., Hanapi, M. N., & Harun, S. (2018). *First flush analysis of urban stormwater runoff from an urban catchment in Johor, Malaysia.* Paper presented at the MATEC Web of Conferences.

CHAPTER 5

ASSESSING BIOTA ACCUMULATION DUE TO CONTAMINATION OF SEDIMENTS BY STORMWATER HEAVY METALS[1]

[1]The content of this chapter is identical to a paper submitted on 27th of June 2020 to the Environmental Toxicology and Chemistry Journal: I. Drygiannaki, M. Bejar, B, D. D. Reible, J. A. Dawson, B. Rao, N. T. Hayman, G. Rosen, M. A. Colvin

5.1 Abstract

Evaluating sediment recontamination due to stormwater discharges is important when evaluating the long-term effectiveness of sediment remedial efforts. In this study, the bioaccumulation of heavy metals in a clam *Macoma nasuta* exposed to stormwater contaminated sediment is assessed. Surficial sediments were collected before and after the winter wet seasons in 2015-2016 and 2016-2017 from Paleta Creek, CA and subjected to *ex situ* bioaccumulation assays and porewater characterization using diffusion gradient in thin film devices. Despite increases in bulk sediment concentration of some metals as a result of stormwater recontamination during wet seasons, significant reductions in biota accumulation and porewater concentrations were observed for all measured metals, Cd, Cu, Hg, Pb, Zn, Ni, and the metalloid As. This was apparently the result of the deposition of stormwater contaminants in low bioavailable forms. All the measured metals and metalloid in biota showed a positive significant correlation with porewater concentrations ($p<0.1$, $\alpha=0.1$) which were a better predictor of biota metal accumulation than bulk sediment concentration. In conclusion, observed bulk sediment recontamination due to stormwater should not be assumed to lead directly to greater biota accumulation without bioavailability assessment.

5.2 Introduction

Contaminated sediment sites pose some of the most difficult remediation and management issues (Reible, 2014; USEPA, 1998). Sediments play a significant role in the release and storage of potentially toxic metals that can lead to ecological and human health risks (Castillo *et al.*, 2013; Durán *et al.*, 2012; Reible, 2014). Heavy metals, like cadmium (Cd), copper (Cu), zinc (Zn), total mercury (Hg), nickel (Ni), lead (Pb), as well as the metalloid arsenic (As) pose serious risks to aquatic ecosystems due to their potential toxicity, non-biodegradable and persistent nature (Zhang *et al.*, 2019; Zhao *et al.*, 2016) presenting an assessment challenge when evaluating their fate and effects in sediments (Eggleton & Thomas, 2004).

One source of contamination in sediments that is particularly difficult to assess and manage is stormwater. Stormwater can lead to sediment contamination as well as recontamination after remediation (Drygiannaki *et al.*, 2020; Reible *et al.*, 2018). Storm events and their discharges may lead to periodic metal remobilization and release of contaminants into the sediment and water (Eggleton & Thomas, 2004; Hamzeh *et al.*, 2014; Rodriguez-Iruretagoiena *et al.*, 2016) or may directly impact the benthic communities of sediments (Hatch & Burton, 1999; Hayman *et al.*, 2020; Schiff & Bay, 2003). It is important to improve the understanding of the effect of storm events on sediment contamination/recontamination in aquatic sediments to develop more effective remedial approaches and evaluate their effectiveness (Leeson *et al.*, 2016). Assessing the bioaccumulation and availability of metals in sediments, like Cd, Ni, As, Zn and Cu, can be challenging due to their complex and often dynamic interactions with sediments (Burton, 2010; Peterson *et al.*, 1996; Zhuang *et al.*, 1994). Sediment bioassays are often

used to assess the exposure of marine organisms within sediment quality assessment programs (ASTM, 1995; Vethaak *et al.*, 2017). Bioaccumulation tests that are performed in the laboratory *ex situ* can generate comparable results to the exposure tests conducted *in situ* if the exposed organisms and conditions are similar to the biota inhabiting the field sediments. The clam species *Macoma nasuta* has been used for bioaccumulation exposure testing of marine and estuarine sediments (Kirtay *et al.*, 2018; Werner *et al.*, 2004). These bivalve species can uptake metals through the ingestion of sediments but also through porewater, burrow and overlying water (Winsor *et al.*, 1990).

Exposure metrics focused on total metal content in sediment have often not predicted biological effects in sediment-dwelling organisms (Crommentuijn & Polder, 1997; Di Toro *et al.*, 1992). The labile metal fraction is typically smaller than the total metals and the total sediment concentration can be misleading (Di Toro *et al.*, 1992). The biologically available fraction of sediment associated-contaminants has been linked to porewater concentration measurements of a variety of contaminants in sediment porewater (Ghosh *et al.*, 2014; Lampert *et al.*, 2015; Lydy *et al.*, 2014; Reible, 2014). Even if the route of exposure is via sediment solids, the porewater in sediments may still indicate the bioavailable contaminant fraction in those solids by indicating or reflecting the labile contaminants. Metals in porewater represent the net effect of the numerous interactions between the dissolved metal phase and the various solid phases in the sediments and provide an indication of the overall chemical activity of the metals in the sediment environment (Ankley *et al.*, 1994; Peijnenburg *et al.*, 2014). Previous studies have shown that porewater concentrations could be an indicator of the free metal ions and labile species in sediments (Leermakers *et al.*, 2005; Zhang *et al.*, 1998; Zhang *et al.*, 2002). Here, diffusive gradient in thin films (DGT)

that do not significantly disturb the sediment environment are used to measure porewater concentrations of metals in laboratory bioassays (Peijnenburg *et al.*, 2014; Reible, 2014; Simpson *et al.*, 2012; Zhang *et al.*, 1995). The DGT method can successfully determine metals in sediment porewater (Harper *et al.*, 1999; Wu *et al.*, 2011; Xu *et al.*, 2017; Zhang *et al.*, 1995) as well as remobilization fluxes of metals in sediments (Harper *et al.*, 1998). Previous studies have also indicated the usefulness of DGTs for biomonitoring (Clarisse *et al.*, 2011), for example, to indicate mercury bioaccumulation (Amirbahman *et al.*, 2013). Studies have also identified relationships between DGT measurements and bioaccumulation in chironomids for Cu and Pb (Roulier *et al.*, 2008).

The scope of the study is to present approaches for assessing the relationship between biological exposure, as indicated by bioaccumulation studies, and physicochemical measures in the stormwater and depositing sediment at Paleta Creek in San Diego Bay, CA. Surficial sediment cores were collected before and after the November to March wet season over two years and at four different locations to reflect spatial variations from the storm discharge point. More than 80% of the annual precipitation in San Diego typically occurs during these months (Climate-Data.org). *Ex situ* bioaccumulation studies were conducted on these cores using the marine clam *Macoma nasuta* for the metals Ni, Cu, Zn, Cd, Pb, and Hg as well as the metalloid As. Physicochemical measurements of the deposited sediments included bulk sediment concentration and porewater concentration, measured by DGTs. Statistical analysis was used to quantify the uncertainty and variability of the measurements and to estimate relationships among different observations. The analyses were used to define seasonal and spatial variations in metal bioaccumulation in bioassays and their relationship to sediment and porewater chemistry. The study is part of

a larger collaborative effort at Paleta Creek that examined the receiving water impacts and resulting bulk sediment recontamination due to stormwater metal runoff (Drygiannaki *et al.*, 2020), and identified the seasonal toxicity to amphipods as a result of pyrethroids (Hayman *et al.*, 2020).

5.3 Materials and Methods

5.3.1 Study area and stormwater assessment

Paleta Creek watershed flows directly through the Naval Base of San Diego that is located on the eastern shoreline in the central portion of San Diego Bay, California, USA (32°40'27.9192"N, 117°6'55.998"W) (Figure 5.1). Paleta Creek is a channelized urban/industrial creek with high flow rates associated with winter storm events, and low dry weather flow rates for the rest of the year. Previous studies have identified stormwater impacts in the benthic community and sediment toxicity at Paleta Creek Mouth in San Diego Bay, CA (Brown & Bay, 2005; Hampton & Chadwick, 2000; Rosen *et al.*, 2017; Yoon & Stein, 2007). As a result, state and regional regulators have prepared an action plan for each contaminant of concern at Paleta Creek, CA (Greenstein *et al.*, 2005). Monitoring of representative stormwater discharges from the location C1W (Figure 5.1) at the mouth of the stormwater conveyance system was used to assess bulk sediment metal recontamination during the storm seasons (Drygiannaki *et al.*, 2020). The stormwater discharge monitoring was also coupled with sediment traps and sediment coring at receiving water sediment locations P17, P11, P08 and P01 at Paleta Creek (Figure 5.1 and Table 5.1).

The stormwater discharge monitoring was also coupled with sediment traps and sediment coring at receiving water sediment locations P17, P11, P08 and P01 at Paleta Creek (Figure

5.1 and Table 5.1). The locations identified for receiving water sediment sampling were part of a larger network of sample locations for other studies and to avoid confusion the original location nomenclature was retatined. P17 is located close to the Paleta Creek storm discharge while P11, P08 and P01 are located further from the creek mouth (Figure 5.1).

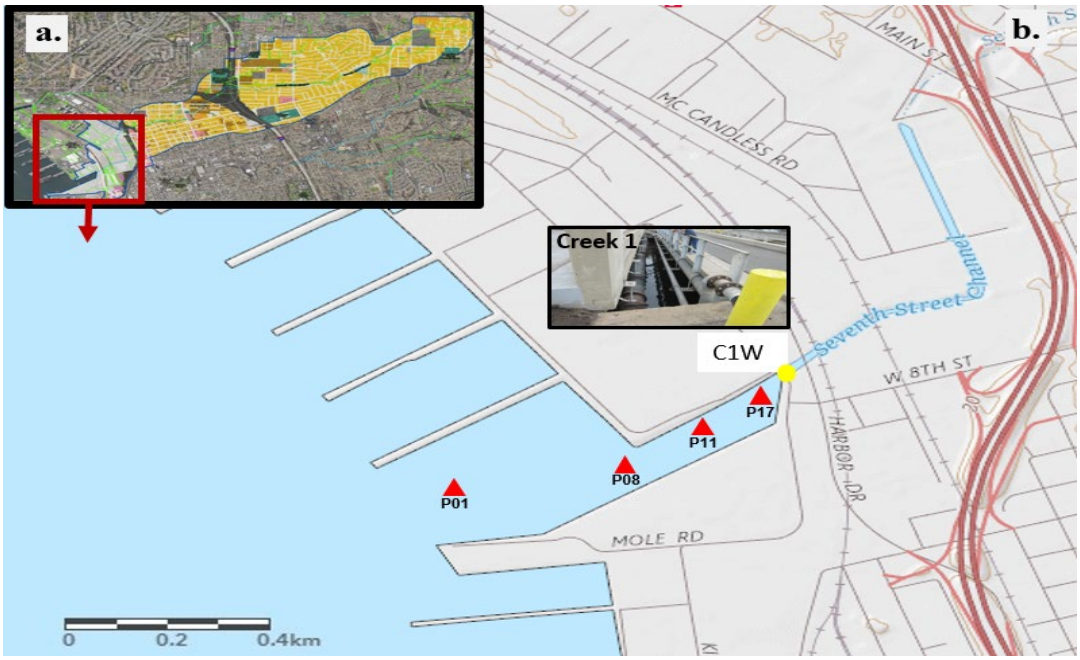

Figure 5.1: Map of the Paleta Creek site (California, USA) with (a) the map of the Paleta Creek watershed, and (b) the locations of the stormwater samples collection (circle) and the sediment samples collection (triangles) in the lower watershed mouth area.

Table 5.1: Sediment sampling in the locations P17, P11, P08, P01 during the years 2015-2017.

Type of sediment	Date	Description
Surficial cores	July 15, 2015	"Pre storm" 2015-16 season
	Oct 19, 2015	"Pre storm" 2015-16 season
	Feb 22, 2016	"Post storm" 2015-16 season
	Sep 8, 2016	"Pre storm" 2016-17 season
	Mar 8, 2017	"Post storm" 2016-17 season
Sediment traps	Oct 19th, 2015 -Feb 22nd, 2016	During 2015-16 storm season

*Seasonal storms at Paleta Creek, CA, have been historically observed from November

In order to evaluate the seasonal changes receiving sediment sampling occurred during the normally dry summer and fall as well as immediately after the end of the normally wet winter season during 2015-16 and 2016-17, as shown in Table 5.1. As shown in Figure 5.2, 75% of the precipitation during 2015-16 and 2016-17 occurred between pre- and post-wet season sampling. Typically more than 80% of precipitation falls between November and March but there were several storm events during summer and fall of 2015 that were deviations from the typical pattern. Pre-storm season sampling was conducted twice during 2015, during July and again October 19, 2015, the latter potentially influenced by the early fall storm events. Pre-post analyses as described herein were conducted with and without the October 19, 2015 samples and no change in conclusions were observed so the October 19, 2015 samples were retained as pre storm season samples.

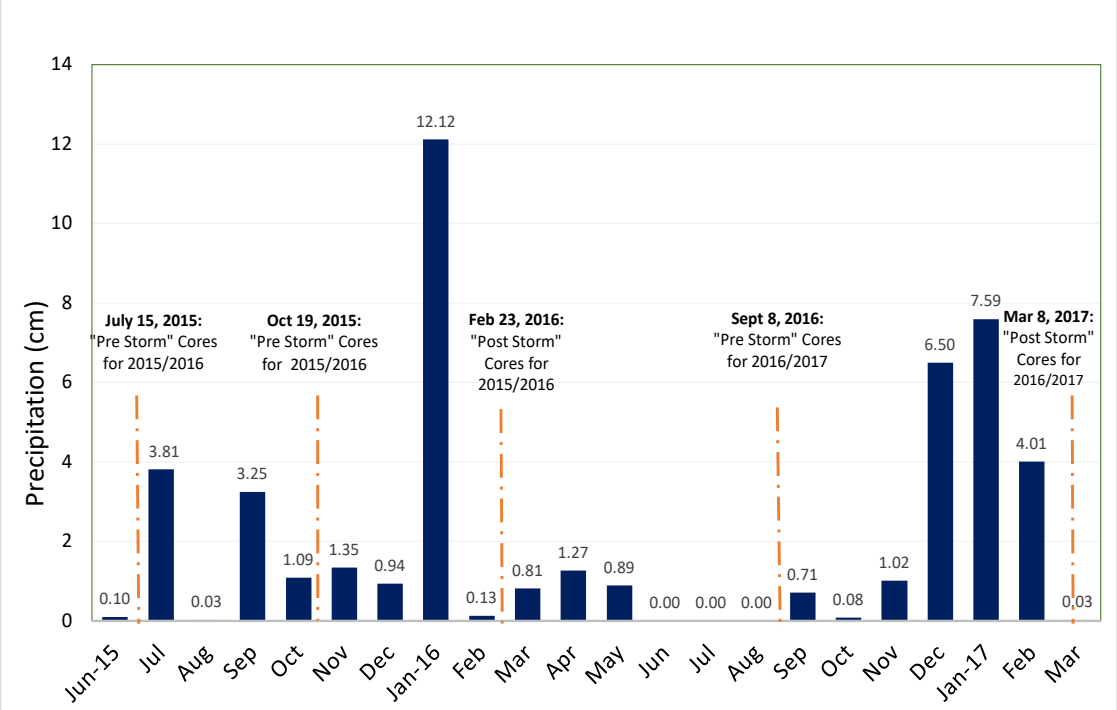

Figure 5.2: Monthly precipitation (in cm) relative to sediment sample collection days, 75% of the precipitation occurred during the "wet" season between pre and post storm season sample events (nominally Oct-March).

5.3.2 Sediment sampling

Samples were collected from each of the locations P17, P11, P08, and P01 (Figure 5.1) before and after storm seasons 15/16 and 16/17 (Table 5.1 and Figure 5.2). Sediment was collected via shallow hand-inserted coring with SCUBA divers in 15/16 and via Van Veen grab sampler followed by subsampling by coring from the grab sampler in 16/17. Multiple intact cores were sampled at each location using cellulose acetate butyrate core liners of 7cm diameter and 28cm length to ensure the collection of surficial sediment (~10cm depth). Two cores were sent vertically to Texas Tech University (TTU) for physical and chemical analyses and were preserved at 4°C until analyzed. The rest of the intact cores were transported to the Naval Information Warfare Center Pacific and were preserved at 4°C until initiation of *ex-situ* bioassays and passive sampler exposures. The upper 3-5 cm of the sediment cores (~100g) was used for both both bioassays and chemical analysis. The sediments in the receiving waters are typically reduced with a redox potential discontinuity with 2 cm of the surface close to shore (P17 and P11) and increasing to ~4 cm furthest from shore (P01) with sulfides increasing below this depth to 150-500 μM (Chadwick *et al.*, 2006). pH in the sediments is 7.4-7.6 while the overlying water is close to saturated with oxygen and pH is ~8. Conditions in the *ex-situ* bioassays are summarized below.

5.3.3 Sediment analyses

Triplicates (~1g dry weight) of each intact sediment core sample were digested using nitric acid, HNO_3, and hydrogen peroxide, H_2O_2, using EPA method 3050B (USEPA, 1996). The digested extracts were analyzed using inductively coupled plasma mass spectrometry, ICP-MS (Perkin Elmer Elan DRC-e), for the metals Ni, Cu, Zn, Cd, Pb, and the metalloid As via EPA Method 200.8 (Creed *et al.*, 1994). Metal recoveries were 87-103% based upon a

standard reference material (SRM 1944). Response criteria for scandium, terbium and indium internal standards were 60-125%. Every 10 samples a blank of 2% v/v HNO_3 and a calibration check standard were analyzed with an acceptance criteria of concentration below lowest calibration point in the blank and 80-120%, respectively. Seven point calibrations with r^2>0.99 and an RSD of <20% over the entire calibration range were required. Calibration ranges for all analytes are included in Table S1 in the Supplementary Information (SI). The practical quantification limit was taken as the lowest calibration concentration meeting the 20% RSD criteria. Any samples not meeting QA criteria were reanalyzed. Average metal sediment concentrations measured for each of the sampling events are included in Table S2, SI.

Mercury analyses proceeded by HNO_3 and HCl, addition for 24h at 20°C, with further oxidization using bromine monochloride (BrCl) to prevent reabsorption of mercury to carbon particles if present in the sample (USEPA, 2013). The extracted Hg was analyzed by EPA Method 1631(USEPA, 2002) the Brooks Rand MERX-T automated system employing cold vapor atomic fluorescence spectrometry. Criteria for recoveries and calibration checks were 77-123%. Other QA procedures were as noted above. Any samples not meeting criteria were reanalyzed.

Triplicate samples (~10g dry weight each sample) of each collected intact sediment core from the pre and post storm season 2016/2017 were processed for particle size distribution to obtain the fractions of clay (<2 μm), fine silt (2-20 μm) and coarse silt (20-63 μm) and sand (>63 μm) (Table S3, SI). The sediment cores from all the seasons and locations were also analyzed for total organic carbon (TOC) (Table S4, SI). The furthest site from the

stormwater discharge (P01) exhibited a higher sand fraction and lower organic carbon that the locations closer to the discharge (P17).

5.3.4 *Ex situ* bioassays to obtain metal tissue accumulation

Ex situ bioaccumulation studies with laboratory-based exposures were conducted by the Naval Systems Center (SSC) Pacific Bioassay Laboratory using intact sediment cores collected as noted in Table 5.1 using the bent-nosed clam *Macoma nasuta*, a deposit-feeding bivalve living at the sediment surface which is abundant in intertidal areas of eastern North Pacific Ocean (Hylleberg & Gallucci, 1975). Sediment trap material deposited during the storm season in 2015/2016 (Table 5.1) was also introduced on the top of "pre storm" sediment collections of 2015 to represent the effect of newly deposited material in a separate treatment identified as "pre+". No significant differences in tissue bioaccumulation and porewater concentrations were noted between the "pre+" and the "post storm" season treatments and the "pre+" were treated as "post storm" treatments.

Five 1 inch small adult clams were exposed for a 28-d bioaccumulation assay. The bioassays were conducted with 3 replicates using intact sediment cores of approximately 100g dry weight. The test protocols for the sediment bioaccumulation exposure were from (ASTM, 1995; USEPA, 1991). A summary of the test conditions and test acceptability criteria for the exposure is shown in Table S5, SI. Briefly, clams were received 4-6 days prior to exposure to allow for acclimation to test conditions and to observe for mortalities. All test chambers were set up with sediment, water and aeration on the day prior to test initiation. Organisms were introduced randomly to test chambers on test "Day 0" with sufficient organisms reserved for characterization of initial metals bioaccumulation. Renewals of overlying water, filtered (0.45 μm) natural seawater collected from San Diego

Bay, were made three times per week over the course of the 28-d exposure. Water was maintained essentially saturated with oxygen at 15±2 °C and 32±2 ppt salinity. Surficial sediments were oxic at the surface as noted previously but more reduced at the bottom of the intact core.

Upon termination of the exposure period (Day 28), surviving organisms were recovered by sieving sediment using a 500 μm sieve, enumerated and then transferred to clean freshwater overnight to purge digested sediment. Survival was >90%. On Day 29, the soft body portions from the clams were dissected from each replicate, rinsed with milli-q deionized water, weighed and frozen in sample collection jars until shipment to the analytical laboratory for digestion, extraction and analysis.

Trace metal (except Hg) in tissue were extracted using HNO_3. Hg was extracted from tissue using HNO_3 and sulfuric acid (H_2SO_4). BrCl was also added to the Hg digestate to prevent the reabsorption of Hg to carbon particles if present. All digested samples were analyzed by the analytical methods noted above except for July 2015 when samples were analyzed (for all metals except Hg) at the SSC, also by ICP-MS. The average tissue concentrations for bioassays from each sampling event and controls are shown in Table S6, SI. Reported concentrations are measured minus the tissue concentration in “Day 0", also shown in Table S6, SI.

5.3.5 Passive porewater sampling and analysis

DGTs were used to measure metal porewater concentrations in the bioassay sediments .DGTs consist of a thin hydrogel layer that allows the mass transport by diffusion of the solutes into a resin that acts as the binding layer as first described by (Davison & Zhang, 1994). DGTs with 0.78mm cross-linked polyacrylamide (APA) diffusive gel,

polyethersulphone filter membrane and 0.4mm Chelex binding layer, acquired from DGT Research, Lancashire, UK, were used to measure the cationic metals Cd, Cu, Zn, Ni, and Pb. DGTs for the measurement of Hg were fabricated by TTU using an agarose based resin-gel layer based on an adaptation of the method described by (Amirbahman *et al.*, 2013). The DGTs for Hg measurements were deoxygenated by nitrogen (N_2) purging in a 10 milli-molar (mM) solution of sodium nitrate ($NaNO_3$) with resin-gel strips. The DGTs were pressed gently into the surface of the sediments to ensure full contact between the sediment and the exposure window/membrane of the DGT. Upon termination of exposure periods, for 2 or 3 days, the DGTs were rinsed immediately with distilled-deionized water to remove the sediment and shipped to the TTU chemistry laboratory for extraction and analysis. Digestion of the DGT resin for Hg used cold (room temperature) HCl followed by BrCl oxidation (USEPA, 2002). Other trace metals were extracted from DGT's resins using the same method as for tissue metal extraction as mentioned above. The digested samples were analyzed by the analytical methods defined previously. The measured porewater concentrations of the study are reported in the Table S7, SI.

5.3.6 Statistical analysis

Statistics using software R were applied to evaluate the significance of the variations across spatial (locations, P01, P08, P11, and P17) and seasonal differences (before and after the storm season) with confidence level $\alpha=0.05$ or 95% confidence in any differences noted. The interaction of the main effects, period and location, was simultaneously examined to identify if the effect of the period depends on the location and likewise the effect of location depends on the period. Statistically significant ($p<0.05$, $\alpha=0.05$) interactions limit the conclusions that can be drawn from the period and location effects separately. Due to non-

detects that were considered as 0 in some of the datasets, the analysis occurred in two steps (Elhai *et al.*, 2008): The first step employed Fisher's exact test (Agresti, 2003) in order to identify whether or not the probability of the concentrations to be zero is driven/associated by location or by period. The second step included a generalized linear model using gamma regression that was applied only to the non-zero, positive values of the dataset. In the cases that the dataset consisted only of non-zero, positive values then only the gamma regression was applied to the dataset. Spearman's rank correlation was applied to evaluate the strength of the association (Hauke & Kossowski, 2011) between the metal tissue accumulation and porewater measured by DGTs as well as bulk sediment concentrations.

5.4 Results and Discussion

5.4.1 Bulk sediment chemistry

As a result of stormwater discharges, surficial sediment concentrations in the receiving waters might be expected to increase. Table 5.2 summarizes the sediment concentration of Ni, Cu, Zn, Cd, Hg, Pb and As at each of the four receiving water locations separated by pre-storm season and post-storm season samples. Tables 5.3 and 5.4 shows the same information for tissue concentrations in bioassays and porewater concentrations in the sediments in the bioassays. All metals and As showed significant increases in sediment concentration toward the stormwater discharge location ($p<0.01$) in post-storm samples (Table 5.5).

The increase in sediment concentration toward the stormwater discharge is illustrated in the top graphs of Figure 5.3 for Ni and Figure 5.4 for Zn. This would suggest that the stormwater has significantly contributed to sediment contamination, particularly when the contamination is associated with larger, rapidly settling particles. Cd, for example, was

primarily associated with sand size (>63 μm particles) and this led to much greater deposition of Cd at P17 and P11 than at more distant locations, Table S2, SI (Drygiannaki *et al.*, 2020). %TOC in sediment cores also increased closer to the stormwater discharge from 0.8% at P01 to 4.0% in P17 (Table S4, SI).

Table 5.2: Average sediment concentrations (mg/kg) with standard deviations in parentheses of the replicate measurements for Ni, Cu, Zn, Cd, THg, Pb, and As before the storm seasons ("pre") and after the storm seasons ("post"). P01 is furthest from the stormwater discharge while P17 is the closest.

	Ni	Cu	Zn	Cd	THg	Pb	As
	mg/kg	mg/kg	mg/kg	mg/kg	mg/kg	mg/kg	mg/kg
P01 Pre	12.8 (3.9)	140 (64.4)	194 (69.5)	0.19 (0.21)	0.38 (0.08)	39.2 (13.0)	6.7 (2.3)
P01 Post	11.4 (0.8)	108 (8.8)	145 (11.5)	0.00 (0.00)	0.26 (0.04)	27.6 (1.3)	4.9 (0.6)
P08 Pre	16.6 (0.8)	213 (27.9)	281 (39.6)	0.12 (0.13)	0.54 (0.04)	78.3 (17.4)	9.1 (0.4)
P08 Post	20.6 (2.0)	259 (7.2)	339 (15.5)	0.09 (0.10)	0.56 (0.02)	84.6 (3.8)	11.6 (1.2)
P11 Pre	18.0 (1.4)	220 (37.6)	396 (80.7)	1.03 (0.77)	0.73 (0.22)	126 (38.6)	8.4 (3.2)
P11 Post	22.8 (4.7)	237 (22.6)	624 (351)	2.32 (2.54)	1.06 (0.60)	257 (191)	8.9 (0.9)
P17 Pre	18.6 (4.0)	260 (74.4)	574 (121)	1.58 (0.22)	0.56 (0.22)	131 (22.5)	8.5 (0.7)
P17 Post	19.0 (1.3)	215 (36.4)	589 (109)	1.45 (0.20)	0.35 (0.04)	134 (28.9)	8.3 (0.2)

Table 5.3: Average tissue concentrations (µg/g dw) with standard deviations in parentheses of the replicate measurements for Ni, Cu, Zn, Cd, THg, Pb, and As before the storm seasons ("pre") and after the storm seasons ("post"). P01 is furthest from the stormwater discharge while P17 is the closest.

	Ni	Cu	Zn	Cd	THg	Pb	As
	µg/g	µg/g	µg/g	µg/g	µg/g	µg/g	µg/g
P01 Pre	0.21 (0.09)	3.1 (1.1)	8.3 (4.9)	0.02 (0.01)	0.05 (0.02)	0.63 (0.23)	2.6 (0.6)
P01 Post	0.11 (0.16)	1.3 (NA[a])	3.0 (4.2)	0.00 (0.00)	0.04 (0.03)	0.42 (NA[a])	1.3 (1.8)
P08 Pre	0.23 (0.06)	3.4 (1.1)	6.2 (1.5)	0.01 (0.01)	0.03 (0.01)	0.91 (0.18)	2.2 (0.6)
P08 Post	0.08 (0.06)	1.6 (0.6)	2.9 (2.5)	0.00 (0.00)	0.01 (0.01)	0.51 (0.10)	1.5 (1.1)
P11 Pre	0.30 (0.17)	3.3 (2.0)	9.8 (4.3)	0.04 (0.04)	0.03 (0.02)	1.78 (0.95)	3.1 (1.4)
P11 Post	0.07 (0.09)	1.1 (0.5)	5.1 (4.8)	0.01 (0.02)	0.01 (0.01)	0.88 (0.33)	0.7 (1.1)
P17 Pre	0.36 (0.23)	5.1 (2.5)	7.7 (4.1)	0.04 (0.02)	0.01 (0.01)	1.84 (1.11)	3.3 (1.6)
P17 Post	0.07 (0.09)	1.1 (0.4)	1.3 (1.7)	0.00 (0.00)	0.00 (0.00)	0.72 (0.17)	0.6 (0.5)

[a]NA: Not available.

Table 5.4: Average porewater concentrations (µg/L) with standard deviations in parentheses of the replicate measurements for Ni, Cu, Zn, Cd, THg, and Pb before the storm seasons ("pre") and after the storm seasons ("post"). There are no As measurements available. P01 is furthest from the stormwater discharge while P17 is the closest.

	Ni	Cu	Zn	Cd	THg	Pb
	µg/L	µg/L	µg/L	µg/L	µg/L	µg/L
P01 Pre	1.3 (0.5)	5.5 (1.3)	28.3 (4.9)	0.07 (0.07)	0.23 (0.09)	0.13 (0.05)
P01 Post	0.8 (0.3)	3.0 (1.5)	20.6 (18.9)	0.02 (0.05)	0.05 (0.02)	0.14 (0.09)
P08 Pre	1.6 (0.4)	12.2 (9.6)	39.4 (8.9)	0.09 (0.05)	0.17 (0.03)	0.37 (0.36)
P08 Post	0.9 (0.3)	7.3 (8.5)	27.1 (36.2)	0.00 (0.00)	0.10 (0.06)	0.32 (0.32)
P11 Pre	3.6 (2.5)	15.8 (10.2)	171 (130)	0.34 (0.32)	0.18 (0.10)	1.28 (0.77)
P11 Post	1.0 (0.7)	6.3 (4.4)	22.6 (16.5)	0.03 (0.03)	0.03 (0.03)	0.52 (0.44)
P17 Pre	1.5 (0.8)	7.8 (7.7)	68.0 (67.6)	0.05 (0.06)	0.07 (0.04)	0.87 (0.69)
P17 Post	0.7 (0.2)	1.7 (1.1)	6.2 (4.6)	0.02 (0.03)	0.00 (0.00)	0.18 (0.14)

Table 5.5: Seasonal and spatial effects on tissue, porewater, and sediment concentrations and significance (p-values if <0.05). "Increase" is associated with trends expected from stormwater contaminants, higher post-storm season concentrations or higher concentration near the stormwater discharge. "Decrease" reflects lower post-storm season concentrations or lower concentration near stormwater discharge.

Sediment							
Effects	Ni	Cu	Zn	Cd	Hg	Pb	As
Period (Post compared to Pre)	Increase (p=0.03)	NS[a]	NS[a]¤	Increase (p<0.01)¤	NS[a]¤	Increase (p<0.01)¤	NS[a]
Location (near discharge compared to far-field)	Increase (p<0.01)	Increase (p<0.01)	Increase (p<0.01)¤	Increase (p<0.01)¤	Increase (p<0.01)¤	Increase (p<0.01)¤	Increase (p<0.01)
Tissue							
Effects	Ni	Cu	Zn	Cd	Hg	Pb	As
Period (Post compared to Pre)	Decrease (p<0.01)	Decrease (p<0.01)	Decrease (p=0.03)	Decrease (p<0.01)*	Decrease (p=0.03)¤	Decrease (p<0.01)	Decrease (p<0.01)¤
Location (near discharge compared to far-field)	NS[a]	NS[a]	NS[a]	Increase (p=0.01)	Decrease (p<0.01)¤	Increase (p<0.01)	NS[a]¤
Porewater							
Effects	Ni	Cu	Zn	Cd	Hg	Pb	As
Period (Post compared to Pre)	Decrease (p<0.01)	Decrease (p<0.01)	Decrease (p<0.01)¤	Decrease (p<0.01)	Decrease (p<0.01)¤	Decrease (p<0.01)	-
Location (near discharge compared to far-field)	Increase (p<0.01)	Increase (p=0.02)	NS[a]¤	Increase (p<0.01)	Decrease (p<0.01)¤	Increase (p<0.01)	-

*: Based upon Fisher's exact test due to excessive 0 values in the dataset.

¤: When there is significant interaction effect (p<0.05) between period and location effects.

[a]NS: not statistically significant changes.

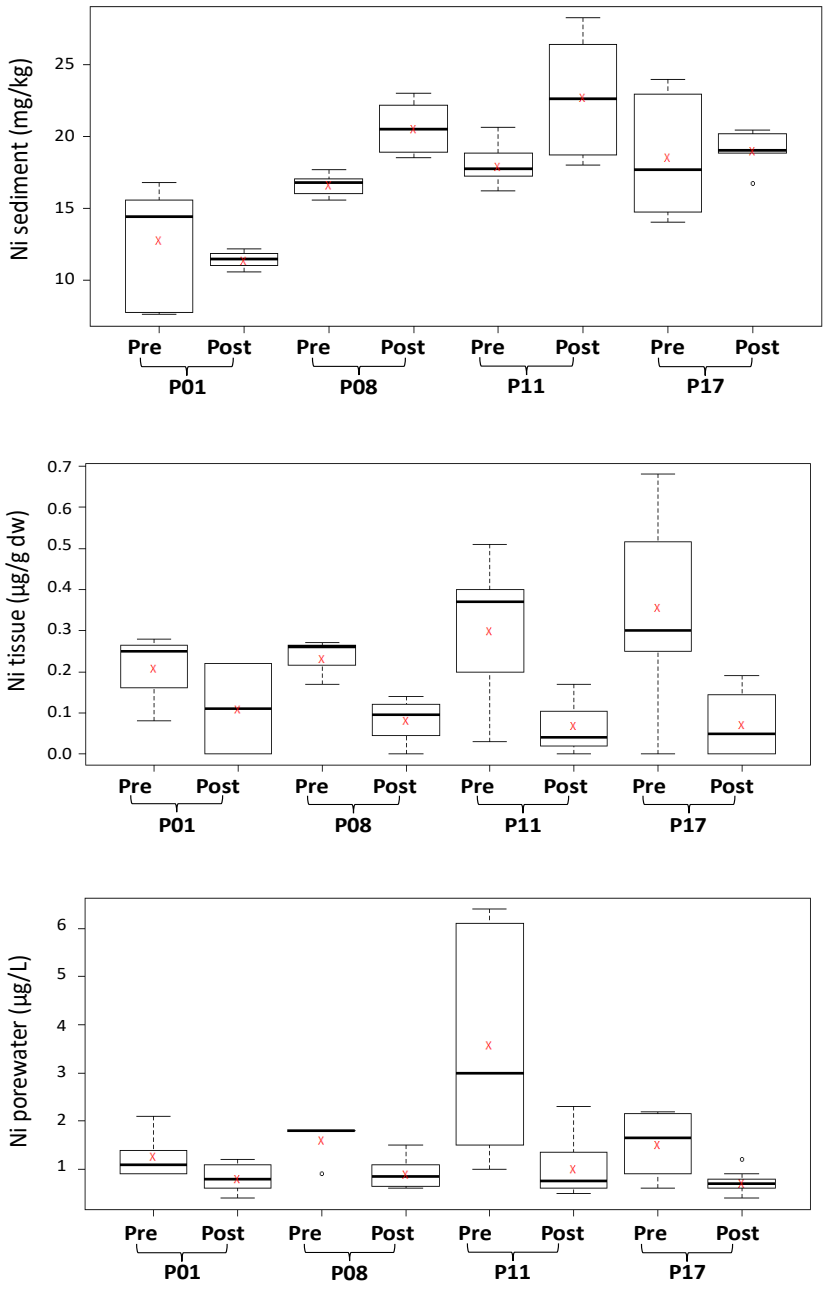

Figure 5.3: Boxplots of Ni tissue concentrations in organisms (top) and porewater concentrations (middle) in ex-situ bioassays and sediment concentrations (bottom) from sites P17, P11, P08, P01 separated by pre-storm season and post-storm season samples. The "x" indicates the mean value of each dataset. Locations are ordered relative to their distance from the stormwater discharge with P17 closest to the Paleta Creek discharge

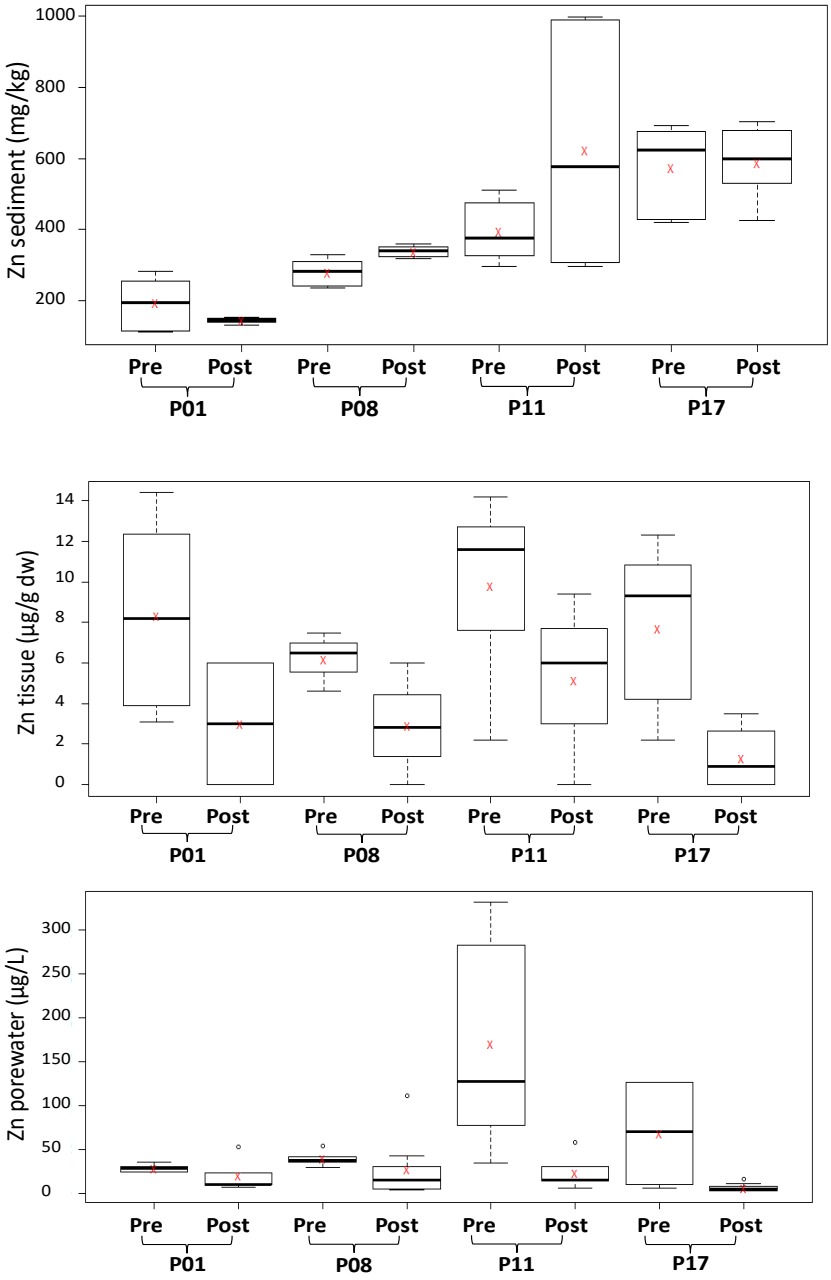

Figure 5.4: Boxplots of Zn tissue concentrations in organisms (top) and porewater concentrations (middle) in ex-situ bioassays and sediment concentrations (bottom) from sites P17, P11, P08, P01 separated by pre-storm season and post-storm season samples. The "x" indicates the mean value of each dataset. Locations are ordered relative to their distance from the stormwater discharge with P17 closest to the Paleta Creek discharge.

Ni, Cd and Pb also showed statistically significant increases in concentration in post-storm season samples relative to pre-storm season samples ($p<0.01$-0.03). Figure 5.3 shows this trend for Ni. Cu, Zn, Hg and As, however, showed no significant differences in concentration post-storm season relative to pre-storm concentrations. Figure 5.4 illustrates the lack of a significant trend between pre-storm and post-storm season for Zn. Zn, Cd, Hg and Pb showed significant interaction effects between location and period (Table 5.2).

The lack of significant differences in sediment concentrations of Cu, Zn, Hg and As with period may reflect the influence of historical sediment contamination as well as the influence of other sources and resuspension from sediments other than the Paleta Creek. Concentrations at location P11, in particular, were elevated and highly variable and may have reflected the effects of historical contamination rather than stormwater discharges (Figure 5.4, top figure). The variability at this location likely also limited the ability to see statistically significant changes in sediment concentrations between pre and post storm samples. A further discussion of the sediment samples and the desirability of using more direct indicators of stormwater deposition such as settling traps can be found in (Drygiannaki *et al.*, 2020).

5.4.2 Sediment bioaccumulation of stormwater contaminants

Although sediment concentrations of all metals tended to increase toward the stormwater discharge location, only Cd and Pb ($p<0.01$) showed significant increases in tissue concentrations in bioassays from sediments collected closer to the discharge (Table 5.5 and Table S6, SI). These metals were associated with relatively large fast settling particles and sediment concentrations also increased closer to the stormwater discharge. Hg bioaccumulation was greatest in sediments from the P01 site, furthest away from the

stormwater discharge, ($p<0.05$, $\alpha=0.05$) despite sediment concentration increases closer to the discharge (Table 5.5 and Table S2, SI). Tissue concentrations of the metals Cu, Zn, and Ni, and the metalloid As were distributed without statistically significant spatial changes despite sediment concentrations increasing closer to the stormwater discharge (Table 5.5).

In addition, although sediment concentrations were either similar or increasing between the pre-storm season conditions and post-season conditions, bioassays showed that the tissue concentrations of all metals decreased significantly ($p<0.05$, $\alpha=0.05$) at all monitored locations in post-wet season samples compared to pre-storm season samples (Table 5.5). Figure 5.3 (middle graph) shows the reduction in tissue concentrations of Ni in the post-storm surficial sediments used in bioassays compared to the pre-storm season samples. Figure 5.4 (middle graph) shows the same behavior for Zn. Figures S1 and S2 in SI shows similar behavior for most other metals in sediment and bioassay tissue concentrations, respectively.

The reduction in biota metal uptake between pre-storm season and post-storm season also meant that there was a significant increase in the potential for biota metal uptake in sediments collected before and after the subsequent dry season. The elevation of biota metal uptake between the end of one storm season and the start of the next one (that is, the higher bioaccumulation in pre-storm season samples shown in Figure 5.2 and 5.3), may be attributed to either changes in bioavailability of the deposited sediment or resuspension events and other sources that brought new contaminants into the sampled sediments or brought historical sediment contamination to the surface. Sediment processes in a stable depositional environment would likely lead to more reduced conditions and less bioavailable metals (Airoldi & Hawkins, 2007) suggesting that resuspension events and

other sources were the likely cause. Resuspension and redistribution of bay sediment e.g. due to propeller wash or bay storms influenced all sampling sites as indicated by greater deposition in settling traps than could be accounted for in stormwater discharges (Drygiannaki *et al.*, 2020).

5.4.3 Porewater in sediments

The above discussion indicated that sediment concentrations of metals tended to increase closer to the stormwater discharge and either increased or stayed approximately constant between pre-and post-storm season sampling while tissue concentrations decreased during the storm season and showed no significant trends with distance from the stormwater discharge. The sediment concentrations of metals did not indicate trends in bioaccumulation in the bioassays. An alternative indicator of metal availability is porewater concentrations in the sediments (Table 5.4 and Figure S3, SI). All metals (no As porewater concentrations were available) showed significant decreases in porewater concentrations between pre-storm season and post-storm season samples ($p<0.01$), consistent with the observed trend in bioaccumulation in the bioassays (Table 5.5). Moreover, when there was a significant trend in bioassay tissue concentration, either increase or decrease with proximity to the stormwater discharge, the porewater concentrations showed the same trend (Table 5.5). Figure 5.3 (bottom graph) illustrates this behavior for Ni and Figure 5.4 (bottom graph) illustrates this behavior for Zn.

5.4.4 Predicting metal biota accumulation

Spearman's rank ratios were used to evaluate the strength of the relationships between tissue biota and porewater in sediment as well as tissue biota with sediment chemistry. The results are summarized in Table 5.6.

Table 5.6: Spearman's rank tissue/sediment and tissue/porewater correlation coefficients, r_s ($-1 \leq rs \leq 1$) and associated p-value.

r_s	Ni	Cu	Zn	Cd	Hg	Pb	As
Tissue vs Sediment	-0.5 (p=0.21)	0.31 (p=0.46)	0.07 (p=0.88)	0.26 (p=0.54)	-0.12 (p=0.78)	0.74 (p=0.05)	0.05 (p=0.94)
Tissue vs Porewater	0.93 (p=0.002)	0.69 (p=0.07)	0.91 (p=0.005)	0.80 (p=0.02)	0.61 (p=0.11)	0.74 (p=0.05)	NA[a]

[a]NA: Not available.

Sediment concentrations did not correlate with bioaccumulation in tissues except Pb with r_s=0.74, p=0.05. Ni and Hg tissues actually showed inverted correlations with sediments, i.e. negative slopes, which indicates that the sediment concentration changes were the opposite of the corresponding changes in tissue bioaccumulation. Zn and As indicated no correlation with sediments (slopes less than 0.1 and p values of 0.88 and 0.94, respectively). Cd and Cu exhibited positive slopes but poor correlations (r_s=0.26, p-0.54 and r_s=0.31, p=0.46, respectively).

In contrast, sediment tissue and porewater in Table 5.6 are all positively correlated with statistically significant correlations (r_s 0.74-0.93, $p<0.05$) for Ni, Zn, Cd, and Pb and slightly weaker for Cu (r_s=0.69, p=0.07) and Hg (r_s=0.61, p=0.11). No porewater measurements of As were available to correlate tissue and porewater of that element. Thus porewater metal concentrations as measured by DGT were a good indicator for *Macoma Nasuta* tissue metal bioaccumulation in these studies. This does not necessarily indicate that porewater exposure was the cause of bioaccumulation in the deposit-feeding organism but that the porewater was an indicator of labile metals available for bioaccumulation. Notably, the porewater metals concentrations and the tissue concentrations all *decreased* in the post-storm season bioassays suggesting that the stormwater contribution to sediment

recontamination did not, at least initially, contribute to greater accumulation to benthic organisms.

5.5 Conclusions

The primary goal of the study was to assess sediment recontamination and biological impacts of stormwater discharges. Although applied to the specific location of Paleta Creek, CA, the methods and analyses may be valuable for similar assessments elsewhere. The metal uptake in *Macoma nasuta* in bioaccumulation assays using sediments collected after the storm seasons were reduced relative to pre-storm season samples for all measured metals, Cd, Hg, Cu, Pb, Zn, Ni, and the metalloid As. This suggests that the stormwater contaminants were discharging in forms largely unavailable to the sediment organisms. The bulk sediment chemistry did not correlate with bioaccumulation with the exception of Pb. Most importantly, sediment recontamination as indicated by stormwater loads and bulk chemistry of the receiving sediments did not indicate biological impacts as indicated by bioaccumulation. The assessment of the biological impacts of stormwater should likely always include direct assessment of the biological endpoints of interest rather than simply the stormwater loads or bulk sediment recontamination.

Moreover, metal concentrations in sediment porewater measured by DGT after the storm seasons decreased consistent with the observed changes in bioaccumulation. Analysis of the metal biota accumulation and DGT measured porewater concentrations showed statistically significant positive correlations ($p<0.05$, $\alpha=0.05$) for most metals and slightly weaker correlations for the others (Hg and Cu). The good correlation between porewater concentrations and bioaccumulation in the same sediments will likely encourage the continued evaluation and use of porewater concentrations as an indicator of metal

availability.

(Drygiannaki *et al.*, 2020) showed that many of the metals associated with the stormwater discharges at Paleta Creek were associated with large (>63µm) particles and based upon this study, these particles were apparently not available for bioaccumulation in *Macoma nasuta*. Left unanswered is whether the reason for the increased bioaccumulation in pre-storm season surficial sediment samples is breakdown of these larger particles to more bioavailable sizes and forms or due to resuspension and deposition of more bioavailable forms from elsewhere in the bay. Study by (Drygiannaki *et al.*, 2020), however, showed that the receiving waters near the Paleta Creek discharge are receiving sediments from resuspension events or other sources that contribute substantially to the total metal load and it is likely that these other sources are important to the pre-storm season sediment bioaccumulation results.

5.6 References

Agresti, A. (2003). *Categorical data analysis* (Vol. 482): John Wiley & Sons.

Airoldi, L., & Hawkins, S. J. (2007). Negative effects of sediment deposition on grazing activity and survival of the limpet Patella vulgata. *Marine Ecology Progress Series, 332*, 235-240.

Amirbahman, A., Massey, D. I., Lotufo, G., Steenhaut, N., Brown, L. E., Biedenbach, J. M., & Magar, V. S. (2013). Assessment of mercury bioavailability to benthic macroinvertebrates using diffusive gradients in thin films (DGT). *Environmental Science: Processes & Impacts, 15*(11), 2104-2114.

Ankley, G. T., Thomas, N. A., Di Toro, D. M., Hansen, D. J., Mahony, J. D., Berry, W. J., Swartz, R. C., Hoke, R. A., Garrison, A. W., & Allen, H. E. (1994). Assessing potential bioavailability of metals in sediments: a proposed approach. *Environmental management, 18*(3), 331-337.

ASTM. (1995). Standard guide for determination of the bioaccumulation of sediment-associated contaminants by benthic invertebrates. *Annual Book of ASTM Standards, 11*, 1140-1189.

Brown, J., & Bay, S. M. (2005). Temporal assessment of chemistry, toxicity and benthic communities in sediments at the mouths of Chollas Creek and Paleta Creek, San Diego Bay. *Southern California Coastal Water Research Project, Draft Report, Westminster, CA*.

Burton, G. A., Jr. (2010). Metal bioavailability and toxicity in sediments. *Critical Reviews in Environmental Science and Technology, 40*(9-10), 852-907.

Castillo, M. A., Trujillo, I. S., Alonso, E. V., de Torres, A. G., & Pavón, J. C. (2013). Bioavailability of heavy metals in water and sediments from a typical Mediterranean Bay (Málaga Bay, Region of Andalucía, Southern Spain). *Marine pollution bulletin, 76*(1-2), 427-434.

Chadwick, D., Kirtay, V., Blake, A., Arias, E., Davidson, B., Guerrero, J., Apitz, S. E., Germano, J., Maa, J., & Smith, C. (2006). *Pathway Ranking for In-place Sediment Management (CU1209). Executive Summary and Site 1 Report--Paleta Creek. SPACE AND NAVAL WARFARE SYSTEMS CENTER PACIFIC SAN DIEGO CA.* Retrieved from

Clarisse, O., Dimock, B., Hintelmann, H., & Best, E. P. (2011). Predicting net mercury methylation in sediments using diffusive gradient in thin films measurements. *Environmental Science & Technology, 45*(4), 1506-1512.

Climate-Data.org. San Diego Climate. Retrieved from https://en.climate-data.org/north-america/united-states-of-america/california/san-diego-714969/

Creed, J., Brockhoff, C., & Martin, T. (1994). *Method 200.8: Determination of trace elements in waters and wastes by inductively coupled plasma-mass spectrometry*. Retrieved from

Crommentuijn, T., & Polder, M. (1997). Maximum permissible concentrations and negligible concentrations for metals, taking background concentrations into account.

Davison, W., & Zhang, H. (1994). In situ speciation measurements of trace components in natural waters using thin-film gels. *Nature, 367*(6463), 546.

Di Toro, D. M., Mahony, J. D., Hansen, D. J., Scott, K. J., Carlson, A. R., & Ankley, G. T. (1992). Acid volatile sulfide predicts the acute toxicity of cadmium and nickel in sediments. *Environmental Science & Technology, 26*(1), 96-101.

Drygiannaki, I., Rao, B., Dawson, J. A., Rakowska, M., Reible, D. D., Hayman, N. T., Rosen, G. H., Colvin, M. A., Chadwick, D. B., Pitt, R., Otto, M., Steets, B., & Ervin, J. (2020). Assessing sediment recontamination from metals in stormwater. *Science of the total environment*, 139726. doi:https://doi.org/10.1016/j.scitotenv.2020.139726

Durán, I., Sánchez-Marín, P., & Beiras, R. (2012). Dependence of Cu, Pb and Zn remobilization on physicochemical properties of marine sediments. *Marine environmental research, 77*, 43-49.

Eggleton, J., & Thomas, K. (2004). A review of factors affecting the release and bioavailability of contaminants during sediment disturbance events. *Environment international, 30*(7), 973-980.

Elhai, J. D., Calhoun, P. S., & Ford, J. D. (2008). Statistical procedures for analyzing mental health services data. *Psychiatry Research, 160*(2), 129-136. doi:https://doi.org/10.1016/j.psychres.2007.07.003

Ghosh, U., Kane Driscoll, S., Burgess, R. M., Jonker, M. T. O., Reible, D., Gobas, F., Choi, Y., Apitz, S. E., Maruya, K. A., & Gala, W. R. (2014). Passive sampling methods for contaminated sediments: practical guidance for selection, calibration,

and implementation. *Integrated Environmental Assessment and Management, 10*(2), 210-223.

Greenstein, D., Bay, S., & Young, D. (2005). Sediment toxicity identification evaluation for the mouths of Chollas and Paleta Creek, San Diego.

Hampton, T. W., & Chadwick, B. (2000). *Quantifying in situ metal contaminant mobility in marine sediments*. Retrieved from

Hamzeh, M., Ouddane, B., Daye, M., & Halwani, J. (2014). Trace metal mobilization from surficial sediments of the Seine River Estuary. *Water, Air, & Soil Pollution, 225*(3), 1878.

Harper, M. P., Davison, W., & Tych, W. (1999). Estimation of Pore Water Concentrations from DGT Profiles: A Modelling Approach. *Aquatic Geochemistry, 5*(4), 337-355. doi:10.1023/A:1009620412373

Harper, M. P., Davison, W., Zhang, H., & Tych, W. (1998). Kinetics of metal exchange between solids and solutions in sediments and soils interpreted from DGT measured fluxes. *Geochimica et Cosmochimica Acta, 62*(16), 2757-2770. doi:https://doi.org/10.1016/S0016-7037(98)00186-0

Hatch, A. C., & Burton, G. A., Jr. (1999). Sediment toxicity and stormwater runoff in a contaminated receiving system: consideration of different bioassays in the laboratory and field. *Chemosphere, 39*(6), 1001-1017.

Hauke, J., & Kossowski, T. (2011). Comparison of values of Pearson's and Spearman's correlation coefficients on the same sets of data. *Quaestiones geographicae, 30*(2), 87-93.

Hayman, N. T., Rosen, G., Colvin, M. A., Chadwick, B. D., Rao, B., Athanasiou, D., Rakowska, M., Drygiannaki, I., Burton, G. A., Jr., & Reible, D. D. (2020). Seasonal Toxicity Observed with Amphipods (Eohaustorius estuarius) at Paleta Creek, San Diego Bay, USA. *Environmental toxicology and chemistry, 39*(1), 229-239.

Hylleberg, J., & Gallucci, V. (1975). Selectivity in feeding by the deposit-feeding bivalve Macoma nasuta. *Marine Biology, 32*(2), 167-178.

Kirtay, V., Conder, J., Rosen, G., Magar, V., Grover, M., Arblaster, J., Fetters, K., & Chadwick, B. (2018). Performance of an in situ activated carbon treatment to reduce PCB availability in an active harbor. *Environmental toxicology and chemistry, 37*(6), 1767-1777.

Lampert, D. J., Thomas, C., & Reible, D. D. (2015). Internal and external transport significance for predicting contaminant uptake rates in passive samplers. *Chemosphere, 119*, 910-916.

Leermakers, M., Gao, Y., Gabelle, C., Lojen, S., Ouddane, B., Wartel, M., & Baeyens, W. (2005). Determination of high resolution pore water profiles of trace metals in sediments of the Rupel River (Belgium) using DET (diffusive equilibrium in thin films) and DGT (diffusive gradients in thin films) techniques. *Water, Air, and Soil Pollution, 166*(1-4), 265-286.

Leeson, A., Thompson, T., Magar, V., Patton, C., Luthy, R., Anderson, K., Bachman, B., Gustavson, k., Markillie, K., Michalsen, M., Rosen, G., Webb, R., & Stackelberg, K. (2016). SERDP and ESTCP Workshop on Research and Development Needs for Long-Term Management of Contaminated Sediments.

Lydy, M. J., Landrum, P. F., Oen, A. M. P., Allinson, M., Smedes, F., Harwood, A. D., Li, H., Maruya, K. A., & Liu, J. (2014). Passive sampling methods for contaminated sediments: State of the science for organic contaminants. *Integrated environmental assessment and management, 10*(2), 167-178.

Peijnenburg, W., Teasdale, P., Reible, D. D., Mondon, J., Bennett, W., & Campbell, P. (2014). Passive sampling methods for contaminated sediments: State of the science for metals. *Integrated environmental assessment and management, 10*(2), 179-196.

Peterson, G., Ankley, G., & Leonard, E. (1996). Effect of bioturbation on metal-sulfide oxidation in surficial freshwater sediments. *Environmental Toxicology and Chemistry: An International Journal, 15*(12), 2147-2155.

Reible, D. (2014). *Processes, assessment and remediation of contaminated sediments*: Springer.

Reible, D. D., Rao, B., Rakowska, M., Athanasiou, D., Drygiannaki, I., Bejar, M., Chadwick, B., Colvin, M., Rosen, G., Burton, G. A., Jr., Stecker, E., Steets, B., Otto, M., & Pitt, R. (2018). Assessment and Management of Stormwater Impacts on Sediment Recontamination. ER-2428, Final Report. *Strategic Environmental Research and Development Program, Alexandria, VA, USA*.

Rodriguez-Iruretagoiena, A., de Vallejuelo, S. F.-O., de Diego, A., de Leão, F. B., de Medeiros, D., Oliveira, M. L. S., Tafarel, S. R., Arana, G., Madariaga, J. M., & Silva, L. F. O. (2016). The mobilization of hazardous elements after a tropical storm event in a polluted estuary. *Science of the total environment, 565*, 721-729. doi:https://doi.org/10.1016/j.scitotenv.2016.05.024

Rosen, G., Chadwick, B., Colvin, M.,, Stransky C., Burton, G. A., Jr., Radford, J., Bailey, H., Cibor, A., Grover, M., & Greenberg, M. (2017). *Demonstration and Commercialization of the Sediment Ecosystem Assessment Protocol*. Retrieved from

Roulier, J., Tusseau-Vuillemin, M., Coquery, M., Geffard, O., & Garric, J. (2008). Measurement of dynamic mobilization of trace metals in sediments using DGT and comparison with bioaccumulation in Chironomus riparius: First results of an experimental study. *Chemosphere, 70*(5), 925-932.

Schiff, K., & Bay, S. (2003). Impacts of stormwater discharges on the nearshore benthic environment of Santa Monica Bay. *Marine environmental research, 56*(1-2), 225-243.

Simpson, S., Yverneau, H., Cremazy, A., Jarolimek, C., Price, H., & Jolley, D. (2012). DGT-induced copper flux predicts bioaccumulation and toxicity to bivalves in sediments with varying properties. *Environmental Science & Technology, 46*(16), 9038-9046.

USEPA. (1991). Evaluation of Dredged Material Proposed for Ocean Disposal_Testing Manual_ EPA 503/8-91/001.

USEPA. (1996). *EPA Method 3050B: Acid Digestion of Sediments, Sludges, and Soils*.

USEPA. (1998). Assessment and Remediastion of Contaminated Sediments (ARCS) Program: Guidance for in-situ subaqueous capping of contaminated sediments.

USEPA. (2002). *Method 1631, Revision E:Mercury in Water by Oxidation, Purge and Trap, and Cold Vapor Atomic Fluorescence Spectrometry*

USEPA. (2013). *Appendix to Method 1631 : total mercury in tissue, sludge, sediment, and soil by acid digestion and BrCl oxidation*. [Anchorage]: [Susitna-Watana Hydroelectric Project].

Vethaak, A. D., Hamers, T., Martínez-Gómez, C., Kamstra, J., de Weert, J., Leonards, P., & Smedes, F. (2017). Toxicity profiling of marine surface sediments: a case study using rapid screening bioassays of exhaustive total extracts, elutriates and passive sampler extracts. *Marine environmental research, 124*, 81-91.

Werner, I., Teh, S. J., Datta, S., Lu, X., & Young, T. M. (2004). Biomarker responses in Macoma nasuta (Bivalvia) exposed to sediments from northern San Francisco Bay. *Marine environmental research, 58*(2-5), 299-304.

Winsor, M. H., Boese, B. L., Lee Ii, H., Randall, R. C., & Specht, D. T. (1990). Determination of the ventilation rates of interstitial and overlying water by the clam Macoma nasuta. *Environmental Toxicology and Chemistry: An International Journal, 9*(2), 209-213.

Wu, Z., He, M., & Lin, C. (2011). In situ measurements of concentrations of Cd, Co, Fe and Mn in estuarine porewater using DGT. *Environmental pollution, 159*(5), 1123-1128. doi:https://doi.org/10.1016/j.envpol.2011.02.015

Xu, J., Zhang, J., Huo, S., Xi, B., He, Z., & Xu, Y. (2017). High-resolution profiles of trace metals assessed by DGT techniques in lake sediment porewaters. *Environmental Earth Sciences, 76*(8), 319. doi:10.1007/s12665-017-6642-5

Yoon, K. V., & Stein, E. (2007). MONITORING AND MODELING OF CHOLLAS, PALETA, AND SWITZER CREEKS.

Zhang, H., Davison, W., Knight, B., & McGrath, S. (1998). In situ measurements of solution concentrations and fluxes of trace metals in soils using DGT. *Environmental Science & Technology, 32*(5), 704-710.

Zhang, H., Davison, W., Miller, S., & Tych, W. (1995). In situ high resolution measurements of fluxes of Ni, Cu, Fe, and Mn and concentrations of Zn and Cd in porewaters by DGT. *Geochimica et Cosmochimica Acta, 59*(20), 4181-4192.

Zhang, H., Davison, W., Mortimer, R., Krom, M. D., Hayes, P. J., & Davies, I. M. (2002). Localised remobilization of metals in a marine sediment. *Science of the total environment, 296*(1-3), 175-187.

Zhang, M., He, P., Qiao, G., Huang, J., Yuan, X., & Li, Q. (2019). Heavy metal contamination assessment of surface sediments of the Subei Shoal, China: Spatial distribution, source apportionment and ecological risk. *Chemosphere, 223*, 211-222. doi:https://doi.org/10.1016/j.chemosphere.2019.02.058

Zhao, G., Lu, Q., Ye, S., Yuan, H., Ding, X., & Wang, J. (2016). Assessment of heavy metal contamination in surface sediments of the west Guangdong coastal region, China. *Marine pollution bulletin, 108*(1-2), 268-274.

Zhuang, Y., Allen, H., & Fu, G. (1994). Effect of aeration of sediment on cadmium binding. *Environmental Toxicology and Chemistry: An International Journal, 13*(5), 717-724.

CHAPTER 6

CONCLUSIONS AND RECOMMENDATIONS FOR FUTURE WORK

6.1 Summary

The dissertation evaluated the impacts of stormwater runoff on sediment recontamination. The aspects that the study examined were the bulk chemistry of sediment effects as well as the biological alterations of organisms living on sediments due to the storms. Stormwater runoff was monitored and characterized to provide the assessment of the receiving water sediment recontamination. Seasonal and spatial advanced statistical analysis for the sediment chemistry, sediment porewater and bioaccumulation estimated the biological responses of deposit-feeders on sediments. Finally, statistical correlation identified the significant relationships among bulk sediment, porewater, and tissue biota and the predictor of biota accumulation.

Stormwater from outlets and discharges was characterized by particle size (μg/L) and normalized by solid concentrations in each particle size, providing the particle-associated concentrations (mg/kg). The stormwater characterization indicated a useful insight of the contaminant association with different settling velocities and therefore depositional potential on the sediment bed. 26% of the discharged solids in the C1W were sands (>63μm) during the high precipitation event and 7% in the low precipitation event. The fact that 60% of the measured particles were sands (>63μm) in the upstream sampling area, C2W, during the low precipitation event shows deposition and accumulation of these particles in the downstream portions of the stormwater conveyance system. Particle size fractionation was able to monitor the particle transport within the studied watershed.

Comparing between the high and the low precipitation event in the main discharge C1W, the contaminant concentrations per volume and the metal concentrations on the stormwater solids were similar because they presented only less than a factor of two differences. Therefore, the similarity of both events can be useful in extrapolating the results to other events. Moreover, the metal concentrations on the solids were used to compare the C1W main discharge with other storm monitored locations related to upstream highway sources as well as navy related outlets. Statistical tools identified that most of the stormwater contaminants, like Cd, Cu, Pb, and Zn, were associated with residential and highway sources from the upstream part of the watershed, while As, Ni, and Hg were significantly influenced by the downstream outlets of the watershed.

Receiving water impacts were evaluated through time-series sampling of the storm discharge close to the main creek location C1W. The initial "first" flush contained the highest concentrations of solids (mg/L) followed by an 80% decrease by the end of the high precipitation event (and similarly in the low precipitation event). Settling traps that used to measure the settling rate in receiving waters indicated 50% greater total mass flux in near shore location P17 compared to the further trap locations P11 and P08. Moreover, 80-85% of the mass flux of the sand sized particles was decreased at the distant locations, P08, P11, and P01 compared to P17; confirming that particles with a diameter greater than 63 μm would require only a few minutes to settle near shore. The estuary model, CH3D, that simulated the hydrodynamics in San Diego Bay during the two monitored events and calculated the expected depositional rates, predicted that the simulated depositional rates of stormwater-discharged solids into receiving waters should be greater in P17 waters than in P01 receiving vicinity.

The comparison of depositional rates for the metals Cd and Cu at various sediment trap locations presented a key observation to identify the stormwater metals that dominated the receiving sediment recontamination. Statistical analysis identified the inability of surficial cores to clearly indicate stormwater sources, due to the cumulative impact of historical sources, compared to settling traps that represented newly deposited sediments. The entire association of Cd with sand particles (>63μm) during the high precipitation event was consistent with the highest Cd mass flux in the near-discharge P17 trap compared to the P01; indicating stormwater dominance in Cd sediment bulk contamination. In contrast, Cu mass flux increased in the sites furthest away from the storm discharge, P08, and P01. In addition to this, the higher Cu concentrations in the sediment traps P01, P08 and P11 compared to the particle-bound Cu concentrations (mg/kg) in stormwater suggested that other more concentrated sources than stormwater were likely contributing to the sediment recontamination for Cu. Other metals showed recontamination sources intermediate between the two metal cases, Cd and Cu. WinSLAMM modeling of the storm metal discharges during the settling trap deployment was compared to the deposited sediment. 100% of Cd was deposited within the studied area, as expected from the association of Cd with coarser particles.

The implications and effects of the above-mentioned sediment recontamination on benthic organisms were also evaluated. The metal uptake in *Macoma nasuta* in samples collected after the storm seasons were reduced significantly ($p<0.05$, $\alpha=0.05$) relative to pre-storm season samples for all measured metals, Cd, Hg, Cu, Pb, Zn, Ni, and As, while sediment concentrations for some metals showed spatial increase in P17 and for most remained constant in seasonal changes. Contaminants associated with large, rapidly settling particles,

like Cd, contributed to rapid recontamination of sediment bulk solid concentration; however, they had no negative effects on benthic organisms. Apparently, stormwater metal contaminants were discharging in forms largely unavailable to the sediment organisms. Simultaneous study at Paleta Creek, however, showed that pyrethroids pesticides were responsible for seasonal sediment toxicity due to stormwater discharges (Hayman *et al.*, 2020).

Metal concentrations in sediment porewater measured by DGTs after the storm seasons decreased consistently with the observed changes in bioaccumulation with statistical significance, $p<0.05$, $\alpha=0.05$. Analysis of the metal biota accumulation and DGT measured porewater concentrations showed positive statistically significant correlations ($p<0.1$, $\alpha=0.1$). This indicated that porewater was a good indicator of labile metals available for bioaccumulation. In contrast to porewater, bulk sediment chemistry correlations with the tissue of biota presented a very weak relationship between bulk sediment and biota accumulation.

Statistics provided quite useful tools to quantify the presence of the measurements' variability and uncertainty, as well as to strengthen the conclusions among different lines of evidence in the study. The statistical methods of the study, like two-way ANOVA, and r^2 and cosineθ similarity, evaluated contributing stormwater sources to sediment recontamination. Moreover, the "two-step statistical model", that included the Fisher's exact test and gamma regression, assessed the contaminated sediment impacts due to stormwater on benthic communities. Finally, Spearman's correlations identified indirect relationships between metal accumulation in marine organisms and labile metals in porewater. These approaches can strengthen decision-making evaluations for sediment

practitioners and stormwater management. Although applied to the specific location of Paleta Creek, CA, the methods and analyses may be valuable for similar assessments elsewhere.

6.2 Future research recommendations

Particle size distribution characterization played an important role in the study for characterizing the metal contaminant association to solids in various particle sizes. Heavy metals in stormwater runoff can occur in particulate-bound forms (>0.45μm), operationally dissolved (<0.45μm), as well as colloidal forms (0.02-0.4μm) (Wu *et al.*, 2001). Given the known particle size association at Paleta Creek discharged contaminants, effective best management practices (BMPs) can be proposed to mitigate the contaminant contributing loads to sediment recontamination. For example, metals that are associated strongly with solids, like the Cd case, can be treated using sedimentation and/or physical filtration based on the size of the solids that the contaminants are bounded (Clark & Pitt, 2012). Also, metals that are associated with particles <1μm can be removed through chemical interactions between the filter media and the particles (Pitt *et al.*, 2009). While metals that are attached to operationally dissolved fractions can be removed from filter media with sorption capacity (Maniquiz-Redillas & Kim, 2014). In order to identify the most effective BMPs for the operationally dissolved fractions in stormwater, it is also recommended to investigate the removal selectivity based on metal speciation, surface interactions, and exchange kinetics. Stormwater metal contaminants that are in colloidal and ionic forms can be reduced using ion-exchange treatment (Clark & Pitt, 2012). However, their valence state and complexation will affect the metal treatability in specific media (Clark & Pitt, 2011).

Regarding the sediment recontamination at Paleta Creek, further investigation of the sources, other than stormwater, that have contributed to the bottom sediments near the P01 vicinity is recommended. For example, Cu deposited on the sediment was found to be strongly associated with outer San Diego bay sources. Cu may be related to anti-fouling paint on the bottom of large vessels that are moored in San Diego Bay, CA (Biggs & D'Anna, 2012; Wang *et al.*, 2016) that eventually settle on the sediment bed. Metal speciation in sediments can provide an insight into the Cu source and propose site-specific remediation and source controlling actions for mitigating the recontamination.

The statistical analysis in the study provided a useful approach to evaluate the seasonal and spatial sediment recontamination due to metals in stormwater with statistical certainty. A similar hypothesis can be applied to stormwater driven organic contaminants, such as PAHs and PCBs, for assessing seasonal and spatial impacts on sediment recontamination and biological effects in sediments at Paleta Creek. Statistics can also be used for testing the relationships of biota organic accumulation with influencing sediment factors, such as dissolved organic matter (Gourlay *et al.*, 2003).

Finally, the study raised questions regarding the increased bioaccumulation in surficial sediment samples in the pre storms season. The potential hypothesis that needs further exploration is either the breakdown of particles with larger sizes (such as Cd) to more bioavailable forms for the clams or the resuspension and deposition of more bioavailable forms from the outer bay during that seasonal period. Metal speciation might be useful to determine the metal-binding sediment components that are driving factors for the seasonal changes in metal availability and accumulation in biota in the field sediments of Paleta Creek. Geochemical recommended methods for speciation of metals can be sequential

extraction techniques, AVS/SEM measurements, and/or scanning electron microscopy, X-ray fluorescence and extended X-ray absorption fine structure (EXAFS) spectroscopy techniques (Allen *et al.*, 1993; Panfili *et al.*, 2005; Tessier *et al.*, 1979).

At the same time, the significant reduction of biota accumulation and porewater in sediments after the storm season should be also examined. Recent studies have demonstrated the importance of colloidal microparticles in the biogeochemical cycling of metals in marine bivalves. Therefore, colloidal assessment and monitoring in sediments are recommended using ultrafiltration and radiolabeling techniques to evaluate the bioavailability of colloid-bound metals in the marine sediments of Paleta Creek (Chin & Gschwend, 1992; Guo *et al.*, 2002; Pan & Wang, 2002).

6.3 References

Allen, H. E., Fu, G., & Deng, B. (1993). Analysis of acid-volatile sulfide (AVS) and simultaneously extracted metals (SEM) for the estimation of potential toxicity in aquatic sediments. *Environmental Toxicology and Chemistry: An International Journal, 12*(8), 1441-1453.

Biggs, T. W., & D'Anna, H. (2012). Rapid increase in copper concentrations in a new marina, San Diego Bay. *Marine pollution bulletin, 64*(3), 627-635. doi:https://doi.org/10.1016/j.marpolbul.2011.12.006

Chin, Y. P., & Gschwend, P. M. (1992). Partitioning of polycyclic aromatic hydrocarbons to marine porewater organic colloids. *Environmental Science & Technology, 26*(8), 1621-1626.

Clark, S. E., & Pitt, R. (2011). *Filtered metals control in stormwater using engineered media.* Paper presented at the World Environmental and Water Resources Congress 2011: Bearing Knowledge for Sustainability.

Clark, S. E., & Pitt, R. (2012). Targeting treatment technologies to address specific stormwater pollutants and numeric discharge limits. *Water research, 46*(20), 6715-6730.

Gourlay, C., Tusseau-Vuillemin, M. H., Garric, J., & Mouchel, J. M. (2003). Effect of dissolved organic matter of various origins and biodegradabilities on the bioaccumulation of polycyclic aromatic hydrocarbons in Daphnia magna. *Environmental Toxicology and Chemistry: An International Journal, 22*(6), 1288-1294.

Guo, L., Santschi, P. H., & Ray, S. M. (2002). Metal partitioning between colloidal and dissolved phases and its relation with bioavailability to American oysters. *Marine environmental research, 54*(1), 49-64.

Hayman, N. T., Rosen, G., Colvin, M. A., Chadwick, B. D., Rao, B., Athanasiou, D., Rakowska, M., Drygiannaki, I., Burton, G. A., Jr., & Reible, D. D. (2020). Seasonal Toxicity Observed with Amphipods (Eohaustorius estuarius) at Paleta Creek, San Diego Bay, USA. *Environmental toxicology and chemistry, 39*(1), 229-239.

Maniquiz-Redillas, M., & Kim, L.-H. (2014). Fractionation of heavy metals in runoff and discharge of a stormwater management system and its implications for treatment. *Journal of Environmental Sciences, 26*(6), 1214-1222.

Pan, J.-F., & Wang, W.-X. (2002). Comparison of the bioavailability of Cr and Fe bound with natural colloids of different origins and sizes to two marine bivalves. *Marine Biology, 141*(5), 915-924.

Panfili, F., Manceau, A., Sarret, G., Spadini, L., Kirpichtchikova, T., Bert, V., Laboudigue, A., Marcus, M. A., Ahamdach, N., & Libert, M.-F. (2005). The effect of phytostabilization on Zn speciation in a dredged contaminated sediment using scanning electron microscopy, X-ray fluorescence, EXAFS spectroscopy, and principal components analysis. *Geochimica et Cosmochimica Acta, 69*(9), 2265-2284. doi:https://doi.org/10.1016/j.gca.2004.10.017

Pitt, R., Clark, S., Steets, B., & Howell, J. (2009). Tests of Biofiltration Media for Engineered Natural Treatment Systems. *Proceedings of the Water Environment Federation, 2009*(7), 7691-7710.

Tessier, A., Campbell, P. G., & Bisson, M. (1979). Sequential extraction procedure for the speciation of particulate trace metals. *Analytical chemistry, 51*(7), 844-851.

Wang, P. F., Rivera-Duarte, I., & Richter, K. (2016). *Evaluation of Resuspension from Propeller Wash in DoD Harbors*. Retrieved from

Wu, J., Boyle, E., Sunda, W., & Wen, L.-S. (2001). Soluble and colloidal iron in the oligotrophic North Atlantic and North Pacific. *Science, 293*(5531), 847-849.

Appendix A

Supplementary information for Chapter 3

Figures

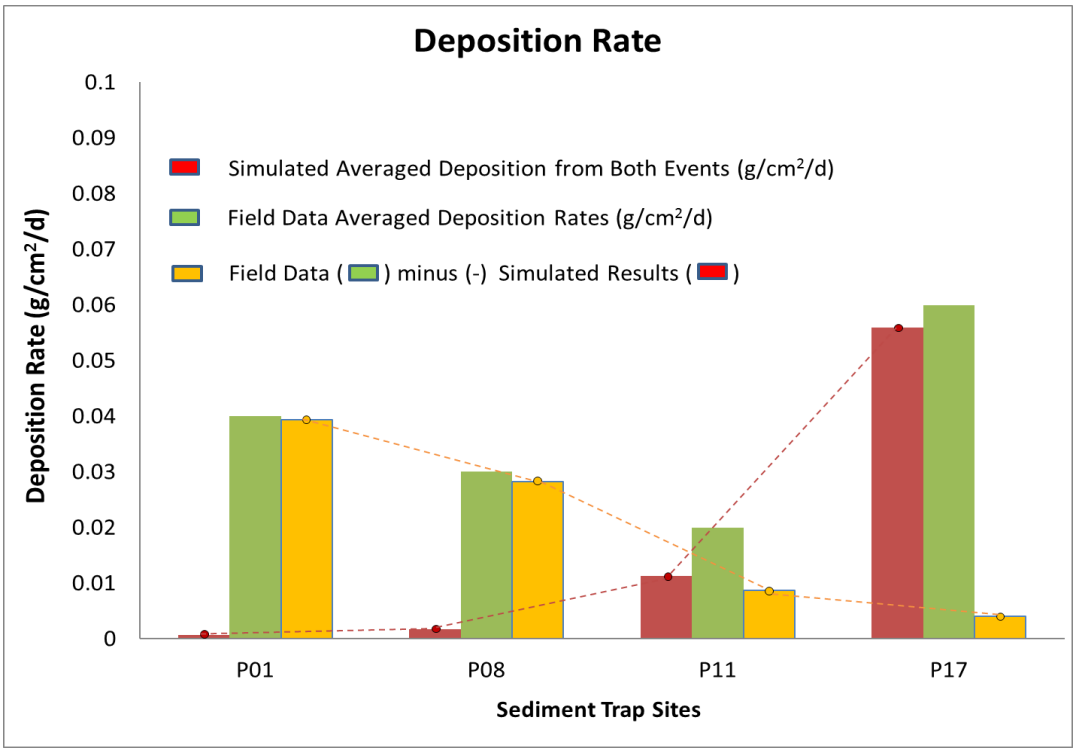

Figure A1: Simulated (obtained from CH3D model) and measured averaged deposition rates (g/cm^2/d) at the four sediment trap locations. The two dashed lines denote the two-source theory with one source from Paleta Creek discharge (red line) and the other source presumably from out-of-the mouth region (e.g. in P01 vicinity).

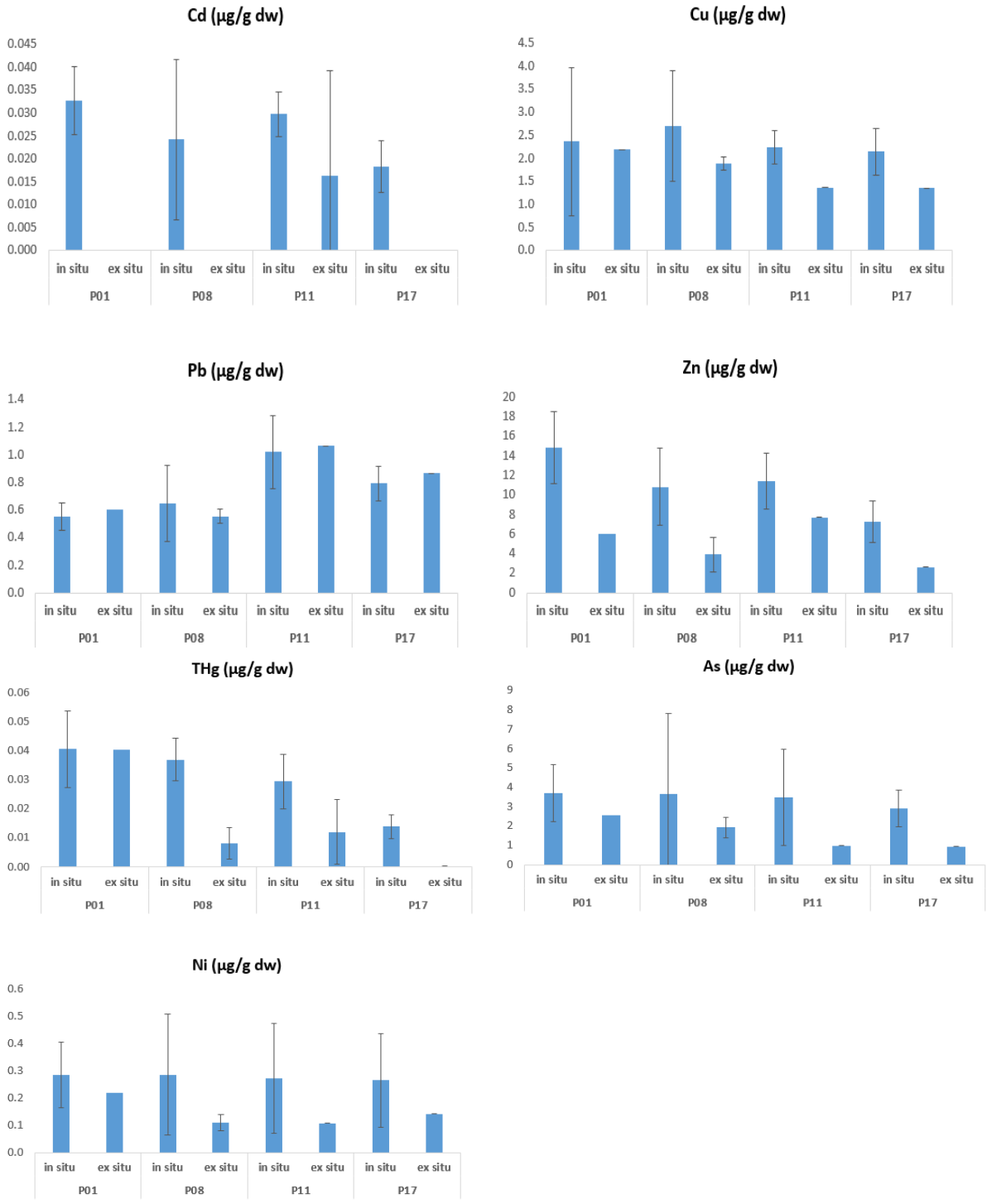

Figure A2: *Ex situ* and *in situ* tissue concentrations for the metals Cd, Cu, Pb, Zn, THg, As, and Ni from the locations P17, P11, P08, and P01 in January 2016 Wet Weather Season of 2015/2016.

Tables

Table A1. Annual mass discharges by different particle sizes in Paleta Creek watershed, obtained by WinSLAMM, as used for the comparison to the extrapolated sediment bed deposition on the sediment bed of Paleta Creek.

	NBSD % contr	NBSD yield grams/ha/yr	NBSD yield <20 um, gm/ha/yr	NBSD yield 20 - 63 um, gm/ha/yr	NBSD yield >63 um, gm/ha/yr	upper % contr	upper yield grams/ha/yr	upper yield <20 um, gm/ha/yr	upper yield 20 - 63 um, gm/ha/yr	upper yield >63 um, gm/ha/yr
Flow	19.2					80.8				
SSC	20.0	640,906	496,702	78,831	65,372	80.0	398,309	141,001	105,154	152,154
As	12.8	43	3.4	11	29	87.2	46	2.6	1.3	42
Cd	27.5	2.6	0.16	0.042	2.4	72.5	1.1	0.12	0.089	0.85
Cu	23.2	175	37	23	116	76.8	91	18	8.8	64
Hg	50.9	0.7	0.15	0.097	0.41	49.1	0.10	0.015	0.0099	0.074
Ni	18.1	32	2.4	5.1	24.21	81.9	22	4.2	2.2	16
Pb	15.8	72	39	5.4	28	84.2	60	11	3.1	46
Zn	19.7	845	112	63	671	80.3	535	83	49	403

Table A2. Statistically significant difference (p-values if $p<0.05$) between *in situ* and *ex situ* measurements using t-test of two sample assuming unequal variances in January 2016 Wet Weather Season of 2015/2016. The used values of *in situ* and *ex situ* t-test examination were averaged among the different locations P17, P11, P08, and P01.

	Cd	Cu	Pb	Zn	THg	As	Ni
p-value	<0.01	0.03	0.89	<0.01	<0.01	0.02	0.01

Coding of statistical analysis using software R

Coding used for two-way ANOVA source identification

```
setwd("C:/Users/idrygian/Desktop/Source ")
library(stringr)
base <- read.csv("sourceDataset_11202019_IDfinal.csv", header=T, strings=F)
base <- base[1:224,-c(6:7)]
base[,1] <- as.factor(base[,1])
base[,2] <- as.factor(base[,2])
#
mmins <- c(0.17, 0.05, 0.02, 0.02, 0.02, 0.006, 0.19)
for(i in 1:224)
{
 if(!is.na(base$Value[i]))
   if(base$Value[i] == 0)
   {
    if(base$Metal[i] == "As")
      base$Value[i] <- 0.17
    if(base$Metal[i] == "Cd")
      base$Value[i] <- 0.05
    if(base$Metal[i] == "Cu")
      base$Value[i] <- 0.02
    if(base$Metal[i] == "Ni")
      base$Value[i] <- 0.02
    if(base$Metal[i] == "Pb")
      base$Value[i] <- 0.02
    if(base$Metal[i] == "THg")
      base$Value[i] <- 0.0006
    if(base$Metal[i] == "Zn")
      base$Value[i] <- 0.17
   }
}
#base <- base[base[,1] %in% c("C1W","C2W"),]
```

```
##############
xAs <- base[base$Metal=="As",]
xCd <- base[base$Metal=="Cd",]
xCu <- base[base$Metal=="Cu",]
xNi <- base[base$Metal=="Ni",]
xPb <- base[base$Metal=="Pb",]
xTHg <- base[base$Metal=="THg",]
xZn <- base[base$Metal=="Zn",]
#############
# Zero checks
sum(xAs$Value<=0, na.rm=T) # 12
sum(xCd$Value<=0, na.rm=T) # 21
sum(xCu$Value<=0, na.rm=T) # 15
sum(xNi$Value<=0, na.rm=T) # 18
sum(xPb$Value<=0, na.rm=T) # 15
sum(xTHg$Value<=0, na.rm=T) # 17
sum(xZn$Value<=0, na.rm=T) # 14
outcomeNames <- c("As", "Cd", "Cu", "Ni", "Pb", "THg", "Zn")
all <- list(xAs, xCd, xCu, xNi, xPb, xTHg, xZn)
library(MASS)
pdf("boxLook.pdf")
  out <- lm(Value ~ Source.Location + Particle.size, data=xAs)
  boxcox(out)
  out <- lm(Value ~ Source.Location + Particle.size, data=xCd)
  boxcox(out)
  out <- lm(Value ~ Source.Location + Particle.size, data=xCu)
  boxcox(out)
  out <- lm(Value ~ Source.Location + Particle.size, data=xNi)
  boxcox(out)
  out <- lm(Value ~ Source.Location + Particle.size, data=xPb)
  boxcox(out)
  out <- lm(Value ~ Source.Location + Particle.size, data=xTHg)
  boxcox(out)
```

```
 out <- lm(Value ~ Source.Location + Particle.size, data=xZn)
 boxcox(out)
dev.off()
#
out1 <- lm(I(log(Value)) ~ Source.Location + Particle.size, data=xAs)
out2 <- lm(I(log(Value)) ~ Source.Location + Particle.size, data=xCd)
out3 <- lm(I(log(Value)) ~ Source.Location + Particle.size, data=xCu)
out4 <- lm(I(log(Value)) ~ Source.Location + Particle.size, data=xNi)
out5 <- lm(I(log(Value)) ~ Source.Location + Particle.size, data=xPb)
out6 <- lm(I(log(Value)) ~ Source.Location + Particle.size, data=xTHg)
out7 <- lm(I(log(Value)) ~ Source.Location + Particle.size, data=xZn)
#
anova(out1)
summary(out1)
```

Coding used for "two-step" model for tissue, porewater and sediment analysis

For tissue analysis

```
setwd("C:/Users/idrygian/Desktop/twostep")
mega <-read.csv("megaData.csv", header=T, strings=F)
base <- mega[,1:5]
base <- base[1:261,] # Removing blank rows
dimnames(base)[[2]] <- c("Outcome","Location","Period","PoreConc","Sample.ID")
library(stringr)
base$Location <- as.factor(str_trim(base$Location))
base$Period <- str_trim(base$Period)
base$Period[base$Period=="Pre"] <- "aPre" #
base$Period <- as.factor(base$Period)
unique(base$Location) # 4 locations
unique(base$Period) # 2 time periods
#
# In order to allow code reuse, going to call PoreConc TConc ...
```

```
dimnames(base)[[2]][4] <- "TConc"
xAs <- base[base[,1]=="As",]
xCd <- base[base[,1]=="Cd",]
xCu <- base[base[,1]=="Cu",]
xNi <- base[base[,1]=="Ni",]
xPb <- base[base[,1]=="Pb",]
xTHg <- base[base[,1]=="THg",]
xZn <- base[base[,1]=="Zn",]
str(xAs)
str(xCd)
str(xCu)
str(xNi)
str(xPb)
str(xTHg)
str(xZn)
#############
# Zero checks
sum(xAs$TConc<=0) # 4
sum(xCd$TConc<=0) # 13
sum(xCu$TConc<=0) # 0
sum(xNi$TConc<=0) # 5
sum(xPb$TConc<=0) # 0
sum(xTHg$TConc<=0) # 8
sum(xZn$TConc<=0) # 5
outcomeNames <- c("As", "Cd", "Cu", "Ni", "Pb", "THg", "Zn")
all <- list(xAs, xCd, xCu, xNi, xPb, xTHg, xZn)
table(xCd$Date, xCd$Location, xCd$Period)
# Looking at this, Date is confounded with Period
##  Doing Cd first since so many 0s; two-step model
###
zerosCd <- xCd[xCd$TConc==0,]
posCd <- xCd[xCd$TConc > 0,]
isNonZero <- as.numeric(xCd$TConc>0)
```

```
test0 <- glm(isNonZero ~ I(Period=="Post") + Location, family=binomial(), data=xCd)
test1 <- glm(TConc ~ Period + Location, family=Gamma(), data=posCd)
test1a <- glm(TConc ~ Period, family=Gamma(), data=posCd)
test1b <- glm(TConc ~ Location, family=Gamma(), data=posCd)
test1c <- glm(TConc ~ Period * Location, family=Gamma(), data=posCd)
# test1, test1a and test1c all fail because the models cannot deal with perfect 0s/Period splits;
### What, if anything, drives 0-values?
summary(test0)
table(isNonZero, xCd$Period)
table(isNonZero, xCd$Location)
fisher.test(table(isNonZero, xCd$Period)) #
fisher.test(table(isNonZero, xCd$Location)) #
### What, if anything, drives the value of non-0-values?
test1b <- glm(TConc ~ Location, family=Gamma(), data=posCd)
test1cx <- glm(TConc ~ 1, family=Gamma(), data=posCd)
#@ Location ME test
anova(test1cx, test1b, test="Chisq") #
#@ Looking at the effects for interpretation ...
summary(test1b)
#@ Making predictions ...
zpred <- round(predict(test0, type="response"),5)
ppred <- round(predict(test1b, type="response"),5)
gpred <- rep(0, dim(xCd)[1])
gpred[isNonZero==1] <- ppred
outCd <- data.frame(xCd, zpred=(1-zpred), gpred)
#@ Making plots ...
png("tissue_all_Cd.png", width = 960)
boxplot(xCd$TConc ~ xCd$Location*xCd$Period, main="Cd tissue concentrations (µg/g dw)", axes=F)
axis(1, at=1:8, labels=c("Pre P01","Pre P08","Pre P11","Pre P17",
  "Post P01","Post P08","Post P11","Post P17"))
axis(2)
box()
suba <- xCd
```

```
XS <- rep(NA, 8)
k = 0
for(j in c("aPre","Post"))
 for(i in c("P01","P08","P11","P17"))
{
 k <- k + 1
 sub <- suba[suba$Location==i & suba$Period==j,]
 if(dim(sub)[[1]] > 0)
   XS[k] <- mean(sub$TConc)
}
points(1:8, XS, pch="X", col="red")
#
dev.off()
#
png("tissue_non0_Cd.png", width = 960)
boxplot(xCd$TConc[isNonZero==1] ~ xCd$Location[isNonZero==1]*xCd$Period[isNonZero==1],
 main="Tissue Cd concentrations (non-0)", axes=F)
axis(1, at=1:8, labels=c("Pre P01","Pre P08","Pre P11","Pre P17",
 "Post P01","Post P08","Post P11","Post P17"))
axis(2)
box()
suba <- posCd
XS <- rep(NA, 8)
k = 0
for(j in c("aPre","Post"))
 for(i in c("P01","P08","P11","P17"))
{
 k <- k + 1
 sub <- suba[suba$Location==i & suba$Period==j,]
 if(dim(sub)[[1]] > 0)
   XS[k] <- mean(sub$TConc)
}
points(1:8, XS, pch="X", col="red")
```

```
#
dev.off()
#
png("tissue_all_Cd_reformated.png", width = 960)
boxplot(xCd$TConc ~ xCd$Period*xCd$Location, main="Cd tissue concentrations (µg/g dw)", axes=F)
axis(1, at=1:8, labels=c("Pre P01","Post P01","Pre P08","Post P08","Pre P11","Post P11",
 "Pre P17","Post P17"))
axis(2)
box()
suba <- xCd
XS <- rep(NA, 8)
k = 0
for(j in c("aPre","Post"))
 for(i in c("P01","P08","P11","P17"))
{
 k <- k + 1
 sub <- suba[suba$Location==i & suba$Period==j,]
 if(dim(sub)[[1]] > 0)
  XS[k] <- mean(sub$TConc)
}
points(c(1,3,5,7,2,4,6,8), XS, pch="X", col="red")
#
dev.off()
#
png("tissue_non0_Cd_reformated.png", width = 960)
boxplot(xCd$TConc[isNonZero==1] ~ xCd$Period[isNonZero==1]*xCd$Location[isNonZero==1],
 main="Tissue Cd concentrations (non-0)", axes=F)
axis(1, at=1:8, labels=c("Pre P01","Post P01","Pre P08","Post P08","Pre P11","Post P11",
 "Pre P17","Post P17"))
axis(2)
box()
suba <- posCd
XS <- rep(NA, 8)
```

```
k = 0
for(j in c("aPre","Post"))
  for(i in c("P01","P08","P11","P17"))
{
  k <- k + 1
  sub <- suba[suba$Location==i & suba$Period==j,]
  if(dim(sub)[[1]] > 0)
    XS[k] <- mean(sub$TConc)
}
points(c(1,3,5,7,2,4,6,8), XS, pch="X", col="red")
#
dev.off()
###
##  Doing Ni next, lots of 0s; two-step model
###
zerosNi <- xNi[xNi$TConc==0,]
posNi <- xNi[xNi$TConc > 0,]
isNonZero <- as.numeric(xNi$TConc>0)
test0 <- glm(isNonZero ~ I(Period=="Post") + Location, family=binomial(), data=xNi)
test1 <- glm(TConc ~ Period + Location, family=Gamma(), data=posNi)
test1a <- glm(TConc ~ Period, family=Gamma(), data=posNi)
test1b <- glm(TConc ~ Location, family=Gamma(), data=posNi)
test1c <- glm(TConc ~ Period * Location, family=Gamma(), data=posNi)
### What, if anything, drives 0-values?
summary(test0)
table(isNonZero, xNi$Period)
table(isNonZero, xNi$Location)
fisher.test(table(isNonZero, xNi$Period)) #
fisher.test(table(isNonZero, xNi$Location)) #
### What, if anything, drives the value of non-0-values?
#@ Interaction test
anova(test1, test1c, test="Chisq")
#@ Period ME test
```

```
anova(test1b, test1, test="Chisq") #
#@ Location ME test
anova(test1a, test1, test="Chisq") #
#@ Looking at the effects for interpretation ...
summary(test1)
#@ Making predictions ...
zpred <- round(predict(test0, type="response"),5)
ppred <- round(predict(test1, type="response"),5)
gpred <- rep(0, dim(xNi)[1])
gpred[isNonZero==1] <- ppred
outNi <- data.frame(xNi, zpred=(1-zpred), gpred)
#@ Making plots ...
png("tissue_all_Ni.png", width = 960)
boxplot(xNi$TConc ~ xNi$Location*xNi$Period, main="Ni tissue concentrations (µg/g dw)", axes=F)
axis(1, at=1:8, labels=c("Pre P01","Pre P08","Pre P11","Pre P17",
  "Post P01","Post P08","Post P11","Post P17"))
axis(2)
box()
suba <- xNi
XS <- rep(NA, 8)
k = 0
for(j in c("aPre","Post"))
  for(i in c("P01","P08","P11","P17"))
{
  k <- k + 1
  sub <- suba[suba$Location==i & suba$Period==j,]
  if(dim(sub)[[1]] > 0)
    XS[k] <- mean(sub$TConc)
}
points(1:8, XS, pch="X", col="red")
#
dev.off()
#
```

```
png("tissue_all_Ni_reformated.png", width = 960)
boxplot(xNi$TConc ~ xNi$Period*xNi$Location, main="Ni tissue concentrations (µg/g dw)", axes=F)
axis(1, at=1:8, labels=c("Pre P01","Post P01","Pre P08","Post P08","Pre P11","Post P11",
 "Pre P17","Post P17"))
axis(2)
box()
suba <- xNi
XS <- rep(NA, 8)
k = 0
for(j in c("aPre","Post"))
 for(i in c("P01","P08","P11","P17"))
{
 k <- k + 1
 sub <- suba[suba$Location==i & suba$Period==j,]
 if(dim(sub)[[1]] > 0)
  XS[k] <- mean(sub$TConc)
}
points(c(1,3,5,7,2,4,6,8), XS, pch="X", col="red")
#
dev.off()
#
png("tissue_non0_Ni.png", width = 960)
boxplot(xNi$TConc[isNonZero==1] ~ xNi$Location[isNonZero==1]*xNi$Period[isNonZero==1],
 main="Tissue Ni concentrations (non-0)", axes=F)
axis(1, at=1:8, labels=c("Pre P01","Pre P08","Pre P11","Pre P17",
 "Post P01","Post P08","Post P11","Post P17"))
axis(2)
box()
suba <- posNi
XS <- rep(NA, 8)
k = 0
for(j in c("aPre","Post"))
 for(i in c("P01","P08","P11","P17"))
```

```
{
 k <- k + 1
 sub <- suba[suba$Location==i & suba$Period==j,]
 if(dim(sub)[[1]] > 0)
   XS[k] <- mean(sub$TConc)
}
points(1:8, XS, pch="X", col="red")
#
dev.off()
#
png("tissue_non0_Ni_reformated.png", width = 960)
boxplot(xNi$TConc[isNonZero==1] ~ xNi$Period[isNonZero==1]*xNi$Location[isNonZero==1],
 main="Tissue Ni concentrations (non-0)", axes=F)
axis(1, at=1:8, labels=c("Pre P01","Post P01","Pre P08","Post P08","Pre P11","Post P11",
 "Pre P17","Post P17"))
axis(2)
box()
suba <- posNi
XS <- rep(NA, 8)
k = 0
for(j in c("aPre","Post"))
 for(i in c("P01","P08","P11","P17"))
{
 k <- k + 1
 sub <- suba[suba$Location==i & suba$Period==j,]
 if(dim(sub)[[1]] > 0)
   XS[k] <- mean(sub$TConc)
}
points(c(1,3,5,7,2,4,6,8), XS, pch="X", col="red")
#
dev.off()
##  Doing THg next, lots of 0s; two-step model
###
```

```
zerosTHg <- xTHg[xTHg$TConc==0,]
posTHg <- xTHg[xTHg$TConc > 0,]
isNonZero <- as.numeric(xTHg$TConc>0)
test0 <- glm(isNonZero ~ I(Period=="Post") + Location, family=binomial(), data=xTHg)
test1 <- glm(TConc ~ Period + Location, family=Gamma(), data=posTHg)
test1a <- glm(TConc ~ Period, family=Gamma(), data=posTHg)
test1b <- glm(TConc ~ Location, family=Gamma(), data=posTHg)
test1c <- glm(TConc ~ Period * Location, family=Gamma(), data=posTHg)
### What, if anything, drives 0-values?
summary(test0)
table(isNonZero, xTHg$Period)
table(isNonZero, xTHg$Location)
fisher.test(table(isNonZero, xTHg$Period)) #
fisher.test(table(isNonZero, xTHg$Location)) #
### What, if anything, drives the value of non-0-values?
#@ Interaction test
anova(test1, test1c, test="Chisq") #
#@ Period ME test
anova(test1b, test1, test="Chisq") #
#@ Location ME test
anova(test1a, test1, test="Chisq") #
#@ Looking at the effects for interpretation ...
summary(test1)
#@ Making predictions ...
zpred <- round(predict(test0, type="response"),5)
ppred <- round(predict(test1, type="response"),5)
gpred <- rep(0, dim(xTHg)[1])
gpred[isNonZero==1] <- ppred
outTHg <- data.frame(xTHg, zpred=(1-zpred), gpred)
#@ Making plots ...
png("tissue_all_THg.png", width = 960)
boxplot(xTHg$TConc ~ xTHg$Location*xTHg$Period, main="THg tissue concentrations (µg/g dw)",
axes=F)
axis(1, at=1:8, labels=c("Pre P01","Pre P08","Pre P11","Pre P17",
```

```
  "Post P01","Post P08","Post P11","Post P17"))
axis(2)
box()
suba <- xTHg
XS <- rep(NA, 8)
k = 0
for(j in c("aPre","Post"))
  for(i in c("P01","P08","P11","P17"))
{
  k <- k + 1
  sub <- suba[suba$Location==i & suba$Period==j,]
  if(dim(sub)[[1]] > 0)
    XS[k] <- mean(sub$TConc)
}
points(1:8, XS, pch="X", col="red")
#
dev.off()
#
png("tissue_all_THg_reformated.png", width = 960)
boxplot(xTHg$TConc ~ xTHg$Period*xTHg$Location, main="THg tissue concentrations (µg/g dw)",
axes=F)
axis(1, at=1:8, labels=c("Pre P01","Post P01","Pre P08","Post P08","Pre P11","Post P11",
  "Pre P17","Post P17"))
axis(2)
box()
suba <- xTHg
XS <- rep(NA, 8)
k = 0
for(j in c("aPre","Post"))
  for(i in c("P01","P08","P11","P17"))
{
  k <- k + 1
  sub <- suba[suba$Location==i & suba$Period==j,]
  if(dim(sub)[[1]] > 0)
```

```
   XS[k] <- mean(sub$TConc)
}
points(c(1,3,5,7,2,4,6,8), XS, pch="X", col="red")
#
dev.off()
#
png("tissue_non0_THg.png", width = 960)
boxplot(xTHg$TConc[isNonZero==1] ~ xTHg$Location[isNonZero==1]*xTHg$Period[isNonZero==1],
  main="Tissue THg concentrations (non-0)", axes=F)
axis(1, at=1:8, labels=c("Pre P01","Pre P08","Pre P11","Pre P17",
  "Post P01","Post P08","Post P11","Post P17"))
axis(2)
box()
suba <- posTHg
XS <- rep(NA, 8)
k = 0
for(j in c("aPre","Post"))
  for(i in c("P01","P08","P11","P17"))
{
  k <- k + 1
  sub <- suba[suba$Location==i & suba$Period==j,]
  if(dim(sub)[[1]] > 0)
    XS[k] <- mean(sub$TConc)
}
points(1:8, XS, pch="X", col="red")
#
dev.off()
#
png("tissue_non0_THg_reformated.png", width = 960)
boxplot(xTHg$TConc[isNonZero==1] ~ xTHg$Period[isNonZero==1]*xTHg$Location[isNonZero==1],
  main="Tissue THg concentrations (non-0)", axes=F)
axis(1, at=1:8, labels=c("Pre P01","Post P01","Pre P08","Post P08","Pre P11","Post P11",
  "Pre P17","Post P17"))
```

```
axis(2)
box()
suba <- posTHg
XS <- rep(NA, 8)
k = 0
for(j in c("aPre","Post"))
 for(i in c("P01","P08","P11","P17"))
{
 k <- k + 1
 sub <- suba[suba$Location==i & suba$Period==j,]
 if(dim(sub)[[1]] > 0)
   XS[k] <- mean(sub$TConc)
}
points(c(1,3,5,7,2,4,6,8), XS, pch="X", col="red")
#
dev.off()
###
##  Doing Zn next, lots of 0s; two-step model
###
zerosZn <- xZn[xZn$TConc==0,]
posZn <- xZn[xZn$TConc > 0,]
isNonZero <- as.numeric(xZn$TConc>0)
test0 <- glm(isNonZero ~ I(Period=="Post") + Location, family=binomial(), data=xZn)
test1 <- glm(TConc ~ Period + Location, family=Gamma(), data=posZn)
test1a <- glm(TConc ~ Period, family=Gamma(), data=posZn)
test1b <- glm(TConc ~ Location, family=Gamma(), data=posZn)
test1c <- glm(TConc ~ Period * Location, family=Gamma(), data=posZn)
### What, if anything, drives 0-values?
summary(test0)
table(isNonZero, xZn$Period)
table(isNonZero, xZn$Location)
fisher.test(table(isNonZero, xZn$Period)) #
fisher.test(table(isNonZero, xZn$Location)) #
```

```
### What, if anything, drives the value of non-0-values?
#@ Interaction test
anova(test1, test1c, test="Chisq") #
#@ Period ME test
anova(test1b, test1, test="Chisq") #
#@ Location ME test
anova(test1a, test1, test="Chisq") #
#@ Looking at the effects for interpretation ...
summary(test1)
#@ Making predictions ...
zpred <- round(predict(test0, type="response"),5)
ppred <- round(predict(test1, type="response"),5)
gpred <- rep(0, dim(xZn)[1])
gpred[isNonZero==1] <- ppred
outZn <- data.frame(xZn, zpred=(1-zpred), gpred)
#@ Making plots ...
png("tissue_all_Zn.png", width = 960)
boxplot(xZn$TConc ~ xZn$Location*xZn$Period, main="Zn tissue concentrations (µg/g dw)", axes=F)
axis(1, at=1:8, labels=c("Pre P01","Pre P08","Pre P11","Pre P17",
  "Post P01","Post P08","Post P11","Post P17"))
axis(2)
box()
suba <- xZn
XS <- rep(NA, 8)
k = 0
for(j in c("aPre","Post"))
  for(i in c("P01","P08","P11","P17"))
{
  k <- k + 1
  sub <- suba[suba$Location==i & suba$Period==j,]
  if(dim(sub)[[1]] > 0)
    XS[k] <- mean(sub$TConc)
}
```

```
points(1:8, XS, pch="X", col="red")
#
dev.off()
#
png("tissue_all_Zn_reformated.png", width = 960)
boxplot(xZn$TConc ~ xZn$Period*xZn$Location, main="Zn tissue concentrations (µg/g dw)", axes=F)
axis(1, at=1:8, labels=c("Pre P01","Post P01","Pre P08","Post P08","Pre P11","Post P11",
 "Pre P17","Post P17"))
axis(2)
box()
suba <- xZn
XS <- rep(NA, 8)
k = 0
for(j in c("aPre","Post"))
 for(i in c("P01","P08","P11","P17"))
{
 k <- k + 1
 sub <- suba[suba$Location==i & suba$Period==j,]
 if(dim(sub)[[1]] > 0)
   XS[k] <- mean(sub$TConc)
}
points(c(1,3,5,7,2,4,6,8), XS, pch="X", col="red")
#
dev.off()
#
png("tissue_non0_Zn.png", width = 960)
boxplot(xZn$TConc[isNonZero==1] ~ xZn$Location[isNonZero==1]*xZn$Period[isNonZero==1],
 main="Tissue Zn concentrations (non-0)", axes=F)
axis(1, at=1:8, labels=c("Pre P01","Pre P08","Pre P11","Pre P17",
 "Post P01","Post P08","Post P11","Post P17"))
axis(2)
box()
suba <- posZn
```

```
XS <- rep(NA, 8)
k = 0
for(j in c("aPre","Post"))
 for(i in c("P01","P08","P11","P17"))
{
 k <- k + 1
 sub <- suba[suba$Location==i & suba$Period==j,]
 if(dim(sub)[[1]] > 0)
   XS[k] <- mean(sub$TConc)
}
points(1:8, XS, pch="X", col="red")
#
dev.off()
png("tissue_non0_Zn_reformated.png", width = 960)
boxplot(xZn$TConc[isNonZero==1] ~ xZn$Period[isNonZero==1]*xZn$Location[isNonZero==1],
 main="Tissue Zn concentrations (non-0)", axes=F)
axis(1, at=1:8, labels=c("Pre P01","Post P01","Pre P08","Post P08","Pre P11","Post P11",
 "Pre P17","Post P17"))
axis(2)
box()
suba <- posZn
XS <- rep(NA, 8)
k = 0
for(j in c("aPre","Post"))
 for(i in c("P01","P08","P11","P17"))
{
 k <- k + 1
 sub <- suba[suba$Location==i & suba$Period==j,]
 if(dim(sub)[[1]] > 0)
   XS[k] <- mean(sub$TConc)
}
points(c(1,3,5,7,2,4,6,8), XS, pch="X", col="red")
#
```

```
dev.off()
###
##  Doing As next, lots of 0s; two-step model
###
zerosAs <- xAs[xAs$TConc==0,]
posAs <- xAs[xAs$TConc > 0,]
isNonZero <- as.numeric(xAs$TConc>0)
test0 <- glm(isNonZero ~ I(Period=="Post") + Location, family=binomial(), data=xAs)
test1 <- glm(TConc ~ Period + Location, family=Gamma(), data=posAs)
test1a <- glm(TConc ~ Period, family=Gamma(), data=posAs)
test1b <- glm(TConc ~ Location, family=Gamma(), data=posAs)
test1c <- glm(TConc ~ Period * Location, family=Gamma(), data=posAs)
### What, if anything, drives 0-values?
summary(test0)
table(isNonZero, xAs$Period)
table(isNonZero, xAs$Location)
fisher.test(table(isNonZero, xAs$Period)) #
fisher.test(table(isNonZero, xAs$Location)) #
### What, if anything, drives the value of non-0-values?
#@ Interaction test
anova(test1, test1c, test="Chisq") # p=0.01; evidence of interaction
#> No point in doing ME tests since strongly significant interaction exists
#@ Looking at the effects for interpretation ...
summary(test1)
#@ Making predictions ...
zpred <- round(predict(test0, type="response"),5)
ppred <- round(predict(test1, type="response"),5)
gpred <- rep(0, dim(xAs)[1])
gpred[isNonZero==1] <- ppred
outAs <- data.frame(xAs, zpred=(1-zpred), gpred)
#@ Making plots ...
png("tissue_all_As.png", width = 960)
boxplot(xAs$TConc ~ xAs$Location*xAs$Period, main="As tissue concentrations (µg/g dw)", axes=F)
```

```
axis(1, at=1:8, labels=c("Pre P01","Pre P08","Pre P11","Pre P17",
  "Post P01","Post P08","Post P11","Post P17"))
axis(2)
box()
suba <- xAs
XS <- rep(NA, 8)
k = 0
for(j in c("aPre","Post"))
  for(i in c("P01","P08","P11","P17"))
{
  k <- k + 1
  sub <- suba[suba$Location==i & suba$Period==j,]
  if(dim(sub)[[1]] > 0)
    XS[k] <- mean(sub$TConc)
}
points(1:8, XS, pch="X", col="red")
#
dev.off()
#
png("tissue_all_As_reformated.png", width = 960)
boxplot(xAs$TConc ~ xAs$Period*xAs$Location, main="As tissue concentrations (µg/g dw)", axes=F)
axis(1, at=1:8, labels=c("Pre P01","Post P01","Pre P08","Post P08","Pre P11","Post P11",
  "Pre P17","Post P17"))
axis(2)
box()
suba <- xAs
XS <- rep(NA, 8)
k = 0
for(j in c("aPre","Post"))
  for(i in c("P01","P08","P11","P17"))
{
  k <- k + 1
  sub <- suba[suba$Location==i & suba$Period==j,]
```

```
  if(dim(sub)[[1]] > 0)
    XS[k] <- mean(sub$TConc)
}
points(c(1,3,5,7,2,4,6,8), XS, pch="X", col="red")
#
dev.off()
#
png("tissue_non0_As.png", width = 960)
boxplot(xAs$TConc[isNonZero==1] ~ xAs$Location[isNonZero==1]*xAs$Period[isNonZero==1],
  main="Tissue As concentrations (non-0)", axes=F)
axis(1, at=1:8, labels=c("Pre P01","Pre P08","Pre P11","Pre P17",
  "Post P01","Post P08","Post P11","Post P17"))
axis(2)
box()
suba <- posAs
XS <- rep(NA, 8)
k = 0
for(j in c("aPre","Post"))
  for(i in c("P01","P08","P11","P17"))
{
  k <- k + 1
  sub <- suba[suba$Location==i & suba$Period==j,]
  if(dim(sub)[[1]] > 0)
    XS[k] <- mean(sub$TConc)
}
points(1:8, XS, pch="X", col="red")
#
dev.off()
#
png("tissue_non0_As_reformated.png", width = 960)
boxplot(xAs$TConc[isNonZero==1] ~ xAs$Period[isNonZero==1]*xAs$Location[isNonZero==1],
  main="Tissue As concentrations (non-0)", axes=F)
axis(1, at=1:8, labels=c("Pre P01","Post P01","Pre P08","Post P08","Pre P11","Post P11",
```

```
  "Pre P17","Post P17"))
axis(2)
box()
suba <- posAs
XS <- rep(NA, 8)
k = 0
for(j in c("aPre","Post"))
  for(i in c("P01","P08","P11","P17"))
{
  k <- k + 1
  sub <- suba[suba$Location==i & suba$Period==j,]
  if(dim(sub)[[1]] > 0)
    XS[k] <- mean(sub$TConc)
}
points(c(1,3,5,7,2,4,6,8), XS, pch="X", col="red")
#
dev.off()
###
##  Doing Cu next, a single 0 (not anymore)
###
xCu <- base[base[,1]=="Cu",]
#indiCu <- which(xCu$TConc==0)
#print(xCu[indiCu,])
#
#val1 <- 0.42637 # smallest non-0 Cu value
#xCu[indiCu,5] <- val1
test1 <- glm(TConc ~ I(Period=="Post") + Location, family=Gamma(), data=xCu)
test1a <- glm(TConc ~ I(Period=="Post"), family=Gamma(), data=xCu)
test1b <- glm(TConc ~ Location, family=Gamma(), data=xCu)
test1c <- glm(TConc ~ Period * Location, family=Gamma(), data=xCu)
#@ Interaction test
anova(test1, test1c, test="Chisq") #
#@ Period ME test
```

```
anova(test1b, test1, test="Chisq") #
#@ Location ME test
anova(test1a, test1, test="Chisq") #
#@ Looking at the effects for interpretation ...
summary(test1)
#@ Making predictions ...
gpred <- round(predict(test1, type="response"),5)
outCu <- data.frame(xCu, gpred)
#@ Making plots ...
png("tissue_all_Cu.png", width = 960)
boxplot(xCu$TConc ~ xCu$Location*xCu$Period,
  main="Cu tissue concentrations (µg/g dw)", axes=F)
axis(1, at=1:8, labels=c("Pre P01","Pre P08","Pre P11","Pre P17",
  "Post P01","Post P08","Post P11","Post P17"))
axis(2)
box()
suba <- xCu
XS <- rep(NA, 8)
k = 0
for(j in c("aPre","Post"))
  for(i in c("P01","P08","P11","P17"))
{
  k <- k + 1
  sub <- suba[suba$Location==i & suba$Period==j,]
  if(dim(sub)[[1]] > 0)
    XS[k] <- mean(sub$TConc)
}
points(1:8, XS, pch="X", col="red")
#
dev.off()
#
png("tissue_all_Cu_reformatted.png", width = 960)
boxplot(xCu$TConc ~ xCu$Period*xCu$Location,
```

```
  main="Cu tissue concentrations (µg/g dw)", axes=F)
axis(1, at=1:8, labels=c("Pre P01","Post P01","Pre P08","Post P08","Pre P11","Post P11",
  "Pre P17","Post P17"))
axis(2)
box()
suba <- xCu
XS <- rep(NA, 8)
k = 0
for(j in c("aPre","Post"))
  for(i in c("P01","P08","P11","P17"))
{
  k <- k + 1
  sub <- suba[suba$Location==i & suba$Period==j,]
  if(dim(sub)[[1]] > 0)
    XS[k] <- mean(sub$TConc)
}
points(c(1,3,5,7,2,4,6,8), XS, pch="X", col="red")
#
dev.off()
#
png("tissue_all_Cu_reformated.png", width = 960)
boxplot(xCu$TConc ~ xCu$Period*xCu$Location, main="Cu tissue concentrations (µg/g dw)", axes=F)
axis(1, at=1:8, labels=c("Pre P01","Post P01","Pre P08","Post P08","Pre P11","Post P11",
  "Pre P17","Post P17"))
axis(2)
box()
suba <- xCu
XS <- rep(NA, 8)
k = 0
for(j in c("aPre","Post"))
  for(i in c("P01","P08","P11","P17"))
{
  k <- k + 1
```

```
 sub <- suba[suba$Location==i & suba$Period==j,]
 if(dim(sub)[[1]] > 0)
   XS[k] <- mean(sub$TConc)
}
points(c(1,3,5,7,2,4,6,8), XS, pch="X", col="red")
#
dev.off()
#
###
##  Lastly Pb, a single 0 (not anymore)
###
xPb <- base[base[,1]=="Pb",]
#indiPb <- which(xPb$TConc==0)
#print(xPb[indiPb,])
#
#val2 <- 0.24413 # smallest non-0 Pb value
#xPb[indiPb,5] <- val2
#
test1 <- glm(TConc ~ I(Period=="Post") + Location, family=Gamma(), data=xPb)
test1a <- glm(TConc ~ I(Period=="Post"), family=Gamma(), data=xPb)
test1b <- glm(TConc ~ Location, family=Gamma(), data=xPb)
test1c <- glm(TConc ~ Period * Location, family=Gamma(), data=xPb)
#@ Interaction test
anova(test1, test1c, test="Chisq") #
#@ Period ME test
anova(test1b, test1, test="Chisq") #
#@ Location ME test
anova(test1a, test1, test="Chisq") #
#@ Looking at the effects for interpretation ...
summary(test1)
#@ Making predictions ...
gpred <- round(predict(test1, type="response"),5)
outPb <- data.frame(xPb, gpred)
```

```
#@ Making plots ...
png("tissue_all_Pb.png", width = 960)
boxplot(xPb$TConc ~ xPb$Location*xPb$Period,
  main="Pb tissue concentrations (µg/g dw)", axes=F)
axis(1, at=1:8, labels=c("Pre P01","Pre P08","Pre P11","Pre P17",
  "Post P01","Post P08","Post P11","Post P17"))
axis(2)
box()
suba <- xPb
XS <- rep(NA, 8)
k = 0
for(j in c("aPre","Post"))
  for(i in c("P01","P08","P11","P17"))
{
  k <- k + 1
  sub <- suba[suba$Location==i & suba$Period==j,]
  if(dim(sub)[[1]] > 0)
    XS[k] <- mean(sub$TConc)
}
points(1:8, XS, pch="X", col="red")
#
dev.off()
#
png("tissue_all_Pb_reformated.png", width = 960)
boxplot(xPb$TConc ~ xPb$Period*xPb$Location, main="Pb tissue concentrations (µg/g dw)", axes=F)
axis(1, at=1:8, labels=c("Pre P01","Post P01","Pre P08","Post P08","Pre P11","Post P11",
  "Pre P17","Post P17"))
axis(2)
box()
suba <- xPb
XS <- rep(NA, 8)
k = 0
for(j in c("aPre","Post"))
```

```
 for(i in c("P01","P08","P11","P17"))
{
 k <- k + 1
 sub <- suba[suba$Location==i & suba$Period==j,]
 if(dim(sub)[[1]] > 0)
   XS[k] <- mean(sub$TConc)
}
points(c(1,3,5,7,2,4,6,8), XS, pch="X", col="red")
#
dev.off()
#
# EOF - Tissue analyses with interaction checks and plots
```

For porewater analysis

```
setwd("C:/Users/idrygian/Desktop/twostep")
mega <-read.csv("megaData.csv", header=T, strings=F)
base <- mega[,6:10]
base <- base[1:296,] # Removing blank rows
dimnames(base)[[2]] <- c("Outcome","Location","Period","PoreConc","Sample.ID")
library(stringr)
base$Location <- as.factor(str_trim(base$Location))
base$Period <- str_trim(base$Period)
base$Period[base$Period=="Pre"] <- "aPre" #
base$Period <- as.factor(base$Period)
unique(base$Location) # 4 locations
unique(base$Period) # 2 time periods
#
# In order to allow code reuse, going to call PoreConc TConc ...

dimnames(base)[[2]][4] <- "TConc"
#xAs <- base[base[,1]=="As",] # No As pore data
xCd <- base[base[,1]=="Cd",]
```

```
xCu <- base[base[,1]=="Cu",]
xNi <- base[base[,1]=="Ni",]
xPb <- base[base[,1]=="Pb",]
xTHg <- base[base[,1]=="THg",]
xZn <- base[base[,1]=="Zn",]
#str(xAs)
str(xCd)
str(xCu)
str(xNi)
str(xPb)
str(xTHg)
str(xZn)
##############
# Zero checks
#sum(xAs$TConc<=0) # No As pore data
sum(xCd$TConc<=0) # 26, all 0s
sum(xCu$TConc<=0) # 0
sum(xNi$TConc<=0) # 0
sum(xPb$TConc<=0) # 1, also a 0
sum(xTHg$TConc<=0) # 0
sum(xZn$TConc<=0) # 0
outcomeNames <- c("Cd", "Cu", "Ni", "Pb", "THg", "Zn")
all <- list(xCd, xCu, xNi, xPb, xTHg, xZn)
###
##  Doing Cd first since so many 0s; two-step model
###

zerosCd <- xCd[xCd$TConc==0,]
posCd <- xCd[xCd$TConc > 0,]
isNonZero <- as.numeric(xCd$TConc>0)
test0 <- glm(isNonZero ~ I(Period=="Post") + Location, family=binomial(), data=xCd)
test1 <- glm(TConc ~ Period + Location, family=Gamma(), data=posCd)
test1a <- glm(TConc ~ Period, family=Gamma(), data=posCd)
```

```
test1b <- glm(TConc ~ Location, family=Gamma(), data=posCd)
test1c <- glm(TConc ~ Period * Location, family=Gamma(), data=posCd)
### What, if anything, drives 0-values?
summary(test0)
table(isNonZero, xCd$Period)
table(isNonZero, xCd$Location)
fisher.test(table(isNonZero, xCd$Period)) #
fisher.test(table(isNonZero, xCd$Location)) #
### What, if anything, drives the value of non-0-values?
#@ Interaction test
anova(test1, test1c, test="Chisq") #
#@ Period ME test
anova(test1b, test1, test="Chisq") #
#@ Location ME test
anova(test1a, test1, test="Chisq") #
#@ Looking at the effects for interpretation ...
summary(test1)
#@ Making predictions ...
zpred <- round(predict(test0, type="response"),5)
ppred <- round(predict(test1, type="response"),5)
gpred <- rep(0, dim(xCd)[1])
gpred[isNonZero==1] <- ppred
outCd <- data.frame(xCd, zpred=(1-zpred), gpred)
#@ Making plots ...
png("pore_all_Cd_reformatted.png", width = 960)
boxplot(xCd$TConc ~ xCd$Period*xCd$Location, main="Cd porewater concentrations (µg/L)", axes=F)
axis(1, at=1:8, labels=c("Pre P01","Post P01","Pre P08","Post P08","Pre P11","Post P11",
  "Pre P17","Post P17"))
axis(2)
box()
suba <- xCd
XS <- rep(NA, 8)
k = 0
```

```
for(j in c("aPre","Post"))
 for(i in c("P01","P08","P11","P17"))
{
 k <- k + 1
 sub <- suba[suba$Location==i & suba$Period==j,]
 if(dim(sub)[[1]] > 0)
   XS[k] <- mean(sub$TConc)
}
points(c(1,3,5,7,2,4,6,8), XS, pch="X", col="red")
#
dev.off()
#
png("pore_non0_Cd_reformatted.png", width = 960)
boxplot(xCd$TConc[isNonZero==1] ~ xCd$Period[isNonZero==1]*xCd$Location[isNonZero==1],
 main="Porewater Cd concentrations (non-0)", axes=F)
axis(1, at=1:8, labels=c("Pre P01","Post P01","Pre P08","Post P08","Pre P11","Post P11",
 "Pre P17","Post P17"))
axis(2)
box()
suba <- posCd
XS <- rep(NA, 8)
k = 0
for(j in c("aPre","Post"))
 for(i in c("P01","P08","P11","P17"))
{
 k <- k + 1
 sub <- suba[suba$Location==i & suba$Period==j,]
 if(dim(sub)[[1]] > 0)
   XS[k] <- mean(sub$TConc)
}
points(c(1,3,5,7,2,4,6,8), XS, pch="X", col="red")
#
dev.off()
```

```
#
###
##  All the rest have nil or one zero value, doing those with all > 0; Cu next
###
xCu <- base[base[,1]=="Cu",]
#
test1 <- glm(TConc ~ I(Period=="Post") + Location, family=Gamma(), data=xCu)
test1a <- glm(TConc ~ I(Period=="Post"), family=Gamma(), data=xCu)
test1b <- glm(TConc ~ Location, family=Gamma(), data=xCu)
test1c <- glm(TConc ~ Period * Location, family=Gamma(), data=xCu)
#@ Interaction test
anova(test1, test1c, test="Chisq") #
#@ Period ME test
anova(test1b, test1, test="Chisq") #
#@ Location ME test
anova(test1a, test1, test="Chisq") #
#@ Looking at the effects for interpretation ...
summary(test1)
#@ Making predictions ...
gpred <- round(predict(test1, type="response"),5)
outCu <- data.frame(xCu, gpred)
#@ Making plots ...
png("pore_all_Cu.png", width = 960)
boxplot(xCu$TConc ~ xCu$Location*xCu$Period,
  main="Cu porewater concentrations (µg/L)", axes=F)
axis(1, at=1:8, labels=c("Pre P01","Pre P08","Pre P11","Pre P17",
  "Post P01","Post P08","Post P11","Post P17"))
axis(2)
box()
suba <- xCu
XS <- rep(NA, 8)
k = 0
for(j in c("aPre","Post"))
```

```
 for(i in c("P01","P08","P11","P17"))
{
 k <- k + 1
 sub <- suba[suba$Location==i & suba$Period==j,]
 if(dim(sub)[[1]] > 0)
   XS[k] <- mean(sub$TConc)
}
points(1:8, XS, pch="X", col="red")
#
dev.off()
#
png("pore_all_Cu_reformatted.png", width = 960)
boxplot(xCu$TConc ~ xCu$Period*xCu$Location,
 main="Cu porewater concentrations (µg/L)", axes=F)
axis(1, at=1:8, labels=c("Pre P01","Post P01","Pre P08","Post P08","Pre P11","Post P11",
 "Pre P17","Post P17"))
axis(2)
box()
suba <- xCu
XS <- rep(NA, 8)
k = 0
for(i in c("P01","P08","P11","P17"))
 for(j in c("aPre","Post"))
{
 k <- k + 1
 sub <- suba[suba$Location==i & suba$Period==j,]
 if(dim(sub)[[1]] > 0)
   XS[k] <- mean(sub$TConc)
}
points(1:8, XS, pch="X", col="red")
#
dev.off()
###
```

```
##  Ni next
###
xNi <- base[base[,1]=="Ni",]
#
test1 <- glm(TConc ~ I(Period=="Post") + Location, family=Gamma(), data=xNi)
test1a <- glm(TConc ~ I(Period=="Post"), family=Gamma(), data=xNi)
test1b <- glm(TConc ~ Location, family=Gamma(), data=xNi)
test1c <- glm(TConc ~ Period * Location, family=Gamma(), data=xNi)
#@ Interaction test
anova(test1, test1c, test="Chisq")
#@ Period ME test
anova(test1b, test1, test="Chisq") #
#@ Location ME test
anova(test1a, test1, test="Chisq") #
#@ Looking at the effects for interpretation ...
summary(test1)
#@ Making predictions ...
gpred <- round(predict(test1, type="response"),5)
outNi <- data.frame(xNi, gpred)
#@ Making plots ...
png("pore_all_Ni.png", width = 960)
boxplot(xNi$TConc ~ xNi$Location*xNi$Period,
  main="Ni porewater concentrations (µg/L)", axes=F)
axis(1, at=1:8, labels=c("Pre P01","Pre P08","Pre P11","Pre P17",
  "Post P01","Post P08","Post P11","Post P17"))
axis(2)
box()
suba <- xNi
XS <- rep(NA, 8)
k = 0
for(j in c("aPre","Post"))
  for(i in c("P01","P08","P11","P17"))
{
```

```
  k <- k + 1
  sub <- suba[suba$Location==i & suba$Period==j,]
  if(dim(sub)[[1]] > 0)
    XS[k] <- mean(sub$TConc)
}
points(1:8, XS, pch="X", col="red")
#
dev.off()
#
png("pore_all_Ni_reformatted.png", width = 960)
boxplot(xNi$TConc ~ xNi$Period*xNi$Location,
  main="Ni porewater concentrations (µg/L)", axes=F)
axis(1, at=1:8, labels=c("Pre P01","Post P01","Pre P08","Post P08","Pre P11","Post P11",
  "Pre P17","Post P17"))
axis(2)
box()
suba <- xNi
XS <- rep(NA, 8)
k = 0
for(i in c("P01","P08","P11","P17"))
  for(j in c("aPre","Post"))
{
  k <- k + 1
  sub <- suba[suba$Location==i & suba$Period==j,]
  if(dim(sub)[[1]] > 0)
    XS[k] <- mean(sub$TConc)
}
points(1:8, XS, pch="X", col="red")
#
dev.off()
###
##  THg next
###
```

```
xTHg <- base[base[,1]=="THg",]
#
test1 <- glm(TConc ~ I(Period=="Post") + Location, family=Gamma(), data=xTHg)
test1a <- glm(TConc ~ I(Period=="Post"), family=Gamma(), data=xTHg)
test1b <- glm(TConc ~ Location, family=Gamma(), data=xTHg)
test1c <- glm(TConc ~ Period * Location, family=Gamma(), data=xTHg)
#@ Interaction test
anova(test1, test1c, test="Chisq") #
#> No point in doing ME tests since strongly significant interaction exists
#@ Looking at the effects for interpretation ...
summary(test1c)
#@ Making predictions ...
gpred <- round(predict(test1, type="response"),5)
outTHg <- data.frame(xTHg, gpred)
#@ Making plots ...
png("pore_all_THg.png", width = 960)
boxplot(xTHg$TConc ~ xTHg$Location*xTHg$Period,
  main="THg porewater concentrations (µg/L)", axes=F)
axis(1, at=1:8, labels=c("Pre P01","Pre P08","Pre P11","Pre P17",
  "Post P01","Post P08","Post P11","Post P17"))
axis(2)
box()
suba <- xTHg
XS <- rep(NA, 8)
k = 0
for(j in c("aPre","Post"))
  for(i in c("P01","P08","P11","P17"))
{
  k <- k + 1
  sub <- suba[suba$Location==i & suba$Period==j,]
  if(dim(sub)[[1]] > 0)
    XS[k] <- mean(sub$TConc)
}
```

```
points(1:8, XS, pch="X", col="red")
#
dev.off()
#
png("pore_all_THg_reformatted.png", width = 960)
boxplot(xTHg$TConc ~ xTHg$Period*xTHg$Location,
  main="THg porewater concentrations (µg/L)", axes=F)
axis(1, at=1:8, labels=c("Pre P01","Post P01","Pre P08","Post P08","Pre P11","Post P11",
  "Pre P17","Post P17"))
axis(2)
box()
suba <- xTHg
XS <- rep(NA, 8)
k = 0
for(i in c("P01","P08","P11","P17"))
  for(j in c("aPre","Post"))
{
  k <- k + 1
  sub <- suba[suba$Location==i & suba$Period==j,]
  if(dim(sub)[[1]] > 0)
    XS[k] <- mean(sub$TConc)
}
points(1:8, XS, pch="X", col="red")
#
dev.off()
###
##  Zn next
###
xZn <- base[base[,1]=="Zn",]
#
test1 <- glm(TConc ~ I(Period=="Post") + Location, family=Gamma(), data=xZn)
test1a <- glm(TConc ~ I(Period=="Post"), family=Gamma(), data=xZn)
test1b <- glm(TConc ~ Location, family=Gamma(), data=xZn)
```

```
test1c <- glm(TConc ~ Period * Location, family=Gamma(), data=xZn)
#@ Interaction test
anova(test1, test1c, test="Chisq") #
#> No point in doing ME tests since significant interaction exists
#@ Looking at the effects for interpretation ...
summary(test1c)
#@ Making predictions ...
gpred <- round(predict(test1, type="response"),5)
outZn <- data.frame(xZn, gpred)
#@ Making plots ...
png("pore_all_Zn.png", width = 960)
boxplot(xZn$TConc ~ xZn$Location*xZn$Period,
  main="Zn porewater concentrations (µg/L)", axes=F)
axis(1, at=1:8, labels=c("Pre P01","Pre P08","Pre P11","Pre P17",
  "Post P01","Post P08","Post P11","Post P17"))
axis(2)
box()
suba <- xZn
XS <- rep(NA, 8)
k = 0
for(j in c("aPre","Post"))
  for(i in c("P01","P08","P11","P17"))
{
  k <- k + 1
  sub <- suba[suba$Location==i & suba$Period==j,]
  if(dim(sub)[[1]] > 0)
    XS[k] <- mean(sub$TConc)
}
points(1:8, XS, pch="X", col="red")
#
dev.off()
#
png("pore_all_Zn_reformatted.png", width = 960)
```

```
boxplot(xZn$TConc ~ xZn$Period*xZn$Location,
  main="Zn porewater concentrations (µg/L)", axes=F)
axis(1, at=1:8, labels=c("Pre P01","Post P01","Pre P08","Post P08","Pre P11","Post P11",
  "Pre P17","Post P17"))
axis(2)
box()
suba <- xZn
XS <- rep(NA, 8)
k = 0
for(i in c("P01","P08","P11","P17"))
  for(j in c("aPre","Post"))
{
  k <- k + 1
  sub <- suba[suba$Location==i & suba$Period==j,]
  if(dim(sub)[[1]] > 0)
    XS[k] <- mean(sub$TConc)
}
points(1:8, XS, pch="X", col="red")
#
dev.off()
#


###
##  No As pore data


###
##  Lastly Pb, which has a single 0-value
###
xPb <- base[base[,1]=="Pb",]
indiPb <- which(xPb$TConc==0)
print(xPb[indiPb,])
#
val2 <- 0.02 # smallest non-0 Pb value
```

```
xPb[indiPb,4] <- val2
#
test1 <- glm(TConc ~ I(Period=="Post") + Location, family=Gamma(), data=xPb)
test1a <- glm(TConc ~ I(Period=="Post"), family=Gamma(), data=xPb)
test1b <- glm(TConc ~ Location, family=Gamma(), data=xPb)
test1c <- glm(TConc ~ Period * Location, family=Gamma(), data=xPb)
#@ Interaction test
anova(test1, test1c, test="Chisq")
#@ Period ME test
anova(test1b, test1, test="Chisq") #
#@ Location ME test
anova(test1a, test1, test="Chisq") #
#@ Looking at the effects for interpretation ...
sumary(test1)
#@ Making predictions ...
gpred <- round(predict(test1, type="response"),5)
outPb <- data.frame(xPb, gpred)
#@ Making plots ...
png("pore_all_Pb.png", width = 960)
boxplot(xPb$TConc ~ xPb$Location*xPb$Period,
  main="Pb porewater concentrations (µg/L)", axes=F)
axis(1, at=1:8, labels=c("Pre P01","Pre P08","Pre P11","Pre P17",
  "Post P01","Post P08","Post P11","Post P17"))
axis(2)
box()
suba <- xPb
XS <- rep(NA, 8)
k = 0
for(j in c("aPre","Post"))
  for(i in c("P01","P08","P11","P17"))
{
  k <- k + 1
  sub <- suba[suba$Location==i & suba$Period==j,]
```

```
 if(dim(sub)[[1]] > 0)
   XS[k] <- mean(sub$TConc)
}
points(1:8, XS, pch="X", col="red")
#
dev.off()
#
png("pore_all_Pb_reformatted.png", width = 960)
boxplot(xPb$TConc ~ xPb$Period*xPb$Location,
 main="Pb porewater concentrations (µg/L)", axes=F)
axis(1, at=1:8, labels=c("Pre P01","Post P01","Pre P08","Post P08","Pre P11","Post P11",
 "Pre P17","Post P17"))
axis(2)
box()
suba <- xPb
XS <- rep(NA, 8)
k = 0
for(i in c("P01","P08","P11","P17"))
 for(j in c("aPre","Post"))
{
 k <- k + 1
 sub <- suba[suba$Location==i & suba$Period==j,]
 if(dim(sub)[[1]] > 0)
   XS[k] <- mean(sub$TConc)
}
points(1:8, XS, pch="X", col="red")
#
dev.off()
#
# EOF - Porewater analyses with interaction checks and plots
```

For sediment core analysis

```
setwd("C:/Users/idrygian/Desktop/twostep")
```

```
mega <-read.csv("megaData.csv", header=T, strings=F)
base <- mega[,11:15]
base <- base[1:376,] # Removing blank rows
dimnames(base)[[2]] <- c("Outcome","Location","Period","SedConc","Sample.ID")
library(stringr)
base$Location <- as.factor(str_trim(base$Location))
base$Period <- str_trim(base$Period)
base$Period[base$Period=="Pre"] <- "aPre" #
base$Period <- as.factor(base$Period)
unique(base$Location) # 4 locations
unique(base$Period) # 2 time periods
#
# In order to allow code reuse, going to call PoreConc TConc ...
dimnames(base)[[2]][4] <- "TConc"
xAs <- base[base[,1]=="As",]
xCd <- base[base[,1]=="Cd",]
xCu <- base[base[,1]=="Cu",]
xNi <- base[base[,1]=="Ni",]
xPb <- base[base[,1]=="Pb",]
xTHg <- base[base[,1]=="THg",]
xZn <- base[base[,1]=="Zn",]
str(xAs)
str(xCd)
str(xCu)
str(xNi)
str(xPb)
str(xTHg)
str(xZn)
##############
# Zero checks
sum(xAs$TConc<=0) # 0
sum(xCd$TConc<=0) # 18, all 0s
sum(xCu$TConc<=0) # 0
```

```
sum(xNi$TConc<=0) # 0
sum(xPb$TConc<=0) # 0
sum(xTHg$TConc<=0) # 0
sum(xZn$TConc<=0) # 0
outcomeNames <- c("As","Cd", "Cu", "Ni", "Pb", "THg", "Zn")
all <- list(xAs, xCd, xCu, xNi, xPb, xTHg, xZn)
###
##  Doing Cd first since so many 0s; two-step model
###
zerosCd <- xCd[xCd$TConc==0,]
posCd <- xCd[xCd$TConc > 0,]
isNonZero <- as.numeric(xCd$TConc>0)
test0 <- glm(isNonZero ~ I(Period=="Post") + Location, family=binomial(), data=xCd)
test1 <- glm(TConc ~ Period + Location, family=Gamma(), data=posCd)
test1a <- glm(TConc ~ Period, family=Gamma(), data=posCd)
test1b <- glm(TConc ~ Location, family=Gamma(), data=posCd)
test1c <- glm(TConc ~ Period * Location, family=Gamma(), data=posCd)
### What, if anything, drives 0-values?
summary(test0)
table(isNonZero, xCd$Period)
table(isNonZero, xCd$Location)
fisher.test(table(isNonZero, xCd$Period)) #
fisher.test(table(isNonZero, xCd$Location)) #
### What, if anything, drives the value of non-0-values?
#@ Interaction test
anova(test1, test1c, test="Chisq") #
#> No point in doing ME tests since significant interaction exists
#@ Looking at the effects for interpretation ...
summary(test1c)
#@ Making predictions ...
zpred <- round(predict(test0, type="response"),5)
ppred <- round(predict(test1, type="response"),5)
gpred <- rep(0, dim(xCd)[1])
```

```
gpred[isNonZero==1] <- ppred
outCd <- data.frame(xCd, zpred=(1-zpred), gpred)
#@ Making plots ...
png("sediment_all_Cd_reformatted.png", width = 960)
boxplot(xCd$TConc ~ xCd$Period*xCd$Location, main="Cd sediment concentrations (mg/kg)", axes=F)
axis(1, at=1:8, labels=c("Pre P01","Post P01","Pre P08","Post P08","Pre P11","Post P11",
 "Pre P17","Post P17"))
axis(2)
box()
suba <- xCd
XS <- rep(NA, 8)
k = 0
for(j in c("aPre","Post"))
 for(i in c("P01","P08","P11","P17"))
{
 k <- k + 1
 sub <- suba[suba$Location==i & suba$Period==j,]
 if(dim(sub)[[1]] > 0)
  XS[k] <- mean(sub$TConc)
}
points(c(1,3,5,7,2,4,6,8), XS, pch="X", col="red")
#
dev.off()
#
png("sediment_non0_Cd_reformatted.png", width = 960)
boxplot(xCd$TConc[isNonZero==1] ~ xCd$Period[isNonZero==1]*xCd$Location[isNonZero==1],
 main="Sediment Cd concentrations (non-0)", axes=F)
axis(1, at=1:8, labels=c("Pre P01","Post P01","Pre P08","Post P08","Pre P11","Post P11",
 "Pre P17","Post P17"))
axis(2)
box()
suba <- posCd
XS <- rep(NA, 8)
```

```
k = 0
for(j in c("aPre","Post"))
  for(i in c("P01","P08","P11","P17"))
{
  k <- k + 1
  sub <- suba[suba$Location==i & suba$Period==j,]
  if(dim(sub)[[1]] > 0)
    XS[k] <- mean(sub$TConc)
}
points(c(1,3,5,7,2,4,6,8), XS, pch="X", col="red")
#
dev.off()
#
png("sediment_all_Cd.png", width = 960)
boxplot(xCd$TConc ~ xCd$Location*xCd$Period,
  main="Cd sediment concentrations (mg/kg)", axes=F)
axis(1, at=1:8, labels=c("Pre P01","Pre P08","Pre P11","Pre P17",
  "Post P01","Post P08","Post P11","Post P17"))
axis(2)
box()
suba <- xCd
XS <- rep(NA, 8)
k = 0
for(j in c("aPre","Post"))
  for(i in c("P01","P08","P11","P17"))
{
  k <- k + 1
  sub <- suba[suba$Location==i & suba$Period==j,]
  if(dim(sub)[[1]] > 0)
    XS[k] <- mean(sub$TConc)
}
points(1:8, XS, pch="X", col="red")
#
```

```
dev.off()
###
##  All the rest have no zero values; Cu next
###
xCu <- base[base[,1]=="Cu",]
#
test1 <- glm(TConc ~ I(Period=="Post") + Location, family=Gamma(), data=xCu)
test1a <- glm(TConc ~ I(Period=="Post"), family=Gamma(), data=xCu)
test1b <- glm(TConc ~ Location, family=Gamma(), data=xCu)
test1c <- glm(TConc ~ Period * Location, family=Gamma(), data=xCu)
#@ Interaction test
anova(test1, test1c, test="Chisq") #
#@ Period ME test
anova(test1b, test1, test="Chisq") #
#@ Location ME test
anova(test1a, test1, test="Chisq") #

#@ Looking at the effects for interpretation ...
summary(test1)
#@ Making predictions ...
gpred <- round(predict(test1, type="response"),5)
outCu <- data.frame(xCu, gpred)
#@ Making plots ...
png("sediment_all_Cu.png", width = 960)
boxplot(xCu$TConc ~ xCu$Location*xCu$Period,
  main="Cu sediment concentrations (mg/kg)", axes=F)
axis(1, at=1:8, labels=c("Pre P01","Pre P08","Pre P11","Pre P17",
  "Post P01","Post P08","Post P11","Post P17"))
axis(2)
box()
suba <- xCu
XS <- rep(NA, 8)
k = 0
```

```
for(j in c("aPre","Post"))
 for(i in c("P01","P08","P11","P17"))
{
 k <- k + 1
 sub <- suba[suba$Location==i & suba$Period==j,]
 if(dim(sub)[[1]] > 0)
   XS[k] <- mean(sub$TConc)
}
points(1:8, XS, pch="X", col="red")
#
dev.off()
#
png("sediment_all_Cu_reformatted.png", width = 960)
boxplot(xCu$TConc ~ xCu$Period*xCu$Location,
 main="Cu sediment concentrations (mg/kg)", axes=F)
axis(1, at=1:8, labels=c("Pre P01","Post P01","Pre P08","Post P08","Pre P11","Post P11",
 "Pre P17","Post P17"))
axis(2)
box()
suba <- xCu
XS <- rep(NA, 8)
k = 0
for(j in c("aPre","Post"))
 for(i in c("P01","P08","P11","P17"))
{
 k <- k + 1
 sub <- suba[suba$Location==i & suba$Period==j,]
 if(dim(sub)[[1]] > 0)
   XS[k] <- mean(sub$TConc)
}
points(c(1,3,5,7,2,4,6,8), XS, pch="X", col="red")
#
dev.off()
```

```
###
##  Ni next
###
xNi <- base[base[,1]=="Ni",]
#
test1 <- glm(TConc ~ I(Period=="Post") + Location, family=Gamma(), data=xNi)
test1a <- glm(TConc ~ I(Period=="Post"), family=Gamma(), data=xNi)
test1b <- glm(TConc ~ Location, family=Gamma(), data=xNi)
test1c <- glm(TConc ~ Period * Location, family=Gamma(), data=xNi)
#@ Interaction test
anova(test1, test1c, test="Chisq") #
#@ Period ME test
anova(test1b, test1, test="Chisq")

#@ Location ME test
anova(test1a, test1, test="Chisq") #
#@ Looking at the effects for interpretation ...
summary(test1)
#@ Making predictions ...
gpred <- round(predict(test1, type="response"),5)
outNi <- data.frame(xNi, gpred)
#@ Making plots ...
png("sediment_all_Ni.png", width = 960)
boxplot(xNi$TConc ~ xNi$Location*xNi$Period,
  main="Ni sediment concentrations (mg/kg)", axes=F)
axis(1, at=1:8, labels=c("Pre P01","Pre P08","Pre P11","Pre P17",
  "Post P01","Post P08","Post P11","Post P17"))
axis(2)
box()
suba <- xNi
XS <- rep(NA, 8)
k = 0
for(j in c("aPre","Post"))
```

```
 for(i in c("P01","P08","P11","P17"))
{
 k <- k + 1
 sub <- suba[suba$Location==i & suba$Period==j,]
 if(dim(sub)[[1]] > 0)
   XS[k] <- mean(sub$TConc)
}
points(1:8, XS, pch="X", col="red")
#
dev.off()
#
png("sediment_all_Ni_reformatted.png", width = 960)
boxplot(xNi$TConc ~ xNi$Period*xNi$Location,
 main="Ni sediment concentrations (mg/kg)", axes=F)
axis(1, at=1:8, labels=c("Pre P01","Post P01","Pre P08","Post P08","Pre P11","Post P11",
 "Pre P17","Post P17"))
axis(2)
box()
suba <- xNi
XS <- rep(NA, 8)
k = 0
for(j in c("aPre","Post"))
 for(i in c("P01","P08","P11","P17"))
{
 k <- k + 1
 sub <- suba[suba$Location==i & suba$Period==j,]
 if(dim(sub)[[1]] > 0)
   XS[k] <- mean(sub$TConc)
}
points(c(1,3,5,7,2,4,6,8), XS, pch="X", col="red")
#
dev.off()
###
```

```
##  THg next
###
xTHg <- base[base[,1]=="THg",]
#
test1 <- glm(TConc ~ I(Period=="Post") + Location, family=Gamma(), data=xTHg)
test1a <- glm(TConc ~ I(Period=="Post"), family=Gamma(), data=xTHg)
test1b <- glm(TConc ~ Location, family=Gamma(), data=xTHg)
test1c <- glm(TConc ~ Period * Location, family=Gamma(), data=xTHg)
#@ Interaction test
anova(test1, test1c, test="Chisq") #
#> No point in doing ME tests since strongly significant interaction exists
#@ Looking at the effects for interpretation ...
summary(test1c)
#@ Making predictions ...
gpred <- round(predict(test1, type="response"),5)
outTHg <- data.frame(xTHg, gpred)
#@ Making plots ...
png("sediment_all_THg.png", width = 960)
boxplot(xTHg$TConc ~ xTHg$Location*xTHg$Period,
  main="THg sediment concentrations (mg/kg)", axes=F)
axis(1, at=1:8, labels=c("Pre P01","Pre P08","Pre P11","Pre P17",
  "Post P01","Post P08","Post P11","Post P17"))
axis(2)
box()
suba <- xTHg
XS <- rep(NA, 8)
k = 0
for(j in c("aPre","Post"))
  for(i in c("P01","P08","P11","P17"))
{
  k <- k + 1
  sub <- suba[suba$Location==i & suba$Period==j,]
  if(dim(sub)[[1]] > 0)
```

```
   XS[k] <- mean(sub$TConc)
}
points(1:8, XS, pch="X", col="red")
#
dev.off()
#
png("sediment_all_THg_reformatted.png", width = 960)
boxplot(xTHg$TConc ~ xTHg$Period*xCu$Location,
 main="THg sediment concentrations (mg/kg)", axes=F)
axis(1, at=1:8, labels=c("Pre P01","Post P01","Pre P08","Post P08","Pre P11","Post P11",
 "Pre P17","Post P17"))
axis(2)
box()
suba <- xTHg
XS <- rep(NA, 8)
k = 0
for(j in c("aPre","Post"))
 for(i in c("P01","P08","P11","P17"))
{
 k <- k + 1
 sub <- suba[suba$Location==i & suba$Period==j,]
 if(dim(sub)[[1]] > 0)
   XS[k] <- mean(sub$TConc)
}
points(c(1,3,5,7,2,4,6,8), XS, pch="X", col="red")
#
dev.off()
###
##  Zn next
###
xZn <- base[base[,1]=="Zn",]
#
test1 <- glm(TConc ~ I(Period=="Post") + Location, family=Gamma(), data=xZn)
```

```
test1a <- glm(TConc ~ I(Period=="Post"), family=Gamma(), data=xZn)
test1b <- glm(TConc ~ Location, family=Gamma(), data=xZn)
test1c <- glm(TConc ~ Period * Location, family=Gamma(), data=xZn)
#@ Interaction test
anova(test1, test1c, test="Chisq") #
#@ Period ME test
anova(test1b, test1, test="Chisq") #

#@ Location ME test
anova(test1a, test1, test="Chisq") #
#@ Looking at the effects for interpretation ...
summary(test1c)
#@ Making predictions ...
gpred <- round(predict(test1, type="response"),5)
outZn <- data.frame(xZn, gpred)
#@ Making plots ...
png("sediment_all_Zn.png", width = 960)
boxplot(xZn$TConc ~ xZn$Location*xZn$Period,
  main="Zn sediment concentrations (mg/kg)", axes=F)
axis(1, at=1:8, labels=c("Pre P01","Pre P08","Pre P11","Pre P17",
  "Post P01","Post P08","Post P11","Post P17"))
axis(2)
box()
suba <- xZn
XS <- rep(NA, 8)
k = 0
for(j in c("aPre","Post"))
  for(i in c("P01","P08","P11","P17"))
{
  k <- k + 1
  sub <- suba[suba$Location==i & suba$Period==j,]
  if(dim(sub)[[1]] > 0)
    XS[k] <- mean(sub$TConc)
```

```
}
points(1:8, XS, pch="X", col="red")
#
dev.off()
#
png("sediment_all_Zn_reformatted.png", width = 960)
boxplot(xZn$TConc ~ xZn$Period*xZn$Location,
  main="Zn sediment concentrations (mg/kg)", axes=F)
axis(1, at=1:8, labels=c("Pre P01","Post P01","Pre P08","Post P08","Pre P11","Post P11",
  "Pre P17","Post P17"))
axis(2)
box()
suba <- xZn
XS <- rep(NA, 8)
k = 0
for(j in c("aPre","Post"))
  for(i in c("P01","P08","P11","P17"))
{
  k <- k + 1
  sub <- suba[suba$Location==i & suba$Period==j,]
  if(dim(sub)[[1]] > 0)
    XS[k] <- mean(sub$TConc)
}
points(c(1,3,5,7,2,4,6,8), XS, pch="X", col="red")
#
dev.off()
###
##  As next
###
xAs <- base[base[,1]=="As",]
#
test1 <- glm(TConc ~ I(Period=="Post") + Location, family=Gamma(), data=xAs)
test1a <- glm(TConc ~ I(Period=="Post"), family=Gamma(), data=xAs)
```

```
test1b <- glm(TConc ~ Location, family=Gamma(), data=xAs)
test1c <- glm(TConc ~ Period * Location, family=Gamma(), data=xAs)

#@ Interaction test
anova(test1, test1c, test="Chisq") #
#@ Period ME test
anova(test1b, test1, test="Chisq") #
#@ Location ME test
anova(test1a, test1, test="Chisq") #
#@ Looking at the effects for interpretation ...
summary(test1c)
#@ Making predictions ...
gpred <- round(predict(test1, type="response"),5)
outAs <- data.frame(xAs, gpred)
#@ Making plots ...
png("sediment_all_As.png", width = 960)
boxplot(xAs$TConc ~ xAs$Location*xAs$Period,
  main="As sediment concentrations (mg/kg)", axes=F)
axis(1, at=1:8, labels=c("Pre P01","Pre P08","Pre P11","Pre P17",
  "Post P01","Post P08","Post P11","Post P17"))
axis(2)
box()
suba <- xAs
XS <- rep(NA, 8)
k = 0
for(j in c("aPre","Post"))
  for(i in c("P01","P08","P11","P17"))
{
  k <- k + 1
  sub <- suba[suba$Location==i & suba$Period==j,]
  if(dim(sub)[[1]] > 0)
    XS[k] <- mean(sub$TConc)
}
```

```
points(1:8, XS, pch="X", col="red")
#
dev.off()
#
png("sediment_all_As_reformatted.png", width = 960)
boxplot(xAs$TConc ~ xAs$Period*xAs$Location,
  main="As sediment concentrations (mg/kg)", axes=F)
axis(1, at=1:8, labels=c("Pre P01","Post P01","Pre P08","Post P08","Pre P11","Post P11",
  "Pre P17","Post P17"))
axis(2)
box()
suba <- xAs
XS <- rep(NA, 8)
k = 0
for(j in c("aPre","Post"))
  for(i in c("P01","P08","P11","P17"))
{
  k <- k + 1
  sub <- suba[suba$Location==i & suba$Period==j,]
  if(dim(sub)[[1]] > 0)
    XS[k] <- mean(sub$TConc)
}
points(c(1,3,5,7,2,4,6,8), XS, pch="X", col="red")
#
dev.off()
###
##  Lastly Pb
###
xPb <- base[base[,1]=="Pb",]
#
test1 <- glm(TConc ~ I(Period=="Post") + Location, family=Gamma(), data=xPb)
test1a <- glm(TConc ~ I(Period=="Post"), family=Gamma(), data=xPb)
test1b <- glm(TConc ~ Location, family=Gamma(), data=xPb)
```

```
test1c <- glm(TConc ~ Period * Location, family=Gamma(), data=xPb)
#@ Interaction test
anova(test1, test1c, test="Chisq") #
#> No point in doing ME tests since strongly significant interaction exists
#@ Looking at the effects for interpretation ...
summary(test1)
#@ Making predictions ...
gpred <- round(predict(test1, type="response"),5)
outPb <- data.frame(xPb, gpred)
#@ Making plots ...
png("sediment_all_Pb.png", width = 960)
boxplot(xPb$TConc ~ xPb$Location*xPb$Period,
  main="Pb sediment concentrations (mg/kg)", axes=F)
axis(1, at=1:8, labels=c("Pre P01","Pre P08","Pre P11","Pre P17",
  "Post P01","Post P08","Post P11","Post P17"))
axis(2)
box()
suba <- xPb
XS <- rep(NA, 8)
k = 0
for(j in c("aPre","Post"))
  for(i in c("P01","P08","P11","P17"))
{
  k <- k + 1
  sub <- suba[suba$Location==i & suba$Period==j,]
  if(dim(sub)[[1]] > 0)
    XS[k] <- mean(sub$TConc)
}
points(1:8, XS, pch="X", col="red")
#
dev.off()
#
png("sediment_all_Pb_reformatted.png", width = 960)
```

```
boxplot(xPb$TConc ~ xPb$Period*xPb$Location,
  main="Pb sediment concentrations (mg/kg)", axes=F)
axis(1, at=1:8, labels=c("Pre P01","Post P01","Pre P08","Post P08","Pre P11","Post P11",
  "Pre P17","Post P17"))
axis(2)
box()
suba <- xPb
XS <- rep(NA, 8)
k = 0
for(j in c("aPre","Post"))
  for(i in c("P01","P08","P11","P17"))
{
  k <- k + 1
  sub <- suba[suba$Location==i & suba$Period==j,]
  if(dim(sub)[[1]] > 0)
    XS[k] <- mean(sub$TConc)
}
points(c(1,3,5,7,2,4,6,8), XS, pch="X", col="red")
#
dev.off()
#
# EOF - Sediment analyses with interaction checks and plots
```

Coding used for Spearman's rank correlations

```
setwd("C:/Users/idrygian/Desktop/Main")
library(stringr)
base <- read.csv("combinedData.csv", header=T, strings=F)
base$Location <- as.factor(str_trim(base$Location))
base$Period <- str_trim(base$Period)
base$Period[base$Period=="Pre"] <- "aPre" #
base$Period <- as.factor(base$Period)
unique(base$Location) # 4 locations
unique(base$Period) # 2 time periods
```

```
#
summary(base$Concen) # No negative values, some big ones?
tapply(base$Concen, base$Source, summary)
tapply(base$Concen, base$Outcome, summary)
urow <- base$Source
for(i in 1:(dim(base)[1]))
  urow[i] <- paste(base$Source[i], base$Outcome[i], base$Location[i], base$Period[i], base$SampleID[i],
  sep="", collapse="")
#
base <- data.frame(base, urow)
#
xAs <- base[base$Outcome=="As",]
xCd <- base[base$Outcome=="Cd",]
xCu <- base[base$Outcome=="Cu",]
xNi <- base[base$Outcome=="Ni",]
xPb <- base[base$Outcome=="Pb",]
xTHg <- base[base$Outcome=="THg",]
xZn <- base[base$Outcome=="Zn",]
str(xAs)
str(xCd)
str(xCu)
str(xNi)
str(xPb)
str(xTHg)
str(xZn)
##############
# Zero checks
sum(xAs$Concen<=0) # 4
sum(xCd$Concen<=0) # 60
sum(xCu$Concen<=0) # 0
sum(xNi$Concen<=0) # 6
sum(xPb$Concen<=0) # 1
sum(xTHg$Concen<=0) # 8
```

```
sum(xZn$Concen<=0) # 5
outcomeNames <- c("As", "Cd", "Cu", "Ni", "Pb", "THg", "Zn")
all <- list(xAs, xCd, xCu, xNi, xPb, xTHg, xZn)
# Machinery
uniquer <- function(sub)
{
 D <- dim(sub)[1]
 ur <- unique(sub$urow)
 M <- length(unique(ur))
 copi <- sub[1:M,]
 for(i in 1:M)
 {
  copi[i,7] <- ur[i]
  subi <- sub[sub$urow==ur[i],]
  copi[i,1] <- subi[1,1]
  copi[i,2] <- subi[1,2]
  copi[i,3] <- subi[1,3]
  copi[i,4] <- subi[1,4]
  copi[i,6] <- subi[1,6]
  copi[i,5] <- median(subi[,5],na.rm=T)
 }
 return(copi)
}
corer <- function(usub)
{
 M <- dim(usub)[1]
 places <- array(NA, M)
 for(i in 1:M)
  places[i] <- paste(usub[i,3],usub[i,4],usub[i,6],sep="",collapse="")
 up <- unique(places)
 K <- length(up)
 tis <- array(NA, K)
 por <- array(NA, K)
```

```
 sed <- array(NA, K)
 for(k in 1:K)
 {
  print(k)
  usubi <- usub[places==up[k],]
  ut <- usubi[usubi[,1]=="Tissue",]
  if(dim(ut)[1]==1)
    tis[k] <- ut[1,5]
  if(dim(ut)[1]>1)
    print(ut)
  uo <- usubi[usubi[,1]=="Porew",]
  if(dim(uo)[1]==1)
    por[k] <- uo[1,5]
  if(dim(uo)[1]>1)
    print(uo)
  us <- usubi[usubi[,1]=="Sedi",]
  if(dim(us)[1]==1)
    sed[k] <- us[1,5]
  if(dim(us)[1]>1)
    print(us)
 }
 out <- data.frame(site=up, tissueVal=tis, porewVal=por, sediVal=sed)
 return(out)
}
plotter <- function(sub, inMain, revi=FALSE)
{
 if(!revi) {
 plot(sub[,2], sub[,4], pch=20, col="brown", main=inMain, xlab="Tissue values",
  ylim=c(0, max(sub[,4], na.rm=T)*1.2), ylab="Other values")
 points(sub[,2], sub[,3], pch=20, col="blue")
 }
 if(revi) {
 plot(sub[,2], sub[,3], pch=20, col="blue", main=inMain, xlab="Tissue values",
```

```
   ylim=c(0, max(sub[,3], na.rm=T)*1.2), ylab="Other values")
  points(sub[,2], sub[,4], pch=20, col="brown")
  }
  legend("topleft", col=c("brown","blue"), pch=20, legend=c("Sediment","Porewater"))
}
# Do everything # c("As", "Cd", "Cu", "Ni", "Pb", "THg", "Zn")
pdf("correlations.pdf")
uAs <- uniquer(xAs)
corAs <- corer(uAs)
plotter(corAs, "As")
cor.test(corAs$tissueVal, corAs$sediVal, method="spearman")  #
cor.test(corAs$tissueVal, corAs$porewVal, method="spearman") #
#
uCd <- uniquer(xCd)
corCd <- corer(uCd)
plotter(corCd, "Cd")
cor.test(corCd$tissueVal, corCd$sediVal, method="spearman")  #
cor.test(corCd$tissueVal, corCd$porewVal, method="spearman") #
#
uCu <- uniquer(xCu)
corCu <- corer(uCu)
plotter(corCu, "Cu")
cor.test(corCu$tissueVal, corCu$sediVal, method="spearman")  #
cor.test(corCu$tissueVal, corCu$porewVal, method="spearman") #
#
uNi <- uniquer(xNi)
corNi <- corer(uNi)
plotter(corNi, "Ni")
cor.test(corNi$tissueVal, corNi$sediVal, method="spearman")  #
cor.test(corNi$tissueVal, corNi$porewVal, method="spearman") #
#
uPb <- uniquer(xPb)
corPb <- corer(uPb)
```

```
plotter(corPb, "Pb")
cor.test(corPb$tissueVal, corPb$sediVal, method="spearman")  #
cor.test(corPb$tissueVal, corPb$porewVal, method="spearman") #
#
uTHg <- uniquer(xTHg)
corTHg <- corer(uTHg)
plotter(corTHg, "THg")
cor.test(corTHg$tissueVal, corTHg$sediVal, method="spearman")  #
cor.test(corTHg$tissueVal, corTHg$porewVal, method="spearman") #
#
uZn <- uniquer(xZn)
corZn <- corer(uZn)
plotter(corZn, "Zn")
cor.test(corZn$tissueVal, corZn$sediVal, method="spearman")  #
cor.test(corZn$tissueVal, corZn$porewVal, method="spearman") #
#
plot(corCd$tissueVal, corCd$sediVal, pch=20, col="brown")
plot(corCd$tissueVal, corCd$porewVal, pch=20, col="blue")
plot(corCu$tissueVal, corCu$sediVal, pch=20, col="brown")
plot(corCu$tissueVal, corCu$porewVal, pch=20, col="blue")
plot(corPb$tissueVal, corPb$sediVal, pch=20, col="brown")
plot(corPb$tissueVal, corPb$porewVal, pch=20, col="blue")
plot(corTHg$tissueVal, corTHg$porewVal, pch=20, col="blue")
plot(corZn$tissueVal, corZn$porewVal, pch=20, col="blue")
dev.off()
#
plot(corTHg$porewVal, corTHg$tissueVal, pch=20, col="blue")
# EOF - comparison of tissue vs sediment/porewater
```

Coding used to obtain the confidence intervals (CIs) for Spearman's rank correlations using the Pearson's correlation method

```
setwd("C:/Users/idrygian/Desktop/Main")
library(stringr)
```

```
base <- read.csv("combinedData.csv", header=T, strings=F)
base$Location <- as.factor(str_trim(base$Location))
base$Period <- str_trim(base$Period)
base$Period[base$Period=="Pre"] <- "aPre" #
base$Period <- as.factor(base$Period)
unique(base$Location) # 4 locations
unique(base$Period) # 2 time periods
#
summary(base$Concen) # No negative values, some big ones?
tapply(base$Concen, base$Source, summary)
tapply(base$Concen, base$Outcome, summary)
urow <- base$Source
for(i in 1:(dim(base)[1]))
  urow[i] <- paste(base$Source[i], base$Outcome[i], base$Location[i], base$Period[i], base$SampleID[i],
  sep="", collapse="")
#
base <- data.frame(base, urow)
#
xAs <- base[base$Outcome=="As",]
xCd <- base[base$Outcome=="Cd",]
xCu <- base[base$Outcome=="Cu",]
xNi <- base[base$Outcome=="Ni",]
xPb <- base[base$Outcome=="Pb",]
xTHg <- base[base$Outcome=="THg",]
xZn <- base[base$Outcome=="Zn",]
str(xAs)
str(xCd)
str(xCu)
str(xNi)
str(xPb)
str(xTHg)
str(xZn)
##############
```

```
# Zero checks
sum(xAs$Concen<=0) # 4
sum(xCd$Concen<=0) # 60
sum(xCu$Concen<=0) # 0
sum(xNi$Concen<=0) # 6
sum(xPb$Concen<=0) # 1
sum(xTHg$Concen<=0) # 8
sum(xZn$Concen<=0) # 5
outcomeNames <- c("As", "Cd", "Cu", "Ni", "Pb", "THg", "Zn")
all <- list(xAs, xCd, xCu, xNi, xPb, xTHg, xZn)
# Machinery
uniquer <- function(sub)
{
 D <- dim(sub)[1]
 ur <- unique(sub$urow)
 M <- length(unique(ur))
 copi <- sub[1:M,]
 for(i in 1:M)
 {
  copi[i,7] <- ur[i]
  subi <- sub[sub$urow==ur[i],]
  copi[i,1] <- subi[1,1]
  copi[i,2] <- subi[1,2]
  copi[i,3] <- subi[1,3]
  copi[i,4] <- subi[1,4]
  copi[i,6] <- subi[1,6]
  copi[i,5] <- median(subi[,5],na.rm=T)
 }
 return(copi)
}
corer <- function(usub)
{
 M <- dim(usub)[1]
```

```
 places <- array(NA, M)
 for(i in 1:M)
  places[i] <- paste(usub[i,3],usub[i,4],usub[i,6],sep="",collapse="")
 up <- unique(places)
 K <- length(up)
 tis <- array(NA, K)
 por <- array(NA, K)
 sed <- array(NA, K)
 for(k in 1:K)
 {
  print(k)
  usubi <- usub[places==up[k],]

  ut <- usubi[usubi[,1]=="Tissue",]
  if(dim(ut)[1]==1)
    tis[k] <- ut[1,5]
  if(dim(ut)[1]>1)
    print(ut)
  uo <- usubi[usubi[,1]=="Porew",]
  if(dim(uo)[1]==1)
    por[k] <- uo[1,5]
  if(dim(uo)[1]>1)
    print(uo)

  us <- usubi[usubi[,1]=="Sedi",]
  if(dim(us)[1]==1)
    sed[k] <- us[1,5]
  if(dim(us)[1]>1)
    print(us)
 }
 out <- data.frame(site=up, tissueVal=tis, porewVal=por, sediVal=sed)
 return(out)
}
```

```
plotter <- function(sub, inMain, revi=FALSE)
{
 if(!revi) {
 plot(sub[,2], sub[,4], pch=20, col="brown", main=inMain, xlab="Tissue values",
  ylim=c(0, max(sub[,4], na.rm=T)*1.2), ylab="Other values")
 points(sub[,2], sub[,3], pch=20, col="blue")
 }
 if(revi) {
 plot(sub[,2], sub[,3], pch=20, col="blue", main=inMain, xlab="Tissue values",
  ylim=c(0, max(sub[,3], na.rm=T)*1.2), ylab="Other values")
 points(sub[,2], sub[,4], pch=20, col="brown")
 }
 legend("topleft", col=c("brown","blue"), pch=20, legend=c("Sediment","Porewater"))
}
# Do everything # c("As", "Cd", "Cu", "Ni", "Pb", "THg", "Zn")
pdf("corLooker.pdf")
uAs <- uniquer(xAs)
corAs <- corer(uAs)
plotter(corAs, "As")
cor.test(corAs$tissueVal, corAs$sediVal, method="pearson")  #
cor.test(corAs$tissueVal, corAs$porewVal, method="pearson") #
#
#data:  corAs$tissueVal and corAs$sediVal
#t = -0.34738, df = 16, p-value = 0.7328
#alternative hypothesis: true correlation is not equal to 0
#95 percent confidence interval:
# -0.5319044  0.3963607
#sample estimates:
#       cor -0.08651975
uCd <- uniquer(xCd)
corCd <- corer(uCd)
plotter(corCd, "Cd")
cor.test(corCd$tissueVal, corCd$sediVal, method="pearson")  #
```

```
cor.test(corCd$tissueVal, corCd$porewVal, method="pearson") #
#
#data:  corCd$tissueVal and corCd$sediVal
#t = 0.66402, df = 16, p-value = 0.5161
#alternative hypothesis: true correlation is not equal to 0
#95 percent confidence interval:
# -0.3282000  0.5858419
#sample estimates:
#      cor 0.1637629
#data:  corCd$tissueVal and corCd$porewVal
#t = -0.70936, df = 14, p-value = 0.4897
#alternative hypothesis: true correlation is not equal to 0
#95 percent confidence interval:
# -0.6243251  0.3409178
#sample estimates:
#      cor -0.1862654
uCu <- uniquer(xCu)
corCu <- corer(uCu)
plotter(corCu, "Cu")
cor.test(corCu$tissueVal, corCu$sediVal, method="pearson")  #
cor.test(corCu$tissueVal, corCu$porewVal, method="pearson") #
#
#data:  corCu$tissueVal and corCu$sediVal
#t = -0.38008, df = 16, p-value = 0.7089
#alternative hypothesis: true correlation is not equal to 0
#95 percent confidence interval:
# -0.5377176  0.3894756
#sample estimates:
#        cor  -0.09459509
#data:  corCu$tissueVal and corCu$porewVal
#t = 0.20938, df = 14, p-value = 0.8372
#alternative hypothesis: true correlation is not equal to 0
#95 percent confidence interval:
```

```
# -0.4523614  0.5367131
#sample estimates:
#       cor 0.05587276
uNi <- uniquer(xNi)
corNi <- corer(uNi)
plotter(corNi, "Ni")
cor.test(corNi$tissueVal, corNi$sediVal, method="pearson")  #
cor.test(corNi$tissueVal, corNi$porewVal, method="pearson") #
#
#data:  corNi$tissueVal and corNi$sediVal
#t = -0.87363, df = 16, p-value = 0.3952
#alternative hypothesis: true correlation is not equal to 0
#95 percent confidence interval:
# -0.6186205  0.2815399
#sample estimates:
#     cor -0.213377
#data:  corNi$tissueVal and corNi$porewVal
#t = -0.68662, df = 14, p-value = 0.5035
#alternative hypothesis: true correlation is not equal to 0
#95 percent confidence interval:
# -0.6206669  0.3461855
#sample estimates:
#       cor  -0.1804936
uPb <- uniquer(xPb)
corPb <- corer(uPb)
plotter(corPb, "Pb")
cor.test(corPb$tissueVal, corPb$sediVal, method="pearson")  #
cor.test(corPb$tissueVal, corPb$porewVal, method="pearson") #
#
#data:  corPb$tissueVal and corPb$sediVal
#t = 1.5093, df = 16, p-value = 0.1507
#alternative hypothesis: true correlation is not equal to 0
#95 percent confidence interval:
```

```
# -0.1363171  0.7038804
#sample estimates:
#    cor  0.35302
#data:  corPb$tissueVal and corPb$porewVal
#t = 1.1408, df = 14, p-value = 0.2731
#alternative hypothesis: true correlation is not equal to 0
#95 percent confidence interval:
# -0.2385640  0.6878911
#sample estimates:
#     cor 0.2916286
uTHg <- uniquer(xTHg)
corTHg <- corer(uTHg)
plotter(corTHg, "THg")
cor.test(corTHg$tissueVal, corTHg$sediVal, method="pearson")  #
cor.test(corTHg$tissueVal, corTHg$porewVal, method="pearson") #
#
#data:  corTHg$tissueVal and corTHg$sediVal
#t = -0.78845, df = 15, p-value = 0.4427
#alternative hypothesis: true correlation is not equal to 0
#95 percent confidence interval:
# -0.6206233  0.3109770
#sample estimates:
#       cor -0.1994846
#data:  corTHg$tissueVal and corTHg$porewVal
#t = 3.8678, df = 16, p-value = 0.001363
#alternative hypothesis: true correlation is not equal to 0
#95 percent confidence interval:
# 0.3379186 0.8772858
#sample estimates:
#     cor 0.6951232
uZn <- uniquer(xZn)
corZn <- corer(uZn)
plotter(corZn, "Zn")
```

```
cor.test(corZn$tissueVal, corZn$sediVal, method="pearson")  #
cor.test(corZn$tissueVal, corZn$porewVal, method="pearson") #
#
#data:  corZn$tissueVal and corZn$sediVal
#t = -0.069059, df = 16, p-value = 0.9458
#alternative hypothesis: true correlation is not equal to 0
#95 percent confidence interval:
# -0.4802618  0.4532607
#sample estimates:
#        cor -0.01726227
#data:  corZn$tissueVal and corZn$porewVal
#t = -0.83182, df = 14, p-value = 0.4195
#alternative hypothesis: true correlation is not equal to 0
#95 percent confidence interval:
# -0.6434964  0.3122837
#sample estimates:
#       cor -0.2170158
plot(corCd$tissueVal, corCd$sediVal, pch=20, col="brown")
plot(corCd$tissueVal, corCd$porewVal, pch=20, col="blue")
plot(corCu$tissueVal, corCu$sediVal, pch=20, col="brown")
plot(corCu$tissueVal, corCu$porewVal, pch=20, col="blue")
plot(corPb$tissueVal, corPb$sediVal, pch=20, col="brown")
plot(corPb$tissueVal, corPb$porewVal, pch=20, col="blue")
plot(corTHg$tissueVal, corTHg$porewVal, pch=20, col="blue")
plot(corZn$tissueVal, corZn$porewVal, pch=20, col="blue")
dev.off()
#
plot(corTHg$porewVal, corTHg$tissueVal, pch=20, col="blue")
# EOF - comparison of tissue vs sediment/porewater
```

Appendix B

Supplementary information for Chapter 4[1]

[1]The content of this appendix is identical to the supplementary information of the published paper in Science of the Total Environment Journal, Vol 737, 2020: I. Drygiannaki, B. Rao, J. A. Dawson, M. Rakowska, D. D. Reible, N. T. Hayman, G. Rosen, M. A. Colvin, B. D. Chadwick, R. Pitt, M. Otto, B. Steets, J. Ervin

Figures

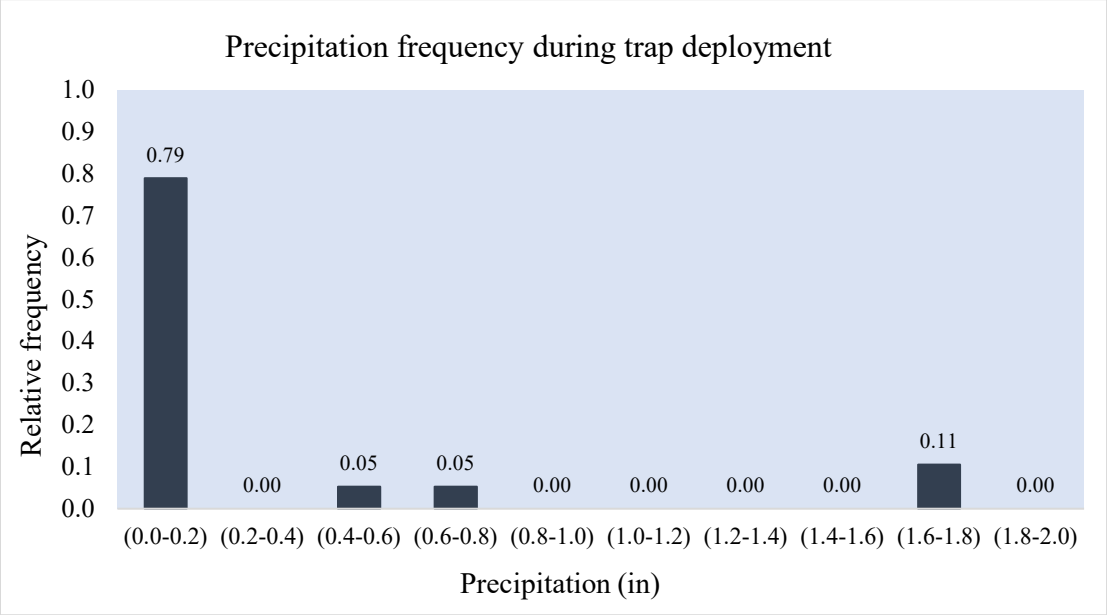

Fig. S1: Precipitation frequency of rainfall (in) during the sediment trap deployment period of 19th of October 2015 until 23rd of February 2016.

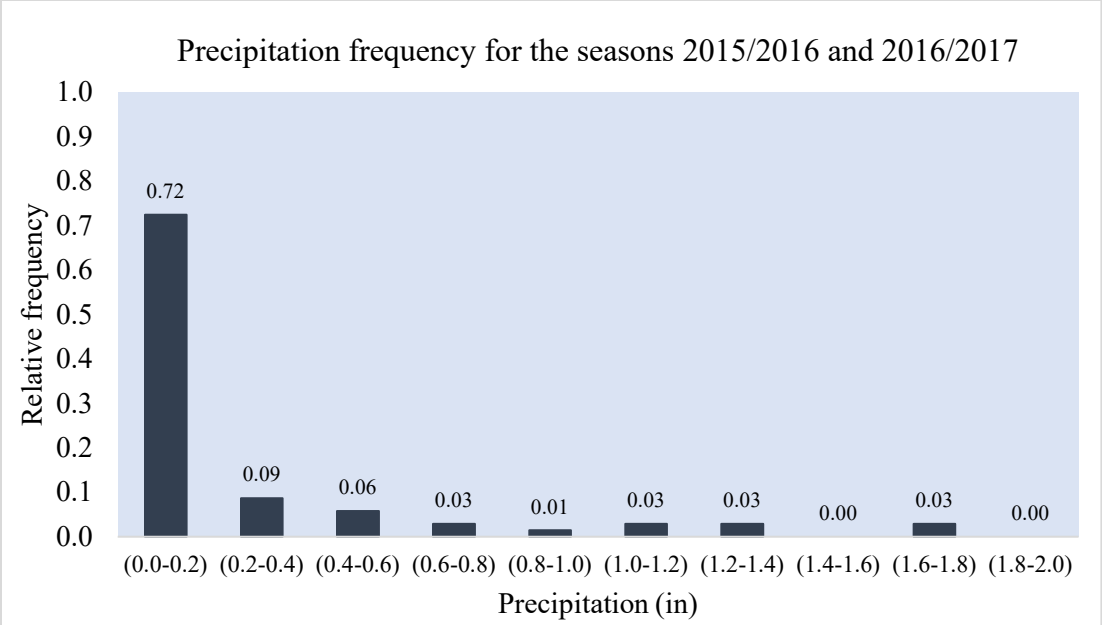

Fig. S2: Precipitation frequency of rainfall (in) during the sampling effort years 2015-2017.

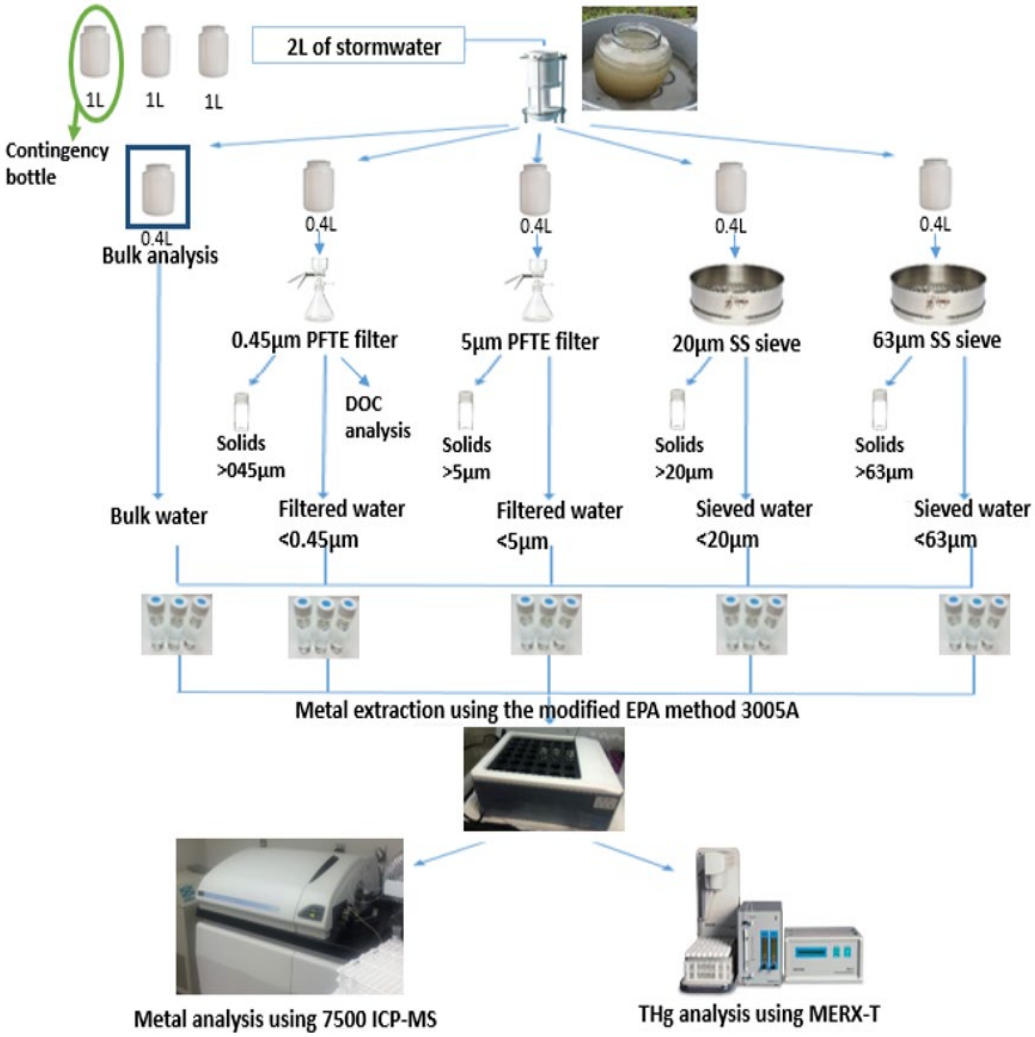

Fig. S3: Particle size fractionation and analysis of stormwater samples.

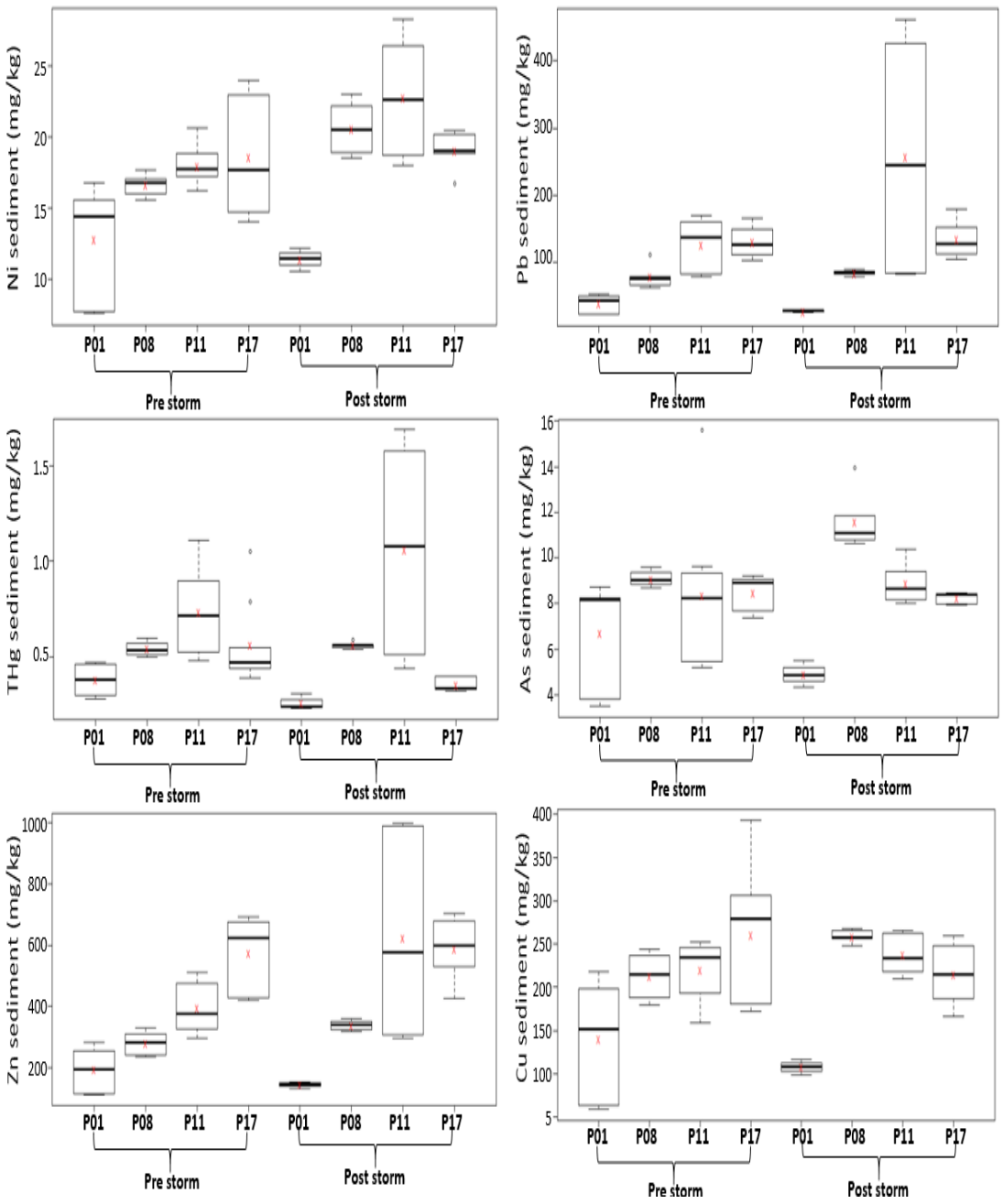

Fig. S4: Boxplots of sediment concentration (mg/kg) for the metals Ni, Hg, Zn, Pb, Cu, and the metalloid As. The red mark indicates the mean value of the dataset.

Tables

Table S1: Size based concentrations of solids, aqueous and particle normalized concentration of Cd and Cu in sampled locations from the 1st storm event and the standard deviations of triplicate samples in parentheses when applicable.

Location	Particle size range (μm)	Solids (mg/L)	Cd-water (μg/L)	Cu-water (μg/L)	Cd-particle (mg/kg)	Cu-particle (mg/kg)
A1W	Bulk	NA[a]	0.62 (0.02)	50.9 (0.6)	NA[a]	NA[a]
	Total (>0.45)	230	0.42 (0.02)	38.0 (0.7)	1.81 (0)	165 (0.0)
	<0.45	NA[a]	0.20 (0.00)	12.9 (0.4)	NA[a]	NA[a]
	0.45-5	0.0	0.00 (0.01)	0.4 (1.4)	NA[a]	NA[a]
	5-20	122	0.14 (0.02)	18.7 (1.7)	1.15 (0.0)	154 (0.0)
	20-63	79.1	0.10 (0.02)	13.3 (1.2)	1.23 (0.0)	168 (0.0)
	>63	28.9	0.17 (0.02)	5.6 (0.9)	6.04 (0.0)	192 (0.0)
A2W	Bulk	NA[a]	0.29 (0.01)	23.0 (0.5)	NA[a]	NA[a]
	Total (>0.45)	231	0.29 (0.01)	15.5 (0.5)	1.24 (0)	67.2 (0.0)
	<0.45	NA[a]	0.00	7.5 (0.1)	NA[a]	NA[a]
	0.45-5	0.0	0.00	1.6 (0.4)	NA[a]	NA[a]
	5-20	199	0.19	9.2 (1.2)	0.9	46.4 (0.0)
	20-63	31.6	0.01 (0.02)	1.0 (1.3)	0.32 (0.0)	31.7 (0.0)
	>63	0.0	0.09 (0.02)	3.7 (0.7)	NA[a]	NA[a]

[a]NA – not applicable. [b]N – salt interference in the solid concentration (>20%).

Table S1, Continued

Location	Particle size range (µm)	Solids (mg/L)	Cd-water (µg/L)	Cu-water (µg/L)	Cd-particle (mg/kg)	Cu-particle (mg/kg)
A3W	Bulk	NA[a]	0.00	12.5 (1.0)	NA[a]	NA[a]
	Total (>0.45)	N[b]	0.00	0.00	0.00	0.0
	<0.45	NA[a]	0.00	12.7 (1.2)	NA[a]	NA[a]
	0.45-5	N[b]	0.00	0.00	0.00	0.0
	5-20	26.0	0.00	0.00	0.00	0.0
	20-63	0.0	0.00	0.6 (1.0)	NA[a]	NA[a]
	>63	1.2	0.00	0.4 (1.4)	0.00	NA[a]
C1W	Bulk	NA[a]	0.41 (0.01)	32.7 (0.6)	NA[a]	NA[a]
	Total (>0.45)	242	0.41 (0.01)	25.0 (1.0)	1.68 (0)	103 (0.0)
	<0.45	NA[a]	0.00	7.8 (0.9)	NA[a]	NA[a]
	0.45-5	23.5	0.00	5.3 (4.3)	0.00	227 (0.2)
	5-20	46.3	0.00	0.0	0.00	0.0
	20-63	108	0.00	5.2 (0.4)	0.00	47.8 (0.0)
	>63	63.5	0.41 (0.01)	17.7 (0.6)	6.38 (0)	278 (0.0)
C2W	Bulk	NA[a]	0.94 (0.02)	75.3 (4.2)	NA[a]	NA[a]
	Total (>0.45)	269	0.94 (0.02)	69.8 (4.2)	3.5 (0.0)	260 (0.0)
	<0.45	NA[a]	0.00	5.5 (0.1)	NA[a]	NA[a]
	0.45-5	1.1	0.00	0.8 (0.2)	0.00	NA[a]
	5-20	114	0.21 (0.01)	13.4 (4.1)	1.8 (0.0)	117 (0.0)
	20-63	99.2	0.15 (0.01)	13.5 (4.2)	1.5 (0.0)	136 (0.0)
	>63	54.4	0.59 (0.02)	42.1 (4.3)	10.8 (0.0)	774 (0.1)

[a]NA – not applicable. [b]N – salt interference in the solid concentration (>20%).

Table S1, Continued

Location	Particle size range (µm)	Solids (mg/L)	Cd-water (µg/L)	Cu-water (µg/L)	Cd-particle (mg/kg)	Cu-particle (mg/kg)
O3W	Bulk	NA[a]	0.40 (0.0)	21.0 (2.1)	NA[a]	NA[a]
	Total (>0.45)	NA[a]	0.19 (0.02)	6.2 (2.1)	NA[a]	NA[a]
	<0.45	NA[a]	0.21 (0.0)	14.8 (0.1)	NA[a]	NA[a]
	0.45-5	NA[a]	0.00	0.3 (0.8)	0.0	NA[a]
	5-20	NA[a]	0.01 (0.0)	0.0	NA[a]	NA[a]
	20-63	0.0	0.03 (0.01)	5.2 (0.9)	0.0	5.2 (0.9)
	>63	5.4	0.16 (0.02)	0.8 (2.3)	NA[a]	NA[a]
O4W	Bulk	NA[a]	0.19 (0.0)	24.1 (0.4)	NA[a]	NA[a]
	Total (>0.45)	184.4	0.19 (0.0)	18.4 (0.4)	1.1 (0.0)	99.6 (0.0)
	<0.45	NA[a]	0.00	5.7 (0.1)	NA[a]	NA[a]
	0.45-5	2.0	0.00	0.9 (0.2)	0.0	NA[a]
	5-20	160	0.00	4.6 (2.9)	0.0	28.5 (0.0)
	20-63	13.8	0.00	8.4 (6.4)	0.0	609 (0.5)
	>63	9.2	0.19 (0.0)	4.6 (5.7)	NA[a]	NA[a]

[a]NA – not applicable. [b]N – salt interference in the solid concentration (>20%).

Table S2: Size based concentration of solids, aqueous and particle normalized concentration of Cd and Cu in sampled locations from the 2nd storm event and the standard deviations of triplicate samples in parentheses when applicable (Outfall O3W and A3W sampling did not occur in 2nd event).

Location	Particle size range (μm)	Solids (mg/L)	Cd-water (μg/L)	Cu-water (μg/L)	Cd-particle (mg/kg)	Cu-particle (mg/kg)
A1W	Bulk	NA[a]	0.00	76.2 (5.0)	NA[a]	NA[a]
	Total (>0.45)	N[b]	0.00	2.4 (11.8)	0.0	N[b]
	<0.45	NA[a]	0.00	73.8 (10.6)	NA[a]	NA[a]
	0.45-5	N[b]	0.00	0.0	0.0	0.0
	5-20	N[b]	0.00	0.0	0.0	0.0
	20-63	20.8	0.00	4.9 (14.0)	0.0	235 (0.7)
	>63	5.2	0.00	4.4 (12.0)	0.0	NA[a]
A2W	Bulk	NA[a]	0.00	62.5 (1.0)	NA[a]	NA[a]
	Total (>0.45)	N[b]	0.00	1.4 (3.1)	0.0	N[b]
	<0.45	NA[a]	0.00	61.1 (3.0)	NA[a]	NA[a]
	0.45-5	N[b]	0.00	0.0	0.0	0.0
	5-20	N[b]	0.00	3.4 (5.2)	0.0	N[b]
	20-63	1.2	0.00	5.3 (5.9)	0.0	NA[a]
	>63	1.4	0.00	1.7 (3.8)	0.0	NA[a]
C1W	Bulk	NA[a]	0.23 (NA)	29.6 (1.8)	NA[a]	NA[a]
	Total (>0.45)	122	0.23 (NA)	15.8 (4.6)	1.87	130 (0.0)
	<0.45	NA[a]	0.00	13.8 (4.3)	NA[a]	NA[a]
	0.45-5	5.4	0.00	0.0	0.00	0.0
	5-20	68.9	0.00	13.1 (2.3)	0.00	190 (0.0)
	20-63	39.1	0.22 (NA)	3.1 (2.8)	5.66	78.3 (0.1)
	>63	8.5	0.01 (NA)	1.4 (2.7)	NA[a]	NA[a]

[a]NA – not applicable. [b]N – salt interference in the solid concentration (>20%).

Table S2, Continued

Location	Particle size range (μm)	Solids (mg/L)	Cd-water (μg/L)	Cu-water (μg/L)	Cd-particle (mg/kg)	Cu-particle (mg/kg)
C2W	Bulk	NA[a]	0.39 (NA)	60.4 (NA)	NA[a]	NA[a]
	Total (>0.45)	723	0.39 (NA)	48.8 (1.6)	0.54	67.6 (0.0)
	<0.45	NA[a]	0.00	11.6 (1.6)	NA[a]	NA[a]
	0.45-5	0.0	0.00	0.0 (NA)	0.00	0.0
	5-20	143	0.00	17.6 (1.0)	0.00	123 (0.0)
	20-63	128	0.20 (NA)	4.0 (NA)	1.55	30.9
	>63	451	0.19 (NA)	28.0 (NA)	0.43	62.1
O4W	Bulk	NA[a]	0.00	49.1 (0.3)	NA[a]	NA[a]
	Total (>0.45)	NA[a]	0.00	6.4 (0.3)	0.00	NA[a]
	<0.45	NA[a]	0.00	42.8 (NA)	NA[a]	NA[a]
	0.45-5	NA[a]	0.00	3.4 (3.5)	0.00	NA[a]
	5-20	NA[a]	0.00	0.4 (4.6)	0.00	NA[a]
	20-63	3.5	0.00	19.1 (3.0)	0.00	NA[a]
	>63	1.5	0.00	0.0	0.00	0.0

[a]NA – not applicable. [b]N – salt interference in the solid concentration (>20%).

Table S3: Size based concentration of solids, aqueous and particle normalized concentration of Pb, Zn, Ni, Hg, and As in sampled locations from the 1st storm event and the standard deviations of triplicate samples in parentheses when applicable.

Location	Particle size range (μm)	Pb-water (μg/L)	Zn-water (μg/L)	Ni-water (μg/L)	Pb-particle (mg/kg)	Zn-particle (mg/kg)	Ni-particle (mg/kg)
A1W	Bulk	32.3 (1.1)	234 (0.6)	11.0 (0.3)	NA[a]	NA[a]	NA[a]
	Total (>0.45)	31.6 (1.1)	199 (0.8)	3.4 (0.3)	138 (0.0)	867 (0.0)	14.6 (0.0)
	<0.45	0.7 (0.0)	34.6 (0.5)	7.6 (0.0)	NA[a]	NA[a]	NA[a]
	0.45-5	0.3 (0.1)	6.0 (1.3)	0.2 (0.2)	NA[a]	NA[a]	NA[a]
	5-20	19.4 (0.9)	71.8 (5.8)	2.9 (0.5)	159 (0.0)	590 (0.0)	23.5 (0.0)
	20-63	2.0 (1.0)	97.0 (6.5)	1.9 (0.8)	24.9 (0.0)	1,230 (0.1)	23.7 (0.0)
	>63	9.9 (1.1)	24.4 (3.2)	0.0 (NA)	342 (0.0)	842 (0.1)	0.0 (NA)
A2W	Bulk	11.7 (0.3)	85.8 (2.9)	7.5 (0.2)	NA[a]	NA[a]	NA[a]
	Total (>0.45)	11.0 (0.3)	73.1 (3.3)	2.0 (0.2)	47.9 (0.0)	317 (0.0)	8.6 (0.0)
	<0.45	0.6 (0.6)	12.7 (1.6)	5.5 (0.0)	NA[a]	NA[a]	NA[a]
	0.45-5	0.0 (NA)	0.0 (NA)	0.8 (0.1)	0.0 (NA)	0.0 (NA)	NA[a]
	5-20	9.2 (0.6)	42.1 (2.8)	0.9 (0.5)	46.2 (0.0)	212 (0.0)	4.7 (0.0)
	20-63	0.0 (NA)	2.7 (2.9)	0.5 (0.5)	0.0 (NA)	86.1 (0.1)	15.2 (0.0)
	>63	3.5 (0.4)	31.7 (3.0)	0.0 (NA)	NA[a]	NA[a]	0.0 (NA)
A3W	Bulk	2.4 (0.0)	28.0 (1.0)	7.8 (0.4)	NA[a]	NA[a]	NA[a]
	Total (>0.45)	1.8 (0.1)	18.3 (1.0)	0.0 (NA)	NA[a]	NA[a]	0.0 (NA)
	<0.45	0.5 (0.1)	9.7 (0.2)	11.1 (3.9)	NA[a]	NA[a]	NA[a]
	0.45-5	0.1 (0.1)	2.9 (0.4)	0.0 (NA)	NA[a]	NA[a]	0.0 (NA)
	5-20	2.4 (0.0)	3.5 (0.8)	0.0 (NA)	90.5 (0.0)	134 (0.0)	0.0 (NA)
	20-63	0.0 (NA)	0.0 (1.6)	0.0 (NA)	0.0 (0.0)	NA[a]	0.0 (NA)
	>63	0.4 (0.1)	11.9 (1.8)	0.4 (0.9)	NA[a]	NA[a]	NA[a]

[a]NA – not applicable. [b]N – salt interference in the solid concentration (>20%).

Table S3, Continued

C1W	Bulk	20.8 (2.5)	152 (9.2)	11.2 (0.2)	NA[a]	NA[a]	NA[a]
	Total (>0.45)	20.1 (2.5)	145 (9.2)	5.0 (0.4)	83.3 (0.0)	599 (0.0)	20.5 (0.0)
	<0.45	0.6 (0.6)	6.8 (0.1)	6.3 (0.3)	NA[a]	NA[a]	NA[a]
	0.45-5	0.6 (0.0)	9.7 (0.2)	2.2 (0.3)	24.7 (0.0)	415 (0.0)	95.3 (0.0)
	5-20	5.2 (0.2)	12.3 (0.4)	0.0	112 (0.0)	266 (0.0)	0.0
	20-63	2.2 (0.2)	17.5 (0.3)	0.0	20.3 (0.0)	161 (0.0)	0.0
	>63	12.2 (2.5)	105 (9.2)	5.0 (0.3)	192 (0.0)	1,660 (0.1)	78.4 (0.0)
C2W	Bulk	45.5 (1.9)	419 (11.8)	19.1 (2.7)	NA[a]	NA[a]	NA[a]
	Total (>0.45)	44.5 (1.9)	397 (11.9)	17.1 (2.7)	165 (0.0)	1,480 (0.0)	63.5 (0.0)
	<0.45	1.1 (0.0)	21.7 (0.6)	2.0 (0.0)	NA[a]	NA[a]	NA[a]
	0.45-5	0.5 (0.2)	2.4 (0.8)	0.2 (0.0)	NA[a]	NA[a]	NA[a]
	5-20	8.9 (3.4)	62.1 (0.8)	2.5 (0.1)	78.0 (0.0)	544 (0.0)	22.1 (0.0)
	20-63	4.4 (8.7)	65.4 (2.2)	3.7 (0.1)	44.1 (0.1)	659 (0.0)	37.8 (0.0)
	>63	30.6 (8.2)	267 (12.0)	10.6 (2.7)	563 (0.2)	4,920 (0.2)	195 (0.0)
O3W	Bulk	3.8 (0.0)	83.2 (8.5)	15.1 (0.3)	NA[a]	NA[a]	NA[a]
	Total (>0.45)	3.3 (0.1)	78.9 (8.5)	1.0 (0.5)	NA[a]	NA[a]	NA[a]
	<0.45	0.5 (0.0)	4.3 (0.2)	14.1 (0.3)	NA[a]	NA[a]	NA[a]
	0.45-5	0.4 (0.0)	5.3 (3.4)	0.0 (NA)	NA[a]	NA[a]	0.0 (NA)
	5-20	3.4 (0.1)	17.7 (3.5)	0.0 (NA)	NA[a]	NA[a]	0.0 (NA)
	20-63	0.0 (0.1)	8.3 (3.8)	1.1 (0.4)	NA[a]	NA[a]	NA[a]
	>63	0.4 (0.1)	47.5 (9.3)	3.2 (0.6)	NA[a]	NA[a]	NA[a]

[a]NA – not applicable. [b]N – salt interference in the solid concentration (>20%).

Table S3, Continued

O4W	Bulk	5.2 (0.1)	92.3 (1.7)	16.7 (0.4)	NA[a]	NA[a]	NA[a]
	Total (>0.45)	4.7 (0.1)	87.2 (1.7)	7.2 (0.4)	25.3 (0.0)	473 (0.0)	39.0 (0.0)
	<0.45	0.6 (0.1)	5.1 (0.3)	9.5 (0.1)	NA[a]	NA[a]	NA[a]
	0.45-5	0.8 (0.1)	5.2 (0.5)	0.1 (0.1)	NA[a]	NA[a]	NA[a]
	5-20	2.3 (1.4)	23.3 (3.0)	0.0 (NA)	14.1 (0.0)	146 (0.0)	0.0 (NA)
	20-63	0.0 (NA)	22.2 (3.2)	4.9 (0.3)	0.0 (NA)	1,610 (0.2)	356 (0.0)
	>63	2.5 (2.2)	36.4 (2.0)	4.7 (0.5)	NA[a]	NA[a]	NA[a]

[a]NA – not applicable. [b]N – salt interference in the solid concentration (>20%).

Location	Particle size range (μm)	Hg-water (μg/L)	As-water (μg/L)	Hg-particle (mg/kg)	As-particle (mg/kg)
A1W	Bulk	0.095 (0.019)	8.6 (0.6)	NA[a]	NA[a]
	Total (>0.45)	0.093 (0.019)	6.7 (0.6)	0.403 (0.000)	29.0 (0.0)
	<0.45	0.003 (NA)	1.9 (0.0)	NA[a]	NA[a]
	0.45-5	0.000 (NA)	0.0 (0.1)	0.000 (NA)	NA[a]
	5-20	0.046 (0.004)	3.0 (0.3)	0.381 (0.000)	24.7 (0.0)
	20-63	0.019 (0.009)	1.6 (0.3)	0.240 (0.000)	19.6 (0.0)
	>63	0.028 (0.020)	2.1 (0.6)	0.962 (0.001)	71.5 (0.0)
A2W	Bulk	0.028 (0.002)	43.3 (9.0)	NA[a]	NA[a]
	Total (>0.45)	0.026 (0.002)	40.7 (9.0)	0.112 (0.000)	177 (0.0)
	<0.45	0.002 (NA)	2.6 (0.0)	NA[a]	NA[a]
	0.45-5	0.000 (NA)	0.3 (0.1)	0.000 (NA)	NA[a]
	5-20	0.015 (0.000)	3.5 (0.6)	0.076 (0.000)	17.8 (0.0)
	20-63	0.000 (NA)	0.4 (0.9)	0.000 (NA)	13.8 (0.0)
	>63	0.011 (0.002)	36.4 (9.0)	NA[a]	NA[a]

Table S3, Continued

A3W	Bulk	0.008 (0.001)	6.1 (0.2)	NA[a]	NA[a]
	Total (>0.45)	0.005 (0.001)	3.0 (0.2)	NA[a]	NA[a]
	<0.45	0.003 (NA)	3.1 (0.1)	NA[a]	NA[a]
	0.45-5	0.001 (0.001)	0.1 (0.2)	NA[a]	NA[a]
	5-20	0.002 (0.001)	0.0 (NA)	0.068 (0.000)	0.0
	20-63	0.000 (NA)	0.2 (0.5)	0.000 (NA)	NA[a]
	>63	0.003 (0.001)	2.7 (0.6)	NA[a]	NA[a]
C1W	Bulk	0.043 (0.005)	38.1 (4.1)	NA[a]	NA[a]
	Total (>0.45)	0.038 (0.005)	36.6 (4.1)	0.159 (0.000)	152 (0.0)
	<0.45	0.005 (NA)	1.5 (0.1)	NA[a]	NA[a]
	0.45-5	0.000 (NA)	0.6 (0.1)	0.000 (NA)	25.6 (0.0)
	5-20	0.007 (0.003)	0.0 (NA)	0.147 (0.000)	0.0
	20-63	0.005 (0.004)	0.8 (0.1)	0.047 (0.000)	7.3 (0.0)
	>63	0.028 (0.006)	35.6 (4.1)	0.433 (0.000)	560 (0.1)
C2W	Bulk	0.078 (0.014)	34.5 (0.9)	NA[a]	NA[a]
	Total (>0.45)	0.075 (0.014)	33.4 (0.9)	0.277 (0.000)	124 (0.0)
	<0.45	0.003 (NA)	1.1 (0.1)	NA[a]	NA[a]
	0.45-5	0.000 (NA)	0.1 (0.1)	NA[a]	NA[a]
	5-20	0.013 (0.001)	1.9 (0.1)	0.116 (0.000)	16.9 (0.0)
	20-63	0.011 (0.004)	1.8 (0.3)	0.113 (0.000)	18.0 (0.0)
	>63	0.051 (0.014)	29.6 (1.0)	0.933 (0.000)	544 (0.0)

[a]NA – not applicable. [b]N – salt interference in the solid concentration (>20%).

Table S3, Continued

O3W	Bulk	0.049 (0.004)	28.1 (15.4)	NA[a]	NA[a]
	Total (>0.45)	0.041 (0.004)	24.0 (15.4)	NA[a]	NA[a]
	<0.45	0.008 (0.000)	4.1 (0.0)	NA[a]	NA[a]
	0.45-5	0.002 (0.001)	0.2 (0.1)	NA[a]	NA[a]
	5-20	0.016 (0.001)	0.0 (0.2)	NA[a]	NA[a]
	20-63	0.008 (0.006)	16.1 (13.4)	NA[a]	NA[a]
	>63	0.015 (0.007)	7.7 (20.5)	NA[a]	NA[a]
O4W	Bulk	0.188 (0.060)	6.0 (0.4)	NA[a]	NA[a]
	Total (>0.45)	0.182 (0.060)	3.8 (0.4)	0.986 (0.000)	20.6 (0.0)
	<0.45	0.006 (NA)	2.2 (0.1)	NA[a]	NA[a]
	0.45-5	0.003 (0.001)	0.0 (NA)	NA[a]	0.0 (NA)
	5-20	0.022 (0.002)	0.8 (0.2)	0.138 (0.000)	5.2 (0.0)
	20-63	0.066 (0.027)	1.8 (0.3)	4.80 (0.002)	134.0 (0.0)
	>63	0.090 (0.066)	1.2 (0.4)	NA[a]	NA[a]

[a]NA – not applicable. [b]N – salt interference in the solid concentration (>20%).

Table S4: Size based concentration of solids, aqueous and particle normalized concentration of Pb, Zn, Ni, Hg, and As in sampled locations from the 2nd storm event and the standard deviations of triplicate samples in parentheses when applicable (Outfall O3W and A3W sampling did not occur in 2*nd* event).

Location	Particle size range (µm)	Pb-water (µg/L)	Zn-water (µg/L)	Ni-water (µg/L)	Pb-particle (mg/kg)	Zn-particle (mg/kg)	Ni-particle (mg/kg)
A1W	Bulk	5.3 (0.3)	71.0 (49.9)	21.9 (1.6)	NA[a]	NA[a]	NA[a]
	Total (>0.45)	4.1 (0.3)	55.0 (50.0)	0.0 (NA)	N[b]	N[b]	0.0
	<0.45	1.3 (0.0)	16.0 (2.7)	24.5 (2.1)	NA[a]	NA[a]	NA[a]
	0.45-5	0.7 (2.1)	6.6 (16.4)	0.0 (NA)	N[b]	N[b]	0.0 (NA)
	5-20	1.0 (2.2)	33.3 (7.4)	2.6 (4.6)	N[b]	N[b]	N[b]
	20-63	1.9 (1.3)	17.6 (17.4)	0.0 (NA)	91.6 (0.1)	849 (0.8)	0.0 (NA)
	>63	0.4 (1.2)	0.0 (NA)	0.0 (NA)	NA[a]	0.0 (NA)	0.0 (NA)
A2W	Bulk	3.2 (0.3)	53.1 (65.2)	22.7 (11.0)	NA[a]	NA[a]	NA[a]
	Total (>0.45)	2.1 (1.6)	31.3 (65.5)	0.0 (NA)	NA[a]	NA[a]	0.0 (NA)
	<0.45	1.1 (0.3)	21.8 (6.6)	24.1 (8.0)	NA[a]	NA[a]	0.0 (NA)
	0.45-5	0.1 (0.4)	44.1 (26.2)	0.0 (NA)	N[b]	N[b]	0.0 (NA)
	5-20	1.6 (0.4)	13.9 (91.0)	3.1 (11.3)	N[b]	N[b]	N[b]
	20-63	0.1 (0.4)	0.5 (104.8)	0.0 (NA)	NA[a]	NA[a]	0.0 (NA)
	>63	0.3 (1.6)	0.0 (NA)	4.1 (11.0)	NA[a]	0.0 (NA)	NA[a]

[a]NA – not applicable. [b]N – salt interference in the solid concentration (>20%).

Table S4, Continued

C1W	Bulk	13.6 (0.7)	141 (11.2)	6.8 (0.1)	NA[a]	NA[a]	NA[a]
	Total (>0.45)	12.5 (0.8)	88.3 (16.6)	3.4 (0.3)	103 (0.0)	724 (0.1)	28.2 (0.3)
	<0.45	1.1 (0.2)	52.2 (12.3)	3.4 (0.3)	NA[a]	NA[a]	NA[a]
	0.45-5	0.2 (0.3)	7.2 (15.3)	0.0	NA[a]	NA[a]	0.0
	5-20	8.0 (0.4)	34.6 (13.4)	3.9 (0.8)	116 (0.0)	503 (0.2)	57.0 (0.0)
	20-63	3.9 (1.7)	20.5 (13.8)	0.0	98.7 (0.0)	523 (0.4)	0.0
	>63	0.4 (1.8)	26.0 (14.7)	0.0 (NA)	NA[a]	NA[a]	0.0
C2W	Bulk	30.0	335	13.9	NA[a]	NA[a]	NA[a]
	Total (>0.45)	28.8 (0.5)	288 (7.1)	11.6 (0.2)	39.9 (0.0)	398 (0.0)	16.1 (0.0)
	<0.45	1.2 (0.5)	47.2 (7.1)	2.2 (0.2)	NA[a]	NA[a]	NA[a]
	0.45-5	0.3 (0.5)	0.0	0.0	0.3 (0.5)	0.0	0.0
	5-20	9.7 (0.0)	85.3 (9.5)	4.8 (0.1)	67.5 (0.0)	595 (0.1)	33.5 (0.0)
	20-63	2.0	35.3	0.5	15.2	275	3.9
	>63	16.9	170	6.5	37.5	376	14.5
O4W	Bulk	1.4 (0.1)	36.0 (10.4)	23.3 (0.4)	NA[a]	NA[a]	NA[a]
	Total (>0.45)	0.0 (NA)	25.6 (10.4)	0.0 (NA)	0.0 (NA)	N[b]	0.0 (NA)
	<0.45	1.5 (0.5)	10.4 (NA)	24.4 (3.8)	0.0 (NA)	NA[a]	NA[a]
	0.45-5	0.0 (NA)	23.0 (NA)	0.0 (NA)	0.0 (NA)	N[b]	0.0 (NA)
	5-20	0.3 (0.3)	0.0 (NA)	1.8 (1.1)	N[b]	0.0 (NA)	N[b]
	20-63	0.0 (NA)	7.0 (NA)	0.0 (NA)	0.0 (NA)	NA[a]	0.0 (NA)
	>63	0.2 (0.1)	29.0 (10.4)	1.0 (0.4)	NA[a]	NA[a]	NA[a]

[a]NA – not applicable. [b]N – salt interference in the solid concentration (>20%).

Table S4, Continued

Location	Particle size range (µm)	Hg-water (µg/L)	As-water (µg/L)	Hg-particle (mg/kg)	As-particle (mg/kg)
A1W	Bulk	0.020 (0.005)	0.0 (NA)	NA[a]	NA[a]
	Total (>0.45)	0.018 (0.005)	NA[a]	N[b]	NA[a]
	<0.45	0.002 (0.001)	NA[a]	NA[a]	NA[a]
	0.45-5	0.001 (0.000)	NA[a]	N[b]	NA[a]
	5-20	0.004 (0.002)	0.0 (NA)	N[b]	0.0 (NA)
	20-63	0.014 (0.011)	0.0 (NA)	0.660 (0.001)	0.0 (NA)
	>63	0.000 (NA)	0.0 (NA)	0.000 (NA)	0.0 (NA)
A2W	Bulk	0.015 (0.001)	0.0 (NA)	NA[a]	NA[a]
	Total (>0.45)	0.011 (0.002)	NA[a]	N[b]	NA[a]
	<0.45	0.004 (0.001)	NA[a]	NA[a]	NA[a]
	0.45-5	0.000 (NA)	NA	0.000 (NA)	NA
	5-20	0.006 (0.000)	0.0 (NA)	N[b]	0.0 (NA)
	20-63	0.002 (0.001)	0.0 (NA)	NA[a]	0.0 (NA)
	>63	0.004 (0.002)	0.0 (NA)	NA[a]	0.0 (NA)
C1W	Bulk	0.026 (0.002)	3.7 (0.3)	NA[a]	NA[a]
	Total (>0.45)	0.023 (0.002)	NA[a]	0.191 (0.000)	NA[a]
	<0.45	0.003 (0.001)	NA[a]	NA[a]	NA[a]
	0.45-5	0.000 (0.001)	NA[a]	NA[a]	NA[a]
	5-20	0.017 (0.002)	NA[a]	0.250 (0.000)	0.0
	20-63	0.005 (0.004)	0.0	0.124 (0.000)	NA[a]
	>63	0.001 (0.004)	0.2 (0.3)	NA[a]	NA[a]

[a]NA – not applicable. [b]N – salt interference in the solid concentration (>20%).

Table S4, Continued

C2W	Bulk	0.046 (0.004)	6.4 (0.1)	NA[a]	NA[a]
	Total (>0.45)	0.044 (0.000)	NA[a]	0.060 (0.000)	NA[a]
	<0.45	0.003 (NA)	NA[a]	NA[a]	NA[a]
	0.45-5	0.000 (0.000)	NA[a]	0.000 (0.000)	NA[a]
	5-20	0.014 (0.001)	NA[a]	0.101 (0.001)	NA[a]
	20-63	0.010 (0.001)	0.8	0.075 (0.001)	6.3
	>63	0.019 (0.005)	2.0	0.042 (0.005)	4.4 (0.0)
O4W	Bulk	0.020 (0.000)	NA	NA[a]	NA[a]
	Total (>0.45)	0.016 (0.000)	NA	N[b]	NA[a]
	<0.45	0.003 (NA)	NA	NA[a]	NA[a]
	0.45-5	0.001 (0.000)	NA	N[b]	NA[a]
	5-20	0.006 (0.001)	0.0 (NA)	N[b]	N[b]
	20-63	0.007 (0.001)	0.0 (NA)	NA[a]	0.0 (NA)
	>63	0.003 (0.000)	NA	NA[a]	0.0 (NA)

[a]NA – not applicable. [b]N – salt interference in the solid concentration (>20%).

Table S5: Method detection limits (MDLs) for two way ANOVA analysis.

	Cd	Cu	Hg	Pb	Zn	Ni	As
MDL (mg/kg)	0.05	0.02	0.001	0.02	0.19	0.02	0.17

Table S6. Significance of seasonal, spatial and their interaction effects on sediment core concentrations (if p-values <0.05, α=0.05). "Increase" is associated with higher sediment concentrations either near the stormwater discharge or at the conclusion of the storm season.

Effects	Cd	Cu	Hg	Pb	Zn	Ni	As
Coupling of period and location	Yes (p<0.01)	No	Yes (p<0.01)	Yes (p=0.02)	Yes (p=0.03)	No	Marginal (p=0.06)
Period (Post compared to Pre)	NA[a]	NS[b]	NA[a]	NA[a]	NA[a]	Increase (p=0.03)	NS[b]
Location (near discharge compared to far-field)	Increase <0.01*	Increase (p<0.01)	NA[a]	NA[a]	NA[a]	Increase (p<0.01)	Increase (p<0.01)

*: Based upon Fisher's exact test due to excessive 0 values in the dataset (Cd exception compared to other metals).

[a]NA: not applicable, when there is statistically significant coupling effect, the period and location effects are not examined separately (Cd exception compared to other metals).

[b]NS: not statistically significant effect/changes.

Table S7: Sediment metal concentration (mg/kg) in the sediment traps of Season 2015/2016 for the metals Cd, Cu, Hg, Zn, Pb, Ni and As and the standard deviations of triplicate samples in parentheses when applicable.

Sediment traps (mg/kg)							
Site	Cd	Cu	Hg	Zn	Pb	Ni	As
P01	ND[a]	306 (30.5)	0.60 (0.01)	446 (91.2)	78.5 (5.2)	26.2 (1.3)	13.1 (0.1)
P08	0.3 (0.1)	300 (12.5)	0.63 (0.05)	407 (36.6)	85.7 (3.4)	28.2 (0.9)	12.5 (0.3)
P11	0.5 (0.1)	316 (34.1)	0.58 (0.04)	450 (46.7)	105 (2.8)	29.1 (0.6)	12.5 (0.2)
P17	1.2 (0.0)	212 (11.2)	0.35 (0.18)	562 (7.1)	126 (2.5)	23.2 (1.2)	7.1 (0.4)

[a]ND – non-detect.

Appendix C

Supplementary information for Chapter 5[1]

[1]The content of this appendix is identical to the supplementary information of a paper submitted on 27th of June 2020 in Environmental Toxicology and Chemistry Journal: I. Drygiannaki, M. Bejar, B, D. D. Reible, J. A. Dawson, B. Rao, N. T. Hayman, G. Rosen, M. A. Colvin

Figures

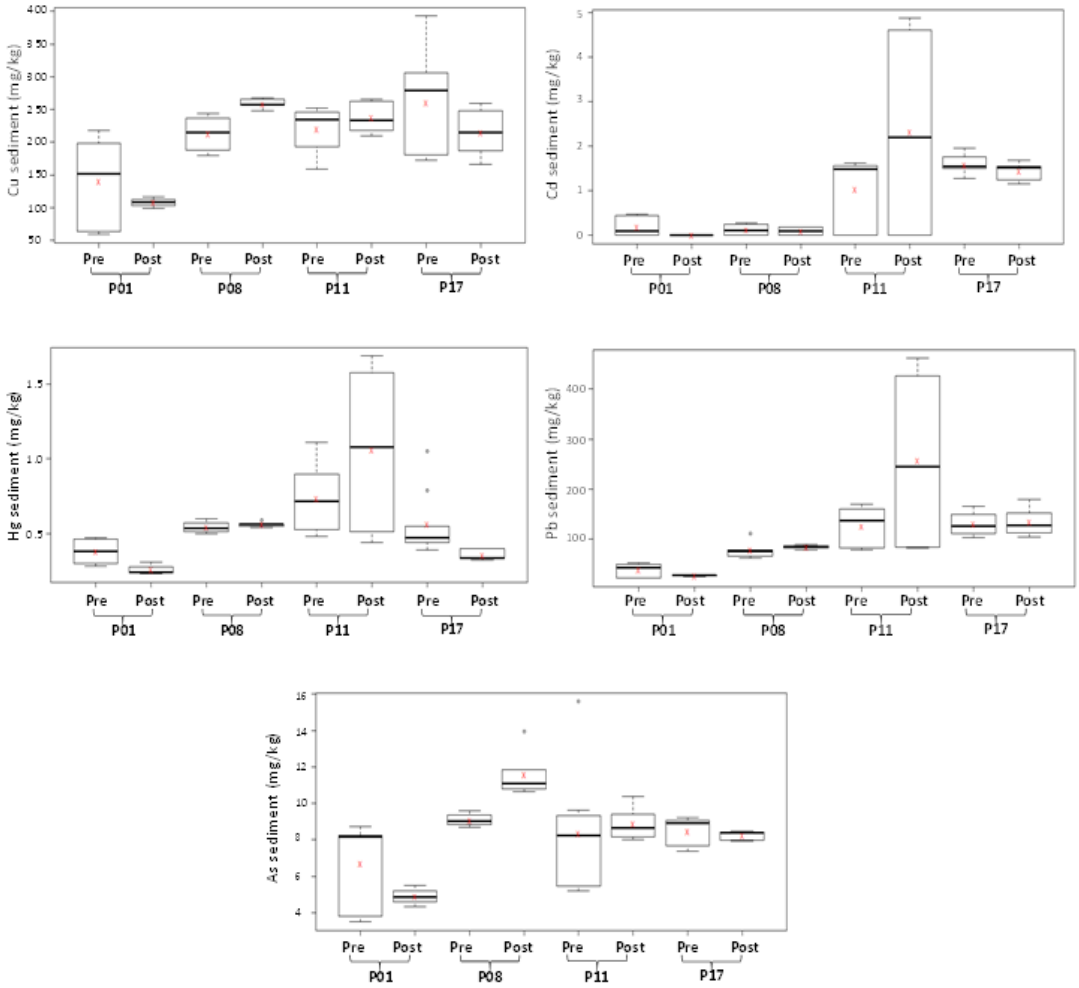

Figure S1: Boxplots of Cu, Cd, Hg, Pb and As sediment concentrations at the sites P17, P11, P08, P01 for the "pre" and "post" storm seasons from 2015 until 2017. The "x" indicates the mean value of each dataset. Locations are ordered relative to their distance from the stormwater discharge with P17 closest to the Paleta Creek discharge.

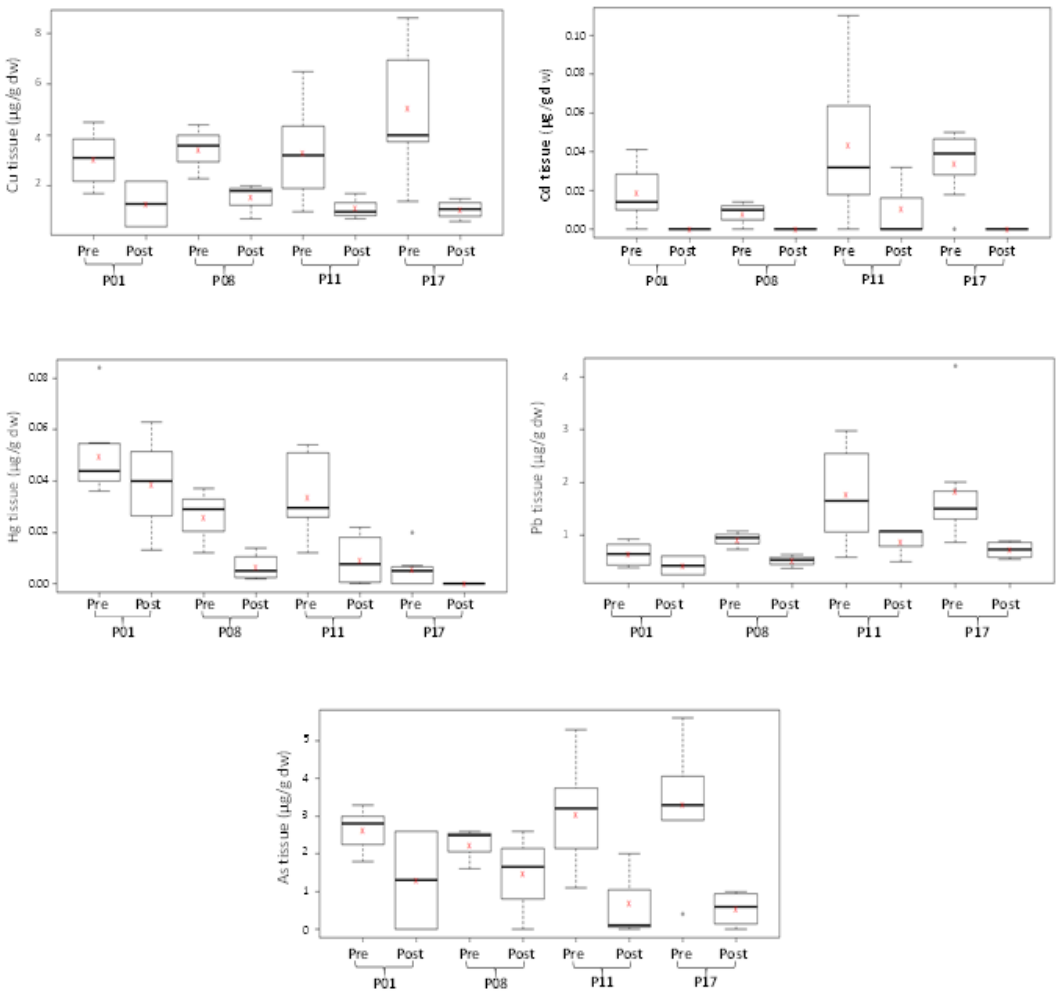

Figure S2: Boxplots of Cu, Cd, Hg, Pb and As tissue concentrations (µg/g dw) at the sites P17, P11, P08, P01 for the "pre" and "post" storm seasons from 2015 until 2017. The "x" mark indicates the mean value of each dataset. Locations are ordered relative to their distance from the stormwater discharge with P17 closest to the Paleta Creek discharge.

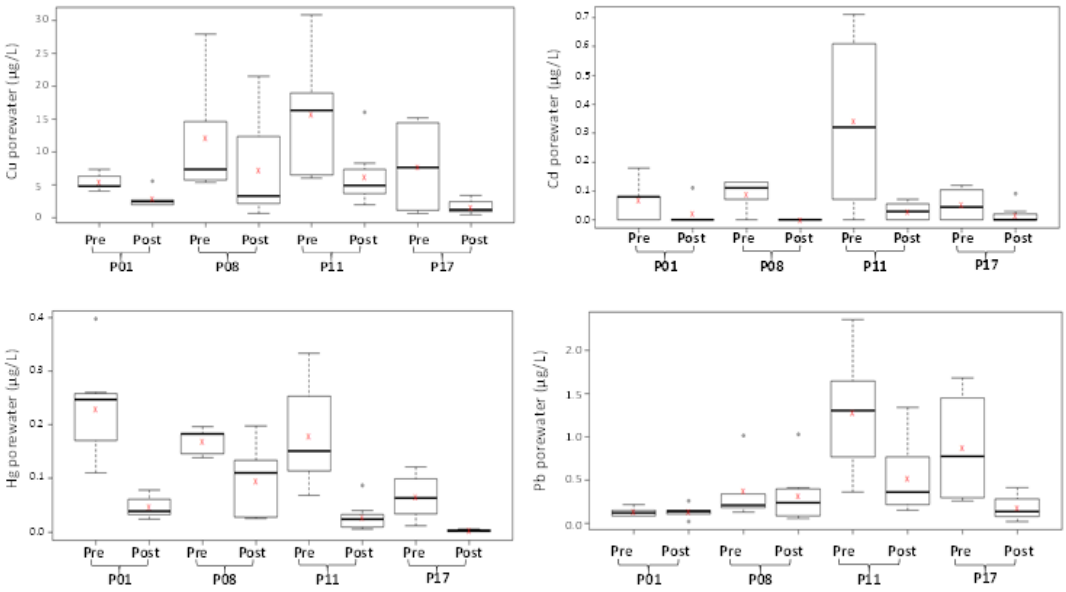

Figure S3: Boxplots of Zn, Cd, Hg, and Pb porewater concentrations (µg/L) at the sites P17, P11, P08, P01 for the "pre" and "post" storm seasons from 2015 until 2017. The "x" indicates the mean value of each dataset. Locations are ordered relative to their distance from the stormwater discharge with P17 closest to the Paleta Creek discharge.

Tables

Table S1: Calibration range of metals that were analyzed using ICP-MS and MERX-T.

Metals	Lower calibration point (ppb)	Higher calibration point (ppb)
Cd	0.2	50
Pb	0.5	50
Cu	1	500
Ni	1	500
Zn	1	500
As	1	100
	Lower calibration point (pg)	**Higher calibration point (pg)**
THg	25	2,500

Table S2: Sediment core concentrations (mg/kg-dry sediment) of the metals Ni, Cu, Zn, Cd, Hg, Pb, and the metalloid As in the monitoring locations P01, P08, P11, and P17 for the months July 2015, October 2015, September 2016, February 2016, and March 2017, and the standard deviations of triplicate samples in parentheses when applicable.

Location	Season	Date	Ni (mg/kg)	Cu (mg/kg)	Zn (mg/kg)	Cd (mg/kg)	Hg (mg/kg)	Pb (mg/kg)	As (mg/kg)
P01	Pre	Jul 15	7.7 (0.1)	61 (2)	113 (1)	0.10 (0.00)	0.29 (0.01)	23 (0)	3.6 (0.2)
		Oct 15	16.1 (0.6)	207 (10)	272 (14)	0.46 (0.01)	0.46 (0.01)	52 (2)	8.1 (0.2)
		Sep 16	14.7 (0.8)	153 (9)	197 (13)	ND[b]	0.39 (0.01)	43 (2)	8.4 (0.3)
	Post	Feb 16	NA[a]	NA[a]	NA[a]	NA[a]	NA[a]	NA[a]	NA[a]
		Mar 17	11.4 (0.8)	108 (9)	145 (12)	ND[b]	0.26 (0.04)	28 (1)	4.9 (0.6)
P08	Pre	Jul 15	NA[a]	NA[a]	NA[a]	NA[a]	NA[a]	NA[a]	NA[a]
		Oct 15	16.9 (0.2)	238 (6)	316 (14)	0.24 (0.03)	0.55 (0.05)	77 (2)	9.3 (0.4)
		Sep 16	16.4 (1.1)	188 (9)	247 (12)	ND[b]	0.53 (0.03)	80 (27)	8.9 (0.3)
	Post	Feb 16	18.8 (0.2)	257 (10)	328 (11)	0.19 (0.00)	0.55 (0.01)	82 (3)	10.8 (0.2)
		Mar 17	22.4 (0.5)	260 (5)	350 (10)	ND[b]	0.57 (0.02)	87 (2)	12.3 (1.5)
P11	Pre	Jul 15	18.1 (2.3)	159-162	388 (19)	1.54 (0.06)	0.71-0.72	139 (30)	5.3 (0.1)
		Oct 15	18.4 (0.5)	244 (8)	492 (18)	1.55 (0.07)	0.97 (0.13)	159 (8)	8.3 (0.1)
		Sep 16	17.5 (1.4)	235 (14)	310 (17)	ND[b]	0.51 (0.04)	80 (2)	11.5 (3.5)
	Post	Feb 16	27.0 (1.1)	254 (18)	940 (92)	4.63 (0.24)	1.61 (0.07)	431 (28)	9.6 (0.7)
		Mar 17	18.6 (0.5)	221 (13)	309 (11)	ND[b]	0.52 (0.08)	84 (0)	8.2 (0.1)
P17	Pre	Jul 15	23.5 (0.5)	335 (50)	685 (13)	1.83 (0.11)	0.79 (0.25)	142 (18)	9.1 (0.1)
		Oct 15	17.8 (0.9)	269 (30)	612 (71)	1.56 (0.05)	0.46 (0.08)	143 (21)	8.7 (0.4)
		Sep 16	14.4 (0.4)	178 (5)	425 (5)	1.36 (0.13)	0.44 (0.05)	107 (4)	7.5 (0.1)
	Post	Feb 16	19.5 (0.8)	246 (15)	681 (20)	1.53 (0.03)	0.34 (0.01)	158 (19)	8.4 (0.0)
		Mar 17	18.6 (1.8)	185 (17)	497 (61)	1.36 (0.27)	0.37 (0.05)	110 (5)	8.1 (0.3)

[a]NA – not applicable because there was not available sediment core for chemical analysis. [b]ND – non-detect.

Table S3: Particle size distribution in percentage (%) of the intact sediment cores sampled in season 2016-2017 and the standard deviations of triplicate samples in parentheses when applicable.

Location	Date	Clay (<2 µm)	Fine silt (2-20 µm)	Coarse silt (20-63 µm)	Sand (>63 µm)
P01	Pre 2016	32.5 (0.4)	14.3 (0.4)	4.2 (0.9)	49.0 (0.3)
	Post 2017	24.4 (0.3)	9.9 (0.3)	3.0 (0.9)	62.7 (0.3)
P08	Pre 2016	38.1 (0.6)	17.5 (0.7)	6.1 (0.2)	38.4 (0.1)
	Post 2017	50.8	29.3	4.0	15.8
P11	Pre 2016	40.5 (0.8)	23.0 (0.3)	1.3 (1.6)	35.2 (0.5)
	Post 2017	36.1	22.9	5.9	35.1
P17	Pre 2016	24.2 (0.3)	22.3 (0.7)	4.8 (1.9)	48.7 (0.8)
	Post 2017	22.9	27.9	11.0	38.2

Table S4: %TOC in the intact sediment cores before the storm seasons ("pre storm") and after the storm seasons ("post storm").

Location	Period	%TOC
P01	Pre storm	0.8
	Post storm	0.7
P08	Pre storm	1.2
	Post storm	1.7
P11	Pre storm	1.7
	Post storm	2.0
P17	Pre storm	4.0
	Post storm	4.5

Table S5: Specifications for 28-day whole sediment bioaccumulation exposure using the bent-nosed clam, *Macoma nasuta.*

Test organisms	Bent-nosed clam, *Macoma nasuta*
Test organism source	Clams: J&G Gunstone Clams, Inc. (Port Townsend, WA)
Test organism size at initiation	Clams: ~1-inch Small Adult
Test duration; endpoint(s)	28 days; survival, bioaccumulation
Test solution renewal	Three-times weekly with filtered seawater
Water Quality Monitoring	Daily (pH, Salinity, Dissolved Oxygen and Temperature); Ammonia at initiation and termination
Feeding	None
Test chamber	1-L glass beakers
Control sediment source	Sediment collected from clam collection site, Discovery Bay, OR
Test sediment depth	3-5 cm (~100g)
Overlying water volume	~750 mL
Test temperature	Clam: 15 ± 2 °C instantaneous
Overlying water	Filtered (0.45 µm) natural seawater collected from near the mouth of San Diego Bay at NIWC-Pacific
Salinity	32 ± 2 ppt
Number of organisms/chamber	Clam: 5
Number of replicates	3
Photoperiod	16 hours light/8 hours dark, ambient laboratory lighting
Aeration	Laboratory filtered air, continuous (1-2 bubbles per second delivered through a Pasteur pipette in laboratory beaker)
Test Protocol	EPA 503/8-91/001, ASTM E-1688-10
Test acceptability criteria	≥ 90% mean survival in controls

Table S6: Tissue concentrations (µg/g-dw) of the metals Ni, Cu, Zn, Cd, Hg, Pb, and the metalloid As in the monitoring locations P01, P08, P11, and P17 for the months July 2015, October 2015, September 2016, February 2016, and March 2017, and the standard deviations of triplicate samples in parentheses when applicable. The reported tissue concentrations (including the control values) are presented after the subtraction of the time 0 tissue concentrations.

Location	Season	Date	Ni (µg/g)	Cu (µg/g)	Zn (µg/g)	Cd (µg/g)	Hg (µg/g)	Pb (µg/g)	As (µg/g)
Time 0	Pre	Jul 15	0.38 (0.09)	2.4 (0.2)	15.3 (2.4)	0.046 (0.004)	0.089 (0.005)	0.11 (0.01)	3.0 (0.2)
		Oct 15	0.27	1.3	13.8	0.057	0.059	0.10	2.7
		Sep 16	0.35	3.0	13.4	0.036	0.105	0.13	2.2
	Post	Feb 16	0.27	1.3	13.8	0.057	0.059	0.10	2.7
		Mar 17	0.41 (0.06)	2.8 (0.4)	19.7 (1.0)	0.044 (0.003)	0.073 (0.004)	0.10 (0.01)	3.3 (0.2)
Control	Pre	Jul 15	NA[a]	NA[a]	NA[a]	NA[a]	NA[a]	NA[a]	NA[a]
		Oct 15	0.23	0.6	6.8	0.032	0.000	0.02	2.5
		Sep 16	NA[a]	NA[a]	NA[a]	NA[a]	NA[a]	NA[a]	NA[a]
	Post	Feb 16	0.23	0.6	6.8	0.032	0.000	0.02	2.5
		Mar 17	NA[a]	NA[a]	NA[a]	NA[a]	NA[a]	NA[a]	NA[a]
P01	Pre	Jul 15	0.22 (0.08)	3.3 (1.2)	6.7 (4.8)	0.015 (0.015)	0.055 (0.018)	0.72 (0.22)	2.7 (0.4)
		Oct 15	0.08	3.1	14.1	0.026	0.041-0.047	0.39	1.8
		Sep 16	0.28	2.0	10.6	0.031	0.036	0.47	3.3
	Post	Feb 16	0.22	2.2	6.0	0.000	0.040	0.60	2.6
		Mar 17	0.00	0.4	0.0	0.000	0.013-0.063	0.24	0.0
P08	Pre	Jul 15	NA[a]	NA[a]	NA[a]	NA[a]	NA[a]	NA[a]	NA[a]
		Oct 15	0.17	2.3	4.6	0.000	0.029	0.72	1.6
		Sep 16	0.26-0.27	3.6-4.4	6.5-7.5	0.010-0.014	0.012-0.037	0.95-1.07	2.5-2.6
	+	+	0.10-0.14	1.78-1.84	2.8-2.9	0.000	0.007-0.014	0.52-0.53	1.6-1.7
	Post	Feb 16	0.09	2.0	6.0	0.000	0.003	0.62	2.6
		Mar 17	0.00	0.7	0.0	0.000	0.002	0.37	0.0
P11	Pre	Jul 15	0.34 (0.15)	3.1 (1.4)	11.0 (3.2)	0.055 (0.043)	0.038 (0.014)	2.06 (1.00)	3.0 (0.9)
		Oct 15	0.03	1.0	2.2	0.000	NA[a]	1.06	1.1
		Sep 16	0.38	6.5	11.6	0.032	0.012	1.06	5.3
	+	+	0.17	1.7	6.0	0.000	0.014-0.022	1.07	2.0
	Post	Feb 16	0.04	1.0	9.4	0.032	0.000	1.07	0.0
		Mar 17	0.00	0.7	0.0	0.000	0.001	0.49	0.1
P17	Pre	Jul 15	0.41 (0.20)	5.3 (2.1)	7.9 (3.4)	0.040 (0.013)	0.006 (0.009)	2.06 (1.24)	4.0 (1.0)
		Oct 15	0.00	1.4	2.2	0.000	0.006	0.86	0.4
		Sep 16	0.46	7.6	12.3	0.038	0.005	1.66	2.9
	+	+	0.19	1.5	1.8	0.000	0.000	0.89	0.9
	Post	Feb 16	0.10	1.2	3.5	0.000	0.000	0.84	1.0
		Mar 17	0.00-0.00	0.6-1.0	0.0-0.0	0.000	0.000	0.54-0.60	0.0-0.3

[a]NA – not available. [+]Treatment in which sediment trap material was added to the pre-storm cores, on the top of this treatment clam exposure occurred.

Table S7: Porewater concentrations (µg/L) of the metals Ni, Cu, Zn, Cd, Hg, and Pb in the monitoring locations P01, P08, P11, and P17 for the months July 2015, October 2015, September 2016, February 2016, and March 2017, and the standard deviations of triplicate samples in parentheses when applicable (Arsenic measurements were not available).

Location	Season	Date	Ni (µg/L)	Cu (µg/L)	Zn (µg/L)	Cd (µg/L)	Hg (µg/L)	Pb (µg/L)
Blank/Travel Controls	Range		0-0.4	0.2-0.5	0.9-1.7	ND	0.002-0.031	0-0.05
P01	Pre	Jul 15	NA[a]	NA[a]	NA[a]	NA[a]	0.256-0.397	NA[a]
		Oct 15	1.5 (0.6)	6.2 (1.3)	31.2 (4.1)	0.11 (0.06)	0.233 (0.037)	0.10 (0.02)
		Sep 16	0.87-0.88	4.1-4.9	24.0-24.0	ND[b]	0.110-0.151	0.15-0.22
	Post	Feb 16	1.0 (0.2)	3.4 (1.9)	14.4 (7.3)	0.04 (0.06)	0.059 (0.020)	0.14 (0.12)
		Mar 17	0.4-0.6	2.0-2.7	7.0-52.6	ND[b]	0.024-0.033	0.11-0.15
P08	Pre	Jul 15	NA[a]	NA[a]	NA[a]	NA[a]	NA[a]	NA[a]
		Oct 15	1.8 (0.0)	9.1 (4.9)	38.1 (3.3)	0.13 (0.01)	0.176 (0.027)	0.44 (0.49)
		Sep 16	0.9-1.8	5.8-28.0	29.6-53.3	0.00-0.07	0.139-0.183	0.21-0.34
	+	+	1.0 (0.2)	1.7 (0.9)	4.6 (1.6)	ND[b]	0.027 (0.002)	0.30 (0.18)
	Post	Feb 16	0.6 (0.1)	3.8 (1.0)	16.5 (4.0)	ND[b]	0.142 (0.050)	0.09 (0.03)
		Mar 17	1.0-1.5	20.2-21.5	42.5-111	ND[b]	0.117-0.144	0.36-1.03
P11	Pre	Jul 15	NA[a]	NA[a]	NA[a]	NA[a]	0.140 (0.018)	NA[a]
		Oct 15	5.2 (1.9)	14.0 (6.6)	247 (107)	0.55 (0.20)	0.279 (0.074)	1.24 (0.44)
		Sep 16	1.0-1.5	6.1-30.8	34.6-77.5	0.00-0.07	0.068-0.108	0.36-2.35
	+	+	1.6 (0.8)	4.0 (2.3)	25.3 (28.2)	0.02 (0.04)	0.013 (0.011)	0.66 (0.61)
	Post	Feb 16	0.6 (0.1)	5.6 (2.4)	19.9 (8.7)	0.04 (0.03)	0.046 (0.038)	0.29 (0.13)
		Mar 17	0.7-0.9	5.4-16.0	15.2-30.1	0.00-0.04	0.022-0.025	0.28-1.07
P17	Pre	Jul 15	NA[a]	NA[a]	NA[a]	NA[a]	0.046-0.116	NA[a]
		Oct 15	2.1-2.2	13.7-15.2	126-127	0.09-0.12	0.089 (0.029)	1.21-1.68
		Sep 16	0.6-1.2	0.7-1.6	5.6-13.4	ND[b]	0.012-0.023	0.26-0.34
	+	+	0.9 (0.3)	1.0 (0.4)	3.0 (0.4)	ND[b]	0.001 (0.000)	0.09 (0.08)
	Post	Feb 16	0.6 (0.1)	1.3 (0.6)	6.6 (3.4)	0.03 (0.05)	0.004 (0.001)	0.12 (0.07)
		Mar 17	0.6-0.7	3.0-3.5	4.9-15.6	0.01-0.03	0.003-0.004	0.36-0.41

[a]NA – not available. [b]ND – non-detect. [+]Treatment in which sediment trap material was added to the pre-storm cores, on the top of this treatment DGT deployment occurred.

Appendix D

Publication regarding seasonal toxicity at Paleta Creek[1]

[1]The content of this appendix is identical to a paper accepted on the 11th of October 2019 in Environmental Toxicology and Chemistry Journal: N. T. Hayman, G. Rosen, M. A. Colvin, B. Chadwick, B. Rao, D. Athanasiou, M. Rakowska, I. Drygiannaki, G. A. Burton Jr, D. D. Reible

Environmental Toxicology and Chemistry—Volume 39, Number 1—pp. 229–239, 2020
Received: 31 May 2019 | Revised: 14 July 2019 | Accepted: 11 October 2019

Environmental Toxicology

Seasonal Toxicity Observed with Amphipods (*Eohaustorius estuarius*) at Paleta Creek, San Diego Bay, USA

Nicholas T. Hayman,[a,*] Gunther Rosen,[a] Marienne A. Colvin,[a] Bart D. Chadwick,[b] Balaji Rao,[c] Dimitrios Athanasiou,[c] Magdalena Rakowska,[c] Ilektra Drygiannaki,[c] G. Allen Burton Jr,[d] and Danny D. Reible[c]

[a]Naval Information Warfare Center Pacific, San Diego, California, USA
[b]Coastal Monitoring Associates, San Diego, California, USA
[c]Texas Tech University, Lubbock, Texas, USA
[d]University of Michigan, Ann Arbor, Michigan, USA

Abstract: To assess potential impacts on receiving systems, associated with storm water contaminants, laboratory 10-d amphipod (*Eohaustorius estuarius*) survival toxicity tests were performed using intact sediment cores collected from Paleta Creek (San Diego Bay, CA, USA) on 5 occasions between 2015 and 2017. The approach included deposition-associated sediment particles collected from sediment traps placed at each of 4 locations during the 2015 to 2016 wet seasons. The bioassays demonstrated wet season toxicity, especially closest to the creek mouth, and greater mortality associated with particles deposited in the wet season compared with dry season samples. Grain size analysis of sediment trap material indicated coarser sediment at the mouth of the creek and finer sediment in the outer depositional areas. Contaminant concentrations of metals (Cd, Cu, Hg, Ni, Pb, and Zn) and organic compounds (polycyclic aromatic hydrocarbons [PAHs], polychlorinated biphenyls [PCBs], and pesticides) were quantified to assess possible causes of toxicity. Contaminant concentrations were determined in the top 5 cm of sediment and porewater (using passive samplers). Whereas metals, PAHs, and PCBs were rarely detected at sufficient concentrations to elicit a response, pyrethroid pesticides were highly correlated with amphipod toxicity. Summing individual pyrethroid constituents using a toxic unit approach suggested that toxicity to *E. estuarius* could be associated with pyrethroids. This unique test design allowed delineation of spatial and temporal differences in toxicity, suggesting that storm water discharge from Paleta Creek may be the source of seasonal toxicity. *Environ Toxicol Chem* 2020;39:229–239. © 2019 SETAC

Keywords: Sediment toxicity; Stormwater; Recontamination; Pyrethroids; Seasonal; Amphipods

INTRODUCTION

Sediment contamination and associated remediation measures are a major challenge for water and sediment program managers and regulators, resulting in significant financial liability (Strategic Environmental Research and Development Program/Environmental Security Technology Certification Program 2016). The potential for recontamination of sediment sites undergoing remediation is also a demonstrated concern, especially when sources of the contamination have not been effectively mitigated (e.g., runoff from storm events; Reible et al. 2018). It is critical not only to understand sources for the recontamination, but also to understand which contaminants are responsible, to better manage mitigation of sediment recontamination. Storm water is considered to be a likely source of this recontamination, although it can be difficult to characterize and identify sources (Brown et al. 1985; Strategic Environmental Research and Development Program/Environmental Security Technology Certification Program 2016). Storm water is comprised of multiple contaminants of concern, including heavy metals, pesticides, and hydrocarbons, present in both water and particulate fractions (Burton and Pitt 2001). Contaminants from storm water events can load contaminants into marine sediment systems (Strategic Environmental Research and Development Program/Environmental Security Technology Certification Program 2016).

The present study is part of a larger effort that characterized recontamination potential of urban sources to the Paleta Creek (San Diego, CA, USA) watershed adjacent to Naval Base San Diego in San Diego Bay (Reible et al. 2018). Paleta Creek is a natural urban/industrial creek with generally higher flows

This article includes online-only Supplemental Data.
* Address correspondence to nicholas.hayman@spawar.navy.mil
Published online 17 October 2019 in Wiley Online Library (wileyonlinelibrary.com).
DOI: 10.1002/etc.4619

associated with winter storm events (measured during this project on the order of approximately 0.6 m^3/s during 2016, and not measured the other years), compared with extended periods with no surface flow during dry weather conditions. The 2161-acre watershed is primarily comprised of residential areas, with some commercial and military uses (Reible et al. 2018). Paleta Creek has been designated a toxic hotspot by the San Diego Regional Water Quality Control Board due to contamination of the sediment and benthic community impacts (SWRCB 1999; Southern California Coastal Water Research Project and Space and Naval Warfare Systems Center 2005). A toxicity identification evaluation concluded that toxicity to amphipods was due to an organic toxicant, but the authors were unable to identify the specific group (Greenstein et al. 2011). However, for any future clean-up action to be successful, continuing sources of contamination must be identified and mitigated to prevent recontamination.

At this site, copper (Cu) and polycyclic aromatic hydrocarbons (PAHs) have been traditionally assumed to be the cause of the observed toxicity (SWRCB 1999; Southern California Coastal Water Research Project and Space and Naval Warfare Systems Center 2005). However, several studies in southern California have attributed this seasonal toxicity of sediments to pyrethroids, using the standard 10-d amphipod acute toxicity test (US Environmental Protection Agency 1994, rather than either Cu or PAHs (e.g., Holmes et al. 2008; Anderson et al. 2010; Lao et al. 2012; Greenstein et al. 2014, 2019). Pyrethroids are commonly used insecticides for residential uses because organophosphates were phased out of household use in the United States (Amweg et al. 2006). Residential runoff in southern California is a major source of pyrethroid contamination in urban creeks, often more important than dry season irrigation runoff (Weston et al. 2009). Due to their chemical characteristics, specifically their hydrophobicity (log octanol/water partition coefficient [K_{OW}] > 5.9) and tendency to associate with sediment particles, sediments in receiving environments may act as a sink for pyrethroids in highly urbanized systems (Gan et al. 2005; Weston et al. 2009; Weston and Lydy 2010). Pyrethroids can cause toxicity in nontarget benthic organisms in the receiving environment (Anderson et al. 2008, 2010; Holmes et al. 2008; Hintzen et al. 2009; Lao et al. 2010, 2012; Van Geest et al. 2014). Thus it is possible that the input of these urban streams has resulted in the seasonal pyrethroid contamination of these receiving environments.

A modified 10-d amphipod acute toxicity test, the toxicity of intact core samples collected in wet and dry seasons over a 2-yr period (2015–2017), was performed with the aim of potentially further identifying the cause(s) of toxicity and the source(s) of contamination.

MATERIALS AND METHODS

Site description

The mouth of Paleta Creek is located on the eastern shoreline in the central portion of San Diego Bay, flowing directly into Naval Base San Diego. The mouth emerges into the bay in a relatively constricted channel area, which then expands into a broader area (Figure 1). The constricted channel area, where sites P11 and P17 were located, will be referred to as the Inner Creek area, whereas the area where the receiving water opens up is referred to as the Outer Creek area and is where site P08 is located. A nearby reference sediment from site P01 was collected to decouple effects from Navy and urban runoff by comparing contaminant concentrations of inner (P17 and P11) and outer creek (P08) sites with the reference sediment.

Sample collection

Two types of sediment samples were collected: intact sediment cores and sediment trap material. Figure S1 in the

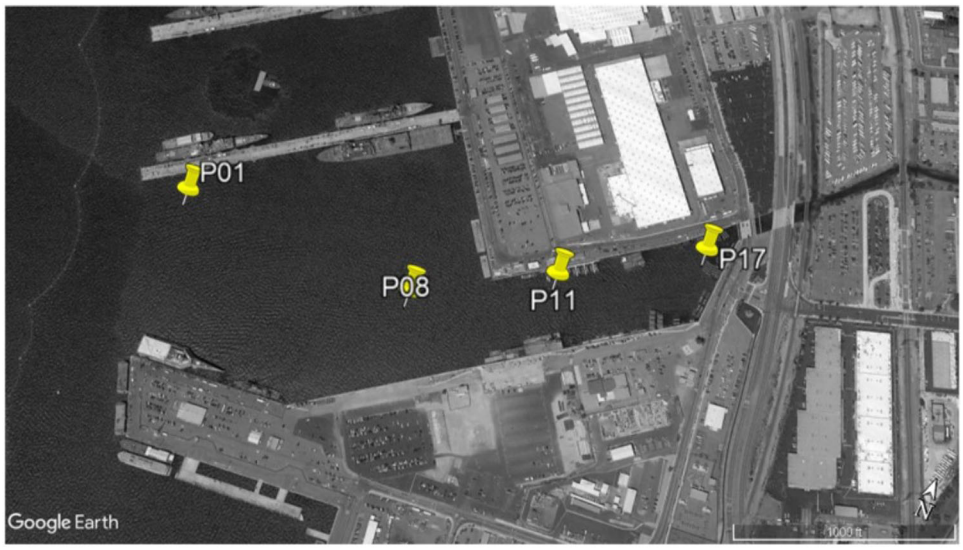

FIGURE 1: Map of the Paleta Creek receiving environment (adjacent to Naval Base San Diego, USA) with study sites indicated. P17 (32.67376, –117.11601) is located near the creek mouth and P11 (32.67265, –117.11800), P08 (32.67165, –117.12000), and P01 (32.67170, –117.12395) are increasingly further away from the creek mouth. Map from Google Earth.

Supplemental Data indicates the timing of each sediment collection (a total of 5 events for intact cores, and 1 event for sediment trap material) in relation to rainfall recorded in San Diego during the study period of June 2015 to March 2017. There were a total of 2 dry and 3 wet weather intact sediment core sampling events. The specific methods for collecting each type of sediment sample are described in the following sections, *Intact sediment core collection* and *Sediment trap material collection*).

Intact sediment core collection

Of the 5 sampling events for intact cores, 2 were dry weather (July 2015 and September 2016) and 3 were wet weather (October 2015, February 2016, and March 2017). All events involved core collection with scuba diver assistance. Following GPS verification of each station location, divers collected cores by pushing cellulose acetate butyrate core liners (7-cm diameter × 28-cm length) approximately 10 cm into the sediment. The divers then capped the ends of the cores. On the boat, overlying water was removed, and samples were placed vertically in coolers. Cores were transported to the Naval Information Warfare Center Pacific for storage at 4 °C until initiation of toxicity and passive sampler exposures.

Sediment trap material collection

Sediment traps consisted of schedule 40 polyvinyl chloride pipe with a trap height of 76.2 cm and a trap diameter of 12.7 cm (5:1 aspect ratio) as described by Blake et al. (2007). A 5-mm stainless steel mesh cover was included on the top end to reduce colonization by macrofauna. The traps were filled with hypersaline brine to retain captured sediment particles, and deployed on the sediment surface for 5 mo, using scuba divers to assist with placement and ensure vertical positioning. Traps were deployed between October 2015 and March 2016 (the 2015/2016 wet season). Two traps were deployed at each of 4 sites: P01 (a reference station), P08, P11, and P17 (Figure 1). The homogenized material from one trap was sent to Texas Tech University (Lubbock, TX, USA) for the same chemical analyses as the intact cores samples, including grain size and other physical parameters, and the homogenized material from the second trap was used for the amphipod toxicity test, described in the following section, *Amphipod toxicity test*. One of the 2 sediment traps from P01 was not recovered successfully, so that material was not assessed for toxicity.

Amphipod toxicity test

For all core samples collected, a 10-d acute amphipod toxicity test was conducted with *Eohaustorius estuarius* using standard methods (US Environmental Protection Agency 1994), with one modification. Instead of homogenizing and sieving sediment samples, cores were collected and tested intact to preserve vertical stratification (Rosen et al. 2017; Kirtay et al. 2018; Fetters et al. 2019), thus more realistically evaluating effects of freshly deposited sediment particles and better replicating in situ conditions. Four toxicity experiments were conducted including cores from: 1) July 2015, 2) October 2015 and February 2016, 3) September 2016, and 4) March 2017.

The day prior to test initiation, all cores were set up in an environmental chamber at 15 °C by adding approximately 500 mL of uncontaminated 0.45-μm filtered seawater and trickle-flow aeration. There were 4 to 6 replicate cores/station, depending on the sampling event. After an overnight equilibration period, 20 amphipods were added to each core. During the test period, water quality (dissolved oxygen, pH, salinity, and temperature) was measured daily, and all parameters were within acceptable ranges (US Environmental Protection Agency 1994). In addition, ammonia was quantified in the overlying water prior to addition of amphipods and prior to test.

During the testing for wet season 2015/2016 cores, 2 additional treatments were added. The first treatment consisted of the October 2015 core with sediment trap material placed on the top of the sediment to mimic particle deposition between the start (October 2015) and end (February 2016) of the wet season. A proportional amount of sediment trap material was added to the top of the core, based on how much material was collected in the recovered sediment trap. This resulted in the height of added sediment on top of October 2015 cores being 2, 1.2, and 3 cm to P08, P11, and P17 cores, respectively. A second additional treatment consisted of the sediment trap material alone. This resulted in a total of 4 treatments, including the intact cores from October 2015 and intact cores from February 2016.

After 10 d, amphipods were sieved from cores using a 0.5-mm stainless steel sieve, and the surviving amphipods were enumerated. All controls met acceptability criteria, with 90% or greater survival (US Environmental Protection Agency 1994).

Chemical and physical analyses

Intact cores collected for chemistry were sent to Texas Tech University for metals (As, Cd, Pb, Zn, Cu, Ni, and Hg), PAHs, polychlorinated biphenyls (PCBs), and pesticide analyses. Pyrethroids were analyzed by Weck Laboratories (Hacienda Heights, CA, USA) for all events, except for March 2017, which was analyzed by Texas Tech University. In general, only the top 5 cm of sediment of the intact core was analyzed. Specifics (including quality assurance/quality control) regarding chemical analyses are available in Reible et al. (2018). All organic contaminants were reported as organic carbon normalized values; metal concentrations were not normalized.

These intact cores were similarly analyzed for physical parameters, including total organic carbon, black carbon, and percentage of moisture. In addition, for cores collected in September 2016 and March 2017, particle size fractionation was performed using a combination of wet sieving and pipette methods to distinguish between coarse sand (>63 μm in diameter), fine sand (20–63 μm in diameter), silt (2–20 μm in diameter), and clay (<2 μm in diameter) following standard protocols as defined in Reible et al. (2018).

Diffusive gradients in thin films (DGT) samplers were deployed in the same containers as amphipods, except for July 2015, when they were exposed in a surrogate chamber (i.e., no amphipods). Single DGT samplers were deployed for 2 d in sediment cores to quantify porewater concentrations of trace metals (Harper et al. 1998; Davison and Zhang 2016).

In addition, triplicate solid-phase microextraction (SPME) fibers were deployed for 28 d to quantify porewater concentrations of PAHs, chlordane, and PCBs (Arthur and Pawliszyn 1990; Mayer et al. 2000) in additional intact cores. Methods to analyze passive samplers from this study are described by Reible et al. (2018).

Bulk sediment chemical and physical (e.g., grain size and total organic carbon) parameters for intact cores were analyzed in the top 5 cm to best estimate the sediment fraction that may have been exposed to the shallow burrowing *E. estuarius* (US Environmental Protection Agency 1994). All parameters (grain size, total organic carbon, black carbon, and percentage of moisture) were measured using standard methods (Reible et al. 2018).

Statistical analyses

Analyses were performed using SYSTAT Ver 12 (SYSTAT Software) and Microsoft Excel 2016. Two series of one-way analyses of variance (ANOVAs) were conducted, one to evaluate the effect of station for each sample date, and the other to assess the effect of sample date at each station. To control for type 1 error, Bonferroni corrections were performed resulting in $\alpha = 0.01$ and 0.0125, respectively. Post hoc Tukey's honestly significant difference tests were performed when one-way ANOVAs revealed significant effects. These data met all relevant assumptions and were not transformed.

Sediment bulk concentrations of trace metals and PCBs were compared with conservative risk thresholds (effect range low [ERL] and effect range median [ERM]) by screening quick reference tables (Buchman 2008), because the relevant literature median lethal concentration (LC50) values were not always available for these contaminants for 10-d amphipod sediment exposures. Sediment concentrations below the ERL are unlikely to elicit toxic effects, and values above the ERM are likely to elicit toxic effects in sensitive species (Long et al. 1995, 1998; Buchman 2008). The ERL and ERM values are based on field observations of a wide range of species responses and do not necessarily indicate a causal relationship (i.e., Zn may exceed the ERM, but is not necessarily the cause of observed toxicity; Long et al. 1995, 1998). Some of these species are more or less sensitive than *E. estuarius*, so these thresholds may not indicate toxicity, although they have been shown to be reasonably reliable with amphipod acute toxicity bioassays (Long et al. 1998). The ERL and ERM values are presented for PAHs as well, but not for pyrethroids (because they have not been developed for these pesticides) or for total chlordane or 4,4′-dichlorodiphenyldichloroethylene (4′,4-DDE; because these contaminants were not detected in sediments).

In addition, toxicity unit analyses were performed for pyrethroids and PAHs, summing them to understand bulk sediment concentrations in terms of toxicity (Holmes et al. 2008; Greenstein et al. 2019). Similar to these studies, relevant pyrethroid literature LC50 values from a similar freshwater amphipod *Hyalella azteca* (when not available for *E. estuarius*) were used to calculate toxicity units by dividing the concentrations of each constituent by literature LC50 values (Table 1). Because these toxicity units were relatively high, the percentage contribution of each pyrethroid analyte to the sum toxicity unit value was calculated. For PAHs, porewater concentrations were calculated using K_{OW} values and bulk sediment concentrations (Swartz et al. 1995). Based on those values, and LC50 values calculated from an amphipod model outlined by Swartz et al. (1995), sum toxicity units were calculated for bulk sediment PAHs. The same analysis was performed again using porewater values obtained from SPME measurements. There were insufficient LC50 literature values to perform toxicity unit analyses for metals or PCBs. Finally, Pearson correlation analyses were performed to determine correlation of the contaminant concentrations with amphipod survival.

TABLE 1: Median lethal concentration (LC50) values of pyrethroids from the literature used in the sum toxic unit calculations

	Literature LC50 (µg/g organic carbon)	
Pyrethroid	*Hyallela azteca*	*Eohaustorius estuarius*
Bifenthrin	—	1.05[a]
Cyfluthrin	—	0.33[b]
Cypermethrin	—	1.41[a]
Deltramethrin/tralomethrin	0.79[d]	—
Fenvalerate/esfenvalerate	0.89[c]	—
L-cyhalothrin	0.45[c]	—
Permethrin		11.16[a]

[a]Anderson et al. 2008.
[b]Greenstein et al. 2014.
[c]Li et al. 2017.
[d]Amweg et al. 2006.

RESULTS

Amphipod survival

There was no significant effect of sampling date at the reference site ($p = 0.086$), but there was a significant effect at 3 other sites, P08 ($p < 0.001$), P11 ($p < 0.001$), and P17 ($p < 0.001$; Figure 2). The observed toxicity (determined by a one-tailed *t* test between the negative control of sediment from amphipod collection site and sample) is noted in Figure 2. To understand the effect of site (reference/P01, P08, P11, P17) on survival, a series of 5 one-way ANOVAs for each sampling date was conducted. There was no significant effect of site for either dry season event, July 2015 ($p = 0.503$) and September 2016 ($p = 0.0444$), although the September 2016 event did show reduced survival at P17 (Figure 3). There were significant effects for the 3 wet weather sampling events, October 2015 ($p < 0.001$), February 2016 ($p < 0.001$), and March 2017 ($p < 0.001$; Figure 3).

Due to 100% mortality of amphipods exposed to the P11 and P17 sediment trap material, and 100% mortality observed in the October 2015 sediment + sediment trap material

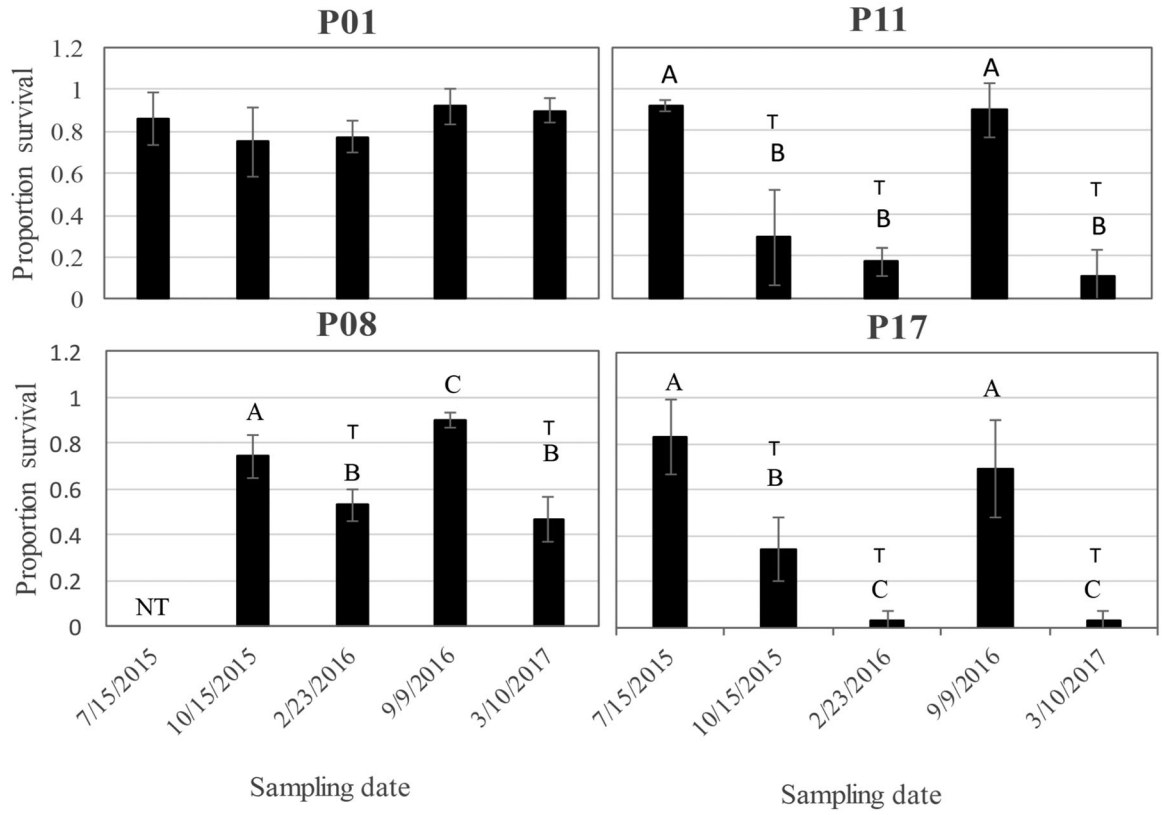

FIGURE 2: *Eohaustorius estuarius* survival at each of 4 sites grouped by sampling location. The letters represent the results of post hoc Tukey tests, indicating differences between sampling dates. Plots with no letters indicate nonsignificant effects of site on the survival of amphipods. "NT" indicates samples that were not tested. A "T" above the bar indicates a significant toxic effect.

treatments, statistical analyses were not performed to compare these treatments with the October 2015 sediment cores (without sediment trap material) or February 2016 cores. However, it is clear that the addition of sediment trap material to P08, P11, and P17 cores collected in October 2015 resulted in reduced amphipod survival compared with unamended October 2015 cores. Furthermore, this addition of trap material resulted in similar, or smaller, survival rates in February 2016 cores (Figure 4).

Physiochemistry of sediment cores

Given the strong seasonal toxicity observed with *E. estuarius*, a variety of toxicants present in the system were measured to determine which ones occurred at 1) concentrations high enough to potentially cause significant toxicity, and 2) concentrations in bulk sediments and/or porewater that correlated with observed toxicity. All measured contaminant concentrations are presented in the Supplemental Data for measured metals, PCBs, PAHs, and pesticides for both bulk sediment concentrations and as results from DGT and SPME measurements (used as proxies for porewater concentrations).

To address the first requirement (that toxicants occurred at concentrations high enough to cause potentially significant toxicity to *E. estuarius*), the ERL and ERM concentrations were used to determine which contaminants were present at concentrations that might result in toxicity if LC50 values could not be located. Values below the ERL are unlikely to elicit toxic effects, whereas values above the ERM may elicit toxic effects (Long et al. 1998).

Organic contaminants measured in the collected sediments were generally below ERL concentrations and well below ERM concentrations, including total PCBs (13% exceeded ERLs, and none exceeded ERMs), total PAHs (11% exceeded ERLs, and none exceeded ERMs), chlordane (not detected in any samples), and 4′,4-DDE (not detected in any samples; Supplemental Data, Tables S1–S3). In addition, SPME-derived porewater PCBs, PAHs, chlordane, and 4′,4-DDE concentrations were well below LC50 values for this species, where data were available (Swartz et al. 1995; Anderson et al. 2010; Phillips et al. 2011; Supplemental Data, Tables S3–S5). Pyrethroids were not targeted for analysis in SPMEs, and thus no porewater data are available for pyrethroids.

For metals (As, Cd, Pb, Zn, Cu, Ni, and Hg), many bulk sediment concentrations were above the ERL (all samples had at least one ERL exceedance) and in some cases, above the ERM (41% had at least one metal above the ERM). Copper and Zn were notably elevated, suggesting possible metal-associated toxicity (Supplemental Data, Table S6). Although there is a published Cu 10-d sediment LC50 (Anderson et al. 2008), toxicity unit calculations showed a maximum value of 0.63, suggesting that Cu had not made a large contribution to the toxicity of these samples to amphipods, especially considering that this maximum value occurred during a dry

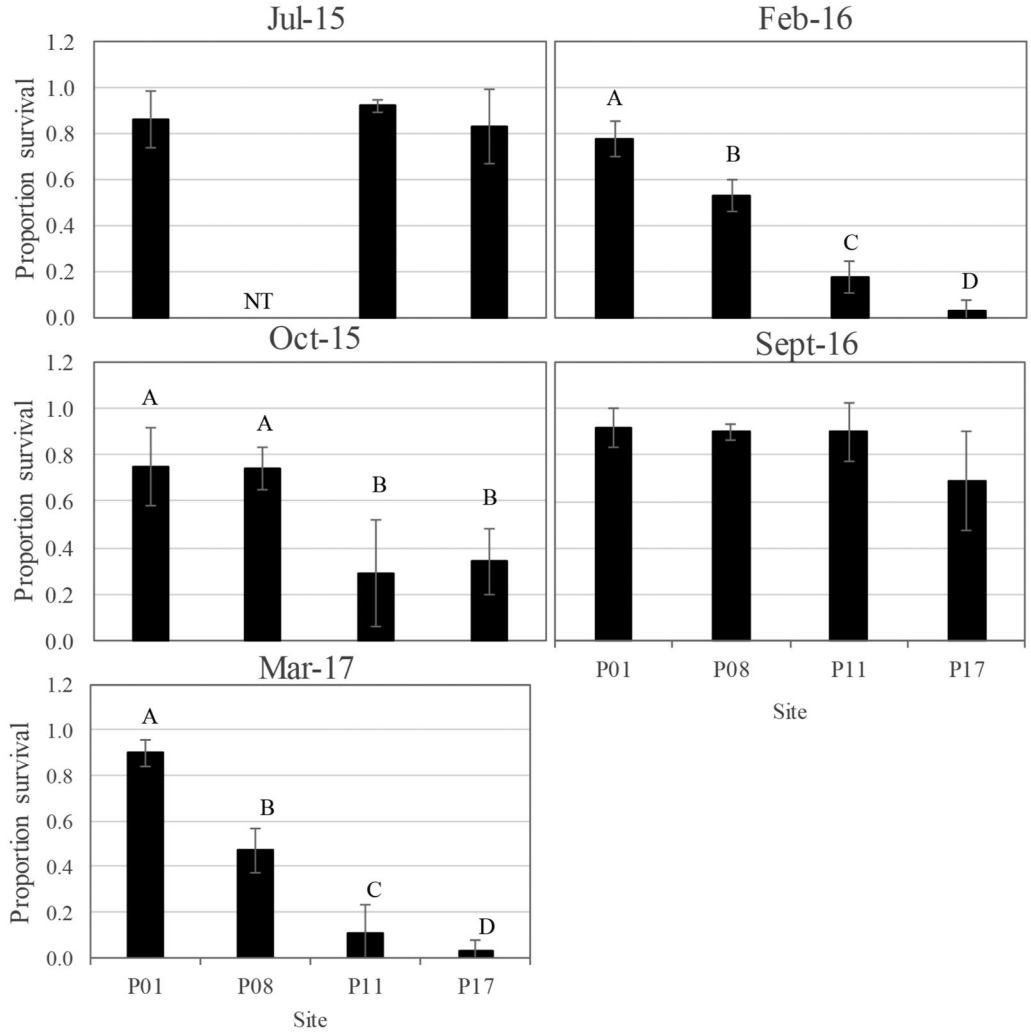

FIGURE 3: *Eohaustorius estuarius* survival at each of 4 sites grouped by sampling date. The letters represent the results of post hoc Tukey tests, indicating differences between sampling dates. Plots with no letters indicate nonsignificant effects of site on the survival of amphipods. "NT" indicates samples that were not tested.

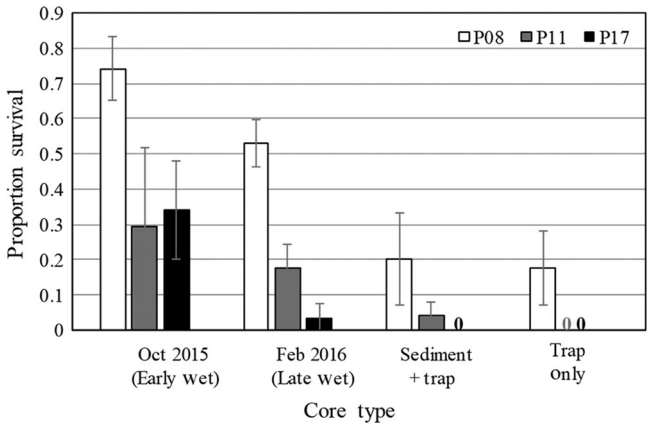

FIGURE 4: *Eohaustorius estuarius* survival for sediment trap material treatments. The first 2 groups of columns are data presented in Figures 2 and 3, shown for comparison with sediment trap treatments. Sediment + Trap indicates sediment + sediment trap material treatment. Trap Only indicates the results from exposure to just the sediment trap material.

weather sampling event (when amphipod survival was >90%). Measured LC50 values for another estuarine amphipod, *Rhepoxynius abronius*, were much lower (generally by at least a factor of 100) than reported LC50 values for Cd and Hg, which were 9810 and 13.1 mg/kg, respectively (Phillips et al. 2011). However, for Zn, with a reported LC50 of 276 mg/kg for *R. abronius* (Phillips et al. 2011), almost every core taken in this study met, or exceeded, this value (Supplemental Data, Table S6). However, this was the case for cores in which no toxicity was observed, so this value is likely too low to be relevant to *E. estuarius*. In our review, no other measured metal concentrations could be associated with reliable or relevant LC50 values from the literature. The DGT-derived metal porewater values were low (highest values for Pb, Cu, and Zn were 20.9, 1.44, and 5.18 μg/L, respectively). These were generally a factor of 10^3 lower than reported 4-d water LC50 values (reviewed in Phillips et al. 2011; Supplemental Data, Table S7).

A sum toxicity unit method for PAHs, first demonstrated by Swartz et al. (1995), was used as another line of evidence to

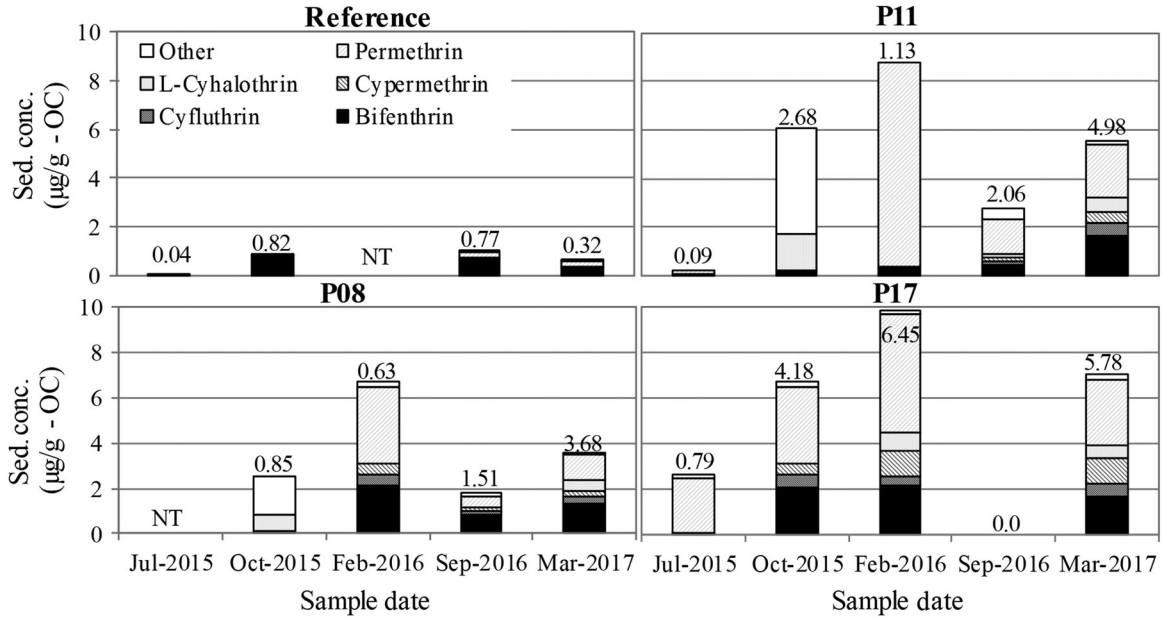

FIGURE 5: Bulk sediment concentrations for pyrethroids in sediment cores, normalized to organic carbon (OC). Pyrethroids detected infrequently were not included in the sum toxicity unit calculations due to insufficient toxicity data and are grouped as "Other." These include deltamethrin/tralomethrin, dichloran, fenvalerate/esfenvalerate, and pendimethalin. Values above the bars represent the calculated sum toxicity unit for the pyrethroids used for analyses. "NT" indicates samples that were not tested.

assess PAH toxicity, because it has been documented that these contaminants are possibly responsible for toxicity observed at this site (Southern California Coastal Water Research Project and Space and Naval Warfare Systems Center 2005; Greenstein et al. 2011). The sum toxicity unit analysis employed both modeled PAH porewater measurements (with a model developed by Swartz et al. [1995] using K_{OW} values and bulk sediment measurements) and porewater values measured using SPME (Supplemental Data, Table S4) and compared those values with porewater LC50 values calculated using an amphipod model from Swartz et al. (1995) that utilized data from 4 marine amphipods, including *E. estuarius* (Supplemental Data, Table S8). Sum toxicity unit values were low (<0.77) for modeled porewater measurements and exceedingly low (<0.039) for porewater concentrations measured using SPME (Supplemental Data, Table S9).

To assess whether pyrethroids might result in significant toxicity to *E. estuarius,* a sum toxicity unit approach was used that has been used previously for evaluating pyrethroid toxicity (Holmes et al. 2008; Lao et al. 2010; Greenstein et al. 2014, 2019). Organic carbon normalized LC50 values from sediment spiking studies were used to determine toxicity units. Pyrethroid data for *E. estuarius* are relatively limited, so when data for *E. estuarius* were not available, LC50 values derived for the freshwater amphipod *H. azteca* were used, because this species has a similar life history (epibenthic, deposit feeder). It is noteworthy, however, that *H. azteca* has been reported to be somewhat more sensitive than *E. estuarius* to pyrethroids (Lao et al. 2010). Regardless, several studies have incorporated *H. azteca* LC50 values when no *E. estuarius* data were available (e.g., Greenstein et al. 2014, 2019), so the results we present are comparable. The LC50 values used in our study are shown in Table 1. The summed toxicity units were as high as 6.35; a value of approximately 2.8 toxicity units corresponded to a 50% effect (Figure 5), and generally the values were higher at inner creek sites and during the wet seasons. The summed toxicity units remained relatively low at the reference site (<1 toxicity unit). The percentage of contributions of each individual pyrethroid toxicity unit to the sum toxicity unit was calculated (Supplemental Data, Table S10).

The percentage of fines in the sediment was determined in cores collected in September 2016 and March 2017, because some studies have indicated that high fines percentage (70–100%) may cause mortality to *E. estuarius,* although there is a lack of agreement regarding an actual fines threshold (Dewitt et al. 1989; Tay et al. 1998; Anderson et al. 2017). Anderson et al. (2017) found that survival was reduced when clay concentrations exceeded 50%, with smaller *E. estuarius* showing less sensitivity than larger ones. However, all the collected cores and sediment trap materials were characterized as having <70% fines (<63 µm in diameter), with the exception of P08 cores collected in March 2018, which had a fines content of 84.2% (Supplemental Data, Table S11). Similarly, clay percentages were all <50%, except for P08 collected in March 2018, which had a clay content of 50.8% (Supplemental Data, Table S11).

Pearson correlations were used to assess the correlation between contaminant concentrations in either sediment or porewater (metals, total PCBs, chlordane) or sum toxicity unit (total PAHs and pyrethroids) and untransformed amphipod survival data (Supplemental Data, Table S12). The following contaminants demonstrated significantly negative correlations (i.e., chemistry parameter measurements increased as amphipod survival decreased) in the sediment phase: Zn ($r = -0.53$, $p < 0.05$), total

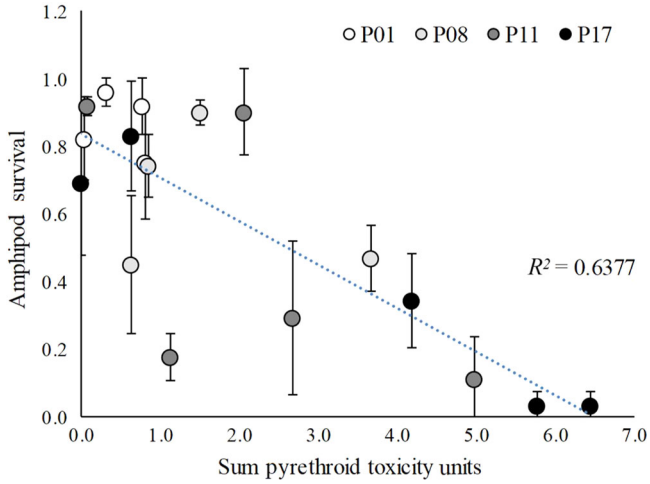

FIGURE 6: Correlation between the sum pyrethroid toxicity units and the proportion of amphipod survival.

PCBs ($r = -0.51$, $p < 0.05$), and pyrethroids ($r = -0.80$, $p < 0.001$). The following contaminants demonstrated significantly negative correlations in the porewater phase: SPME-measured total PAH ($r = -0.51$, $p < 0.05$), and total chlordane ($r = -0.73$, $p < 0.001$). Pyrethroids are the only contaminant to both occur at concentrations high enough to cause the observed toxicity and be highly correlated with amphipod survival (Figure 6).

Physiochemical parameters of sediment traps

Similar to the cores, sediment trap material did not exceed the ERM for any of the measured organic contaminants (total PCBs, total PAHs, and pesticides excluding pyrethroids), although some ERL concentrations were exceeded infrequently (Supplemental Data, Table S13–S15). In addition, the sediment trap material did exceed the ERL (for at least one metal in all samples), and in some cases the ERM (either Cu or Zn in all samples), for the measured trace metals (As, Cd, Pb, Zn, Cu, Ni, and Hg; Supplemental Data, Table S16). The bulk concentrations of pyrethroids, and the resulting sum toxicity unit values, are presented in Figure 7, showing an increase in sum toxicity unit values at sites closer to the mouth of Paleta Creek, although these values were not as high as those reported for the intact cores. The relative contribution of individual pyrethroid analytes to the sum toxicity unit value are summarized in the Supplemental Data, Table S17. Grain-size analysis of the sediment trap material (Supplemental Data, Table S11) indicated that the percentage of fines were 93.1, 90.3, 89.8, and 53.7% for stations P01, P08, P11, and P17, respectively. Although these values may suggest the potential to cause *E. estuarius* mortality, these data were not included in the correlation analysis because the sediment trap material frequently resulted in total mortality of the amphipods (i.e., no variation), making these data inappropriate for analysis.

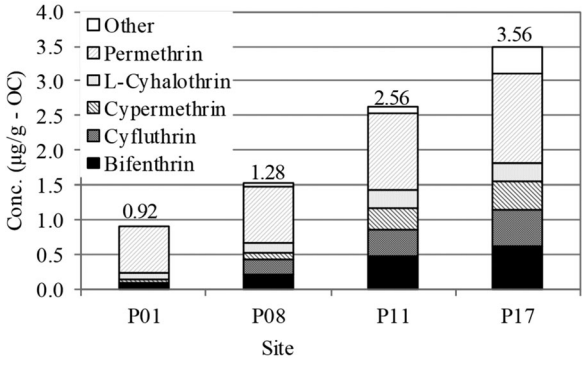

FIGURE 7: Bulk sediment concentrations for pyrethroids in sediment trap material, collected over the 2015/2016 wet weather season (October 2015–February 2016), separated by station. Pyrethroids detected infrequently were not included in sum toxicity unit calculations due to insufficient toxicity data and are grouped as "Other." These include deltamethrin/tralomethrin, dichloran, fenvalerate/esfenvalerate, and pendimethalin. Values above the bars represent the calculated sum toxicity unit for pyrethroids used for analyses. OC = organic carbon.

DISCUSSION

In the present study, a clear seasonal pattern in acute toxicity to the estuarine amphipod *E. estuarius* was observed over a 2-yr period at the mouth of Paleta Creek. In cores collected after significant antecedent dry periods (July 2015 and August 2016), high survival was generally observed at all stations (Figure 2). However, in cores collected after rain events (October 2015, February 2016, and March 2017) there was significant mortality at P08, P11, and P17, but not at P01 (Figure 2). In addition, reduced amphipod survival was greater in late wet season samples (February 2016 and March 2017) than earlier in the wet season (October 2015). This may have resulted from differences in rainfall and runoff quantity (Figure 2). Furthermore, cores collected during the wet season showed a clear spatial trend of amphipod survival, with reduced survival closer to the creek mouth, whereas this trend was not apparent in the dry season (Figure 3). In combination, these results suggest that contaminant toxicity is related to storm water discharge and that Paleta Creek may be the source. Finally, it appears that this effect is ephemeral, because it did not occur during dry season monitoring events.

Pyrethroid pesticides are the most likely cause for seasonal toxicity. They were the only organic contaminant class likely to cause toxicity to *E. estuarius* (demonstrated by sum toxicity unit values), and there was a strong correlation of sum toxicity unit values and amphipod survival (Figures 6 and 7). The sum toxicity unit analysis with pyrethroids demonstrated a similar pattern, resulting in a strong correlation between amphipod mortality and summed pyrethroid toxicity units (Figure 5). The coefficient of determination (r^2) calculated from this relationship was 0.638, which suggests that a majority of the variation in amphipod survival can be described by the sum toxicity unit values, although it is possible that other factors are also involved. Furthermore, available data regarding degradation of pyrethroids (30–90 d, with the exception of bifenthrin at 629 d), agree with observed ephemeral toxicity (Li et al. 2017). It is apparent from the pyrethroid analyses that whereas bifenthrin was consistently the largest contributor to toxicity in all core sediments (20–100%), during the second

season (2016/2017) cyfluthrin, and to a lesser degree other pyrethroids, became larger contributors to the overall sum toxicity unit values (Supplemental Data, Table S10). Although PCB sediment concentrations and chlordane porewater concentrations correlated significantly with amphipod toxicity, both were at relatively low concentrations, and were unlikely responsible for the toxic response (reviewed by Phillips et al. 2011).

Although some metals were elevated (i.e., Zn, Hg, and Cu, notably), previous research has suggested that *E. estuarius* is relatively insensitive to Cu (McPherson and Chapman 2000; Anderson et al. 2008) and likely other metals, although appropriate LC50 values of *E. estuarius* are not available for either Zn or Hg. Further DGT measurements were relatively low (in the low ppb range), and were a factor of 10^3 lower than reported water LC50 values for this species for 4-d exposures. Note that direct comparisons between DGT and porewater LC50 values are not possible, because these measurements are operationally different (some dissolved organic carbon–bound metal ions present in dissolved metal measurements are excluded by DGT; Davison and Zhang 2016). However, DGT measurements have been shown to be relevant to the bioavailable fraction (e.g., Degryse and Smolders 2016). Thus these low values suggest that most of the metals were likely not bioavailable in these sediments.

The only metal that was correlated significantly with amphipod mortality was Zn, possibly because Zn concentrations were higher during the wet season: increased storm water runoff generally increases Zn concentrations in sediment, and thus is not indicative of a causal relationship with amphipod survival. Given the apparently low bioavailability of Zn (from DGT measurements) and the much stronger correlation with pyrethroids (present at concentrations likely to cause toxicity), it is unlikely that Zn was driving this seasonal toxicity. Furthermore, although many of the sediment core measurements were above the reported sediment LC50 values for *R. abronius*, these samples included those without observable toxicity, suggesting that this LC50 value is too low to be applicable to *E. estuarius*.

The sediment + trap material treatment simulated particle deposition during the wet season and provided another line of evidence of the contribution of Paleta Creek contaminants as a potential source of seasonal toxicity (Figure 4). Trap material increased the toxicity of all stations (P08, P11, and P17) relative to unmanipulated intact cores, suggesting that particles contributed to the increase in mortality (Figure 4). Fines were unlikely responsible for mortality, given that they were not at levels as high as literature values that report only modest reductions in survival (Anderson et al. 2017). Furthermore, fines content generally increased in sediment traps further from the creek mouth, whereas toxicity was highest nearest the mouth. Thus, amphipod mortality and high fines/clay were not well correlated, suggesting that fine/clay percentages were not driving the observed toxicity in these treatments. The data suggest that storm water–associated particles from the creek may be a source of pyrethroids because pyrethroid sum toxicity units from the sediment traps decreased as they moved further from the creek mouth, matching the toxicity pattern (Figure 7). Note that the sediment trap material + core treatments were representative of a worst case scenario. It is possible that amphipods were unable to burrow past the sediment trap material (all of these specific laboratory treatments consisted of at least 1 cm of trap material), resulting in trap material bias. Finally, the percentage of contribution of each individual pyrethroid to the sum toxicity unit value in the sediment material suggests that Paleta Creek discharge is primarily loading cyfluthrin (44–56%) and *L*-cyhalothrin (16–23%), and, to a lesser degree, bifenthrin (11–18%; Supplemental Data, Table S17).

Our results are similar to others in Southern California, including San Diego Bay, suggesting that pyrethroids may be the cause of seasonal toxicity (Holmes et al. 2008; Anderson et al. 2010; Greenstein et al. 2014, 2019). Pyrethroids may be especially relevant in highly urbanized watersheds, such as Paleta Creek, because they have replaced organophosphates as a common household insecticide (Amweg et al. 2006; Weston and Lydy 2010; Tang et al. 2018) and are becoming increasingly relevant in agricultural settings as well. They have been detected worldwide in a variety of environmental media, such as surface water and sediment, making them critical to consider at potentially impacted sites (Tang et al. 2018). Following the correlation analysis, 63.8% of the variation in amphipod survival was described by pyrethroid sum toxicity units; this finding suggests that although pyrethroids are a significant driver of toxicity, there are other contaminants or parameters that may explain the observed toxicity, including some of those documented in the present study, such as Zn.

Understanding not only the responsible contaminants, but also the source of contamination, is critical to efforts to mitigate sediment contamination. Utilizing multiple lines of evidence, the results of the present study strongly suggest that Paleta Creek is an active source of pyrethroid contamination during the wet seasons. Without considering the source, and appropriately mitigating it, remediation efforts may fail due to recontamination of the site (Strategic Environmental Research and Development Program/Environmental Security Technology Certification Program 2016). For example, in the Paleta Creek receiving environment, if pyrethroid contamination from the creek is not considered, future amendments to reduce sediment toxicity may fail, because pyrethroids may continue to be a contaminant source at the site. Our study demonstrates that a better understanding of potential linkages between the source (storm water in the present study) and sediment contamination can be developed through delineation of spatial and temporal trends combined with novel storm particle treatment techniques. The novel combination of methods that we employed could increase the likelihood of appropriate determination of the contaminants of concern (including others yet to be determined) responsible for causing the observed toxicity, and its source, ultimately leading to effective use of available resources to assist remediation and regulatory compliance.

Supplemental Data—The Supplemental Data are available on the Wiley Online Library at DOI: 10.1002/etc.4619.

Acknowledgment—The present study was funded by the US Department of Defense's Strategic Environmental Research and Development Program (project ER-2428). We would like to thank J. Munson-Decker, M. Bejar, and M. Hudson for laboratory and field support that made this project successful.

Data Availability Statement—Data are available from the corresponding author on request (nicholas.hayman@spawar.navy.mil).

REFERENCES

Amweg EL, Weston DP, You J, Lydy MJ. 2006. Pyrethroid insecticides and sediment toxicity in urban creeks from California and Tennessee. *Environ Sci Technol* 40:1700–1706.

Anderson BS, Lowe S, Phillips BM, Hunt JW, Vorhees J, Clark S, Tjeerdema RS. 2008. Relative sensitivities of toxicity test protocols with the amphipods *Eohaustorius estuarius* and *Ampelisca abdita*. *Ecotoxicol Environ Saf* 69:24–31.

Anderson BS, Phillips BM, Hunt JW, Clark SL, Voorhees JP, Tjeerdema RS, Casteline J, Stewart M, Crane D, Mekebri A. 2010. Evaluation of methods to determine causes of sediment toxicity in San Diego Bay, California, USA. *Ecotoxicol Environ Saf* 73:534–540.

Anderson B, Phillips B, Voorhees J. 2017. The effects of kaolin clay on the amphipod *Eohaustorius estuarius*: Part two. Contribution No. 822. Final Report. San Francisco Estuary Institute Clean Water Program, Richmond, CA, USA.

Arthur CL, Pawliszyn J. 1990. Solid phase microextraction with thermal desorption using fused silica optical fibers. *Anal Chem* 62:2145–2148.

Blake AC, Chadwick DB, White PJ, Jones CA. 2007. User's guide of assessing sediment transport at Navy facilities. TR-1960. Technical Report. SPAWAR Systems Center San Diego, San Diego, CA, USA.

Brown RC, Pierce RH, Rice SA. 1985. Hydrocarbon contamination in sediments from urban stormwater runoff. *Mar Pollut Bull* 16:236–240.

Buchman MF. 2008. Screening Quick Reference Tables (SQuiRTs). US National Oceanic and Atmospheric Administration, Office of Response and Restoration Division, Seattle, WA.

Burton GA Jr, Pitt R. 2001. *Stormwater Effects Handbook: A Tool Box for Watershed Managers, Scientists and Engineers*. CRC/Lewis, Boca Raton, FL, USA.

Davison W, Zhang H. 2016. Introduction to DGT. In Davison W, ed, *Diffusive Gradients in Thin-Films for Environmental Measurements*, 1st ed. Cambridge University, Cambridge, UK, pp 1–10.

Degryse F, Smolders E. 2016. DGT and bioavailability. In Davison W, ed, *Diffusive Gradients in Thin-Films for Environmental Measurements*. Cambridge University, Cambridge, UK, pp 216–262.

Dewitt TH, Swartz RC, Lamberson JO. 1989. Measuring the acute toxicity of estuarine sediments. *Environ Toxicol Chem* 8:1035–1048.

Fetters K, Rosen G, Kirtay V, Chadwick B, Conder J, Sacks VP, Grover M, Magar V. 2019. Demonstration and validation of enhanced monitored natural recovery at a pesticide contaminated sediment site. *J Soil Sediment*. DOI: 10.1007/S11368-019-02386-4

Gan J, Lee SJ, Liu WP, Haver DL, Kabashima JN. 2005. Distribution and persistence of pyrethroids in runoff sediments. *J Environ Qual* 841:836–841.

Greenstein DJ, Bay SM, Young DL. 2011. Sediment toxicity identification evaluation for the mouths of Chollas and Paleta Creeks, San Diego. 699. Final Report. Southern California Coastal Water Research Project, Costa Mesa, CA, USA.

Greenstein DJ, Bay SM, Young DL, Asato S, Maruya KA, Lao W. 2014. The use of sediment toxicity identification evaluation methods to evaluate clean up targets in an urban estuary. *Integr Environ Assess Manag* 10:260–268.

Greenstein DJ, Parks AN, Bay SM. 2019. Using spatial and temporal variability data to optimize sediment toxicity identification evaluation (TIE) study designs. *Integr Environ Assess Manag* 15:248–258.

Harper MP, Davison W, Zhang H, Tych W. 1998. Kinetics of metal exchange between solids and solutions in sediments and soils interpreted from DGT measured fluxes. *Geochem Cosmochim Acta* 62:2757–2770.

Hintzen EP, Lydy MJ, Belden JB. 2009. Occurrence and potential toxicity of pyrethroids and other insecticides in bed sediments of urban streams in central Texas. *Environ Pollut* 157:110–116.

Holmes RW, Anderson BS, Phillips BM, Hunt JW, Crane DB, Mekebri A, Connor V. 2008. Statewide investigation of the role of pyrethroid pesticides in sediment toxicity in California's urban waterways. *Environ Sci Technol* 42:7003–7009.

Kirtay V, Conder J, Rosen G, Magar V, Grover M, Arblaster J, Fetters K, Chadwick B. 2018. Performance of an in situ activated carbon treatment to reduce PCB availability in an active harbor. *Environ Toxicol Chem* 37:1767–1777.

Lao W, Tsukada D, Greenstein DJ, Bay SM, Maruya KA. 2010. Analysis, occurrence, and toxic potential of pyrethroids, and fipronil in sediments from an urban estuary. *Environ Toxicol Chem* 29:843–851.

Lao W, Tiefenthaler L, Greenstein DJ, Maruya KA, Bay SM, Ritter K, Schiff K. 2012. Pyrethroids in Southern California coastal sediments. *Environ Toxicol Chem* 31:1649–1656.

Li H, Cheng F, Wei Y, Lydy MJ, You J. 2017. Global occurrence of pyrethroid insecticides in sediment and the associated toxicological effects on benthic invertebrates: An overview. *J Hazard Mater* 324:258–271.

Long ER, McDonald DD, Smith SL, Calder FD. 1995. Incidence of adverse biological effects within ranges of chemical concentrations in marine and estuarine sediments. *Environ Manage* 19:81–97.

Long ER, Field LJ, MacDonald DD. 1998. Predicting toxicity in marine sediments with numerical sediment quality guidelines. *Environ Toxicol Chem* 17:714–727.

Mayer P, Vaes WHJ, Wijnker F, Legierse KCHM, Kraaij R, Tolls J, Hermens JLM. 2000. Sensing dissolved sediment porewater concentrations of persistent and bioaccumulative pollutants using disposable solid-phase microextraction fibers. *Environ Sci Technol* 34:5177–5183.

McPherson C, Chapman P. 2000. Copper effects on potential sediment test organisms: The importance of appropriate sensitivity. *Mar Pollut Bull* 40:656–665.

Phillips B, Anderson B, Lowe S. 2011. RMP Sediment Toxicity Study 2009-2010: Determining causes of sediment toxicity in the San Francisco Estuary. Contribution No. 626. Final Report. Regional Monitoring Program for Water Quality in the San Francisco Estuary, San Francisco, CA, USA.

Reible D, Rao B, Rakowska M, Athanasiou D, Drygiannaki I, Bejar M, Chadwick B, Rosen G, Colvin M, Burton GA. 2018. Assessment and management of stormwater impacts on sediment recontamination. ER-2428. Final Report. Strategic Environmental Research and Development Program, Alexandria, VA, USA.

Rosen G, Chadwick DB, Colvin M, Stransky C, Burton A, Radford J, Bailey H, Cibor A, Grover M, Greenberg M. 2017. Demonstration and commercialization of the Sediment Ecosystem Assessment Protocol. Space and Naval Warfare Center Pacific Technical Report #3052, for the Department of Defense's Environmental Security Technology Certification Program, January 2017. Alexandria, VA, USA. [cited 2019 April 2]. Available from: http://www.dtic.mil/dtic/tr/fulltext/u2/10314

Southern California Coastal Water Research Project and Space and Naval Warfare Systems Center. 2005. Sediment assessment study for the mouths of Chollas and Paleta Creek, San Diego: Phase 1. Final Report. San Diego Regional Water Quality Control Board, San Diego, CA, USA.

Strategic Environmental Research and Development Program/Environmental Security Technology Certification Program. 2016. SERDP and ESTCP workshop on research and development needs for long-term management of contaminated sediments. In Leeson A, Thompson T, Magar V, Patton C, Luthy RG, Anderson K, Bachman B, Gustavson K, Markillie K, Michalsen M, eds. US Department of Defense, Alexandria, VA, USA.

Swartz RC, Schults DW, Ozretich RJ, Lamberson JO, Cole FA, Ferraro SP, Dewitt TH, Redmond MS. 1995. ΣPAH: A model to predict the toxicity of polynuclear aromatic hydrocarbon mixtures in field-collected sediments. *Environ Toxicol Chem* 14:1977–1987.

SWRCB. 1999. Consolidated Toxic Hot Spots Cleanup plan List and Findings. Sacramento, CA, USA.

Tang W, Wang D, Wang J, Wu Z, Li L, Huang M, Xu S, Yan D. 2018. Pyrethroid pesticide residues in the global environment: An overview. *Chemosphere* 191:990–1007.

Tay KL, Doe K, Jackman P, MacDonald A. 1998. Assessment and evaluation of the effects of particle size, ammonia, and sulfide on the acute lethality test. Technical Report. Environmental Canada Atlantic Division. Dartmouth, NS, Canada.

US Environmental Protection Agency. 1994. Methods for assessing the toxicity of sediment-associated contaminants with estuarine and marine amphipods. Office of Research and Development, Washington, DC.

Van Geest JL, Burridge LE, Kidd KA. 2014. Toxicity of two pyrethroid-based anti-sea lice pesticides, AlphaMax® and Excis®, to a marine amphipod in aqueous and sediment exposures. *Aquaculture* 434:233–240.

Weston DP, Lydy MJ. 2010. Urban and agricultural sources of pyrethroid insecticides to the Sacramento-San Joaquin Delta of California. *Environ Sci Technol* 44:1833–1840.

Weston DP, Holmes RW, Lydy MJ. 2009. Residential runoff as a source of pyrethroid pesticides to urban creeks. *Environ Pollut* 157:287–294.

